2016

Synthesis and Characterization of Transition Metal Pincer Complexes on a Silica Polyamine Composites for Catalytic Applications

Abdul Goni

Synthesis and Characterization of Transition Metal Pincer Complexes on a Silica Polyamine Composites for Catalytic Applications

By
Md Abdul Goni
M.S. in Chemistry, Tennessee State University, Nashville, TN 37209

Dissertation

Presented in Partial Fulfillment of the Requirements for the Degree of Doctor of Philosophy, in Inorganic Chemistry
The University of Montana
Missoula, MT
Fall 2016

Approved by

Dr. Edward Rosenberg, Committee Chair
Department of Chemistry

Dr. J.B. Alexander Ross, Committee Member
Department Chemistry

Dr. Garon Smith, Committee Member
Department of Chemistry

Dr. Orion Berryman, Committee Member
Department of Chemistry

Dr. Nicholas Natale, Committee Member
Department of Biomedical and Pharmaceutical Sciences

Synthesis and Characterization of Transition Metal Pincer Complexes on a Silica Polyamine Composite for Catalytic Applications

Chairperson: Prof. Edward Rosenberg, Department of Chemistry and Biochemistry

Abstract

There are two main parts of this dissertation: (i) Investigation of the most efficient method for loading and synthesizing catalytically active pincer metal complexes on a silica polyamine composite, BP-1, and (ii) study of the catalytic activity of the immobilized pincer complexes on the BP-1 surface.

Three methods were investigated to immobilize pincer complexes on BP-1 using PONOP pincer complexes of Ru, Rh, Ni and Pd. Method 1, appeared to be the most suitable and effective process to load the pincer complexes: the immobilization proceeded by a two-step Mannich reaction with the addition of preassembled pincer metal complexes to BP-1. The complexes on BP-1 were characterized by solid state NMR, FT-IR, elemental analysis, and metal digestion studies. The model solution experiments between pincer complexes and n-butylamine revealed electrophilic substitution in both the meta- and para-position of pyridine ring of the pincer complexes by Mannich intermediate.

The catalytic reactivity of immobilized (PNN)RuH(Cl)(CO) and (PONOP)RuH(Cl)(CO) on BP-1 was studied in the dehydrogenative coupling of alcohols to esters and H_2 reactions. Moderate to good ester yields were realized with both immobilized systems without using any base and in the presence of KOH. The homogeneous reactions required a base for catalysis. The amine functionality on BP-1 functioned as a base to generate active pincer catalyst on the BP-1 surface. Both immobilized catalysts were recycled for multiple alcohol reaction cycles. BP-1-Ru-PNN showed alcohol conversions up to five cycles, whereas BP-1-Ru-PONOP was found to be survived up to the fourth catalytic cycle. Four control experiments were carried out using alcohol and both of the immobilized systems. The results revealed the heterogeneity of alcohol catalysis by both BP-1-Ru-PNN and BP-1-Ru-PONOP systems. The composite catalysts were also tested in amide formation reactions from amines and alcohols. Instead of generating amides, the imines formations were realized by the coupling of amines in both cases.

This study opened a new catalytic method for important metal pincer complexes in their known catalytic reactions where the requirement of using a base is eliminated for the catalysis by the utilization of a solid support with basic functionality. It also suggested different immobilization approaches which will save the relatively expensive pincer catalysts for multiple uses in catalysis.

Acknowledgements

I have spent almost four and half years living in Missoula for my graduate study at the university of Montana. This is such as a wonderful place to live and work. I could never have imagined how fast these days would be gone. First of all, my all thanks and praises to the Almighty Lord Who awarded me all talent and intellectual ability to perform graduate study and research at this stage. I would like to thank Prof. Edward Rosenberg for giving me the opportunity to perform my graduate research in his lab. He is a wonderful person, not only as a mentor and advisor, but also as a man and his equal will be hard to find. Thank you so much, Prof. Edward Rosenberg, for being so patient and kind with me throughout my graduate study at the university of Montana. I also have to thank Dr. Glenn Pinson and Dr. Geoffrey Abbott who were in the lab when I arrived and took their time to introduce me to all of the apparatus and facilities in the lab. Special thanks to Dr. Geoffrey Abbott who taught me all the procedures and operations of solid state NMR. Thanks to all the members of the Rosenberg group for their support. My sincere thanks to Dr. Earle Adams for his help and patience regarding all my issues with the solid-state NMR instrument. I would like to thank all faculty and stuff of the Department of Chemistry and Biochemistry for being so friendly, helpful, and supportive to students and making the chemistry department a wonderful place to study and research. I would also like to offer thanks to the Graduate School and the Department of Chemistry and Biochemistry for supporting me as a TA for the last four years. I want to acknowledge my friends Dr. Md. Mainul Hossain and Dr. Aeysha Sharmin for being supportive and helpful as I settled in Missoula.

I would like to thank my Mom and Dad who sacrificed their whole life to educate and take care of me and my other siblings. I owe so much gratitude to my elder brother, who provided me all financial support, and encouragement, and caring during my college and Bachelor's studies. Words might not be enough to convey my gratitude to him. I would like to thank my loving and caring wife, and soul mate Nahid Sultana. I always strongly appreciate all her care and encouragement to me. She has sacrificed a lot for me during my Master's and PhD study in the USA, and she was so supportive and understanding, particularly in all those late nights and weekends when I had to work and stay in the lab.

Table of Contents

Chapter 3
Methods study for the immobilization of metal pincer complexes on silica polyamine composites, BP-1

Chapter 4

Synthesis, characterization, and catalytic study of PNN pincer complex of ruthenium on BP-1

Chapter 5

Catalytic study on alcohol dehydrogenation reactions on silica polyamine composites, BP-1 by immobilized (PONOP)RuH(Cl)(CO) (1)

Chapter 6

Formation of imines from primary amines on the silica polyamine composite, BP-1, by immobilized (PNN)RuH(Cl)(CO) and (PONOP)RuH(Cl)(CO)

Chapter 7

Conclusions and Future Work

List of Tables and Schemes

List of Figures

List of Abbreviations

AA	Atomic Absorption
BP-1	Polyallylamine Coated Particles
CPMAS	Cross-Polarization Magic Angle Spinning
FT-IR	Fourier Transform Infrared
NMR	Nuclear Magnetic Resonance
PNN	{2-(di-*tert*-butylphosphinomethyl)-6-(di-ethylaminomethyl)} pyridine
Ru-PNN	(PNN)RuH(Cl)(CO) [{2-(di-*tert*-butylphosphinomethyl)-6-(di-ethylaminomethyl)} pyridine] ruthenium hydrido chloro carbonyl
PONOP	2,6-bis(di-*tert*-butylphosphinito)pyridine
Ru-PONOP	(PONOP)RuH(Cl)(CO) {2,6-bis(di-*tert*-butylphosphinito) pyridine}ruthenium hydrido chloro carbonyl
SPC	Silica Polyamine Composites
SS-NMR	Solid State Nuclear Magnetic Resonance
SL	Solid-Liquid Method
SV	Solid-Vapor method

Chapter 1

Introduction and Background

1.1 Catalysis: General statement

Catalysis is a process which exists in every sphere of nature. Numerous chemical transformations observed in a wide variety of biological systems in nature over millions of years are catalyzed by naturally occurring enzyme catalysts.[1] These catalyst molecules involve complex compounds with large molecular weight structures and work very selectively in various complex biological reaction systems.[2] Catalysis has been a key focus in chemical transformations since the industrial revolution began. It offers many advantages in chemical reaction systems by reducing time and energy requirements and results in overall chemical processes with increased environmental sustainability.[3] The principle on which a catalytic compound works is to decrease the energy barrier between the reactants and products by providing an alternative reaction path (Figure 1.1). It functions in a very specific way and under ideal conditions, allows for more efficient reactions, results in the selective formation of desired products and eliminates the possibility of side reactions occurring. Compared to the enzyme catalysts observed in nature, the catalysts designed and synthesized by human beings are relatively simple, soluble molecules with lower masses or insoluble inorganic solids.[2,3]

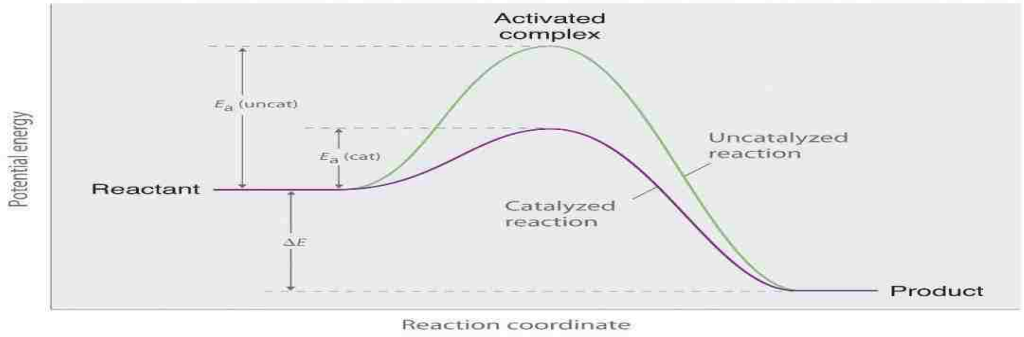

Figure 1.1: The potential energy diagrams for a single-step exothermic reaction in the presence and absence of a catalyst.[4]

Catalytic processes can be divided into three main categories: homogeneous catalysis, heterogeneous catalysis, and bio-catalysis. In this dissertation, we will mainly focus on homogeneous and heterogeneous catalysis. Both homogeneous and heterogeneous catalytic systems have several advantages and disadvantages. Table 1.1 summarizes the characteristics of heterogeneous and homogeneous catalysis.[5]

Table 1.1: Comparison of the advantages and disadvantages of homogeneous and heterogeneous catalysis

Parameter/Factor	Homogeneous	Heterogeneous
Form	Soluble metal complexes, usually mononuclear	Metals, metal oxides, metal complexes on a solid support
Active site	Excellent accessibility to active sites, no mass transfer limitations, no pressure drop	Poorly defined. Continuous operation frequently applied
Phase	Liquid	Gas/Solid, Liquid/Solid
Temperature	Low (<250°C)	Relatively higher
Activity	High Activity in terms of *TON and *TOF	Low to moderate. Resistance to drastic operational conditions
Selectivity	High	Low
Diffusion	Facile	Can be very important
Heat transfer	Facile	Can be problematic
Reaction mechanisms	Excellent catalyst description. Reasonably well understood mechanisms	Poorly understood mechanisms. Choice of large variety of supports, e.g. silica, alumina, zeolites, carbon etc.
Catalyst modification	Easy	Difficult
Product separation	Generally very problematic and difficult	Very simple and easy
Catalyst recycling	Expensive	Very simple

*TON = Turnover number = moles of product/moles of catalyst ; *TOF= TON/Time

In modern synthetic chemistry the recycling and reuse of relatively expensive catalyst systems has become an important goal. In addition, the separation of catalysts from product streams poses an economic and environmental challenge to satisfy some of the Green Chemistry

criteria.[6] Though the catalyst design, selectivity, and activity are the major outputs of homogeneous catalysis, the easy purification of the product and facile reuse of the relatively expensive catalytic materials make heterogeneous catalysis more applicable in large scale commercial operations in industry.[7] Approximately 85% of all chemical processes in industry are run catalytically where the relative ratio of the applications of homogeneous to heterogeneous catalysis is about 25:75.[8,9] Therefore, to achieve an ideal and excellent catalytic system, one should design and constitute a hybrid catalytic species which would combine both aspects and features of homogeneous and heterogeneous catalysis.

1.2 General immobilization approaches

Heterogenization of homogeneous catalysts on suitable supports has become an expanding area of research because it offers accessibility to both homogeneous and heterogeneous catalysis in a single platform. Today the field of catalysis is mainly dominated by metal catalysis. Transition metal compounds with a wide variety of organic-inorganic ligands are the largest class of homogeneous metal catalysts that are now extensively used in various chemical transformations.[10] Types of heterogeneous catalysts could be the bulk metal catalyst compound on a suitable solid support or only metal particles on that support. These support materials may be varied in their sizes and can be as small as a few nanometers. There are many synthetic techniques that have been reported and utilized to immobilize molecular organometallic catalysts on various support materials.[8,9] Some of them utilize non-covalent interactions between catalysts and supports.[8,9] Figure 1.2 depicts the common methodologies to immobilize catalyst compounds on solid supports.

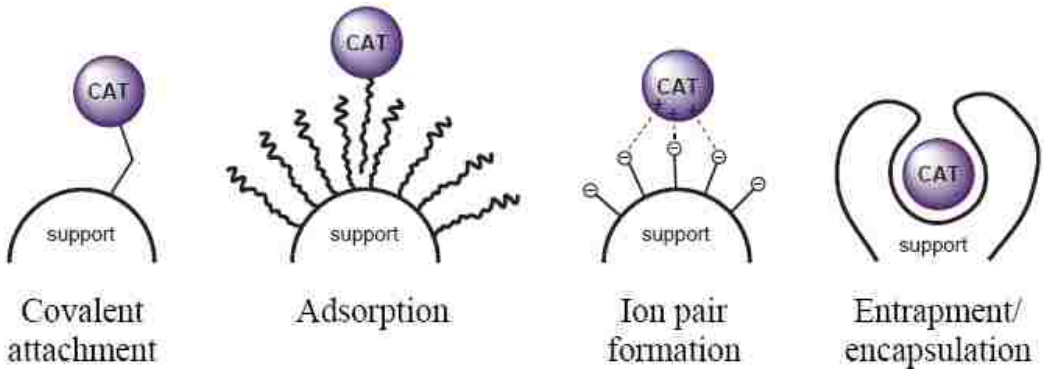

Figure 1.2: Different approaches for immobilization of homogeneous catalyst on solid supports[9]

Table 1.2: Comparison of the advantages and disadvantages of different immobilization approaches[9]

Immobilization method	Covalent ligand binding	Physisorption	Ion pair	Encapsulation
Applicability	Broad	Restricted	Restricted	Restricted
Drawbacks	Preparation	Competition with solvents	Competition with polar or ionic substrates	Substrate size, Diffusion

Comparison of different immobilization approaches is listed in Table 1.2. However, the most versatile, widely used effective method for the immobilization of homogeneous catalysts is to attach them to suitable supports by the formation of covalent bonds between the solid support and the ligand of the catalyst complex.[8,9,10,11,12] Immobilization by covalent attachment can be done in two ways: (i) pre-formed complex immobilization or (ii) step-wise synthesis of the complex on the support.[8-12] The types and natures of the solid supports are crucial for the catalytic activity of the loaded complexes. A large variety of solid supports have been used to heterogenize homogeneous catalyst compounds such as: dendrimers, functionalized organic polymers, and inorganic support systems: alumina, silica, silica–alumina, and cation exchange resins.[11,13,14] However, silica materials have shown to be the most viable and facile support for the catalyst

molecules in terms of activity, recycling, and easy separation of the product from the reaction mixtures.[15,16]

1.3 Pincer ligands and their complexes in catalysis

Controlling the properties of metal centers by a well-defined ligand system is an ultimate goal in modern inorganic and organometallic chemistry. There are many ligand systems reported in the literature. However, among them, pincer ligands and their complexes have drawn increasing interest in recent years. Extensive research has been carried out recently on metal pincer chemistry.[17,18,19] This is due to the higher thermal stability, structural variability, and outstanding catalytic activity of metal pincer complexes in various chemical transformations.[20, 21,22] Pincer-type ligands offer control over coordination geometry of metal complexes due to the extreme variability in the ligand design.[23] The first pincer type ligand was synthesized by Moulton and Shaw in 1976.[24] Since then, a wide variety of pincer ligands have been developed. Their chemistry at metal centers, and catalytic reactions are also being explored.[25-27]

Pincer ligands are types of chelating agents that bind tightly to metal centers with three adjacent coplanar sites in meridional configurations.[22] Pincer ligands are named after their particular coordination mode to the metal centers and are abbreviated by the letters of three donor atoms that are coordinated to the metal center in the complex: e.g., the PNP, PNN, SCS, PCP, or NCN pincer. They are usually tridentate ligands. They feature a central aromatic ring with a heteroatom (Y) and which is ortho-disubstituted with two electron-donor substituents (E) (Figure 1.3).[22] These substituents (E) can be connected to the central aromatic backbone by different spacers (A), such as methylene groups (-CH_2-), amines (-NR-) or oxygen atoms (-O-). The (un)substituted aromatic ring can be either a pyridine ring (Y= N) or a benzene ring (Y= C). Thus

either neutral or anionic pincer ligands can be obtained. The neutral lone pair donors (E), are typically amines (NR_2), phosphines (PR_2), phosphites ($P(OR)_2$), ethers (OR), thio-ethers (SR), or even N-heterocyclic carbenes (NHCs), arsines (AsR_2), and seleno-ethers (SeR).[22,34] The donor groups need not be identical, and pincer ligand systems with two different donor atoms have also been reported.[28,29]

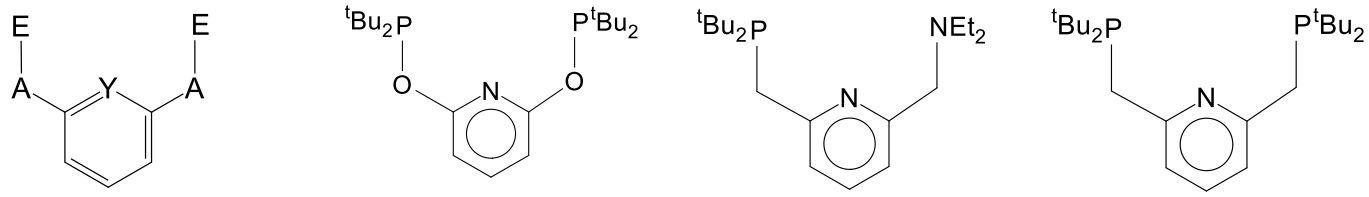

(a) (b) (c) (d)

General structure of pincer ligands | PONOP | PNN | PNP

E = NR_2, PR_2, $P(OR)_2$, OR, SR, AsR_2, SeR ;

Y = N, C ; A = CH_2, NH(R), O ; R = alkyl, aryl

Figure 1.3: Schematic diagram of: (a) Pincer ligands, (b) Pincer ligand, PONOP (c) Pincer ligand, PNN and (d) Pincer ligand, PNP

Pincer ligands can coordinate with the metal center in a meridional way via the two electron-donor groups and with the formation of metal-carbon σ bonds (benzene-based pincer complexes) or metal-nitrogen bonds (pyridine-based pincer complexes). Thus, a wide variety of different EYE pincer ligands are accessible by modifying one or more of the parameters in the general structure of the ligand; that is, the donor groups, the aromatic ring and its substitution, or the spacer groups (Figure 1.3).[22] However, so far, the most widely-utilized and effective pincer ligands are those containing phosphines or phosphites as donor groups.[22, 30] The pincer ligand PNP, PNN, and PCP have been shown to be excellent alternatives to traditional phosphine ligands which

are poisonous, air sensitive, and unrecoverable, and which degrade at higher reaction temperatures.[18,22] They have been found to form complexes with a large variety of transition metals such as Pd, Pt, Ru, Os, Rh, Ir, Ni. [31,32,33]

The pincer-type complexes consist of a metal center and a pincer skeleton. The pincer skeleton is a tridentate ligand which is connected to the metal *via* metal-carbon σ bond or two dative bonds between metal and donor heteroatoms and these bonds provide the unique stability of these complexes, thus avoiding the dissociation of the metal from the pincer ligands and the decomposition of the complexes. In addition, the donor atoms and their corresponding substituents allow tuning of the steric and electronic properties of the complexes. Metal complexation with pincer ligands usually occurs with the formation of two five-membered metallocycles [MXn(EYE)Lm] (Figure 1.4).[22,34] However, very few examples are known that contain a two-carbon linkage between the aryl-carbon and the E-donor atoms, which results in the formation of six membered metallocycles.[34]

Pincer metal complexes have tremendous applications in a wide range of catalytic reactions which include: aldol condensation,[35] double Michael addition and Kharasch addition,[36] transfer hydrogenation,[37] transfer dehydrogenation,[38] allylicstannylation[39] and allylic alkylation reactions.[40]

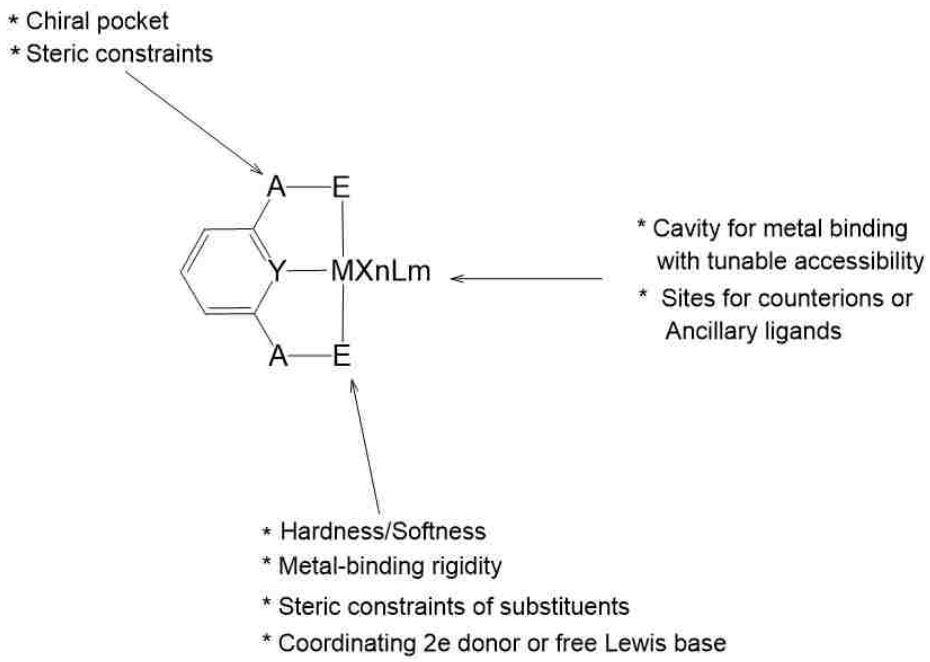

Figure 1.4: Schematic diagram of metal pincer complexes [22,34]

One relatively recent, interesting application of pincer metal complexes is in esterification, which is one of the most fundamental and important reactions in organic synthesis.[41] PNP and PNN pincer complexes of ruthenium have shown the most promising and interesting catalyst, for dehydrogenative coupling of alcohols to esters along with the liberation of hydrogen, [41, 42, 43] hydrogenation of esters,[44] hydrogenation of amides to alcohols and amines,[44] and other reaction systems. [45-53]

Section 1.4: Immobilization of pincer complexes on various solid supports

Though a large variety of pincer ligands and their metal complexes are now accessible (Figures 1.3 & 1.4), and their interesting catalytic reactivity has been shown in the literature, they are still relatively expensive and their synthetic procedures are not easy and straight-forward. Therefore, there is a growing demand for the immobilization of valuable pincer catalyst complexes on suitable supports which will allow reusing them in multiple catalytic

cycles. In addition, immobilization provides a means for separating expensive pincer catalysts through simple filtration.

Recent studies have reported various methods of immobilizing pincer complexes on a range of solid supports, including inorganic materials (alumina, silica), dendrimers, and functionalized organic polymers.[54-56] Silica materials appear to be the most suitable solids for immobilization of organometallic pincer catalysts.[6,57] Pozo *et al.* reported the immobilization of (NHC)NN-pincer complexes on a mesoporous silica (MCM-41) support by covalent binding of the pincers to silica via a pendant alkoxysilane group.[13] Platinum and palladium pincers, [C_6H_3(2,6-CH_2NMe_2)$_2$] catalysts functionalized with para-ethynyl-groups, were immobilized on azido-functionalized silica materials for C–C coupling reactions using "click " chemistry.[58] Palladium PCP pincer complexes were tethered on polymer and silica supports through amide or ether linkages and applied in the Heck reaction of iodobenzene and n-butylacrylate.[59] Brookhart *et al.* reported the immobilization of PCP and POCOP iridium pincer complexes for transfer dehydrogenation of alkanes on different types of solid supports using three approaches: the covalent attachment of a phenoxide functionalized iridium pincer to a Merrifield's resin with chlorobenzyl moieties, covalent bonding of iridium pincers with a pendant alkoxysilane group to silica, and the adsorption of iridium pincers containing basic functional groups on g-Al_2O_3 through a Lewis acid/Lewis base interaction.[60] Goldman *et al.* demonstrated the immobilization of bis-phosphinite-tert-butyl-iridium pincer complexes on γ-Al_2O_3 by two methods: covalent attachment to trimethoxysilyl substituted iridium pincers with hydroxyl-functionalized Al_2O_3 and binding of para-functionalized POCOP iridium pincers to a coordinately-unsaturated surface, Al ion site, in Al_2O_3.[61] The dihydride pincer complex [IrH_2(POCOP)]was also anchored on a mesoporous silica (SBA-15) by the reaction of hydride with surface silanol groups and utilized as a heterogeneous

catalyst for alkene hydrogenation reactions.[62] Pd(II)-SCS pincer complexes were covalently immobilized on porous silica, poly(norborene) and cross-linked Merrifield resin supports by C.W. Jones *et al.* and applied in the Heck reaction.[63,64] G. van Koten *et al.* reported the anchoring of PCP and SCS palladium pincer complexes on ordered mesoporous silicas through a carbamate linkage between *para*-tri-alkoxysilane-functionalized palladium pincers and silica using a grafting process, and utilized the supported catalysts in C-C bond formation reactions.[16] NCN-pincer palladium and platinum complexes were also tethered to silica for applications as Lewis acid catalysts.[6]

Several important applications of pincer catalysts require a basic environment or deprotonation to activate the catalyst or substrate. For example, the Ru-PNN and Ru-PNP catalyzed dehydrogenative coupling reactions developed by Milstein require deprotonation of the pincer arm to generate the active catalyst.[65] More recently, an Fe-PNP complex has been shown to reduce CO_2 to formate at low pressures and also requires a base.[50] The PNP pincer, $Ir(H)_3(2,6\text{-}(iPr_2P)_2)NC_5H_3$ has been shown to be a highly efficient catalyst for reduction of CO_2 to formate and requires a 10% aqueous KOH solution.[66] Similarly, the nickel PONOP pincer, $NiH(2,6\text{-}(iPr_2PO)_2)NC_5H_3$), has been shown to be an effective hydrosilation catalyst in the presence of an aqueous base.[67] Both of these systems would benefit from the elimination of the basic co-reagents by using a surface that could provide the required base. For CO_2 reduction, water would still be required. There are also a variety of Pd(PCP) and Pd(POCOP) pincer complexes that have been applied to C-C coupling reactions. On reaction with a base, however, many of these release Pd(0) nanoparticles and would not be suitable for immobilization on surfaces for multiple cycles.[68] On the other hand, there are many reaction types, including aldol-type condensations with

electrophiles that do require bases using PCP and POCOP frameworks.[68] Thus, there is a large class of pincer catalyzed reactions that would benefit from a basic surface.

The types and natures of the support materials and linkers can have significant effects on the catalytic reactions of pincer metal complexes. In our study, we have used a unique solid support, silica polyamine composites (SPCs), to immobilize some very important pincer metal complexes. These SPCs offer a basic plat-form on their surfaces. The silica polyamine composites (SPCs) are organic-inorganic hybrid composite materials that have been commercially developed and have been used industrially for applications in the recovery and removal of transition metals, precious metals, and mercury from diverse waste streams and mining leaches (Scheme 1.1).[69-72]

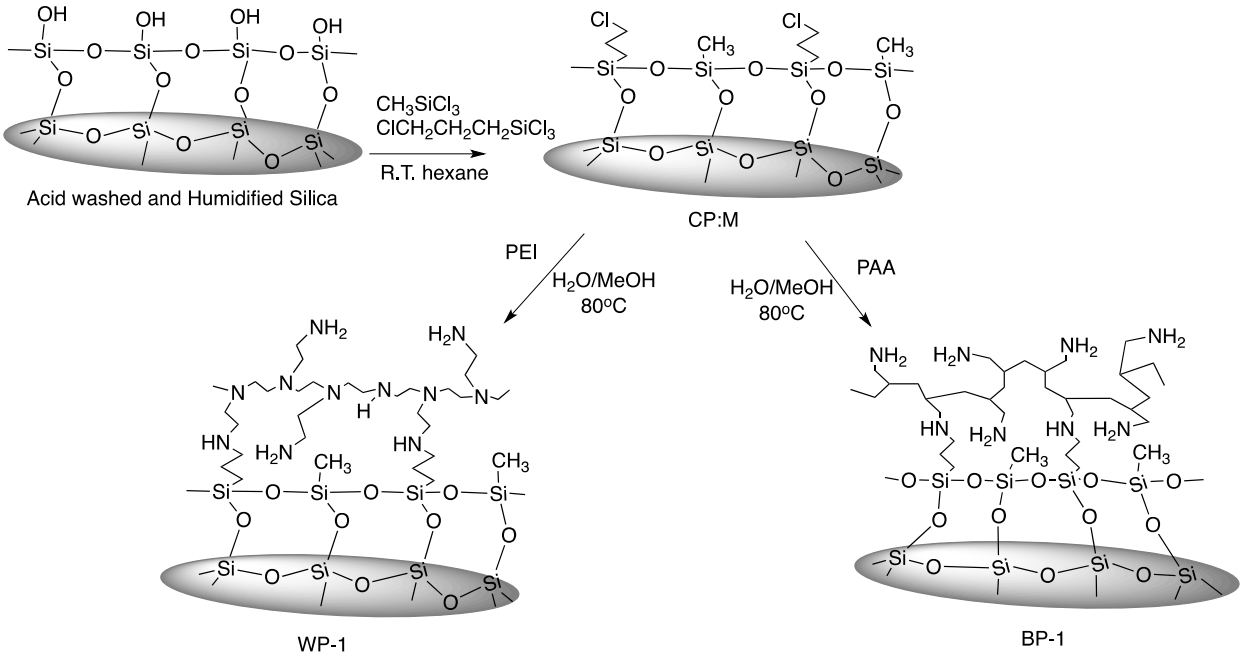

Scheme 1.1: Synthesis of silica polyamine composites.

The SPCs offer the high ligand loading of polymeric supports with the greater porosity and matrix rigidity of amorphous silica.[72] The SPCs yield silica gel-polyamine surfaces that can be

used as chelating agents (Scheme 1.1). The polyamines are covalently bound at multiple points to the silane layers providing additional stability,[70] and can be further modified with ligands that make them selective for a given metal or group of metals.[72] These SPC materials do not shrink or swell, and can tolerate temperatures up to 200°C, and have been shown to have long, usable lifetimes.[72]

The performance of catalysts in heterogeneous systems greatly depends on the nature of the support surfaces.[73,74] The surfaces of silica polyamine composites could alter the electronic properties of the catalytically active species or complexes bound to the surfaces and could also control molecular access to the active sites of the catalysts in heterogeneous systems in a different way than simple oxide or polystyrene supports. For example, the unmodified amines offer the opportunity to act as base co-catalysts and permit tuning of the surface pH (Zeta potential). They have silane-polyamine linkage that extends the complex away from the surfaces. Recently, we reported the successful use of rhodium, palladium and ruthenium salts immobilized on SPC surfaces for selective hydrogenation of olefins and the selective oxidation of phenol to catechol.[75] These studies required the thermal stability of the SPCs and this stability has been confirmed by DTG (Differential Thermogravimetry) analysis.[76] In addition, a series of luminescent ruthenium complexes with various types of ligands have also been successfully immobilized on SPC.[77] Given the ease of modification of the SPC amine surface with aromatic ligands using the Mannich Reaction without prior *para*-substitution[71,78] and its ability to provide a basic surface for catalysis, SPC would appear to be a suitable candidate for the immobilization of metal pincer complexes.

Chapter 2: Project Goals

In this dissertation, we focus on the synthesis and immobilization of pincer ligands and metal pincer complexes on SPC surfaces for catalytic applications. Our high level of interest in pincer complexes is attributable to their tunable properties, thermal stability, and recent applications across a broad spectrum of catalytic reactions.[18-20,22,41-55] In addition SPC with pincers would offer higher porosity and greater rigidity than the polystyrene systems and because of the use of polyamine it provides higher loading than the pendent siloxane and distancing from the oxide surface to give a more kinetically accessible catalytic site. The basic amine groups present on the surface of the SPC provide additional possibilities to utilize them as a co-catalyst. The addition of a base is required in the dehydrogenation of alcohols and related reactions by pincer metal complexes, and in the case of the SPC this may occur *in situ*. So, the initial goal of this project is to synthesize and characterize various pincer complexes on a silica polyamine composite, BP-1. The overall goal is to investigate the catalytic reactivity of immobilized pincer complexes on SPC-BP-1 in their well-known catalytic reactions.[41-42] The specific aims of this dissertation are listed below:

Specific Aim 1: To develop the effective methods to load and synthesize pincer ligands and metal pincer complexes on SPC-BP-1.

Specific Aim 2: To **c**onstruct the PONOP pincer ligand and metal PONOP pincer complexes on SPC-BP-1 by the best method. Investigate the catalytic activity of these immobilized M-PONOP pincer complexes on SPC-BP-1.

Specific Aim 3: To **sy**nthesize and characterize the PNN pincer ligand and metal-PNN pincer complexes on SPC-BP-1 and to screen the catalytic performance of PNN pincer complexes on BP-1 in different chemical transformations.

Specific Aim 4: To recycle the immobilized catalysts and investigate the catalytic performances of the immobilized PNN and PONOP metal pincer complexes on SPC-BP-1 in multiple cycles in the respective reaction systems.

Chapter 3

Methods study for the immobilization of metal pincer complexes on silica polyamine composites, BP-1

3.1 Introduction

3.1.1 The type of pincer ligand and metal pincer complex used in the methods study

Synthesis of the most widely used pincer ligands and catalytically active metal pincer complexes is relatively difficult and involves multi-step synthetic procedures. Therefore, the immobilization of metal pincer complexes on a suitable solid support has become an expanding area of research.

Most of the recent reports on the immobilization of pincer complexes required para-functionality on the preassembled pincer complex to anchor them to various solid supports by covalent linkages. The major drawback of this approach is the need for modification in the structures of pincer ligands or metal pincer complexes in order to construct an attachable unit like a meta- or para- functionality. This leads to more synthetic steps and higher preparation costs in the process which also sometimes makes it difficult to isolate and separate substituted pincer metal complexes from the starting materials. It might also have negative consequences in the catalytic reactivity of pincer complexes regarding the presence of substituents in the ligand backbone structures of the pincer complexes. Here we investigated various methods to immobilize pincer metal complexes that do not require the introduction of *para*- or *meta*-functionality in the pincer structure and the support surfaces provide a basic functionality that can act as a co-catalyst for reactions requiring base. Though a wide variety of pincer ligands are now accessible, the most widely utilized pincer ligands are those with phosphinites and phosphines donor atoms in their structures.[22,30] An attractive multi-dentate nitrogen-phosphorus pincer ligand for the purposes of

immobilization on the SPC surface is 2,6-bis(di-*tert*-butylphosphinito)pyridine (PONOP, Figure 1.3b). The phosphinite ligand in this system is relatively air-stable in comparison to other pincer ligand systems, and can be easily synthesized prior to immobilization and after (vide infra). This flexibility offers the opportunity to try different routes to immobilization of the pincer ligand. Herein we report three methods for loading and synthesizing the transition metal PONOP pincer complexes on an SPC with the goal of evaluating the best pathway for immobilization.

3.1.2 Immobilization of metal pincer complexes by Mannich reaction

The Mannich reaction is one of the most powerful synthetic methodologies for the formation of carbon-carbon bond. [79,80] It was discovered by a German chemist, Carl Ulrich Franz Mannich in 1912.[79,80] It is a condensation reaction which involves a nucleophilic addition of an amine to a carbonyl compound followed by dehydration. It forms an imine or an iminium ion which is called a Mannich base. This imine compound can act as an electrophile and potentially react with compounds containing acidic protons. In the Mannich reaction, usually primary or secondary amines or ammonia are employed for the activation of formaldehyde or a carbonyl group. The scheme 3.1 shows the mechanism of imine formation in the Mannich reaction between an amine and formaldehyde in the presence of catalytic amount of acid. The reaction is usually carried out in a polar protic solvent such as water, methanol, or ethanol. This reaction is also known as amino alkylation.

Mannich reactions have found extensive applications in the syntheses of naturally and biologically active compounds: peptides, nucleotides, antibiotics, alkaloids and different medicinal compounds such as rolitetracycline (Mannich base of tetracycline), fluoxetine (antidepressant), tramadol, tolmetin (anti-inflammatory drug) and azacyclophanes.[80,81,82] Other

applications include: paint- and polymer chemistry, catalysts and mechanism of formalin tissue crosslinking.[83,84]

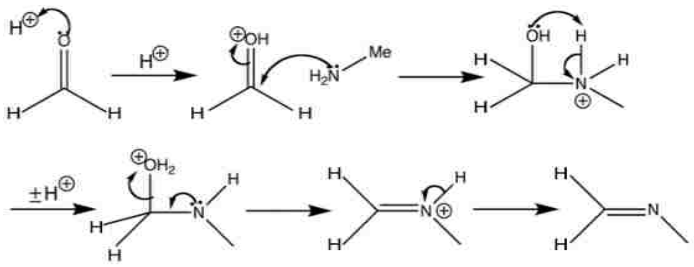

imine

Scheme 3.1: Formation of imine from formaldehyde and amine in Mannich reaction[79,80]

We chose the Mannich reaction for the immobilization of pincer metal complexes on SPC-BP-1 because of our prior successes with this reaction system in loading aromatic molecules on SPC.[71,78] In the previous study from our group, a series of luminescent ruthenium bipyridyl and phenanthroline complexes was successfully immobilized on SPC-BP-1 by Mannich reaction.[77] In addition, this reaction provides an opportunity to immobilize the pincer metal complexes on BP-1 surface directly by electrophilic substitution reaction in the pyridine moiety of the pincer complexes by Mannich base. It also eliminates the requirement of having functionality or substituent in the structures of metal pincer complexes to load and synthesize them on a solid support.

3.2 Experimental

3.2.1 General methods and materials

The SPC referred to as BP-1, was synthesized using poly(allylamine) (MW = 11-15 Kg, NitoboBuseki, Japan) and has been commercialized as a metal sequestering material for the mining and remediation industries (Scheme 1.1).[69-72] The solvents used were reagent grade. Tetrahydrofuran was distilled from benzophenoneketyl and methylene chloride and acetonitrile

were distilled from calcium hydride. 2,6-dihydroxy pyridine hydrochloride (Sigma Aldrich) and $(PPh_3)_3RuH(Cl)(CO)$, $NiCl_2.6H_2O$ and $(PPh_3)_3RhCl$ were purchased from Strem Chemicals, USA. $PdCl_2(CH_3CN)_2$ was synthesized by a previously reported procedure.[85-86] 2,6-bis(di-*tert*-butylphosphinito)pyridine (PONOP) was synthesized according to the reported literature procedure.[87] Elemental analysis (C, H, N, P and Cl) were performed by Galbraith Laboratories, Inc, Knoxville, Tennessee, USA. Solid-state CPMAS ^{13}C and ^{31}P NMR were obtained on a Varian NMR Systems 500 MHz spectrometer at 125 and 206 MHz respectively, with spinning speeds of 7-10 KHz. ^{13}C and ^{31}P chemical shifts are reported relative to external *tetra*-methylsilane and phosphoric acid respectively. Solution ^{1}H and ^{31}P NMR were obtained on Varian 500 NMR systems spectrometer at 500 and 206 MHz or a Bruker Advanced spectrometer at 400 and 169 MHz respectively. Infrared spectra were recorded as KBr pellets on a Thermo-Nicolet 633 FTIR spectrometer. Loading of the metals on BP-1was determined by digesting the composite samples with the mixture of conc. HCl and conc. HNO_3 mixtures (6:1)[77] and the metal concentration in the digest was determined by Atomic Absorption (AA Spectrometer S Series, Thermo-electron Corporation, USA). All reactions were carried out under a dry nitrogen atmosphere using standard Schlenk techniques.

3.2.2 Immobilization of M(PONOP) pincer complexes on BP-1 by direct reaction with the preformed complex (method 1) (M= Ru, Pd, Ni, Rh)

5g of BP-1 (containing 1.6 mmol N/g) was mixed with a reagent solution of 25 mL aqueous HCHO (38%, 345 mmol) and 0.5 mL glacial acetic acid (17.4M, 8.74 mmol) in a 250 mL flask equipped with an overhead stirrer. The suspension was stirred for 3-4 h at room temperature yielding the surface-bound imine intermediate. The resulting composite was filtered and then washed several times with 95% ethanol, filtered, and then dried under a vacuum overnight (yield:

5.16 g). This dried intermediate composite product was used for immobilization of each of the following complexes on BP-1.

3.2.2.1 Immobilization of (PONOP)RuH(Cl)(CO) on BP-1

500 mg (0.885 mmol) of (PONOP)RuH(Cl)(CO)[87] and 25 mL of distilled THF were added to 5g of dried imine intermediate in a three-necked round bottom flask equipped with an overhead stirrer and a condenser. The mixture was degassed by an applied vacuum (30 mmHg). The temperature of the mixture was raised to 70°C and the reaction mixture was refluxed overnight with stirring under N_2. The composite product was then filtered and washed four times with THF and four times with CH_2Cl_2 and then dried overnight under high vacuum yielding 5.34 g of BP-1-(PONOP)RuH(Cl)(CO)(**1**) product. IR spectra (KBr pellet): 1952 cm^{-1} (s) (νCO). Elemental analysis and NMR data are given in Table 3.1.

3.2.2.2 Immobilization of M(PONOP) complexes on BP-1 (M = Pd, Ni, Rh)

The procedure described above was used for the immobilization of the Pd and Ni complexes using 500 mg of [(PONOP)PdCl]Cl[20] and [(PONOP)NiCl]Cl[20] respectively. Conditions and solvents are shown in Scheme 3 and the yields for the resulting composites, BP-1-[(PONOP)PdCl]Cl(**2**), BP-1-[(PONOP)NiCl]Cl(**3**) were 5.41 g and 5.17 g respectively. Elemental analysis and NMR data are given in Table 3.2 and 3.3.

(PONOP)RhCl was previously reported[88] but was synthesized here by a different route; the reaction of PONOP (50 mg, 0.125 mmol) with $Rh(PPh_3)_3Cl$ (116 mg, 0.125 mmol) in dried C_6H_6, refluxed overnight under N_2 (yield: 46 mg, 0.086 mmol, 69%). ^1H NMR (500 MHz, CD_2Cl_2): δ 7.58 (t, J_{H-H}= 5.0 Hz, 1H, *p*-C_5H_3N), 7.12 (d, J_{H-H}= 5.0 Hz, 2H,*m*-C_5H_3N), 1.34 (vt, J_{P-H}= 15.0 Hz, 36H, P-C(CH_3)$_3$). $^{31}P\{^1H\}$ NMR (500 MHz, CD_2Cl_2): δ 197.8 (d, J_{Rh-P}= 370 Hz),

500 mg of (PONOP)RhCl made by this route using the conditions shown in Scheme 4 yielded 5.21 g of BP-1-(PONOP)RhCl (**4**). Solid-state ^{13}C and ^{31}P NMR data and the elemental analysis data are given in Table 3.4.

3.2.3 Immobilization of M(PONOP) pincers on BP-1 by ligand grafting followed by addition of metal complexes (method 2)

3.2.3.1 Immobilization of PONOP on BP-1

Using the method for making the imine intermediate given in section 3.2.2, 500 mg (1.25 mmol) of PONOP[87] in 30 mL distilled THF was added to 5 g of the imine intermediate and the mixture was degassed for 10 minutes by applied vacuum. The mixture was refluxed overnight with stirring under N_2. The resulting composite product was cooled and then filtered and washed five times with distilled THF and four times with CH_2Cl_2 and dried overnight under high vacuum (yield, 5.23 g). Elemental analysis: C 12.71 %, H 2.50%, N 2.46%, P 0.497%. Solid-state CPMAS ^{13}C NMR, δ: 163 (pyridine), 47.9 (CH_2 polyamine), 33.3 (*tert*-butyl), 23.4 (*tert*-butyl), -6.5 (Si-CH_3). CPMAS ^{31}P NMR: δ 52.4

3.2.3.2 Preparation M(PONOP) pincers on BP-1 loaded with PONOP by method 2

500 mg (0.525 mmol) of $(PPh_3)_3RuH(Cl)(CO)$ was combined with 5 g of BP-1 loaded with PONOP in a three-necked flask equipped with overhead stirrer and a condenser. 25 mL of distilled THF was added and the mixture was degassed for 10 minutes by applied vacuum. The reaction mixture was refluxed under N_2 overnight. The resulting composite BP-1-(PONOP)RuH(Cl)(CO)(**1**), product was cooled, then filtered, and washed five times with THF and four times with CH_2Cl_2 and then dried overnight under high vacuum (yield, 5.72 g).

The procedure was repeated for the synthesis of BP-1-[(PONOP)PdCl]Cl(**2**), BP-1-[(PONOP)NiCl]Cl(**3**) and BP-1-(PONOP)RhCl(**4**) by method 2 with the addition of the respective

metal compounds, $PdCl_2(CH_3CN)_2$, $NiCl_2.6H_2O$ and $(PPh_3)_3RhCl$ and using the solvents, distilled CH_2Cl_2, absolute EtOH and C_6H_6 respectively (Scheme 3.2). A similar procedure was followed to separate and dry each of the composite products (yield: 5.58g, 5.45g and 5.41g respectively). Solid-state ^{13}C and ^{31}P NMR data elemental analysis data are given in Table 3.1-3.4.

3.2.4 Immobilization of M(PONOP) pincers on BP-1 by stepwise construction of the PONOP on BP-1 followed by addition of metal complexes (method 3)

3.2.4.1 Stepwise construction of PONOP on BP-1

To 5g of the imine intermediate prepared according to section 3.2.2 was added 1.2 g (10.81 mmol) of 2,6-dihydroxy pyridine [obtained by the addition of NaOH (328 mg, 8.2 mmol) to2,6-dihydroxy pyridine hydrochloride (1.21 g, 8.2 mmol) in 25 mL absolute EtOH adjusted to pH=9]. 30 mL of absolute EtOH was added and the mixture was degassed by applied vacuum for 10 minutes. The temperature of the mixture was raised to 65-70°C and the reaction was carried out for 24 hours under N_2. The solvent was then removed and the resulting composite product was washed four times with absolute EtOH, three times with distilled THF, three times with CH_2Cl_2 and three times with CH_3OH and then dried under vacuum. This dried composite product was then transferred to a three-necked round bottom flask equipped with an overhead stirrer. 30 mL of distilled THF was added and the mixture was degassed by an applied vacuum. 2.85 mL (16 mmol) of N,N-di-isopropylethyleneamine (DIEPA) and 3.1 mL (16 mmol) of $(^tBu)_2PCl$ were mixed with the composite mixture in THF under N_2. The mixture was then stirred for 24 h at room temperature under N_2 to complete the reaction. The solvent was then removed from the final composite product and the product was washed four times with CH_2Cl_2, four times with THF and four times with EtOH and finally dried overnight under high vacuum (yield: 5.20 g). Elemental analysis:

C 12.54 %, H 2.40%, N 2.38%, P 0.485%. Solid-state CPMAS ^{13}C NMR, δ: 163 (pyridine), 47.9 (CH_2 polyamine), 33.3 (*tert*-butyl), 23.4 (*tert*-butyl), - 6.5 (Si-CH_3). CPMAS ^{31}P NMR: δ 52.4

3.2.4.2 Immobilization M(PONOP) pincers on BP-1 by addition of metal compounds to pre-constructed PONOP (method 3)

Each of the four pincer immobilized complexes BP-1-(PONOP)RuH(Cl)(CO)(**1**), BP-1-[(PONOP)PdCl]Cl(**2**), BP-1-[(PONOP)NiCl]Cl(**3**) and BP-1-(PONOP)RhCl(**4**) were made on BP-1 following the same procedure as in section 3.3.2. Yields of the composite products were 5.67 g, 5.48 g, 5.36 g and 5.29 g respectively. Elemental analysis, solid-state ^{13}C and ^{31}P NMR data are given in Table 3.1-3.4.

3.2.5 Determination of the metal content of M(PONOP) pincers on BP-1 by digestion and AAS

Loading of the metals on BP-1 as M(PONOP) pincers (M= Ru, Pd, Ni, Rh) by the three methods was determined by digestion of the composites by a previously reported procedure.[77] 40 mg of each of the composite samples loaded with metal pincers was heated overnight at 500°C. The samples were cooled to room temperature and 0.5 mL of HF was added into each of them. Then 0.5 mL of a mixture of conc. HCl and conc. HNO_3 (6:1) was added. Finally, each of the digest solutions was diluted with deionized water until it made up a total volume of 4.5 mL. Metal concentrations in the digest solutions were determined by Atomic Absorption Spectroscopy after construction of standard calibration curves with absorption ranges of 0.001 to 2, using standard solutions (Fischer Scientific), and diluted five times to give the appropriate absorbance. The results obtained in mmol/g of composite are given in Table 3.5 (calibration curves were made in the following absorbance ranges for Ru, 0.001 to 0.02; for Pd, 0.5 to 2; for Ni, 0.02 to 0.8; for Rh, 0.003 to 0.06.

3.2.6 Experimental procedure for the reaction between n-butylamine and PONOP in solution

200 µL (2 mmol) of n-butylamine was added to 200 µL (38%, 2 mmol) of HCHO solution. 20 µL (0.35 mmol) of glacial acetic acid (17.4 M) was added and the reaction mixture was stirred for 3-4 hours at room temperature under N_2. The resulting imine intermediate was extracted with distilled CH_2Cl_2 and then anhydrous Na_2SO_4 was added to remove any trace H_2O. Solvent was then removed and the product was dried under high vacuum. 0.8 g (2 mmol) PONOP was combined with the dried imine intermediate in 8 mL distilled THF. The reaction was carried out at 60°C overnight under N_2. Solvent was removed by rotary evaporation. The product was purified by column chromatography eluting with the mixture of THF and hexane and then dried under high vacuum (yield: 0.58 g, 1.19 mmol, 60%). ^{31}P NMR: δ 112.46 (s), δ 117.13 (s, br), and δ 118.62(s). ^{1}H NMR (two isomers): δ 0.74 (t, J_{H-H}= 10.0 Hz, 3H, CH_3), 0.89 (sextet, J_{H-H}= 5.0 Hz, 2H, CH_2), 1.61 (sextet, J_{H-H}= 7.0 Hz, 2H, CH_2), 1.24 (d, J_{P-H}= 15.0 Hz, 36H, P-C(CH_3)$_3$),1.89 (s, 36H, P-C(CH_3)$_3$), 2.26 (pent, J_{H-H}= 5.0 Hz, 2H, CH_2), 2.81 (pent, J_{H-H}= 5.0 Hz, 2H, CH_2), 2.40 (t, J_{H-H}= 7.5 Hz, 2H, CH_2), 2.61 (t, J_{H-H}= 7.5 Hz, 2H, CH_2),2.98 (d, J_{H-H}= 7.5 Hz, 2H, CH_2),2.53 (s, 2H, CH_2), 10.32 (s, br, 1H, N-*H*), 8.57 (s, 2H, *m*-pyridine, *para*-isomer),7.56 (s, br, 1H, pyridine, *meta*-isomer), 7.37 (s,br,1H, pyridine, *meta*-isomer).

3.2.7 Experimental procedure for the reaction between (PONOP)RuH(Cl)(CO) and n-butylamine in solution

200 µL (2 mmol) of n-butylamine was added to 200 µL (38%, 2 mmol) of HCHO solution. 20 µL (0.35 mmol) of glacial acetic acid (17.4 M) was added and the reaction mixture was stirred 3-4 hours at room temperature under N_2. The resulting imine intermediate was extracted with distilled CH_2Cl_2 and then anhydrous Na_2SO_4 was added to remove any trace H_2O. Solvent was then removed and the product was dried under high vacuum. 1.12 g (2 mmol) of

(PONOP)RuH(Cl)(CO) was combined with the dried imine intermediate in 15mL distilled THF. The reaction was carried out at 66°C for 24 h under N_2. Solvent was removed and the resulting product was washed with pentane and CH_2Cl_2. The product was purified by column chromatography eluting with the mixture of THF and hexane and then dried under high vacuum (yield: 0.73 g, 1.13 mmol, 57%). ^{31}P NMR (C_6D_6): δ 62.57 (s), 58.06 (s), and 57.43 (s). ^{1}H NMR (C_6D_6) (two isomers): δ 0.77 (t, J_{H-H}=7.5 Hz, 3H, CH_3), 1.09 (sextet, J_{H-H}= 7.4 Hz, 2H, CH_2), 3.09 (sextet, J_{H-H}= 8.1 Hz, 2H, CH_2), 0.28 (s, 36H, P-C(CH_3)$_3$), 1.19 (pent, J_{H-H}= 6.8 Hz, 2H, CH_2), 2.45 (pent, J_{H-H}= 7.5 Hz, 2H, CH_2), 0.84 (t, J_{H-H}= 7.5 Hz, 2H, CH_2), 1.45 (d, J_{H-H}= 12.4 Hz, 2H, CH_2), 3.52 (s, 2H,CH_2), 5.48 (s, br, 1H, N-*H*), 8.02 (s, 2H, m-pyridine, para-isomer),7.72 (dd, J_{H-H}= 6.6 Hz, 2H, pyridine, *meta*-isomer). IR spectra(ATR): 1942 cm^{-1} (s)(νCO), 2036 cm^{-1}(s) (νRu−H).

Section 3.3 Results and discussion

The PONOP ligand and the PONOP transition metal complexes were synthesized following previously reported literature procedures (Scheme 3.2).[20,87] Three different approaches have been attempted for immobilization of the PONOP pincer transition metal complexes on BP-1. The first approach involved a direct reaction of the preassembled pincer complexes using a two step Mannich reaction. In method 2, the preformed PONOP ligand was anchored on BP-1 using the same Mannich procedure followed by the addition of the appropriate transition metal compound. In method 3, the PONOP ligand was constructed on BP-1 using three sequential reactions on the composite surface (Scheme 3.3) and the subsequent synthesis of pincer complexes was accomplished by the addition of the transition metal compound. Treatment of BP-1 with 38% aqueous formaldehyde yielded the imine-BP-1 intermediate product, which was the electrophile that reacted with the pyridine ring of the PONOP (Schemes 3.3 & 3.4). The metal compounds used

were $(PPh_3)_3RuH(Cl)(CO)$, $PdCl_2(CH_3CN)_2$, $NiCl_2.6H_2O$ and $(PPh_3)_3RhCl$. The reaction pathways for methods 2 and 3 are illustrated in Schemes 3.3 and 3.4.

The actual position of electrophilic aromatic substitution of the pyridine ring by the imine intermediate in the Mannich reaction could not be determined from the solid-state NMR data due to the poor resolution of the aromatic resonances. Substitution at the *meta*-position would be expected on electronic grounds while *para*-substitution might be expected on steric grounds. To clarify this point, two model solution experiments were conducted. One was with PONOP and n-butylamine, and another was performed between (PONOP)RuH(Cl)(CO) and n-butylamine.

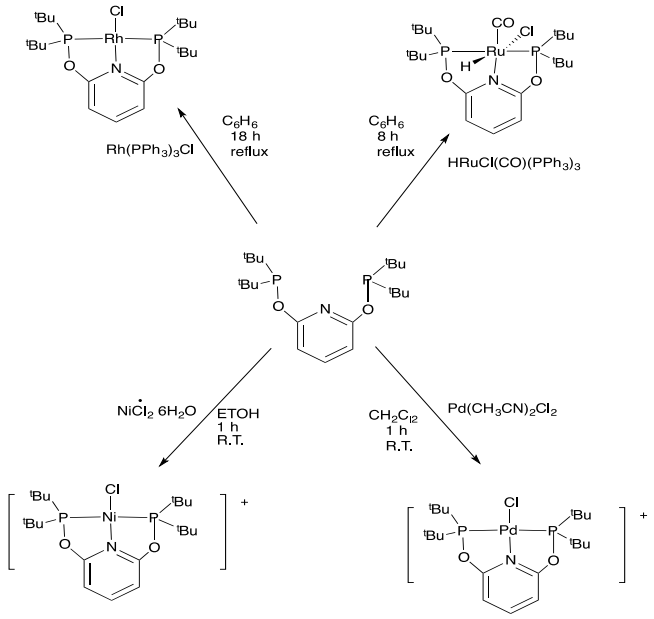

Scheme 3.2: Synthesis of (PONOP)RuH(Cl)(CO), [(PONOP)PdCl]Cl, [(PONOP)NiCl]Cl, and (PONOP)RhCl.[20,87]

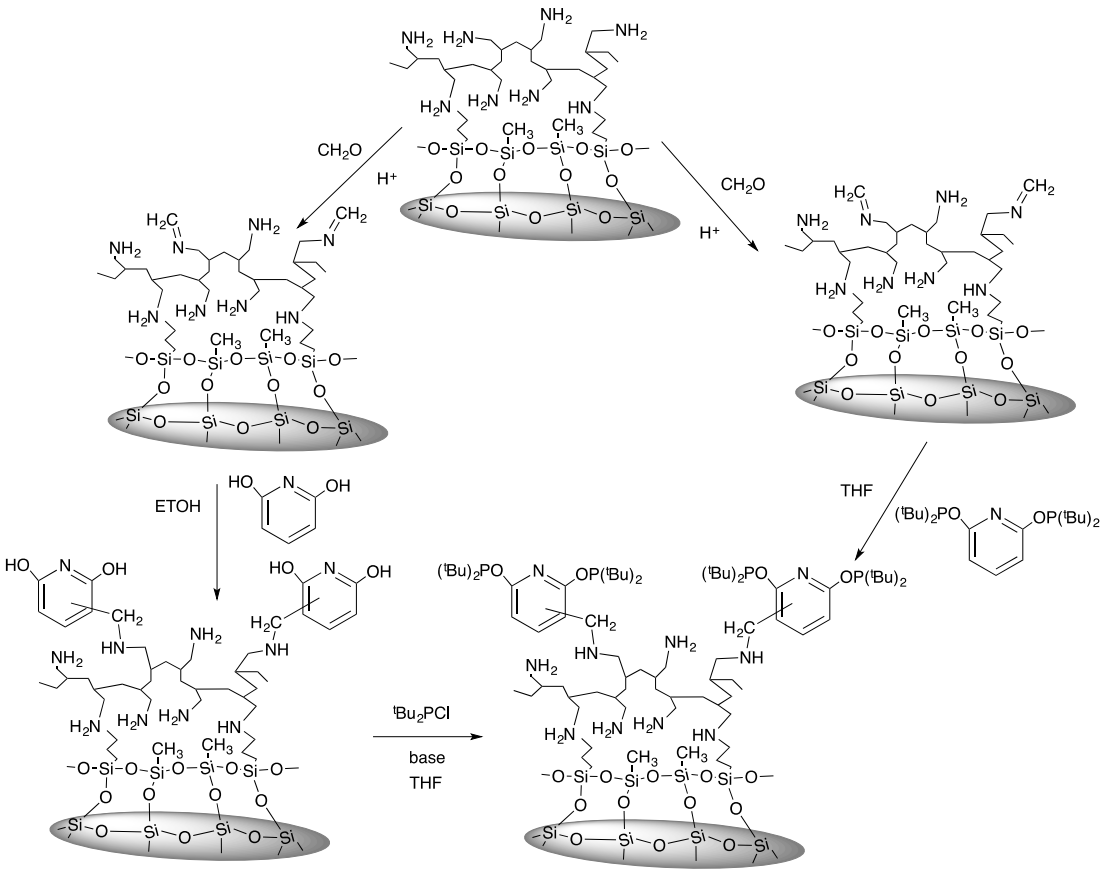

Scheme 3.3: The two methods for immobilization of the PONOP ligand on BP-1

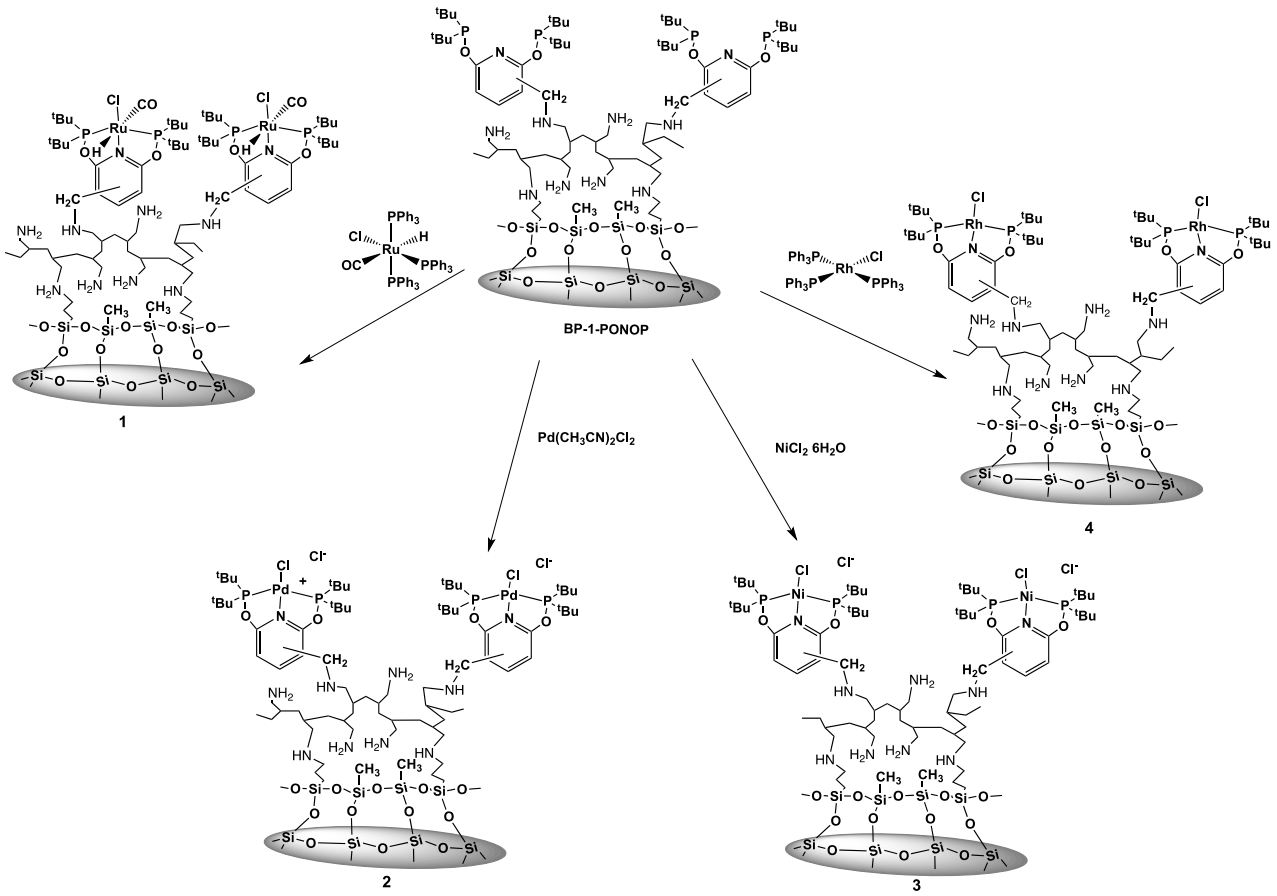

Scheme 3.4: Proposed structures for the immobilized PONOP pincer ligand complexes (conditions for addition of the metal compounds were the same as shown in Scheme 3.2)

3.3.1 Characterization of the immobilized PONOP pincer ligand and its complexes

Anchoring of the PONOP ligand on BP-1 by methods 2 & 3 is supported by the observation of resonance for the *tert*-butyl carbons at δ 33.3 and 23.4 and the pyridine carbons at δ 163 in the solid-state CPMAS ^{13}C NMR spectra. A broad resonance at δ 52.4 in the solid-state ^{31}P NMR spectra is also consistent with the loading of the ligand on BP-1. It should be noted that the resonances observed for CPMAS ^{31}P NMR spectra of the ligand PONOP on BP-1 are shifted significantly to up field compared to those observed in solution phase (δ 151.3).[20,87] This might be due to the electronic environment and nature of the surface of SPC-BP-1. Previous studies also showed significant up field chemical shifts for the pincer ligands and their complexes upon

immobilization on to solid supports.[61] However, CPMAS ^{13}C resonances of the immobilized PONOP ligand and their complexes showed a good agreement with the resonances found in solution (δ 163.1, pyridine ; δ 35.5, *tert*-butyl carbons).[87] The solid-state CPMAS ^{13}C NMR spectra of the ligand and the four complexes on BP-1 displayed additional resonances at δ -4 to -6 due to the methyl groups bound to Si from the methyl trichlorosilane used in the silanization of the starting silica gel. The resonances in the range of δ 40-50 are assigned to the CH and CH_2- groups of poly(allylamine) and the propyl anchors bound to starting BP-1.[69] The increase in N content after correction for the weight gain by methods 2 and 3 was too small to allow an accurate determination of the P/N ratio for the immobilized ligand.

The imine-functionalized BP-1 intermediate showed a characteristic $\nu_{C=N}$ at~ 1662cm^{-1} which is not observed in the spectra of pristine BP-1 (Figure B10 in Appendix B). Upon reaction with the PONOP ligand or the corresponding pincer complexes only a small decrease in intensity of this resonance was observed indicating only partial loading of the complexes. This was also supported by the results of the metal digestion study that indicate low loading of the complexes (Table 3.5). IR spectra of (PONOP)RuH(Cl)(CO) immobilized on BP-1 showed a metal carbonyl stretch at 1952 cm^{-1} for all three synthetic methods (Figure B3 in Appendix B). Given that the carbonyl stretch for this complex in solution is 1933 cm^{-1}. This indicates that there is a change in the electronic environment at the metal center of the complex upon attachment on BP-1.[87] This large change in the CO stretch could be due to the formation of hydrogen bonds between the hydride in this complex and an amine lone pair and/or an amine hydrogen. There is considerable evidence for both of these interactions in the solid-state structures of amine-substituted carbonyl hydride complexes.[89] However, it is difficult to predict the magnitude and direction of the frequency change, especially if both interactions are present. Metal carbonyl stretching frequency

of (PONOP)RuH(Cl)(CO)-n-butylamine (**6**) from the model solution experiment was found to be 1942 cm^{-1} (Figure B2 in Appendix B). This clearly indicates that attachment of a substituent in the PONOP ligand of the complex can cause a large shift of CO resonances in the IR spectra.[90] Observation of a CO stretch does support the formation of BP-1-(PONOP)RuH(Cl)(CO)(**1**) on BP-1 by the three methods. The IR spectra of the other three supported PONOP metal complexes (**2**), (**3**) & (**4**) were not informative except for the appearance of a small increase in the intensities of the band at ~2930cm^{-1} assignable to the C-H stretches and the observed residual imine at ~1662 cm^{-1}. The CPMAS ^{13}C and ^{31}P NMR of complexes **1-4** (Scheme 3.4) along with their elemental analyses are shown in Table 3.1 -3.4. Representative spectra are given in Figures 3A-10A in the Appendix A. For **1** made by method 1, the *tert*-butyl groups appear as relatively sharp resonances at δ 33.86 and 23.95 and the pyridine carbons appear as a broad resonance at δ 163.55 in the solid-state CPMAS ^{13}C NMR spectra. The IR data indicates that the unreacted C=N bond survives the conditions for binding the pincer ligand to the surface. The chemical shift of this bond is at ~ δ 161, and is observed prior to reaction with the pincer or pincer ligand complex but overlaps with the broad pyridine resonance. Interestingly, all the ^{13}C NMR spectra of the surface bound pincers show a sharp component at ~ δ 161 suggesting that the unreacted imine persists, consistent with the IR data (Figures A1, A3, A5, A7, A10 in Appendix A). The CH_2 groups attached to the amine of the polymer appear as relatively sharp resonances centered at δ 48.53. Solid-state CPMAS ^{31}P NMR of composite **1** exhibited a resonance at δ 58.05. Taken together, these data confirm the presence of (PONOP)RuH(Cl)(CO) on BP-1. The composite **1**, made by methods 2 and 3, showed the same overall pattern of resonances as for method 1 but had slightly different chemical shifts for tert-butyl groups. However, an additional resonance at δ 129.72 in the CPMAS ^{13}C spectrum of composite **1** is attributed to triphenyl phosphine and a resonance at δ 44.45 in the CPMAS ^{31}P

spectrum is also assigned to PPh_3. Apparently, triphenyl phosphine is entrained in the composite matrix during the reaction of the starting Ru complex with BP-1 loaded with PONOP. Repeated washings with toluene failed to remove all of the triphenyl phosphine, but did decrease the relative intensity of the ^{31}P NMR resonance at δ 44.45. The Cl analysis for method 1 gives a value of 0.076 mmol/g while the phosphorous analysis gives 0.060 mmol/g (P/Cl =0.79). Theoretically there should be twice as much phosphorous per gram but the higher Cl content can be attributed to residual chloride from unreacted chloropropyl groups after polyamine anchoring to the silica gel (Cl content in BP-1 is 0.21% or 0.060 mmol/g). However, for methods 2 and 3, the P/Cl ratio decreases to 0.35 and 0.38 suggesting the introduction of chlorine during the immobilization reaction, probably via dehydrohalogenation of the Ru complex by basic amine sites (Table 3.1). Dehydrohalogenation of a Ru-PONOP pincer complex to give a Ru^0 has been previously reported. [87]

Table 3.1: CPMAS ^{13}C and ^{31}P NMR data and Elemental Analyses for Composite **1**

Method	CPMAS ^{31}P NMR(δ)	CPMAS^{13}C NMR(δ ppm)	Elemental Analysis	P/Cl
1	58.1	163.5 (pyridine), 48.5 (CH_2 polyamine), 33.8 (*tert*-butyl), 23.9 (*tert*-butyl), -5.9 (Si-CH_3)	C 12.57 %, H 2.75%, N 2.42%, P 0.189%, Cl 0.27%	0.79
2	58, 44.4	163.2 (pyridine), 129.7 (PPh_3), 49.9 (CH_2 polyamine), 35.1 (*tert*-butyl), 25.4 (*tert*-butyl), - 4.7 (Si-CH_3)	C 14.16 %, H 2.94%, N 2.62%, P 0.502%, Cl 1.65%	0.35
3	58, 44.4	163.2 (pyridine), 129.7 (PPh_3), 49.9 (CH_2 polyamine), 35.1 (*tert*-butyl), 25.4 (*tert*-butyl), - 4.7 (Si-CH_3)	C 13.77 %, H 2.84%, N 2.52%,P 0.489%, Cl 1.50%	0.38

The formation of BP-1-[(PONOP)PdCl]Cl (**2**), by all three methods gave relatively sharp resonances at δ 33.3 and 23.2 for the *tert*-butyl carbons and a broad resonance at δ 162.9 for the pyridine moiety in the CPMAS ^{13}C NMR spectra. The resonances associated with the polymer

appear at δ 48.4, and a single broad peak is observed for ^{31}P NMR at δ 65. As for **1** the same pattern of resonances is observed for **2** made by method 2 or 3, but with small differences in chemical shifts (Table 3.2). The P/Cl ratio in **2** for method 1 is 0.61 when it should be 1, even lower than for **1**. Here, as for **1** the P/Cl ratio decreases by the about the same amounts going from method 1 to methods 2 and 3. In this case, however, formation of $PdCl_2$ amine complexes in competition with PONOP is probably the reason, even in the case of method 1.

Table 3.2: CPMAS ^{13}C and ^{31}P NMR data and Elemental Analyses for Composite **2**

Method	CPMAS^{31}P NMR (δ)	CPMAS ^{13}C NMR (δ)	Elemental Analyses	P/Cl
1	65	162.9 (pyridine), 48.4 (CH_2 polyamine), 33.3 (*tert*-butyl), 23.2 (*tert*-butyl), - 6.1(Si-CH_3)	C 11.79 %, H 1.89%, N 1.95%, P 0.161%, Cl 0.30%	0.61
2	65	162.9 (pyridine), 48.4 (CH_2 polyamine), 33.3 (*tert*-butyl), 23.2 (*tert*-butyl), - 6.1(Si-CH_3)	C 12.78%, H 2.31%, N 2.22%, P 0.495%, Cl 1.42%	0.38
3	65.1	162.8 (pyridine), 48.2 (CH_2 polyamine), 33.2 (*tert*-butyl), 23.1 (*tert*-butyl), - 6.3 (Si-CH_3)	C 12.18 %, H 2.10%, N 2.12%, P 0.483%, Cl 1.29%	0.44

As for **1** and **2,** BP-1-[(PONOP)NiCl]Cl (**3**) exhibited the usual resonances in the CPMAS ^{13}C NMR at δ 165.6 for the pyridine ring and δ 34.3 & 25.6 for the *tert*-butyl carbons respectively. The CPMAS ^{31}P NMR showed a resonance at δ 63.6. Overall this pattern is very similar to **2** and the chemical shifts were very similar for all three methods. However, in the case of **3** the resonances associated with the silanes are shifted slightly down-field. Although the actual P/Cl ratios are somewhat different, the overall pattern is similar to that of **2** with the amount of Cl for methods 2 and 3 increasing relative to 1 and indicating competitive formation of $NiCl_2$ amine complexes in competition with the complexes of PONOP.

Table 3.3: CPMAS ^{13}C and ^{31}P NMR data and Elemental Analyses for Composite **3**

Method	CPMAS $^{31}PNMR$ (δ)	CPMAS ^{13}C NMR (δ)	Elemental Analyses	P/Cl
1	63.6	165.6 (pyridine), 50.2 (CH_2 polyamine), 34.3 (*tert*-butyl), 25.6 (*tert*-butyl), - 4.6 (Si-CH_3)	C 11.68 %, H 2.12%, N 1.55, P 0.118%, Cl 0.21%	0.64
2	63.6	165.6 (pyridine), 50.2 (CH_2 polyamine), 34.3 (*tert*-butyl), 25.6 (*tert*-butyl), - 4.6 (Si-CH_3)	C 12.49 %, H 2.62%, N 1.95%, P 0.497%, Cl 1.10%	0.52
3	63.5	165.4 (pyridine), 50 (CH_2 polyamine), 34.1 (*tert*-butyl), 25.4 (*tert*-butyl), - 4.89 (Si-CH_3)	C 13.48 %, H 2.41%, N 1.95%, P 0.487%, Cl 1.08%	0.52

BP-1-(PONOP)RhCl (**4**) made by method 1 exhibited the expected *tert*-butyl resonance at δ 32.8 and 23.6 and also a broad resonance at δ 164.5 for the pyridine moiety and the usual resonances associated with the polymer. When made by methods 2 and 3, a resonance at δ 126.6 is assignable to the phenyl groups on triphenyl phosphine in the CPMAS ^{13}C NMR and the ^{31}P-NMR spectrum showed two resonances a major resonance at δ 60.5 ppm assigned to phosphorus atoms in the complex, and an additional resonance at δ 30.9 assignable to triphenyl phosphine. From this data, it would appear that triphenyl phosphine is trapped in the pores of the silica gel in the process of formation of **4** and **1** with methods 2 & 3. The composite **4** made by method 1 showed almost the same resonances for *tert*-butyl and pyridine carbons, however, the silane resonance is slightly shifted to downfield. The P/Cl ratio for the synthesis of **4** by method 1 is lower than for **1** even after correcting for the residual Cl due to chloropropyl silane. The reason for this not clear at this time. The P/Cl ratios observed for **4** made by methods 2 and 3 are higher than for **1,** indicating that there is more entrapped triphenyl phosphine than for **1**.

Table 3.4: CPMAS ^{13}C and ^{31}P NMR data and Elemental Analyses for Composite **4**

Method	CPMAS ^{31}P NMR (δ)	CPMAS ^{13}CNMR (δ)	Elemental Analyses	P/Cl
1	60.8	164 (pyridine), 49.4 (CH_2 polyamine), 34.4 (*tert*-butyl), 24.3 (*tert*-butyl), - 5.1 (Si-CH_3)	C 12.58 %, H 2.42%, N 1.53%, P 0.143%, Cl 0.24%	0.68
2	60.5, 30.9	164.5 (pyridine), 126.6 (PPh_3), 48.5 (CH_2 polyamine), 32.8 (*tert*-butyl), 23.6 (*tert*-butyl), - 6.3 (Si-CH_3)	C 14.89 %, H 2.83%, N 2.43%, P 0.516%, Cl 1.46%	0.41
3	60.5, 30.9	164.5 (pyridine), 126.6 (PPh_3), 48.5 (CH_2 polyamine), 32.8 (*tert*-butyl), 23.6 (*tert*-butyl), - 6.36 (Si-CH_3)	C 14.75 %, H 2.73%, N 2.13%,P 0.508%, Cl 1.43%	0.40

Table 3.5: Loading of Metal or Complex on BP-1 (mmol of ligand or complex / g of BP-1)

Composite	Method of loading	mmol complex /g BP-1by AAS	mmol ligand/g BP-1 from P analysis	RSD for metal analysis (±%)	% N sites loaded
1	Method 1	**0.039**	**0.031**	**2.50**	**2.44**
	Method 2	**0.068**	**0.081**	**1.80**	**4.25**
	Method 3	**0.045**	**0.079**	**2.40**	**2.81**
2	Method 1	**0.081**	**0.026**	**0.15**	**5.06**
	Method 2	**0.244**	**0.080**	**0.05**	**15.25**
	Method 3	**0.230**	**0.078**	**0.01**	**14.38**
3	Method 1	**0.014**	**0.019**	**0.89**	**0.88**
	Method 2	**0.139**	**0.080**	**0.35**	**8.69**
	Method 3	**0.069**	**0.078**	**1.20**	**4.31**
4	Method 1	**0.015**	**0.023**	**0.33**	**0.94**
	Method 2	**0.042**	**0.083**	**1.20**	**2.63**
	Method 3	**0.039**	**0.082**	**1.40**	**2.44**

The elemental analyses reported in Tables 3.1-3.4 leave a lot to be desired with regard to determining actual pincer complex loading in light of the side reactions that give rise to excess Cl in all cases, even to using method 1 and the presence of excess phosphine in the case of **4** and **1** with method 2 & 3. However, a comparison of the metal loading with the phosphorous analysis should considerably clarify the situation. The results of the metal analysis obtained by digestion

of **1** – **4** along with the calculated metal loading and its comparison with phosphine loading are given in Table 3.5.

Comparing %P from elemental analysis with the % Ru from metal analysis for **1**, made by methods 1 and 2, the loadings of **1** are in reasonable agreement, being 0.031 mmol/g and 0.039 mmol/g for method 1 and 0.068 and 0.081 for method 2, for the two analytical methods (Table 3.5). In the case of **3** both methods 1 and 3 give reasonable agreement between the results of metal digestion and phosphorus analysis, being 0.014 and 0.019 mmol/g and0.069 mmol/g and 0.078 mmol/g, respectively (Table 3.5). However, the data for method 2 shows poor agreement between values for phosphorus and metal analysis. All three methods used for composite **2** gave very high Pd values relative to the phosphorus content. This is consistent with the high chloride content and points to the competitive formation of $PdCl_2$ polyamine complexes. In all three methods, the ratio of pincer ligand to total Pd is ~1:3. However, even the high Cl content cannot account for all the Pd, suggesting the formation of Pd nanoparticles, as has been previously reported for Pd salts on BP-1[64,71] in addition to the formation of $PdCl_2$-amine complexes. Interestingly, only method 2 for complex **3** shows a significant excess of metal. This can be accounted for by the formation of $NiCl_2$ polyamine complexes if one assumes that all the pincers are complexed to Ni (0.14 mmol Ni/g total 0.08 mmol/g for pincer, 0.31 mmol/g total Cl, 0.16 needed for pincer, leaving 0.15 mmol/g excess chloride and 0.060 excess nickel that requires 0.12 Cl, adding the 0.060 mmol/g for residual chloropropyl gives a good Cl mole balance for **3**). Composite **4** yielded low loading by method 1, but with comparable values between P and Rh loading. Methods 2 and 3 showed high phosphorus values as a result of entrained triphenyl phosphine that was detected by CPMAS ^{13}C and^{31}P NMR (Table 3.1and 3.4). Overall methods 2 and 3 provide higher metal loading as a result of better loading of the ligand to the surface, but there was evidence of side reactions that

resulted in the formation of metal-halide-polyamine complexes in the case of 2 and 3 and metal nanoparticles in the case of **2**. Thus, method 1 gives cleaner results at the expense of higher loading relative to methods 2 and 3.[90]

1 g of BP-1 contains 1.6 mmol of nitrogen (N) sites based on its elemental analysis.[71,72] One could expect higher loading of the pincers considering the availability of amine densities on the BP-1 surface. In fact, all amine functionality might not be readily accessible to bind with metal pincers due to the steric hindrance of the bulky pincer complexes. The % of N sites on BP-1 occupied with four pincer complexes by the three methods has been estimated from the ratio of mmol metal/g to the mmol N/g. The overall nitrogen site occupancy by actual pincer-metal complexes is in the range of 1− 4% (Table 3.5). The higher values reported in Table 3.5 for **2** are due to competitive metal loading via halide-polyamine complexes and/or Pd nanoparticles. The lower amounts (1−4%) should be sufficient for catalytic studies based on the data from catalysis.[91,92]

The impact of immobilization of the PONOP metal pincer complexes on surface area, structure and porosity of the silica polyamine composite, BP-1, was assumed to be negligible, particularly considering the extent of loading of the pincers (<0.3 mmol complex/g BP-1) (Table 3.5). Our previous studies on covalent tethering of luminescent Ru complexes on BP-1 with similar loading did not show any measurable changes in the porosity and structure of the composite surface.[71,77]

3.3.2 Determination of the regiochemistry of the Mannich reaction between PONOP and n-butyl amine in solution

In the first step of the model solution reaction, n-butyl amine was treated with 38% formaldehyde solution, which yielded the imine intermediate. Then the PONOP ligand was added to the imine intermediate in the second step, which formed a mixture of isomeric products.

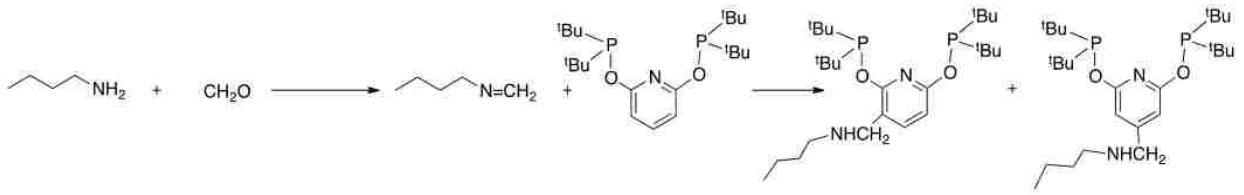

1.0 (*meta*-isomer, **5i**) 0.30 (*para*-isomer, **5ii**)

Scheme 3.5: Reaction between PONOP and n-butyl amine in solution

^{31}P NMR spectra of the product mixture displayed three resonances (Figure 3.1). A broad resonance at δ 117.13 integrated in an approximately 1:1 ratio with a resonance at δ 112.46. The broadness of the resonance at δ 117.13 is attributed to hindered rotation of the *tert*-butyl groups of one of the phosphorus atoms of the PONOP ligand as a result of steric crowding with the n-butyl group in the *meta*-position. It represents the partial averaging of different conformations of the di-*tert*-butyl group. As expected, the *para*-isomer exhibits only one resonance at δ 118.62 and integrates in a ratio of 0.3:1 with the *meta*-isomer resonances.

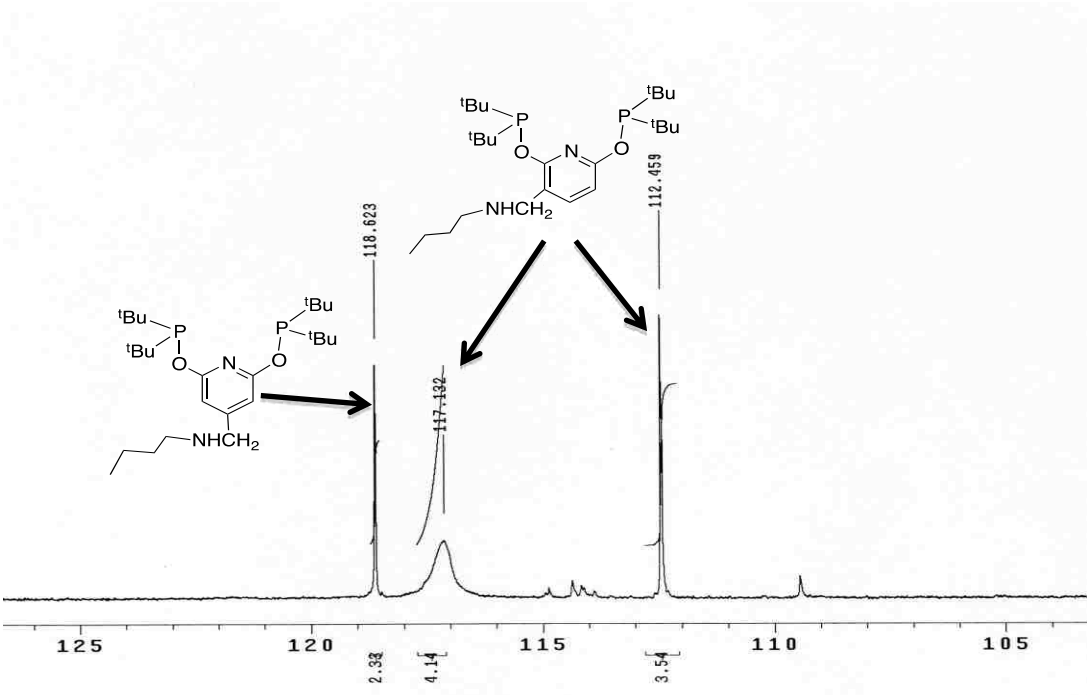

Figure 3.1: ^{31}P NMR spectrum of the isomers formed from n-butyl amine reaction with PONOP.

3.3.3 Determination of the regiochemistry of the Mannich reaction between (PONOP)RuH(Cl)(CO) and n-butyl amine in solution

Given that using the preassembled metal complex proved to be the best way to bind the pincer complexes to the SPC surface,[90] we thought it would be relevant to repeat the model solution reaction sequence with (PONOP)RuH(Cl)(CO). In this case Ru-PONOP complex was combined with the imine intermediate in the second step (Scheme 3.6). The results are remarkably similar to the model solution reaction between the PONOP ligand and n-butylamine. Again, two isomers are obtained in a 0.3:1 *para*-to-*meta* ratio and in very similar yield (57% for Ru(PONOP) and 60% for PONOP) (Figure 3.1 & 3.2). This illustrates that the presence of the metal has little influence on the regiochemistry and the efficiency of the Mannich reaction with the PONOP system. However, the broadness of one of the ^{31}P resonances seen in the PONOP reaction is not observed in the reaction of the Ru-PONOP with n-butyl amine. This is not surprising in light of the geometry changes of the (^{t}Bu)$_2$P groups relative to the meta-n-butyl amine that occur on coordination of Ru^{2+}. It is also worthy of noting that the ^{31}P chemical shifts of the Ru-PONOP resonances in solution are very similar to those observed in the solid state being δ 60.57, 58.06, 57.43 (Table 3.1). ^{1}H NMR spectrum of complex **6** shows many resonances which are difficult to interpret. These could be due to the formation of isomeric products as well as the presence of a trace amount of unreacted starting materials such as imines, amines and formaldehydes (Figure A23 in Appendix A). The CO stretching frequency of the complex **6** is observed at 1942 cm^{-1} while the unsubstituted complex shows a CO stretching frequency of 1933 cm^{-1} (Figures B1 & B2 in Appendix B). This clearly indicates the sensitivity of the CO stretch to the environment. Taken together with the solution ^{31}P NMR data, it provides further proof that the pincer ligand structure is conserved on grafting to the SPC surface.

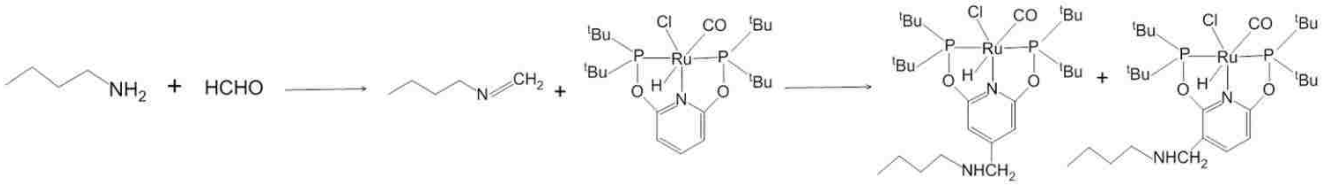

0.3 (*para*-isomer, **6i**) 1 (*meta*-isomer, **6ii)**

Scheme 3.6: Reaction between (PONOP)RuH(Cl)(CO) and n-butyl amine in solution

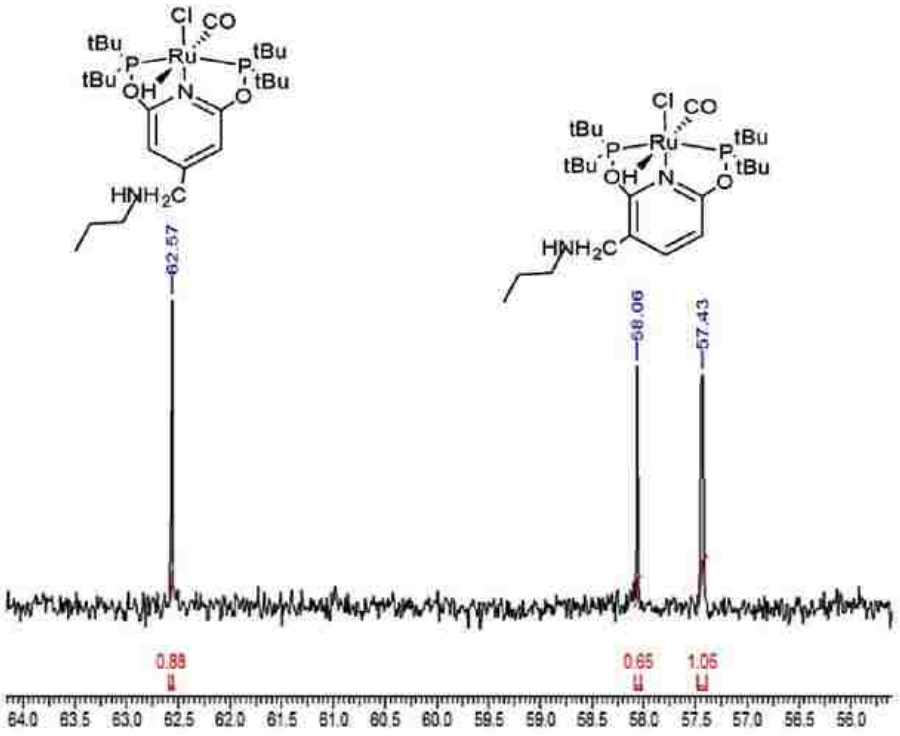

Figure 3.2: ^{31}P NMR spectrum of the isomers (**6**) formed from n-butylamine reaction with (PONOP)RuH(Cl)(CO)

Chapter 4

Synthesis, characterization, and catalytic study of PNN pincer complex of ruthenium on BP-1

4.1 Introduction

4.1.1 Pyridine-based metal pincer complexes and their catalytic reactivity

In most chemical processes involving homogeneous catalysis by metal complexes, the role of the ligand is only to impart or control the critical properties of the metal center of the complex. Ligands themselves do not participate or become directly involved in catalytic reaction processes in bond-making and bond breaking with the substrate compounds. Pincer ligands are exceptional compounds which actively cooperate with the metal center of the catalyst complex in bond activation processes in different chemical transformations.[45-53] They are bulky, electron-rich species that can stabilize unsaturated metal complexes by coordinating with metal centers in a synergistic manner and participate in unusual bond activation and catalytic processes. Their interplay facilitates chemical transformation processes. Pyridine- and acridine- based pincer ligands and their metal complexes undergo bond-breaking and bond-making processes by the deprotonation of a pyridinyl methylenic proton, which leads to the aromatization and dearomatization of the ligand systems.[45-53] In this process, a base is required to extract a proton from the pincer arms of the ligand structures. These dearomatized pincer complexes function as active catalyst and can potentially activate different types of chemical bonds (H–Y, Y=H, OH, OR, NH_2, NR_2, C) by the efficient cooperation between the metal and the pincer ligand, thereby regaining aromatization (Scheme 4.1).[93,94] It is interesting to note that in this overall process there is no change in the oxidation states of the metal center.[65,95,96]

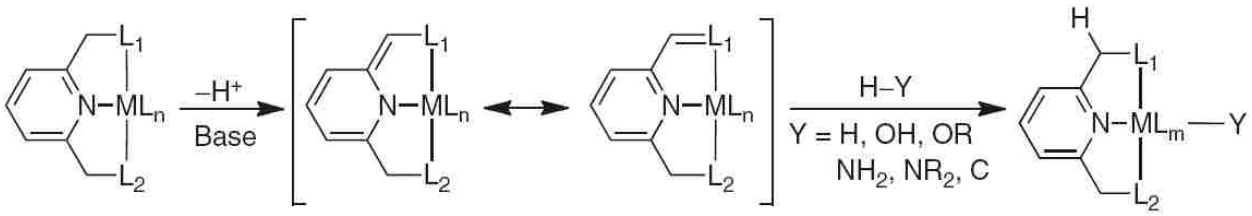

Scheme 4.1: Metal–pincer ligand interaction and cooperation in the aromatization–dearomatization processes of pyridine and acridine based pincer metal complexes.[93,94]

4.1.2 Catalytic reactivity of (PNN)RuH(Cl)(CO) pincer complex

(PNN)RuH(Cl)(CO) pincer complex was originally discovered by D. Milstein's research group in 2005.[41] It was synthesized by the reaction of $RuH(Cl)(CO)(PPh_3)_3$ with the pincer ligand PNN (2-(di-*tert*-butylphosphinomethyl)-6-diethylaminomethyl)pyridine.[41] In the structure of the complex, three donor atoms (two nitrogen and one phosphorus) from PNN ligands coordinate to the metal center (Figure 4.1). Since 2005, the complex has shown outstanding catalytic performance in a wide range of chemical transformations which include: dehydrogenation of alcohols to the corresponding esters,[41] hydrogenation of esters to alcohols,[65,97] and amide formations from alcohols and amines.[52,65] Our high level of interest in PNN pincer complex systems for immobilization purpose was largely due to their interesting catalytic reactivity in various chemical transformations.[45-53]

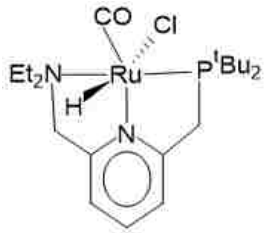

Figure 4.1: Structure of (PNN)RuH(Cl)(CO) [{2-(di-*tert*-butylphosphinomethyl)-6-(di-ethylaminomethyl)}pyridine]ruthenium hydrido chloro carbonyl

One of the most fundamental and important reactions in organic chemistry is esterification.[41] Most of the reaction systems for ester formations require the use of stoichiometric amounts of acid or base promoters and coupling agents, and involve reactive intermediates derived from alcohols or acids (Schemes 4.2) which lead a large amount of waste being generated.

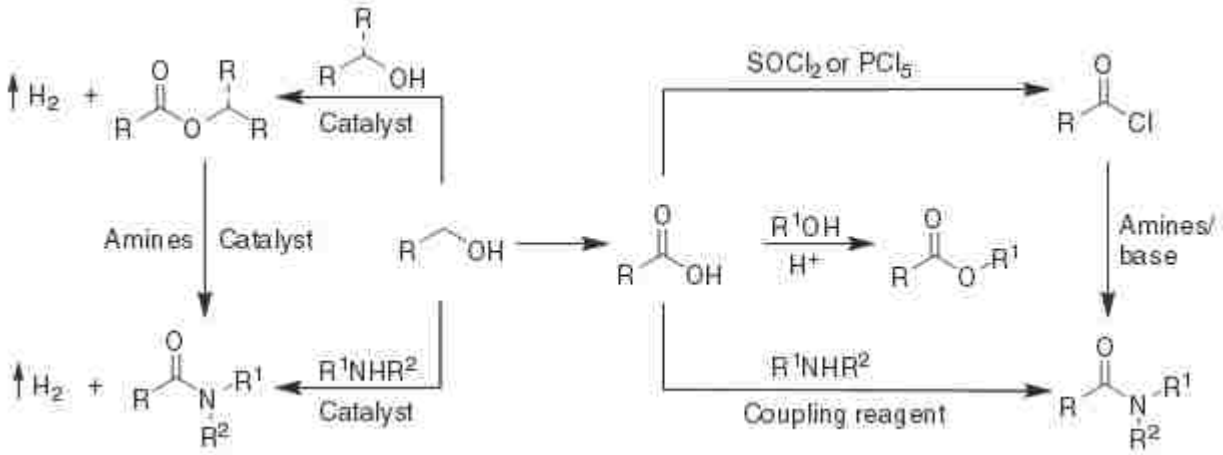

Scheme 4.2: Synthesis of esters and amides: conventional versus catalytic synthetic methods.[94]

The common method utilized for making an ester involves the reaction between an acid or acid derivatives and an alcohol.[94] Formation of esters without the use of acid is relatively rare. However, an attractive alternative route for synthesizing ester compounds is the direct catalytic transformation of alcohols to esters by the dehydrogenative coupling of alcohols which would be environmentally friendly and atom-efficient.[41] An interesting and exceptional approach in homogeneous catalytic systems is the application of metal pincer complexes to synthesize esters directly from alcohols.[41] PNN [(2-(di-*tert*-butylphosphinomethyl)-6-diethylaminomethyl)pyridine] pincer complex of Ru has been shown to be an exceptional catalyst for the efficient and selective dehydrogenation of primary alcohols to esters with the liberation of hydrogen in high turnover numbers under relatively mild and neutral conditions.[41,65]

In 2005 David Milstein reported the dehydrogenative coupling of alcohols to esters and hydrogen catalyzed by (PNN)RuH(Cl)(CO) in solution (Table 4.1).[41] The general reaction of the conversion of alcohols to esters and hydrogen catalyzed by (PNN)RuH(Cl)(CO) is given below:

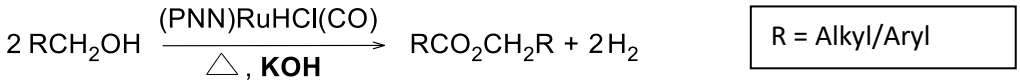

Scheme 4.3 : General reaction- dehydrogenative coupling of alcohols to esters and H_2 catalyzed by (PNN)RuH(Cl)(CO)

Table 4.1: Alcohol dehydrogenation reactions catalyzed by (PNN)RuH(Cl)(CO) in solution[41]

Catalyst (PNN)RuH(Cl)(CO)	KOH (equiv)	Alcohol	Temp (°C)	Time (h)	Total alcohol conversion (%)	Yield (%) Ester	Yield (%) Aldehyde
0.1 mol%	1	1-hexanol	157	24	90.3	90	0.3
,,	0	1-hexanol	157	24	0	0	0
,,	1	benzyl alcohol	115	72	100	99.5	0.5
,,	0	Benzyl alcohol	115	72	0	0	0

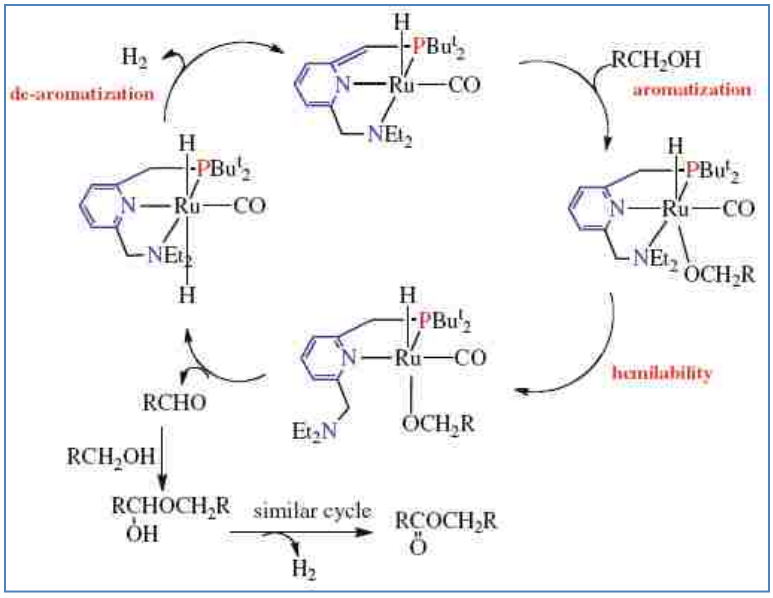

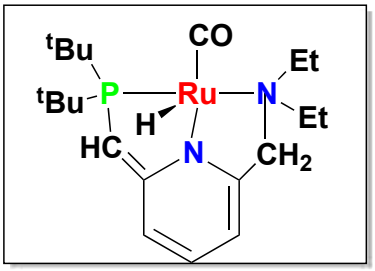

Active Catalyst

a **b**

Scheme 4.4 : (a) Postulated mechanism for dehydrogenative coupling of alcohols to esters catalyzed by (PNN)RuH(Cl)(CO). (b) Active catalyst formed by the deprotonation of pincer arm by KOH.[41]

From the Table 4.1 it is clear that an external base was required in the catalytic reaction system to covert alcohols to esters. No reaction took place in the absence of a base. The function of the base was to deprotonate the pincer arm to generate dearomatized (PNN-)RuH(CO) (Scheme 4.4) which worked as an active catalytic species in the reaction systems.[41]

We investigated the dehydrogenative coupling of alcohol reaction systems on BP-1 surfaces with immobilized (PNN)RuH(Cl)(CO). We here hypothesize that the amine functionality on the BP-1 surface (Scheme 1.1) might satisfy the requirement for a base needed for the formation of active pincer catalyst on BP-1 surface upon immobilization of the pincer complex on BP-1.

4.2 Experimental

4.2.1 Experimental procedure for immobilization of (PNN)RuH(Cl)(CO) on BP-1

(PNN)RuH(Cl)(CO) was immobilized on BP-1 by a two-step Mannich reaction following the procedures similar to those described in the section 3.2.2.[90] 5g of BP-1 (containing 1.6 mmol N/g) was mixed with a reagent solution of 25 mL aqueous HCHO (38%, 345 mmol) and 0.5 mL glacial acetic acid (17.4M, 8.74 mmol) in a 250 mL flask equipped with an overhead stirrer. The suspension was stirred for 3–4 hours at room temperature yielding the surface-bound imine intermediate. The resulting composite was filtered and then washed several times with 95% ethanol, and then dried under vacuum overnight (yield: 5.19 g). 500 mg (0.885 mmol) of (PNN)RuH(Cl)(CO)[41] and 25 mL of distilled 1,4-dioxane were added to 5g of dried imine intermediate in a three-necked round bottom flask equipped with an overhead stirrer and a condenser. The mixture was degassed by applied vacuum (30 mmHg). The reaction mixture was refluxed overnight with stirring under N_2. The composite product was then filtered and washed four times with 1,4-dioxane, four times with acetone, and four times with CH_2Cl_2 and then dried overnight under high vacuum yielding 5.30 g of BP-1-(PNN)RuH(Cl)(CO) (**7**) product. Elemental analysis: C 12.74%, H 2.95%, N 2.84%, P 0.11%, Cl 2.30%. Solid-state CPMAS ^{13}C NMR, δ (ppm): 162.4 (pyridine), 33.5 (CH_2 polyamine), 56.7 (ethyl), 23.7 (*tert*-butyl), 15.1 (*tert*-butyl), -6.0 (Si-CH_3). CPMAS ^{31}P NMR, δ (ppm): 49.5. IR spectra (KBr pellet): 1948 cm^{-1} (s) (ν CO).

4.2.2 Experimental procedure for model solution reaction between (PNN)RuH(Cl)(CO) and n-butyl amine

200 µL (2 mmol) of n-butyl amine was added to 200 µL (38%, 2 mmol) of HCHO solution. 20 µL (0.35 mmol) of glacial acetic acid (17.4 M) was added and the reaction mixture was stirred overnight at room temperature under N_2. The resulting imine intermediate was extracted with

distilled CH_2Cl_2 and then anhydrous $Na_2SO_4$was added to remove any trace H_2O. Solvent was then removed by rotary evaporation and the product was dried under high vacuum. 0.9 g (2 mmol) of (PNN)RuH(CO)Cl was combined with the dried imine intermediate in 10 mL distilled THF. The reaction was carried out at 66°C for 24 hours under N_2. Solvent was removed by rotary evaporation and the resulting product was washed with pentane and CH_2Cl_2. The product was purified by column chromatography eluting with the mixture of THF and hexane and then dried under high vacuum (yield: 0.72g, 1.26 mmol, 63%). ^{31}P NMR (Acetone-d_6): δ 89.79 (s), 90.36 (s), and 96.97 (s). ^{1}H NMR (Acetone-d_6) (three isomers) (δ ppm): 0.77 (t, J_{H-H}= 4.0 Hz, 3H, C*H*$_3$), 0.80 (t, J_{H-H}= 8.0 Hz, 3H, C*H*$_3$), δ 1.56 (t, J_{H-H}= 8.0 Hz, 3H, C*H*$_3$), δ 1.35 (t, J_{H-H}= 4.0 Hz, 3H, C*H*$_3$), δ 3.06 (t, J_{H-H}= 8.0 Hz, 3H, C*H*$_3$), 3.48 (m, 1H, N(C*H*HMe)$_2$), 3.31(m, 1H, N(C*H*HMe)$_2$), 1.22 (sextet, J_{H-H}= 8.1 Hz, 2H, C*H*$_2$), 1.74 (s, 18H, P-C(C*H*$_3$)$_3$), 5.05 (s, 2H, C*H*$_2$), 4.74 (s, br, 1H, N-*H*), 7.97 (s, 2H, *m*-pyridine, *para*-isomer), 7.58 (dd, J_{H-H}= 4.0 Hz, 2H, pyridine, *meta*-isomer),1.42 (pent, J_{H-H}= 8.1 Hz, 2H, C*H*$_2$), 3.59 (d, J_{H-H}= 12.0 Hz, 2H, C*H*$_2$), -15.43 (d, J_{PH} = 28Hz, 1H, Ru-H). IR (ATR): 1931 cm^{-1} (s)(νCO), 2016 cm^{-1}(s) (νRu−H).

4.2.3 Experimental procedure for the deprotonation of (PNN)RuH(Cl)(CO)-n-butyl amine

58 mg (0.1 mmol) of Ru-PNN-n-butyl amine was dissolved in THF (5mL). 11.2 mg (0.1 mmol) of KO^{t}Bu was added at -31°C and the mixture was stirred for 7 hours and then filtered. The volume of the deep-red filtrate was reduced to 0.5 mL under vacuum and 5 mL pentane was added to precipitate brown-red product. The product (**9**) was then separated and washed three times with 2 mL pentane and dried under vacuum (37 mg, 0.07 mmol, 69%). ^{31}P NMR (Acetone-d_6): δ 97.07 (s), 109.73 (s), and 109.78 (s). ^{1}H NMR (δ ppm) (Acetone-d_6) (three isomers): 0.78 (t, J_{H-H}= 4.0 Hz, 3H, C*H*$_3$), 3.07 (t, J_{H-H}= 4.0 Hz, 3H, C*H*$_3$), 4.17 (t, J_{H-H}= 8.0 Hz, 3H, C*H*$_3$), 1.22 (sextet, J_{H-H}= 8.0 Hz, 2H, C*H*$_2$), 0.78 (sextet, J_{H-H}= 4.0 Hz, 2H, C*H*$_2$), 1.56 (m, 1H, N(C*H*HMe)$_2$), 2.12(m, 1H,

N(C*H*HMe)$_2$), 1.96 (s, 2H, CH_2), 1.67(s, 2H, CH_2), 1.92 (vt, J_{P-H} = 4.0 Hz, 9H, P-C(CH_3)$_3$), 1.93 (vt, J_{P-H} = 4.0 Hz, 9H, P-C(CH_3)$_3$), 5.27 (s, 1H, =CHP), 5.27 (s, br, 1H, N-*H*), 7.57 (dd, J_{H-H}= 8.0 Hz, 2H, pyridine, *meta*-isomer), -16.6 (d, J_{P-H} = 16Hz, 1H, Ru-H). IR (ATR): 1929cm^{-1} (s) (νCO), 2041cm^{-1}(s) (νRu−H).

4.2.4 Experimental procedure for the catalytic dehydrogenation of 1-hexanol with deprotonated (PNN-)RuH(CO)-n-butyl amine

The complex (PNN-)RuH(CO)-n-butyl amine (**9**) (0.01 mmol) was dissolved in 1-hexanol (10 mmol) in a small round bottom flask which was then equipped with a condenser. The solution was heated at 157°C under an argon flow for 56 hours. Conversion of 1-hexanol was measured at different time intervals by GC using an HP 5 column on an Agilent 6890N GC-MS system. 1-Hexanol conversions: 28% (after 2.5 hours reaction), and 66% (after 56 hours reaction)

4.2.5 Experimental procedure for the catalytic dehydrogenation of 1-hexanol with deprotonated (PNN-)RuH(CO)-n-butyl amine in presence of toluene

The complex (PNN-)RuH(CO)-n-butyl amine (**9**) (0.01 mmol) was dissolved in 1-hexanol (10 mmol) in a small round bottom flask and 2 mL of toluene was added. The flask was then equipped with a condenser and the system was degassed by an applied vacuum. The solution was refluxed under argon flow for 56 hours. Conversion of 1-hexanol was measured at different time intervals by GC using an HP 5 column on an Agilent 6890N GC-MS system. 1-Hexanol conversions: 23 % (after 2.5 hours reaction), and 59% (after 56 hours reaction)

4.2.6 Experimental procedures for alcohol dehydrogenation reactions catalyzed by immobilized (PNN)RuH(Cl)(CO) on BP-1 in the absence of a base and with KOH

200 mg of BP-1-Ru-PNN (**7**) (0.007 mmol catalyst on BP-1) was placed in a small round-bottom flask. 21 mmol of alcohol was added. In the case of 1-hexanol, 400 mg of BP-1-Ru-PNN

was added into 35 mmol of alcohol. The mixture was degassed by an applied vacuum. The mixture was then heated with slow stirring under an inert atmosphere of argon. The reaction mixture was cooled to room temperature and the composite catalyst was separated by filtration. The resulting liquid product mixture was analyzed by GC-MS using an HP 5 column on an Agilent 6890N GC-MS system. Total alcohol conversion and reaction conditions in each of the alcohols catalysis are summarized in Table 4.2.

Table 4.2: Conversion of alcohol to corresponding esters and hydrogen with immobilized (PNN)RuH(Cl)(CO) on BP-1 in the absence of a base and with KOH.

Alcohol	Base (mmol)	Catalyst / Alcohol ratio (mmol)	Reaction Temp (°C)	Reaction Time (Hours)	Total alcohol conversion (%)	Turnover frequency (Hour $^{-1}$)
1-Hexanol	-	0.02/50	157	56	50 (49% Hexyl hexanoate and 0.5% 1-Hexanal) Range: 49-51	22
	0.02	0.02/50	157	56	62 (61% Hexyl hexanoate and 0.8% 1-Hexanal) Range: 61-63	28
1-Heptanol	-	0.01/30	176	48	52 (51% Heptyl heptanoate and 1% 1-Heptanal) Range: 51-52	33
	0.01	0.01/30	176	48	64 (62% Heptyl heptanoate and 2% 1-Heptanal) Range: 63-65	40
Benzyl alcohol	-	0.01/30	178	60	48 (38% Benzyl benzoate and 10% Benzaldehyde) Range: 47-49	24
	0.01	0.01/30	178	60	55 (43% Benzyl benzoate and 12% Benzaldehyde) Range: 54-57	28
2-octanol	-	0.01/30	178	48	53% 2-octanone Range: 52-53	33
	0.01	0.01/30	178	48	58% 2-octanone Range: 57-60	36

4.2.7 Experimental procedures for alcohol dehydrogenation reactions catalyzed by immobilized (PNN)RuH(Cl)(CO) on BP-1 in the presence of solvent

4.2.7.1 Reaction protocols for 1-hexanol catalysis with immobilized (PNN)RuH(Cl)(CO) on BP-1 (**7**) in the presence of toluene

400 mg of BP-1-Ru-PNN (**7**) (0.014 mmol catalyst on BP-1) and 35 mmol of 1-hexanol were mixed in a small round-bottom flask. 2mL toluene was added. The mixture was degassed by an applied vacuum. The mixture was then refluxed with slow stirring under an inert atmosphere of argon for 56 hours. The reaction mixture was cooled to room temperature. The liquid product mixture and the catalyst were separated by filtration. Formation of hexyl hexanoate was determined by GC an HP 5 column on an Agilent 6890N GC-MS system. Total 1-hexanol conversion: 0 %

4.2.7.2 Reaction protocols for 1-hexanol catalysis with immobilized (PNN)RuH(Cl)(CO) on BP-1 (**7**) in the presence of toluene and KOH

400 mg of BP-1-Ru-PNN (**7**) (0.014 mmol catalyst on BP-1) and 0.014 mmol KOH were suspended into 35 mmol of 1-hexanol in a small round-bottom flask. 2mL toluene was added. The flask was equipped with a water condenser. The mixture was degassed by an applied vacuum. The mixture was then refluxed with slow stirring under an inert atmosphere of argon for 56 hours. The reaction mixture was cooled to room temperature. The liquid product mixture and catalyst were separated by filtration. Formation of hexyl hexanoate was determined by GC-MS using an HP 5 column on an Agilent 6890N GC-MS system. Total 1-hexanol conversion: 0 %

4.2.7.3 Reaction protocols for 1-heptanol catalysis with immobilized (PNN)RuH(Cl)(CO) on BP-1 (**7**) in the presence of dichlorobenzene

200 mg of BP-1-Ru-PNN (**7**) (0.007 mmol catalyst on BP-1) and 21 mmol of 1-heptanol were mixed in a small round-bottom flask. 2mL dichlorobenzene was added. The mixture was degassed by an applied vacuum. The mixture was then refluxed with slow stirring under an inert atmosphere of argon for 48 hours. The reaction mixture was cooled to room temperature. The liquid product mixture and catalyst were separated by filtration. Formation of heptyl heptanoate and 1-heptanal was determined by GC using an HP 5 column on an Agilent 6890N GC-MS system. Total 1-heptanol conversion: 33%. Heptyl heptanoate: 32%. 1-heptanal: 1%

4.2.7.4 Reaction protocols for 1-heptanol catalysis with immobilized (PNN)RuH(Cl)(CO) on BP-1 (**7**) in the presence of dichlorobenzene and KOH

200 mg of BP-1-Ru-PNN (**7**) (0.007 mmol catalyst on BP-1) and 0.007 mmol KOH were suspended into 21 mmol of 1-heptanol in a small round-bottom flask. 2mL dichlorobenzene was added. The flask was equipped with a water condenser. The mixture was degassed by an applied vacuum. The mixture was then refluxed with slow stirring under an inert atmosphere of argon for 48 hours. Reaction mixture was cooled to room temperature. Liquid product mixture and catalyst were separated by filtration. Formation of heptyl heptanoate and 1-heptanal was determined by GC using an HP 5 column on an Agilent 6890N GC-MS system. Total conversion: 40%. Heptyl heptanoate: 38% . 1-heptanal: 2%

4.2.8 Experimental procedures for cycle study in alcohol dehydrogenation reactions with immobilized (PNN)RuH(Cl)(CO) on BP-1 (7)

4.2.8.1 Reaction protocols for conversion of alcohols to corresponding esters and hydrogen with the solid-liquid method (Slow stirring the mixture of catalyst and alcohol) (No base used)

In the solid-liquid method, alcohols and BP-1-Ru-PNN (**7**) mixtures were stirred slowly with a small magnetic stir bar under an inert atmosphere of argon. Temperature and other reactions conditions were described in Table 4.2 and section 4.2.6. When the reaction was stopped, the composite catalyst and liquid product mixture was separated by filtration and then the catalyst was washed with acetone, toluene, and CH_2Cl_2 and dried under high vacuum. The liquid product mixtures were analyzed by GC using an HP 5 column on an Agilent 6890N GC-MS system. The dried BP-1-Ru-PNN (**7**) was used for the next cycle and the overall procedure was repeated. Yields and conversion of alcohols to corresponding esters in each of the successive cycles are given in Table 4.5-4.10.

4.2.8.2 Reaction protocols for conversion of alcohols to corresponding esters and hydrogen with solid-vapor method (passing the alcohol vapor over the catalyst bed) (No base used)

The ratio of the catalyst, BP-1-Ru-PNN (**7**) to alcohol used in the new method was similar to those applied in the solid-liquid method. In the solid-vapor method, the required amount of composite catalyst (as mentioned in sections 4.2.6 and Table 4.2) was placed in a glass frit. The frit was then equipped with a small round bottom flask containing the appropriate amount of alcohols (sections 4.2.6). A water condenser was placed on the top of the frit. The whole system was then degassed by an applied vacuum. Alcohol vapor was created by heating the alcohol in the round bottom flask and was then passed through the composite catalyst bed. The alcohol vapor condensed as it moved up from the catalyst bed, and then back to the round bottom flask, through the catalyst bed, and the process was repeated as the reaction proceeded. After the reaction was over, the system was cooled to room temperature and the apparatus was disassembled. The liquid product mixture was collected and then analyzed by GC using an HP 5 column on an Agilent 6890N GC-MS system. The composite catalyst was washed with acetone, toluene, and CH_2Cl_2 and dried under high vacuum. The dried composite catalyst was used for next cycle and the overall

procedure was repeated. Yields and conversion of alcohols to corresponding esters are given in the Table 4.5-4.10. Solid state CPMAS NMR data and FT-IR data on BP-1-Ru-PNN (7) after catalysis are given in Table 4.3. The results of elemental analysis and metal digestion study on BP-1-Ru-PNN (7) after catalysis are shown in Table 4.4.

Table 4.3: Characterization of BP-1-Ru-PNN (**7**) after catalysis by solid state NMR, FT-IR, metal digestion, and elemental analysis using solid-vapor method

Alcohol catalysis	Solid-state CPMAS ^{13}C NMR, δ (ppm)	IR spectra (KBr pellet) (ν CO)
Cycle 1	162.5 (pyridine), 62.3 (Ethyl), 31.5 (CH_2 polyamine), 22.1 (*tert*-butyl), 13.7 (*tert*-butyl), - 4.3 (Si-CH_3).	1944 cm^{-1}
Cycle 2	162.1 (pyridine), 63.2 (Ethyl),31.6(CH_2 polyamine), 22.0 (*tert*-butyl), 13.6 (*tert*-butyl), - 4.3 (Si-CH_3).	1944 cm^{-1}
Cycle 3	162.5 (pyridine), 63.1 (Ethyl),29.0(CH_2 polyamine), 22.2 (*tert*-butyl), 13.6 (*tert*-butyl), - 4.2 (Si-CH_3)	-

Table 4.4: Elemental analysis data of BP-1-Ru-PNN (7) after catalysis using solid-vapor method

Alcohol catalysis	Cycle 1			Cycle 3		
	Elemental analysis	Amount of complex remaining (mmol/gm BP-1) from elemental	Amount of complex remaining (mmol/gm BP-1) from metal digestion	Elemental analysis	Amount of complex remaining (mmol/gm BP-1) from elemental	Amount of complex remaining (mmol/gm BP-1) from metal digestion
1-Hexanol	C 12.44%, H 2.87%, N 2.10%, P 0.09%, Cl 1.80%.	0.028	0.031	C 13.96%, H 3.10%, N 2.01%, P 560 ppm, Cl 1.64%.	0.018	0.023
1-Heptanol	C 12.71%, H 2.46%, N 2.10%, P 0.08%, Cl 2.00%	0.025	0.029	C 14.11%, H 3.28%, N 1.78%, P 430 ppm, Cl 1.55%	0.014	0.019
Benzyl alcohol	C 12.98%, H 2.18%, N 1.98%, P 0.06%, Cl 1.78%	0.020	0.028	C 14.27%, H 3.17%, N 1.53%, P 410 ppm, Cl 1.20%	0.013	0.017

Table 4.5: Cycle study on 1-hexanol catalysis with BP-1-Ru-PNN (**7**) using the **solid-liquid (SL)** and **solid-vapor (SV)** methods

Alcohol	Reaction configuration	Catalyst / Alcohol ratio (mmol)	Reaction Temp (°C)	Reaction Time (Hours)	Total 1-hexanol conversion (%)	Decrease in 1-hexanol conversion between two cycles (%)	Turnover frequency (Hour $^{-1}$)
1-Hexanol 1st Cycle	SL	0.02/50	157	56	50	-	22
	SV	0.02/50	Passing alcohol vapor over catalyst bed	56	51	-	23
1-Hexanol 2nd Cycle	SL	0.02/50	157	56	42	16	19
	SV	0.02/50	Passing alcohol vapor over catalyst bed	56	47	8	21
1-Hexanol 3rd Cycle	SL	0.02/50	157	56	34	19	15
	SV	0.02/50	Passing alcohol vapor over catalyst bed	56	41	12	18
1-Hexanol 4th Cycle	SL	0.02/50	157	56	25	26	11
	SV	0.02/50	Passing alcohol vapor over catalyst bed	56	36	12	16
1-Hexanol 5th Cycle	SL	0.02/50	157	56	13	48	6
	SV	0.02/50	Passing alcohol vapor over catalyst bed	56	26	28	12

Table 4.6: Comparison between the decrease in 1-hexanol conversions and the loading of the complex remaining on BP-1 after catalysis with BP-1-Ru-PNN (**7**) using the **solid-vapor (SV)** and **solid-liquid (SL)**methods

Cycle	Method	Total conversion of 1-hexanol (%)	Decrease in conversion (%) between the cycles	Amount of complex remaining (mmol/gm BP-1) after cycle based on Ru analysis	Decrease in loading of Ru-PNN (%) between the cycles
1	SV	51 (Hexyl hexanoate 50% and 1-Hexanal 0.8%)	-	0.031	13
	SL	50 (Hexyl hexanoate 49% and 1-Hexanal 0.8%)	-	0.026	27
3	SV	41 (Hexyl hexanoate 40% and 1-Hexanal 0.7%)	20	0.023	25
	SL	34(Hexyl hexanoate 33% and 1-Hexanal 0.8%)	32	0.018	31
5	SV	26 (Hexyl hexanoate 25% and 1-Hexanal 0.5%)	36	0.015	35
	SL	13(Hexyl hexanoate 12% and Hexanal0.5%)	62	0.007	61

Table 4.7: Cycle study on 1-heptanol catalysis with BP-1-Ru-PNN (**7**) using the **solid-liquid (SL)** and **solid-vapor (SV)** methods

Alcohol	Reaction configuration	Catalyst/ Alcohol ratio (mmol)	Reaction Temp (°C)	Reaction Time (Hours)	Total 1-heptanol conversion (%)	Decrease in 1-heptanol conversion between two cycles (%)	Turnover frequency (Hour $^{-1}$)
1-Heptanol 1st Cycle	SL	0.01/30	176	48	52	-	33
	SV	0.01/30	Passing alcohol vapor over catalyst bed	48	50	-	31
1-Heptanol 2nd Cycle	SL	0.01/30	176	48	35	32	22
	SV	0.01/30	Passing alcohol vapor over catalyst bed	48	42	16	26
1-Heptanol 3rd Cycle	SL	0.01/30	176	48	21	40	13
	SV	0.01/30	Passing alcohol vapor over catalyst bed	48	33	21	21
1-Heptanol 4th Cycle	SL	0.01/30	176	48	10	52	6
	SV	0.01/30	Passing alcohol vapor over catalyst bed	48	22	33	14
1-Heptanol 5th Cycle	SL	0.01/30	176	48	5	50	3
	SV	0.01/30	Passing alcohol vapor over catalyst bed	48	13	40	8

Table 4.8: Comparison between the decrease in 1-heptanol conversions and the loading of the complex remaining on BP-1 after catalysis with BP-1-Ru-PNN (**7**) using the **solid-vapor (SV)** and **solid-liquid (SL)** methods

Cycle	Method	Total conversion of 1-heptanol after each cycle (%)	Decrease in conversions between the cycles (%)	Amount of complex remaining (mmol/gm BP-1) after each cycle based on Ru analysis	Decrease in loading of Ru-PNN between the cycles (%)
1	SV	50 (Heptyl heptanoate 48% and 1-Heptanal 2%)	-	0.029	19
	SL	52 (Heptyl heptanoate 51% and 1-Heptanal 1%)	-	0.024	33
3	SV	33 (Heptyl heptanoate 31% and 1-Heptanal 2%)	34	0.019	35
	SL	21(Heptyl heptanoate20% and 1-Heptanal 1%)	59	0.010	58
5	SV	13 (Heptyl heptanoate 12% and 1-Heptanal 1%)	60	0.008	62
	SL	5 (Heptyl heptanoate 4% and 1-Heptanal 0.5%)	76	-	-

Table 4.9: Cycle study on benzyl alcohol catalysis with BP-1-Ru-PNN (**7**) using the **solid-liquid (SL)** and **solid-vapor (SV)** methods

Alcohol	Reaction configuration	Catalyst/ Alcohol ratio (mmol)	Reaction Temp (°C)	Reaction Time (Hours)	Total benzyl alcohol conversion (%)	Decrease in benzyl alcohol conversion between two cycles (%)	Turnover frequency (Hour $^{-1}$)
Benzyl alcohol 1st Cycle	SL	0.01/30	178	60	48	-	24
	SV	0.01/30	Passing alcohol vapor over catalyst bed	60	52	-	26
Benzyl alcohol 2nd Cycle	SL	0.01/30	178	60	32	33	16
	SV	0.01/30	Passing alcohol vapor over catalyst bed	60	43	17	22
Benzyl alcohol 3rd Cycle	SL	0.01/30	178	60	18	43	9
	SV	0.01/30	Passing alcohol vapor over catalyst bed	60	34	21	17
Benzyl alcohol 4th Cycle	SL	0.01/30	178	60	10	44	5
	SV	0.01/30	Passing alcohol vapor over catalyst bed	60	21	38	11
Benzyl alcohol 5th Cycle	SL	0.01/30	178	60	5	50	3
	SV	0.01/30	Passing alcohol vapor over catalyst bed	60	12	42	6

Table 4.10: Comparison between the decrease in benzyl alcohol conversions with the loading of the complex remaining on BP-1 after catalysis with BP-1-Ru-PNN (**7**) using the **solid-vapor (SV)** and **solid-liquid (SL)** methods

Cycle	Method	Total conversion of benzyl alcohol (%)	Decrease in conversions between the cycles (%)	Amount of complex remaining (mmol/gm BP-1) after each cycle based on Ru analysis	Decrease in loading of Ru-PNN between the cycles (%)
1	SV	52 (Benzyl benzoate 40% and Benzaldehyde 12%)	-	0.028	22
	SL	48 (Benzyl benzoate 38% and Benzaldehyde 10%)	-	0.023	36
3	SV	33 (Benzyl benzoate 28% and Benzaldehyde 5%)	37	0.017	39
	SL	18 (Benzyl benzoate16% and Benzaldehyde 2%)	63	0.009	61
5	SV	12 (Benzyl benzoate 9% and Benzaldehyde 3%)	64	0.006	65
	SL	5 (Benzyl benzoate 4% and Benzaldehyde 1%)	72	-	-

4.2.9 Experimental procedures for control experiments with immobilized (PNN)RuH(Cl)(CO) on BP-1 (7)

4.2.9.1 Experimental procedure for the control experiment with 1-hexanol and BP-1-Ru-PNN (**7**) in the absence of a base

400 mg of BP-1-Ru-PNN (**1**) (0.014 mmol Ru-PNN on BP-1) was placed in a small round-bottom flask. 35mmol of 1-hexanol was added. The flask was equipped with a condenser. The mixture was degassed by an applied vacuum. Then the following steps were done:

Step 1: The mixture of 1-hexanol and BP-1-Ru-PNN (**7**) was stirred slowly for 4-5 hours under an inert atmosphere of argon. 100µL of the resultant liquid was collected and diluted with toluene and analyzed by GC-MS using an HP 5 column on an Agilent 6890N GC-MS system). Yield (1-hexanol conversion): 0%.

Step 2: The mixture was stirred and heated overnight (about 15-16 hours) at 157°C under the flow of argon. The mixture was then cooled to room temperature. 100µL of the resultant liquid was taken and diluted with toluene and the analyzed by GC-MS. Yield (1-hexanol conversion):30%.

Step 3: The resultant mixture of 1-hexanol and BP-1-Ru-PNN (**7**) from step 2 was stirred by heating at 157°C under the flow of argon for further 4 hours. The reaction mixture was cooled to room temperature and the liquid product mixture was separated from the **7**. 100µL of the liquid mixture was diluted with toluene and analyzed by GC-MS. Yield (1-hexanol conversion): 4%.

Step 4: The resultant liquid product mixture obtained from step 3 was separated from the catalyst and placed in a small round bottom flask equipped with a condenser and degassed by an applied vacuum. In the absence of the catalyst, it was stirred and heated at 157°C under an inert

atmosphere of argon overnight (about 15-16 hours). It was then cooled to room temperature and analyzed by GC-MS. Yield (1-hexanol conversion): 2-3%.

4.2.9.2 Experimental procedure for the control experiment of with 1-hexanol and BP-1-Ru-PNN (**7**) in the presence of KOH

400 mg of BP-1-Ru-PNN (**7**) (0.014 mmol Ru-PNN on BP-1) and 0.014 mmol of KOH were mixed in a small round-bottom flask. 35 mmol of 1-hexanol was added. The mixture was degassed by an applied vacuum. Then steps 1 to 4 described in section 4.2.9.1 were repeated. Conversion of 1-hexanol in each of the steps was determined by using GC-MS. The results are as follows: Step1: No conversion; Step 2: 36% ; Step 3: 7% and Step 4: 3%.

4.2.10 Experimental procedures for control experiments with BP-1 and silica gel

4.2.10.1 Experimental procedure for the control experiment between alcohol and BP-1

200 mg of BP-1 (containing 1.6 mmol of N/g) was placed in a small round-bottom flask. 21 mmol of alcohol was added to it. The mixture was degassed by an applied vacuum. The mixture was then heated with slow stirring under an inert atmosphere of argon. The reaction mixture was then cooled to room temperature. The liquid product mixture and BP-1 were separated by filtration. The resulting liquid mixture was analyzed by GC-MS using an HP 5 column on an Agilent 6890N GC-MS system. The results are shown in Table 4.11.

4.2.10.2 Experimental procedure for the control experiments between alcohol and silica gel

200 mg of silica gel (10 nm average pore diameter, 250−600 μm particle size, 450 m^2/g surface area was obtained from Qing Dao Mei Gow, Qing Dao, China) was placed in a small round-bottom flask. 21 mmol of alcohol was added to it. The mixture was degassed by an applied vacuum. The mixture was then heated with slow stirring under an inert atmosphere of argon. The reaction mixture was then cooled to room temperature. The liquid product mixture

and silica gel were separated by filtration. The resulting liquid mixture was analyzed by GC-MS using an HP 5 column on an Agilent 6890N GC-MS system. The results are shown in Table 4.11.

Table 4.11: The results of control experiments of alcohols with BP-1 and silica gel respectively

Alcohol	BP-1 /Silica gel used (200 mg)	Alcohol used (mmol)	Reaction Temp (°C)	Reaction Time (Hours)	Total alcohol conversion (%)
1-Hexanol	BP-1	21	157	56	0
	Silica gel	21	157	56	0
1-Heptanol	BP-1	21	176	48	0
	Silica gel	21	176	48	0
Benzyl alcohol	BP-1	21	178	60	0
	Silica gel	21	178	60	0
2-octanol	BP-1	21	178	48	0
	Silica gel	21	178	48	0

4.2.11 Experimental procedure for the filtration test

200 mg of BP-1-Ru-PNN (**7**) was suspended into 1,4-dioxane in a round-bottom flask. The mixture was refluxed for two hours and then filtered while still hot. The filtrate was placed in a round-bottom flask and 21 mmol of 1-heptanol added. The flask was equipped with a condenser and the mixture was heated at 176°C under the flow of argon for 48 hours. The resultant liquid was analyzed by GC-MS using an HP 5 column on an Agilent 6890N GC-MS system. Yield (1-Heptanol conversion): 0 %.

4.3 Results and discussion

4.3.1 Immobilization of (PNN)RuH(Cl)(CO) on BP-1

The PNN [(2-(di-*tert*-butylphosphinomethyl)-6-di-ethylaminomethyl)pyridine] ligand and (PNN)RuH(Cl)(CO) were synthesized by the previously reported procedure.[41] The PNN pincer

complex of Ru was immobilized on BP-1 surfaces by method 1 following a two-step Mannich reaction as described in section 3.2.2. The complex on BP-1 was characterized by solid-state NMR, FT-IR, elemental analysis, and metal digestion study. Solid-state CPMAS ^{13}C spectra of the tethered complex showed resonances at δ 162.4 ppm for the pyridine carbons, 23.7 ppm for *tert*-butyl carbons, and 56.7 ppm for the carbons from the ethyl groups in the complex (Figure A16 in Appendix A), which were similar to the resonances observed for the complex in solution.[41] In addition CPMAS ^{31}P NMR spectra displayed single resonance at δ 49.5 ppm indicating the successful loading of the complex on BP-1 surfaces (Figure A15). The carbonyl group in the complex showed *ν*CO stretch at 1948 cm^{-1} in the FT-IR spectra evidence that the heterogenization of the complex on the composite, BP-1 (Figure B8 in Appendix B).

Upon immobilization, a large shift in CO frequency of the complex was realized in comparison to the solution phase (1901 cm^{-1})[41] which might be due to the change in electronic environment around the complex on BP-1.[90] Similar shifts of the CO frequency was also noticed in the case of (PONOP)RuH(Cl)(CO) on BP-1.[90] The FT-IR spectra of the product, (PNN)RuH(Cl)(CO)-n-butyl amine (**8**), from the model solution study between (PNN)RuH(Cl)(CO) and n-butyl amine displayed CO stretching frequency at 1931 cm^{-1} (Figure 6B in Appendix B) indicating that attachment of an alkyl chain in the pyridine ring of the complex could dramatically affect the electronic environment of the complex, which might result in the large shift of the CO stretching frequency. Loading of the complex was found to be 0.038 mmol/gm BP-1 based on the metal digestion study. The % P analysis from elemental analysis data provided the loading of the complex, 0.035 mmol/gm BP-1 which showed a very good agreement with the results of the metal digestion study confirming the presence of (PNN)RuH(Cl)(CO) on BP-1. For

the catalytic study we estimated the loading of the complex 0.036 mmol/gm BP-1 which was the average of the two loading data obtained by metal digestion and elemental analysis methods.

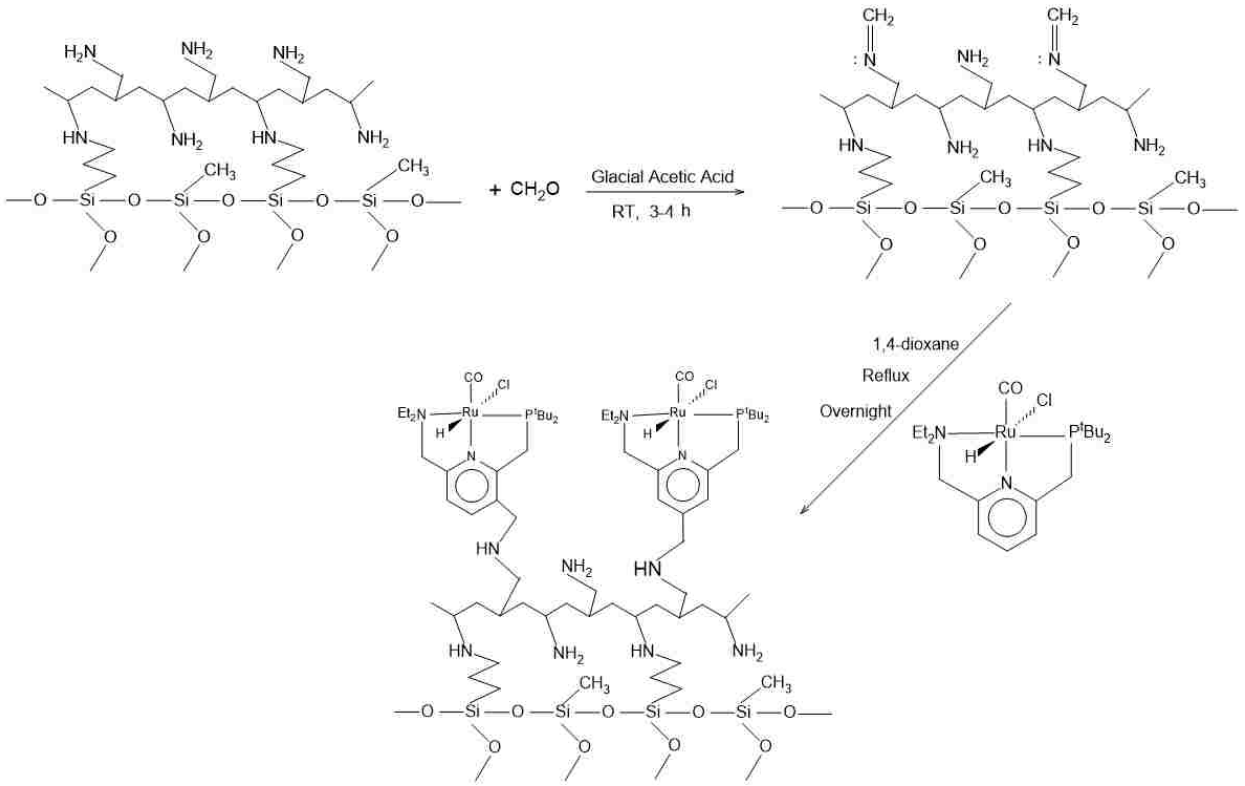

BP-1-Ru-PNN (**7**)

Scheme 4.5: Immobilization of (PNN)RuH(Cl)(CO) on BP-1 by the Method 1

4.3.2 Model solution reaction between (PNN)RuH(Cl)(CO) and n-butyl amine

Determination of the actual position of the substitution in the pyridine moiety of (PNN)RuH(Cl)(CO) upon immobilization on the BP-1 surface was relatively difficult, as in the Ru-PONOP-BP-1 system, due to the poor resolution of the solid-state NMR data. The presence of two different donor atoms in the structure of (PNN)RuH(Cl)(CO) might affect the position of electrophilic substitution in the pyridine ring of the complex. Therefore, the goal of this experiment was to investigate whether the *meta*- or *para*- position of the pyridine ring of the (PNN)RuH(Cl)(CO) complex was involved in electrophilic substitution by Mannich imine

intermediate. The experimental procedure was similar to that applied to the Ru-PONOP complex as described in Chapter 3.

The model solution experiment was conducted between (PNN)RuH(Cl)(CO) and n-butylamine following a two-step reactions. The first step was the formation of a Mannich imine intermediate (Scheme 4.6) by the reaction of n-butyl amine with 38% formaldehyde solution in the presence of catalytic amount of glacial acetic acid, which yielded a Mannich imine intermediate. In step 2, (PNN)RuH(Cl)(CO) was added into the imine intermediate in THF solvent and the mixture was heated at 66°C under N_2 overnight (Scheme 4.6). Analyses of the product with ^{31}P NMR spectroscopy showed three resonances at δ 89.97, 90.36, and 96.97 ppm (Figure 4.2), indicate the formation of the mixture of three isomers. The resonance at δ 89.97 ppm could be for the *para*-isomer. Two *meta*-isomers showed resonances at δ 89.97 and 90.36 ppm with almost equal integration. The relative intensity of the resonances suggested the formation of about 84% *meta*-isomers (42% each) and 16% *para*-isomer. These results demonstrated that electrophilic substitution predominantly occurs at the *meta*-position of the pyridine structure of the complex during the loading or immobilization of (PNN)RuH(Cl)(CO) on BP-1. The appearance of two resonances for the *meta*-isomers indicates that electrophilic substitution could be at both meta positions of the pyridine ring of the complex (Figure 4.2). Likewise in the (PONOP)RuH(Cl)(CO)-n-butyl amine system (**6**), the meta isomers could be predominant due to the electronic ground and *ortho*-isomer would be preferable due to the steric hindrances.[90] ^1H NMR of the spectrum of **8** was too complicated to resolve because of the formation of the mixtures of three isomers. However, the resonances for *tert*-butyl, n-butyl chain, and pyridine protons were realized in the spectra (Figure A25 in Appendix A). The appearance of additional unexpected resonances in the ^1H NMR spectrum might be due to the presence of a trace amount of unreacted

amines, formaldehyde, imines, and the starting complex remaining after purification of the product **8**. FT-IR spectrum of the isomeric product displayed carbonyl stretch at 1931 cm^{-1} (Figure B6 in Appendix B) which was higher by 30 cm^{-1} from the original complex (1901cm^{-1}).[41] This suggests that CO stretching frequency for the (PNN)RuH(Cl)(CO) complex could be shifted dramatically upon the attachment of a functional group or an alkyl chain with the pyridine backbone of the complex due to the change of the electronic environment.[90] These results rationalized the appearance of the CO stretching frequency at 1948 cm^{-1} upon immobilization of (PNN)RuH(Cl)(CO) on BP-1 which was much higher than that of the original complex (1901cm^{-1}) before loading. The surface functionality, steric, and electronic environment on BP-1 surfaces might cause the change in CO resonance in the FT-IR.[90]

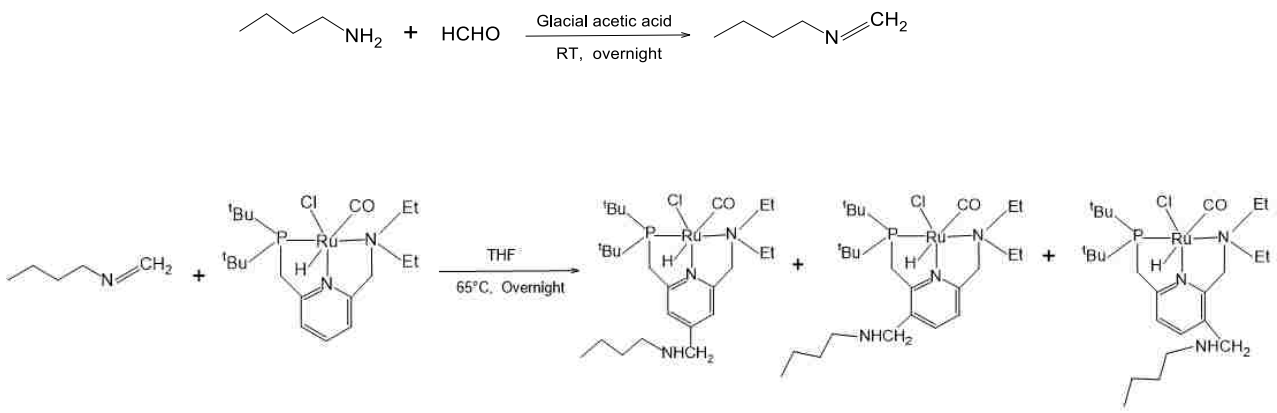

1 Ru-PNN-n-butyl amine (*para*-isomer, **8i**)

3 Ru-PNN-n-butyl amine (*meta*-isomers, **8ii, 8iii**)

Overall yield: 63%

Scheme 4.6: Reaction between (PNN)RuH(Cl)(CO) and n-butyl amine

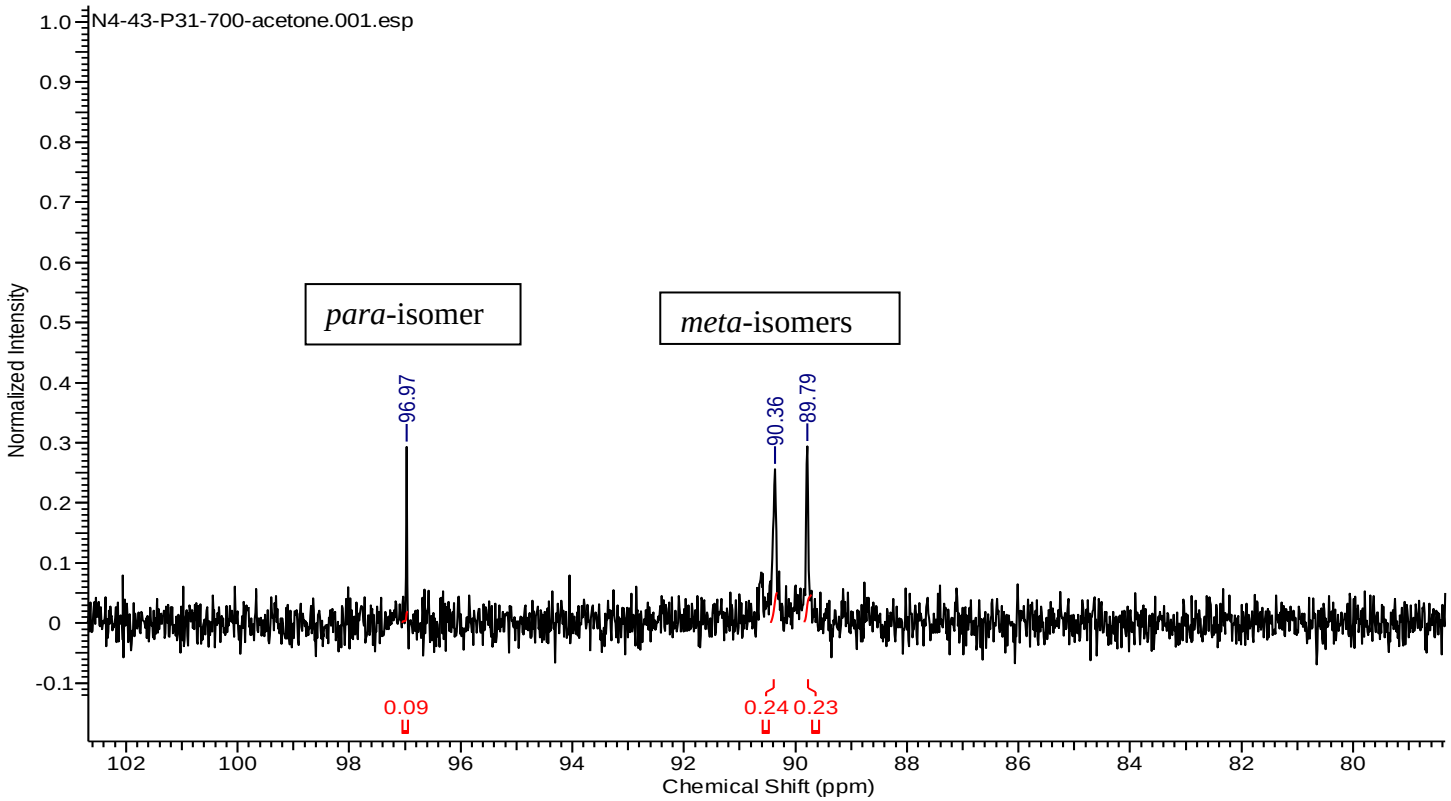

Figure 4.2: ^{31}P NMR spectrum of the isomers (**8)** formed from n-butylamine reaction with (PNN)RuH(Cl)(CO)

4.3.3 Deprotonation of the product, (PNN)RuH(Cl)(CO)-n-butyl amine (8), from the model solution reaction and alcohol catalysis

Introduction of an alkyl chain or any functional group in the pincer complex structures might impact their catalytic reactivity. Very few examples are reported in the literature about how the substituents in the pincer complexes structure affects their catalytic reactivity.[97] It would be very interesting to see how the addition of an alkyl chain in the structure of (PNN)RuH(Cl)(CO) affects the catalytic reactivity of the resulting complex. The objective of this study was to investigate the catalytic reactivity of (PNN)RuH(Cl)(CO)-n-butyl amine (**8**) in the alcohol dehydrogenation reactions. The first step of this study was to deprotonate the product (**8**) obtained from the model solution reaction by a base to generate active catalytic complex following the

similar procedure to that used with the (PNN)RuH(Cl)(CO).[41] The next step was to apply the deprotonated active catalytic complex in the alcohol conversion reactions. The catalytic reactions were conducted in the absence of solvent as well as in the presence of toluene.

Chemical treatment of (PNN)RuH(Cl)(CO)-n-butyl amine (**8**) with KO^{t}Bu results in the formation of deprotonated or dearomatized (PNN-)RuH(CO)-n-butyl amine (**9**) (Scheme 4.7). The complex was characterized by NMR and FT-IR. ^{31}P NMR showed three resonances at δ 97.07 (s), 109.73 (s), and 109.78 (s) which indicates the formation of three isomeric products (Figure 4.3). The resonance at δ 97.07 could be for deprotonated *para*-isomer. The other two resonances appeared as an overlapping doublet at δ 109.73 (s), and 109.78(s) which might be due to two *meta*-isomers (Figure 4.3). ^{1}H NMR data was too complicated to interpret because of the formation of isomeric product mixtures. However, as in the case of **8**, the resonances for *tert*-butyl, pyridine, and n-butyl protons were also observed in the spectra of the deprotonated product **9** (Figure A27 in Appendix A). In comparison to the spectra of **8**, the change in the resonances observed at the pincer arm region of the spectra of **9,** which could be due to the deprotonation that occurred during the reaction. FT-IR spectra of the deprotonated product showed the CO stretching frequency at 1929 cm^{-1}, which was not much different than before deprotonation (1931 cm^{-1}) (Figures B6 & B7 in Appendix B). Very similar carbonyl stretching frequency differences were observed with (PNN)RuH(Cl)(CO) before (1901 cm-1) and after deprotonation (1889 cm^{-1}) reported by David Milstein *et al*.[41]

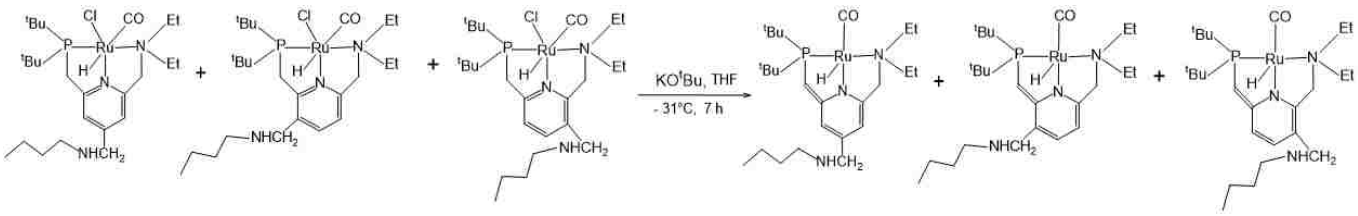

1 (*para*-isomer) **(9i)**

4 (*meta*-isomers) **(9ii, 9iii)**

Overall yield: 69%

Scheme 4.7: Formation of dearomatized active catalyst (PNN-)RuH(CO)-n-butyl amine (**9**) from the reaction of (PNN)RuH(Cl)(CO)-n-butyl amine (**8**) with KO^{t}Bu

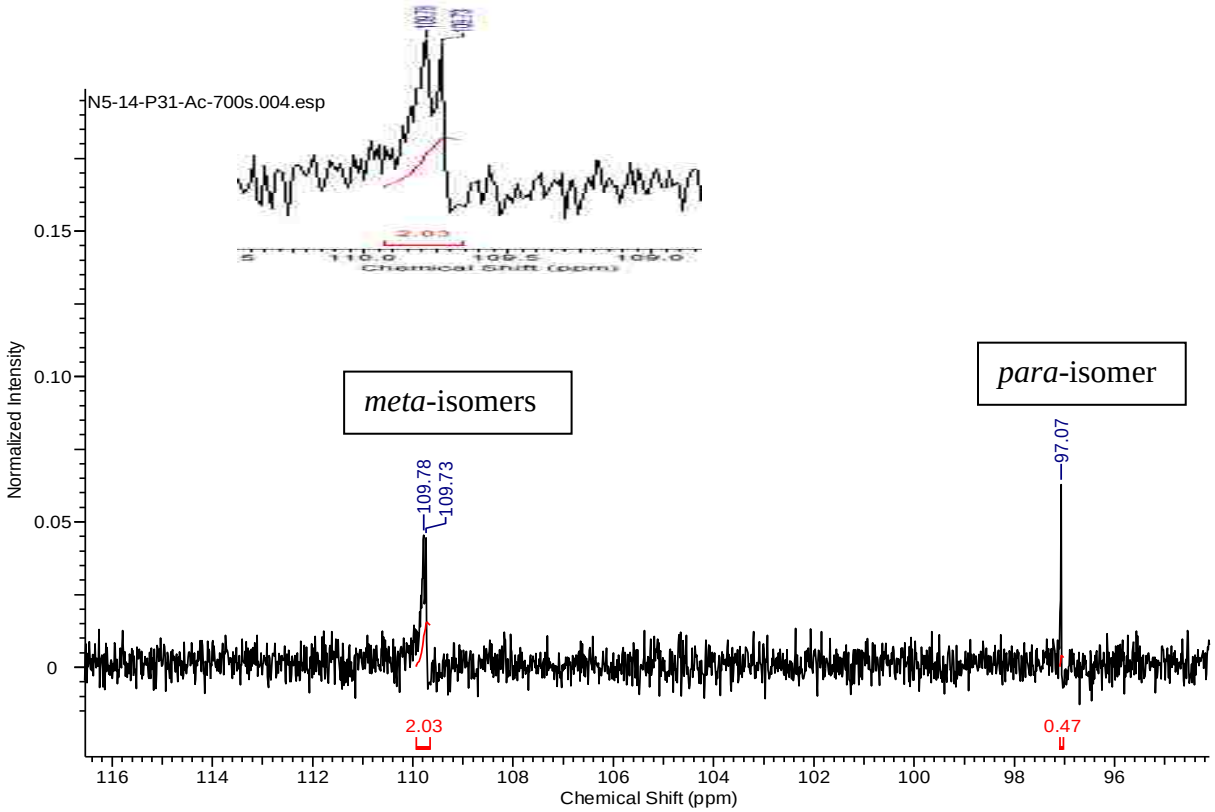

Figure 4.3: ^{31}P NMR spectrum of the isomeric products (**9**) formed from the deprotonation of (PNN)RuH(Cl)(CO)-n-butylamine by KO^{t}Bu

1-Hexanol catalysis with 0.1 mol% of (PNN-)RuH(CO)-n-butyl amine (**9**) at 157°C under an argon flow yielded only 28% product after 2.5 hours (Scheme 4.8). However, the dearomatized

original complex, (PNN-)RuH(CO), with similar reaction conditions showed about 91% conversion of 1-hexanol after 2.5 hours.[41] When the reaction was continued for 56 hours, total conversion was found to be 66% with 65% hexyl hexanoate and 0.5% 1-hexanal. In the presence of toluene, the reaction with **9** yielded only 23% after 2.5 hours. A similar reaction with 0.1 mol% dearomatized (PNN-)RuH(CO) provided 99% conversion of 1-hexanol to hexyl hexanoate in the presence of toluene after 6 hours,[41] whereas only 59% conversion was realized when the 1-hexanol catalysis was conducted with deprotonated (PNN-)RuH(CO)-n-butyl amine complex (**9**) in toluene for 56 hours.

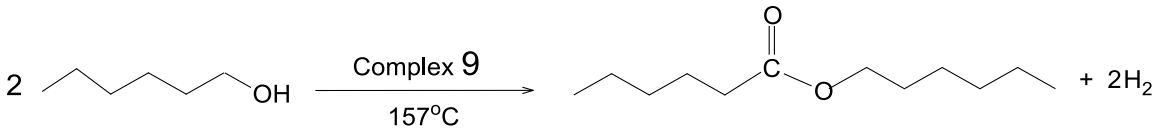

a

Yield: 28% (after 2.5 hour)

66% (after 56 hours)

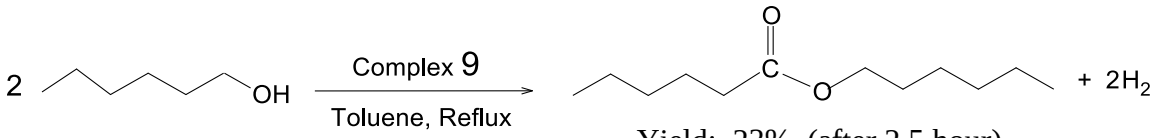

b

Yield: 23% (after 2.5 hour)

59% (after 56 hours)

Scheme 4.8: 1-Hexanol catalysis by the dearomatized Ru-PNN-n-butylamine (**9**):
(a) in the absence of solvent and (b) in toluene

The turnover frequencies were also considerably less in comparison to those of the Milstein active catalyst.[41] These results indicate that introduction of n-butyl amine substituent in the structure of (PNN)RuH(Cl)(CO) complex decreases its catalytic reactivity. One possible explanation is that an amine on the alkyl chain can form a five-coordinate complex through the intramolecular reactions

(Figure 4.4) which might inhibit the catalytic reactivity of the resulting complex. It could also be due to the low selectivity and steric hindrances of the long n-butyl chain for orientation effect.

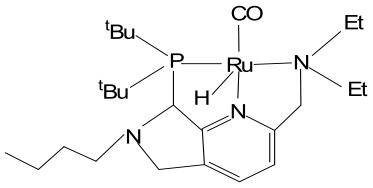

Figure 4.4: Possible structure of the five-coordinated complex created through an intramolecular reaction of the amine with the spacer carbon of the pincer complex **9**

4.3.4 Catalytic study on silica polyamine composites by immobilized (PNN)RuH(Cl)(CO) on BP-1

4.3.4.1 Dehydrogenative coupling of alcohols to esters and hydrogen with immobilized (PNN)RuH(Cl)(CO) on BP-1 (7)

The catalytic reactions were carried out with (PNN)RuH(Cl)(CO) on BP-1 (**7**) in three primary alcohol systems: 1-hexanol, 1-heptanol, and benzyl alcohol and a secondary alcohol, 2-octanol. All reactions on BP-1-Ru-PNN (**7**) were conducted following two conditions: in the absence of base and with the addition of KOH. The results were compared with the homogeneous systems reported by Milstein *et al.*[41] The catalyst to alcohol ratio used in the reaction system was 0.007:21 (equivalent to 0.01:30) except in the case of 1-hexanol where 0.014 mmol of catalyst was used with 35 mmol of alcohol (equivalent ratio, 0.02:50) (Table 4.2) . However, in all cases, excess alcohols were used in comparison to the catalyst-to- alcohol ratios used previously in the homogeneous reaction system.[41] Catalysis of alcohols with BP-1-Ru-PNN (7**)** produced the corresponding esters and hydrogen. However, in some cases aldehydes were also formed along with major ester products.

The catalytic reaction of 1-hexanol on BP-1 with 0.04 mol% of immobilized Ru-PNN at 157°C for 56 hours resulted in the formation of hexyl hexanoate, hydrogen, and a trace of 1-hexanal with overall conversion of 50% (Scheme 4.9a). When KOH (equivalent to Ru-PNN) was used, conversion increased to 62% (Scheme 4.9b). Homogeneous reaction with the same catalyst investigated by Milstein *et al.* reported the conversion as 91 to 95% after 24 hours,[41] following similar reaction conditions in the presence of KOH with catalyst-to-alcohol mmol ratio of 0.01:10.[41] Heterogeneous catalysis on BP-1 with 0.01 mmol catalyst to 50 mmol 1-hexanol ratio provided relatively lower overall conversion of 39% in the absence of a base and 45 % when 0.01 mmol of KOH was used. When the catalyst was doubled (0.02 mmol), hexyl hexanoate yields improved to 51-62%.

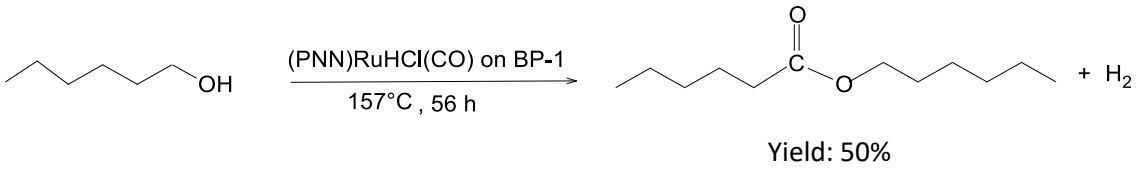

Yield: 50%

a

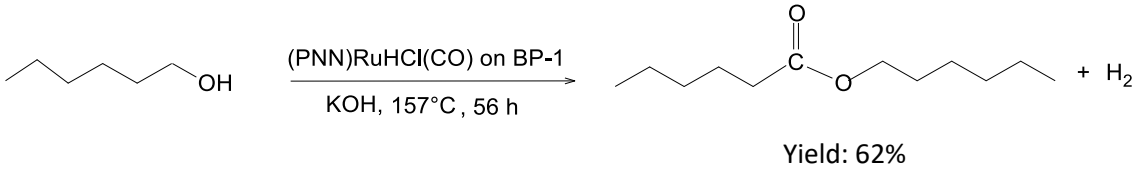

Yield: 62%

b

Scheme 4.9: Formation of hexyl hexanoate and H_2 from 1-hexanol with immobilized °C (PNN)RuH(Cl)(CO) on BP-1 (**7**): (a) in the absence of base and (b) with KOH

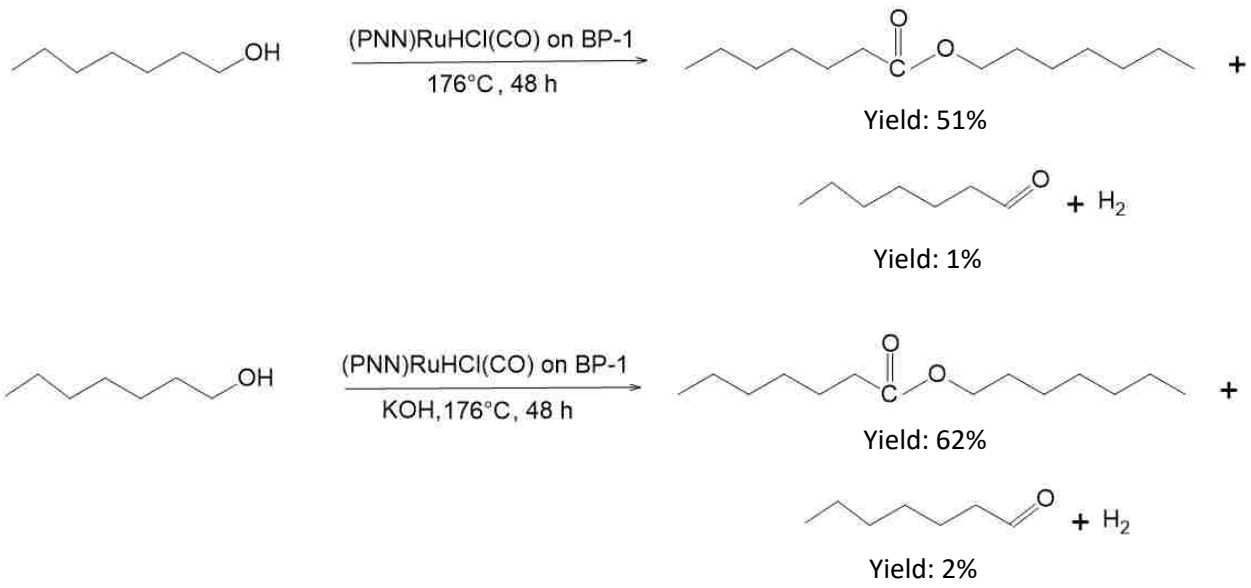

Scheme 4.10: Formation of heptyl heptanoate, 1-heptanal, and H_2 from 1-hexanol with immobilized (PNN)RuH(Cl)(CO) on BP-1 (**7**): (a) in the absence of base and (b) with KOH

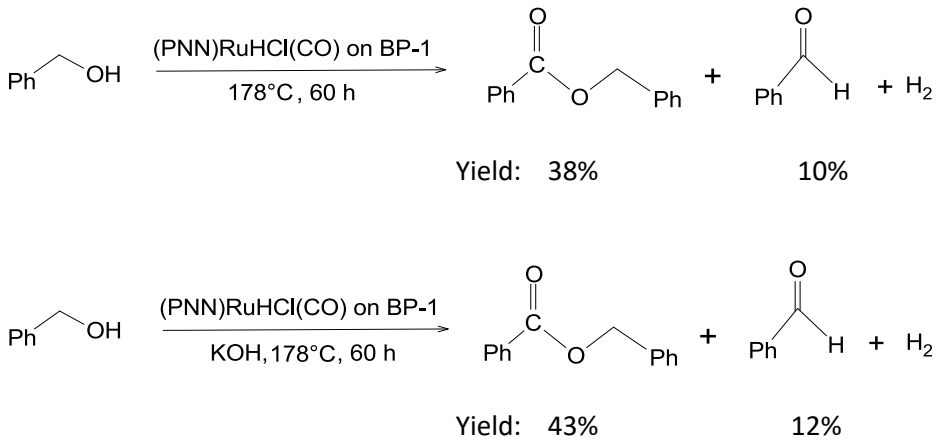

Scheme 4.11: Formation of benzyl benzoate, benzaldehyde, and H_2 from benzyl alcohol with immobilized (PNN)RuH(Cl)(CO) on BP-1 (**7**): (a) in the absence of base and (b) with KOH

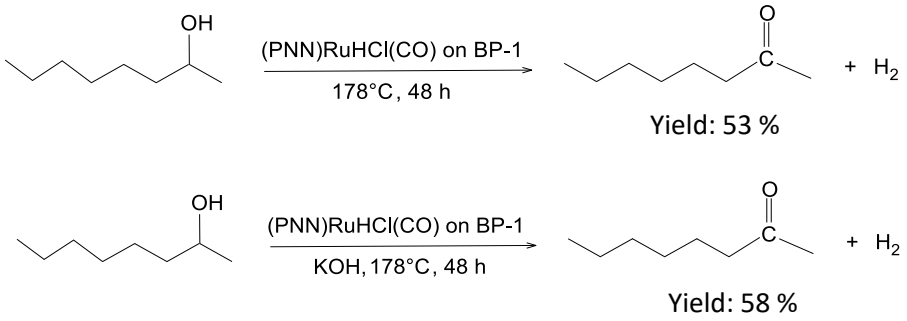

Scheme 4.12: Formation of 2-octanone and H_2 from 2-octanol with BP-1-Ru-PNN (**7**): (a) in the absence of base and (b) with KOH

1-heptanol catalysis with 0.03 mol% Ru-PNN on BP-1 (**7)** showed total 52% conversion with 51% of heptyl heptanoate and 1% 1-heptanal when the reaction was carried out at 176°C for 48 hours under argon. However, with KOH (1 equivalent to Ru-PNN), conversion improved to 64% (62 % heptyl heptanoate and 2% 1-heptanal) (Scheme 4.10). Upon heating the mixture of benzyl alcohol with 0.03 mol% BP-1-Ru-PNN at 178°C for 60 hours, benzyl benzoate and benzaldehyde were formed at 38% and 10 % yields respectively with the liberation of H_2 (Scheme 4.11). With the addition of KOH (equivalent to Ru) total conversion increased to 55%, with 43% benzyl benzoate and 12% benzaldehyde whereas the homogeneous reaction system with 0.1 mol% Ru-PNN provided 93% yield with only 1% benzaldeyde.[41] The percentage of benzaldehyde formation was observed to be a bit higher with the BP-1-Ru-PNN system, which could be due to the influence of the support surface. The secondary alcohol, 2-octanol, yielded a ketone, 2-octanone and hydrogen with a conversion of 53% when treated with 0.03 mol% Ru-PNN on BP-1 (**7)** following the reaction at 178°C for 48 hours under argon. When the KOH equivalent to Ru was used, the 2-octanone yield was increased to 58% with the liberation of H_2 (Scheme 4.12). No ester formation was realized in the secondary alcohol catalysis.

No reaction occurred in the homogeneous system between (PNN)RuH(Cl)(CO) and alcohols when there was no base.[41] Heterogeneous alcohol catalysis with BP-1-Ru-PNN produced esters and H_2 in the absence of base as well as with KOH. However, a longer reaction period and lower reaction yields were realized in the case of all alcohol catalysis with immobilized Ru-PNN on BP-1 system (**7**) in comparison to homogeneous systems which might be due to the several factors such as different functionality and electronic environment on BP-1 surface and catalyst decomposition. The homogeneous systems used 0.1 mol% catalyst whereas in our study, 0.03 mol% of immobilized catalyst was utilized in the alcohol catalysis and excess amount of alcohol was used in each case. These could also affect the alcohol conversion rate in the heterogeneous systems.

The formation of moderate to good conversion of alcohols to corresponding esters and H_2 in the absence of KOH provided evidence that amine functionality on the BP-1 surface functioned as a required base to deprotonate the pincer arm (-CH_2 group) of (PNN)RuH(Cl)(CO) and formed deprotonated or dearomatized active catalyst, [(PNN-) RuH(CO)] on BP-1 (Scheme 4.13). Though an amine is a weaker base than KOH, the higher temperature and surface confinement made the deprotonation favorable.[92] The scheme 4.13 shows how the amine functionality on the BP-1 surface potentially worked to generate active pincer catalytic complex on BP-1. Both the original and dearomatized Ru-PNN complexes could be present on BP-1 after immobilization. It was difficult to figure out the approximate proportion of deprotonated/ dearomatized active catalyst to the original complex [(PNN)RuH(Cl)(CO)] present on BP-1 after immobilization. FT-IR and solid state NMR spectra did not provide much information about the differences in the resonances between the two forms of the complexes on BP-1.

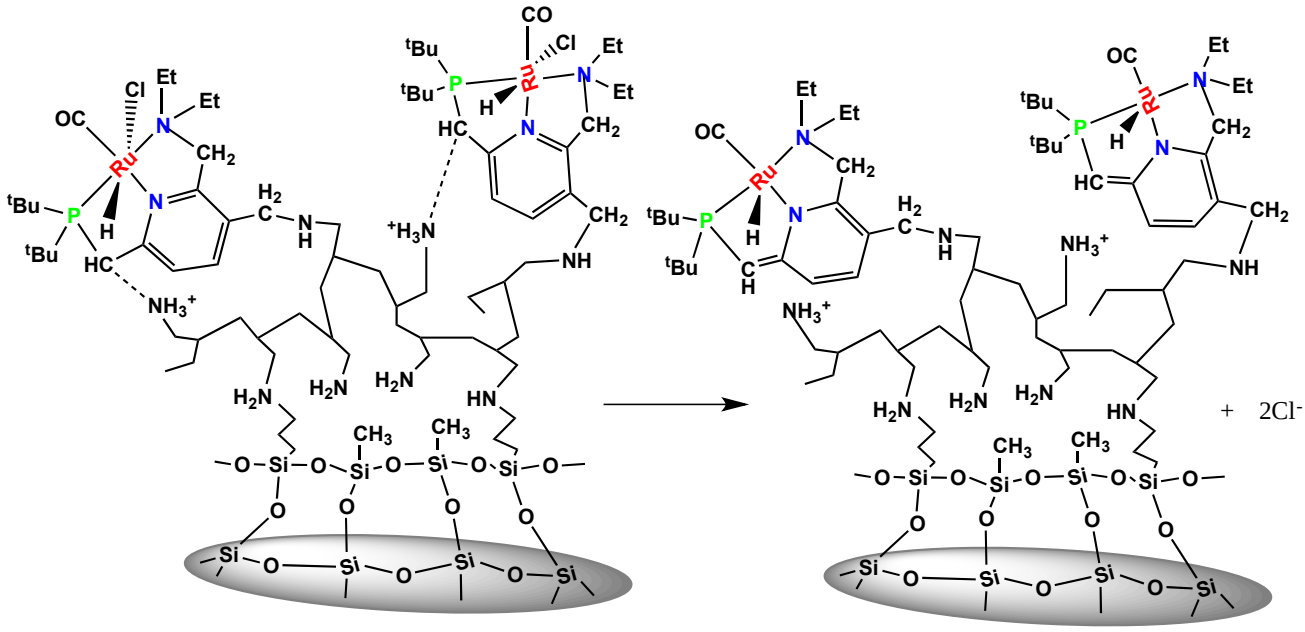

Scheme 4.13: Deprotonation of pincer arm (-CH_2 group) in (PNN)RuH(Cl)(CO) by amine on BP-1 surface

However, better conversion of alcohols was observed in all four cases when the catalytic reactions were conducted in the presence of KOH. This indicates that all loaded or immobilized Ru-PNN molecules might not be deprotonated by the surface amines. Application of KOH might result in the generation of more dearomatized [(PNN-)RuH(CO)] complex on BP-1 and enhance the catalytic conversion of alcohols.

4.3.4.2 Effect of solvents in the heterogeneous catalysis of alcohols with immobilized (PNN)RuH(Cl)(CO) on BP-1 (7)

The reaction of 1-hexanol with 0.04 mol% of BP-1-Ru-PNN (**7**) in 2 mL of toluene with refluxing under argon for 56 hours did not yield any ester. Equivalent KOH on BP-1 in the 1-hexanol catalysis reaction in toluene also resulted in no product formation, which gives evidence that alcohol catalysis does not occur on BP-1 at a lower temperature. However, in the

homogeneous reaction systems with similar reaction conditions showed 95% conversion of 1-hexanol to hexyl hexanoate in toluene.[41] When the 1-hepatanol reaction was carried out with BP-1-Ru-PNN (**7**) in the presence of 2 mL dichlorobenzene following catalyst-to-alcohol ratio of 0.01:30 (mmol) and refluxed for 48 hours under argon, only 33% heptyl heptanoate was formed. The presence of KOH (equivalent to Ru) in the 1-heptanol catalysis in dichlorobenzene increased the reaction yield to 40% after 48 hours. These results suggested that presence of solvent in the heterogeneous alcohol catalytic reaction system decreased the reaction kinetics. A longer period of reaction was needed to complete the reaction and the overall yields are reduced in comparison to the reactions with neat alcohol. Introduction of KOH in the reaction system with dichlorobenzene did not change the reaction kinetics significantly; however, an increase of the formation of heptyl heptanoate was noticed. The selectivity of a catalyst has always been an issue in heterogeneous catalytic reaction systems. One might predict that the presence of solvent in the alcohol in multi-phase catalysis reactions could decrease the selectivity of the immobilized catalyst, affect mass transfer kinetics, and thus slow down the formation of products.[98,99]

4.3.5 Cycle study on dehydrogenative coupling of alcohols to esters and hydrogen by immobilized (PNN)RuH(Cl)(CO) on BP-1(7) by solid-liquid and solid-vapor methods

The major advantage of heterogeneous catalytic reactions is easy recycling of important catalysts, which offers opportunities to reuse the catalysts in multiple cycles of reaction. However, the stability of catalysts on solid surfaces, physical and chemical properties of support solids, performance of catalysts in each reaction cycle, and subsequent yields of products in the respective cycle are important factors to be considered in most heterogeneous reactions.[100-102] One of the main objectives of this dissertation was to investigate the recyclability of immobilized

(PNN)RuH(Cl)(CO) on BP-1 (7) in alcohol dehydrogenative coupling reaction systems. To achieve this objective we have studied the catalytic performance of immobilized Ru-PNN on BP-1 in dehydrogenation of alcohols reaction systems up to five cycles. All reactions were carried out following two reaction configurations named, "solid-liquid" and "solid-vapor". No base was used in the cycle study. In the solid-liquid method, alcohol catalysis was conducted with traditional reaction systems which involved the heating of the mixtures of alcohols and BP-1-Ru-PNN (**7**) with slow stirring and heating under an inert atmosphere of argon. In the solid-vapor method, alcohol compounds were heated enough to allow them to pass alcohol vapor over the BP-1-Ru-PNN (**7**) bed, whereas catalyst-to-alcohol ratios remained the same in both reaction configurations. Figure 4.5 depicts the reaction configuration by the solid-liquid and solid-vapor methods.[103] Conversions of alcohols in each of the cycles accompanied with turnover frequency were determined (Table 4.5-4.1-0). The immobilized catalyst complex was characterized after catalytic reaction cycles by solid-state NMR and FT-IR. The amount of the complex remaining on BP-1after catalysis was estimated by metal digestion study as well as the elemental analysis of the resulting composite catalysts.

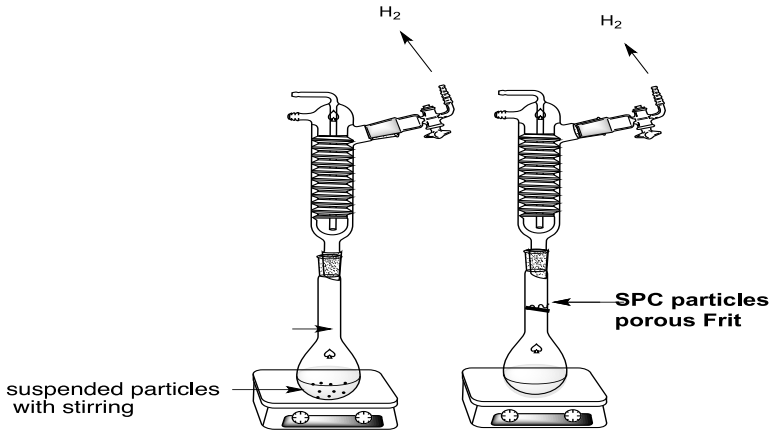

Figure 4.5: Schematic diagram for alcohol catalysis with the Solid-Liquid and the Solid-Vapor methods.

4.3.5.1 Cycle study on 1-hexanol catalysis by immobilized BP-1-Ru-PNN (7)

In the first cycle, 1-hexanol conversion was found to be almost the same (~50%) using both solid-liquid and solid-vapor methods with a turnover frequency of 23 h^{-1}. However, in cycle 2, formation of hexyl hexanoate was decreased to 42 % following the solid-liquid method and 47% using the solid-vapor method. It dropped to 34 % in the cycle 3 when the solid-liquid method was applied, however, 41% hexyl hexanoate formation was still observed while the reaction was carried out by passing 1-hexanol vapor on BP-1-Ru-PNN (**7**) (Table 4.5). Further reduction of hexyl hexanoate yields was realized with both solid-vapor and solid-liquid methods when the reaction was continued to a fourth cycle (Table 4.5). Only 13% hexyl hexanoate was formed in the fifth cycle of reaction with the solid-liquid method; however, using the solid-vapor method it was doubled to 26 % (Table 4.5-4.6).

The loading of the complex was found to be 0.031 mmol/gm BP-1 after the first cycle of reaction with the solid-vapor method (Table 4.6). This demonstrated that about 13% of the catalyst was leached off from BP-1 which showed good agreement with the corresponding decrease of the yield of hexyl hexanoate (8-16% from Cycle 1 to 2 with solid-liquid and solid-vapor methods). A similar reduction of 1-hexanol conversions was realized as we moved from cycle 2 to 3 using both the solid-liquid and solid-vapor methods (Table 4.5). However, a much higher decrease of hexyl hexanoate yield was observed from cycle 3 to 4 with the solid-liquid method (26%) in comparison to the solid-vapor method which showed only 12% decrease. This could be due to the higher leaching of Ru-PNN in the solid-liquid method. The loading data observed after cycle 3 with the solid-liquid method was 0.018 mmol complex/gm BP-1, which is 31% decrease from cycle 1, whereas the solid-vapor method provided 0.023 mmol complex/gm BP-1, 25% less than cycle 1 (Table 4.5). The overall decrease of the 1-hexanol conversions from cycle 1 to 3 was 20% with

the solid-vapor method and 32% using the solid-liquid method, which correlates with the corresponding loss of the catalyst from BP-1 during catalysis (Table 4.6). Phosphorus analysis data on the resulting composite BP-1-Ru-PNN (**7)** from cycles 1 to 3 with solid-vapor method (0.028 mmol complex/gmBP-1 and 0.018 complex/gmBP-1) provided a good agreement with the results of metal analysis (Table 4.4) which also showed evidence of the loss of catalyst from cycle 1 to 5. The turnover frequencies varied from 6-23 h^{-1} from cycles 1 to 5 with both methods (Table 4.5).

4.3.5.2 Cycle study on 1-heptanol catalysis by immobilized (PNN)RuH(Cl)(CO) on BP-1 (7)

1-Heptanol catalysis with 0.03 mol% Ru-PNN on BP-1(**7**) with the solid-liquid and solid-vapor reaction configurations gave similar conversions in the first cycle with the major product heptyl heptanoate, and the minor product being 1-heptanal, accompanied by the liberation of H_2 (Table 4.7). In the second cycle, the total 1-heptanol conversion decreased from 50 % to 42 % using the solid-vapor method and 52% to 35% with the solid-liquid method, indicating the loss of catalytic performance of Ru-PNN. On going from Cycle 2 to 3, further reduction of reaction yields was realized by the both methods. Cycle 4 gave only 22 % overall conversion with solid-vapor method which was a 33% decrease from cycle 3 and a much higher reduction in comparison to the ester yields observed from cycle 2 to 3, where 1-heptanol conversion dropped by only 21% (Table 4.7 & 4.8). The total 1-heptanol conversion was even further decreased in the same cycles when the reaction was conducted with the solid-liquid method (40% decrease from cycle 2 to 3 and 52% reduction from cycle 3 to 4) (Table 4.7). Cycle 5 showed only 5% yield of heptyl heptanoate with the solid-liquid method, whereas the solid-vapor method provided a yield about 3 times higher (13%) (Table 4.7). The loading data of **7** after catalysis demonstrated that the catalytic reactivity of BP-1-Ru-PNN- was reduced by 33% after the first cycle of 1-heptanol

catalysis when the reaction was performed with the solid-liquid method which was twice of the reduction noticed for the solid-vapor method where only a 19% decrease was realized (Table 4.7 & 4.8).

The amount of Ru-PNN on BP-1 after the third cycle of catalysis was found to be 0.019 mmol/gm BP-1 with the solid-vapor method which implies a decrease or loss of 35% of the complex from cycle 1. This is more or less consistent with the corresponding reduction of 1-heptanol conversion from cycle 1 to 3, which was also observed to be 34% (Table 4.7 & 4.8). This was also confirmed by the loading of Ru-PNN on BP-1 obtained from phosphorus analysis after cycle 3, which was 0.014 mmol complex/gm BP-1 (Table 4.4). Similar agreement was observed between reduction of 1-heptanol conversions and the corresponding loading of the complex on BP-1 from cycle 3 to 5. No Ru content was found in the resulting composite after the fifth cycles of catalysis of 1-heptanol, meaning that Ru-PNN survived on BP-1 surfaces up to the fifth catalytic cycles.

4.3.5.3 Cycle study on benzyl alcohol catalysis by immobilized (PNN)RuH(Cl)(CO) on BP-1 (7)

The chemical reaction of benzyl alcohol with 0.03 mol% of immobilized Ru-PNN on BP-1 resulted in 52% conversion of benzyl alcohol to 40% benzyl benzoate and 12 % benzaldehyde in the first catalytic run with the solid-vapor method, whereas when using the solid-liquid method total conversion was 48% with 38 % benzyl benzoate and 10 % benzaldehyde respectively (Table 4.9). Repetition of the reaction in cycle 2 led to 32% conversion of benzyl alcohol using the solid-liquid method with turnover frequency of 16 h^{-1}, which was approximately 33% less than in cycle 1 (Table 4.9). Application of the solid-vapor method in the same cycle generated 43 % conversion of benzyl alcohol, which was only 17% less than in cycle 1. As in the 1-heptanol and 1-hexanol

reaction systems, reduction of the ester yields in benzyl alcohol catalysis could be rationalized by the corresponding decrease of the loading of the complex obtained from the resulting BP-1-Ru-PNN after of benzyl alcohol catalysis which was found to be 0.023mmol/gm BP-1 after first cycle with the solid-liquid method, indicating 36% leaching of the catalyst at cycle 1 (Table 4.10). Before the catalysis the loading of the Ru-PNN was 0.036 mmol complex/gm BP-1. A considerable decrease in ester yields was also noticed from cycle 2 to 3 (43% with the solid-liquid method and 21% with the solid-vapor method) (Table 4.9). The solid-liquid method showed the benzyl alcohol conversion to be only 10% in cycle 4 but the conversion was observed doubled 21% when the solid-vapor method was used. These results demonstrated the decrease of benzyl alcohol conversion by 44% using the solid-liquid method and 38% using the new method in comparison to cycle 3 (Table 4.9). The amount of Ru-PNN remaining on BP-1 after cycle 3 was observed to be 0.017 mmol complex/gm BP-1, which showed that 39% of the catalyst from cycle 1 was leached off by cycle 3 with the solid-vapor method. In the same reaction cycle, the loss of Ru-PNN was about 61% when the solid-liquid method was applied (Table 4.10). Only 12% of overall conversion of benzyl alcohol was noticed in fifth cycle of catalysis with the solid-vapor method but it was reduced to 5% with the solid-liquid method (Table 4.9). Phosphorus analysis data from BP-1 Ru-PNN after the first cycle of catalysis with the solid-vapor method showed the loading of the complex to be 0.020 mmol complex/gm BP-1 which conformed with the results of Ru metal analysis (0.028 mmol complex/gm BP-1) provided further proof that the Ru-PNN catalyst stayed on the BP-1 surface after catalysis, though considerable leaching was realized (Table 4.4).

4.3.5.4 Comparison of cycle study on the catalysis of three alcohol systems by immobilized (PNN)RuH(Cl)(CO) on BP-1 (7) using the solid-liquid (SL) and solid-vapor (SV) methods

In the three alcohol reaction systems used in the cycle study, the solid-vapor method provided better alcohol conversions than the solid-liquid method in all 5 cycles. Mechanical stirring of the composite solid, BP-1-Ru-PNN (**7**), with alcohols for a longer reaction period might have degraded some BP-1 particles during the course of reactions, which might have resulted in the higher leaching of the immobilized catalyst from BP-1 surfaces and thus caused more decrease of the reaction yields in the solid-liquid method. The decrease of the ester yields from cycle 1 to 5 using both methods indicated that the catalyst, Ru-PNN leached off the BP-1 surface in each of the reaction cycles irrespective of the alcohols used in the catalytic reactions. This was also evidenced by the loading of Ru-PNN observed on the resulting composite BP-1-Ru-PNN (**7)** after catalysis (Table 4.4). The reaction yields were drastically decreased between cycles 3 to 4 and 4 to 5 in comparison to cycles 1 to 2 and 2 to 3 (Table 4.5, 4.7, 4.9). This could be because recycling the catalyst for multiple cycles of reactions at higher temperature might have decreased the stability of the immobilized catalyst on the BP-1 surfaces and increased the chance of leaching or decomposition of the catalyst in the later reaction cycles.

There was very good agreement between the reduction of alcohol conversions and the corresponding loss of the catalyst from BP-1 in the successive cycles of three alcohol catalysis by both the solid-liquid and solid-vapor methods (Table 4.6, 4.8, 4.10). Turnover frequencies for alcohol catalysis were found to be varied from cycle to cycle and were considerably lower than those observed in homogeneous reactions[41] as one would expect in heterogeneous reaction systems because of relatively lower reaction yields. Leaching of the catalyst was found to be relatively lower in cycles 1 and 2 irrespective of the configuration of catalytic reactions. In addition, the

decrease in alcohol conversions between two successive cycles was relatively lower in the 1-hexanol reaction system in comparison to 1-heptanol and benzyl alcohol, which implied the relatively lower leaching of the complex in 1-hexanol catalytic reaction systems. This was also supported by the higher loading of the complex found after the fifth cycle of 1-hexanol catalysis with the solid-vapor method, which was 0.015 mmol complex/gm BP-1 (Table 4.6). 1-hexanol catalysis was carried out at 157°C, while the corresponding reaction temperatures for 1-heptanol and benzyl alcohol reaction were 176°C and 178°C. Higher reaction temperatures in the 1-heptanol and benzyl alcohol reaction systems might have enhanced the leaching or decomposition of Ru-PNN from BP-1surfaces and caused the relatively higher decrease of the corresponding reaction yields in comparison to the 1-hexanol system.

Immobilized Ru-PNN on BP-1 (**7**) lost its catalytic activity in each cycle by both methods, which was evidenced by the reduction of alcohol conversion observed in the corresponding catalytic cycles. In some cases, the reduction of alcohol conversions between two successive reaction cycles was relatively lower than the corresponding loss or degradation of the catalyst from the BP-1 surface as estimated from Ru analysis (Table 4.6, 4.8, 4.10). This could be due to the formation of more deprotonated Ru-PNN species on BP-1 in the repeated cycles of catalysis because the loss of some catalysts from the BP-1 surface might reduce the steric hindrance and make more amines accessible to the pincer arm for deprotonation. The dearomatized complex, (PNN-)RuH(CO) might be leached off or decomposed from the BP-1 surface more readily than the original pincer complex.

FT-IR spectra of the resulting composite, BP-1-Ru-PNN (**7**) after catalysis showed metal carbonyl stretch at 1944 cm^{-1} which was very similar to that observed in the original immobilized catalyst before catalysis (1948 cm^{-1}). This confirmed the presence of Ru-PNN on BP-1 after

catalysis. However, IR data from cycles 3 to 5 were not very informative because of the low abundance of the complex on BP-1. A good correlation was also realized between the results of phosphorus and Ru-analysis of the resulting composite after catalysis which gave further evidence of the existence of Ru-PNN on BP-1 after catalysis. Slightly higher percentages of carbon and hydrogen were observed in the elemental analysis of BP-1-Ru-PNN (7) after cycle 3, which could be due to the unreacted alcohols and/or product esters remaining on the composite after washing. Solid-state ^{13}C NMR spectra of the BP-1-Ru-PNN (**7**) after catalysis displayed expected resonances for pyridine carbons at δ 162.5 and for the *tert*-butyl and ethyl carbons of the complex at δ 22.1 and 62.3 ppm respectively which were very similar to those observed for the complex on BP-1 before catalysis (Figure A17 in Appendix A). This suggested that the Ru-PNN complex remained intact on BP-1after catalysis. However, the relative intensity of resonances decreased in CPMAS solid state ^{13}C NMR spectra of the resulting composite going from cycle 1 to 3 (Figures A17-A19). This demonstrated the gradual leaching of the complex from the BP-1 surfaces at each cycle of the reactions which was consistent with the relative decrease of the alcohol conversions noticed from cycle to cycle. The immobilized Ru-PNN completely leached off after the fifth catalytic cycle as evidence by the loading of the complex from the resulting composite except in the 1-hexanol system where a trace of catalyst might have remained on BP-1 as observed from the loading data (Table 4.6). This was further supported by the solid-state CPMAS ^{13}C and ^{31}P NMR spectra of the resulting composite where there were no resonances appeared for the immobilized Ru-PNN after cycle 5. Solid-state CPMAS ^{31}P NMR spectra of BP-1-Ru-PNN (**7**) did not show any resonance even after the first cycle of catalysis, which could be due to the low abundance of the complex on BP-1. There was no regular trend observed in the reduction of alcohol conversions between two successive cycles of catalysis irrespective of the methods used. In all three catalytic

systems very good agreement was found between the degree of the reduction of ester yields and the corresponding loss/leaching of Ru-PNN in the successive cycles, which rationalized the decrease of alcohol conversions from cycle to cycle. Turnover frequencies (h^{-1}) for all three alcohol reaction systems varied from cycle to cycle (Table 4.5, 4.7, 4.9); however, they were considerably lower than those observed in the homogeneous systems.[41]

4.3.6 Control experiments with 1-hexanol and BP-1-Ru-PNN (7) system

Heterogeneous catalysis is a very important process frequently used in industry because it saves expensive catalyst complexes for multiple cycles of reactions. However, loss or degradation of catalysts from support solids has always been a major concern in its applications to large-scale commercial production. It was quite clear that the decrease of reaction yields in the multiple cycles of catalytic reactions with 1-hexanol, 1-heptanol, and benzyl alcohol were due to the leaching or decomposition of catalysts from BP-1 surfaces. These observations lead to a major concern: whether alcohol catalysis occurring on BP-1 surfaces was truly heterogeneous in nature or whether the complexes leached off the BP-1 surfaces into solutions at the beginning of the reactions and then perform catalysis. Literature reports have shown a lot of controversy regarding the heterogeneous catalytic processes on a solid surface with immobilized catalysts, particularly when leaching or decrease of performance of catalysts observed in repeated reaction cycles.[12,63-64,104] In our catalytic study, we assumed two possibilities: (i) immobilized catalysts remained on the BP-1 surfaces during catalysis and performed alcohol catalysis on the surfaces, then leached off or decomposed at the end of the catalytic reactions. (ii) immobilized catalysts leached off from the BP-1 surfaces at the beginning of the catalytic reactions and mixed with reactant alcohols and the catalysis was accomplished in the solution phase. The main goal of the control experiments was to clarify these possibilities and to prove the heterogeneity of the catalytic processes occurring on

the BP-1 surfaces with immobilized Ru-PNN complex. The experiments were carried out with 1-hexanol by BP-1-Ru-PNN (**7**) in the absence of a base and with the addition of 1 equivalent of KOH.

The control experiments involved four steps reactions. In the first step, the mixture of 1-hexanol and BP-1-Ru-PNN (**7)** was stirred at room temperature under argon for 4-5 hours. The resulting liquid mixture was tested by GC-MS. No conversion of alcohol was observed in this step, which means alcohol catalysis on BP-1 with immobilized Ru-PNN did not occur at room temperature. In step 2 when 1-hexanol and BP-1-Ru-PNN (**7)** were heated at 157°C under the flow of argon for about 16 hours, 30% hexyl hexanoate yield was noticed. This suggested that higher reaction temperature is required for alcohol catalysis on BP-1-Ru-PNN (7). In step 3, the resultant reactant mixture from step 2 was heated further at 157°C for about 3-4 hours, and 4% conversion of 1-hexanol alcohol was found. This result indicated that the reaction was not yet completed and the longer reaction period would be required to complete the reaction, as well as the Ru-PNN catalyst remaining on the BP-1 surface during catalysis. After step 3, the liquid mixture was separated from BP-1-Ru-PNN (**7**). Then the resultant liquid mixture was heated in step 4 at 157°C for 15 hours under argon in the absence of the catalyst, BP-1-Ru-PNN (**7)**. GC-MS analysis on the product mixture from step 4 showed only 2-3% conversion, which clearly showed that immobilized Ru-PNN remained intact on the BP-1surface during catalysis, otherwise considerable conversion of 1-hexanol should have been realized at this stage. This also confirmed that immobilized Ru-PNN is catalyzing alcohol reactions on BP-1 surface to form corresponding esters and H_2 as well as that the catalytic reaction proceeded in a heterogeneous manner. The appearance of a very small amount of conversion of alcohol (2-3%) in step 4 might have been due to the leaching of a very small amount of Ru-PNN from BP-1 surfaces, which could be negligible

considering the total conversion of alcohol at the end of the corresponding catalytic reaction. When the same control experiment was carried out in the presence of 1 equivalent of KOH, following steps 1 to 4, similar results were observed in each of the steps except the formation relatively more ester yield (36%) in step 2. This further confirmed the heterogeneity of the alcohol catalysis reaction on BP-1 by immobilized Ru-PNN (**7**) complex even in the presence of a base. However, the reduction of alcohol conversions in the cycle study (cycles 2 to 5) and respective decrease in the loading of the complex on the resulting composite BP-1-Ru-PNN (**7)** reflected the leaching of the catalyst from BP-1 surface which occurred in the catalytic reactions. Based on the results of our control experiments, we are strongly convinced that the immobilized Ru-PNN caused the alcohol catalysis and remained on the BP-1 surfaces during catalysis and then leached away or decomposed at the end of reaction. Formation of a significant percentage/proportion of reaction yields within the first 25-30 hours of catalytic reactions also supported that.

4.3.7 Control experiments with BP-1 and silica gel

The physical and chemical properties of solid supports as well as their stability are very important in the heterogeneous catalytic reactions.[12,14-17] An ideal and suitable solid support must be neutral or non-reactive toward the catalytic reactions. Since BP-1 was synthesized from modified silica gel, it was important to see any influence of silica gel or BP-1 in the alcohol catalytic processes. Silica materials were reported to be chemically inert toward many reactants because they do not have pronounced functionality on their surfaces, which can induce side reactions in the catalytic processes.[12]

The objective of the control experiments with BP-1 and silica gel was to investigate any reactivity or participation of BP-1 or silica gel in alcohol catalytic processes. The experiments were conducted using three alcohols with BP-1 and silica gel separately. The reactions of BP-1

with 1-hexanol, 1-heptanol, and benzyl alcohol respectively, following similar conditions to those described in sections 4.2.6 and Table 4.2, did not produce any esters, aldehyde or H_2. Similarly, chemical treatment of silica gel with 1-hexanol, 1-heptanol, and benzyl alcohol respectively did not result in any product formation. This confirms the neutrality and non- reactivity of BP-1 and silica gel in alcohol catalytic reactions. In the filtration experiment, immobilized catalysts BP-1-Ru-PONOP (**1**) and BP-1-Ru-PNN (**7**) were heated with 1,4-dioxane separately. The resulting filtrate was tested for catalytic activity in the reaction with 1-heptanol. No alcohol conversions were realized with the filtrate, which confirmed that the complexes were covalently immobilized on BP-1 and no physiosorption was involved in the immobilization processes.

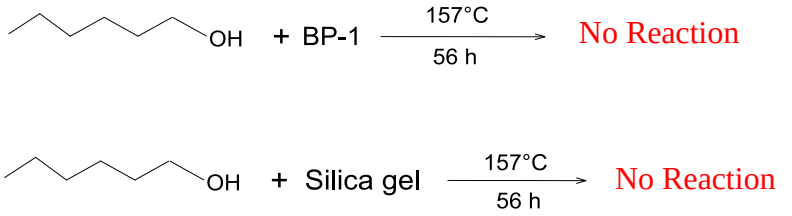

Scheme 4.14: Reaction of 1-hexanol with: (a) BP-1 and (b) silica gel

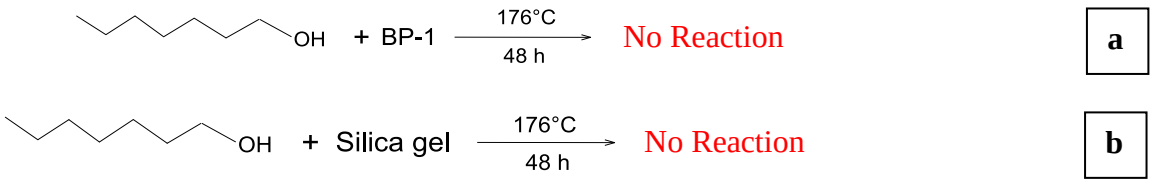

Scheme 4.15: Reaction of 1-heptanol with: (a) BP-1 and (b) silica gel

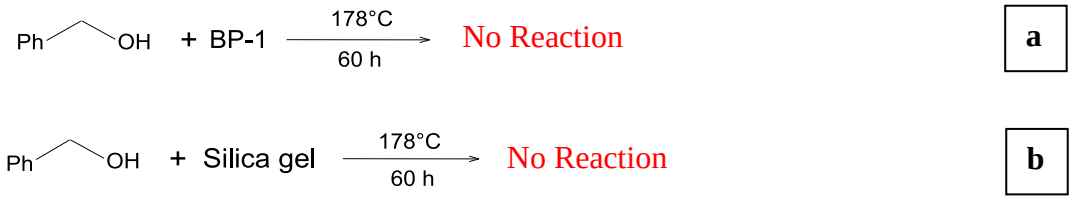

Scheme 4.16: Reaction of benzyl alcohol with: (a) BP-1 and (b) silica gel

Chapter 5

Catalytic study on alcohol dehydrogenation reactions on silica polyamine composites, BP-1 by immobilized (PONOP)RuH(Cl)(CO) (1)

5.1 Introduction

PONOP [2,6-bis(di-*tert*-butylphosphinito)pyridine] is an interesting and attractive pincer ligand. It was first reported by Milstein and coworkers.[87,105] It can easily be coordinated to different transition metals such as Ru, Rh, Ni, Pd, Ir, and form interesting stable complexes.[20, 87,105] PONOP analogues POCOP metal complexes have already been shown to catalyze various chemical transformations.[106-111] PONOP *trans*-hydride ruthenium complex has exhibited reactivity toward water and eletrophiles.[87] Though many PONOP metal complexes have been shown in the literature, to date, there have been no reports of catalysis with (PONOP)RuH(Cl)(CO) pincer complex system.[20,87,105] However, its analogue, (PNN)RuH(Cl)(CO) has shown very interesting catalytic reactivity in various chemical transformations.[41,45-53] In light of this perspective, we became interested in investigating the catalytic reactivity of (PONOP)RuH(Cl)(CO) in dehydrogenative coupling of alcohols reactions in solution. The interesting results of our heterogeneous alcohol catalysis with the BP-1-Ru-PNN (7) system motivated us to explore the catalytic reactivity of (PONOP)RuH(Cl)(CO) on BP-1 as well. Immobilized BP-1-Ru-PONOP obtained by method 1 was used in this catalytic study. Scheme 5.1 shows the general reactions of dehydrogenative coupling of alcohol reactions by immobilized Ru-PONOP on BP-1 (**1**).

$$2\ RCH_2OH \xrightarrow[\triangle]{\text{(PONOP)RuHCl(CO) on BP-1}} RCO_2CH_2R + 2H_2 \qquad R = \text{Alkyl/Aryl}$$

Scheme 5.1: General reaction of alcohol dehydrogenation by BP-1-Ru-PONOP (**1**)

5.2 Experimental

5.2.1 Experimental procedures for catalytic study in dehydrogenative coupling of alcohols to esters and hydrogen by (PONOP)RuH(Cl)(CO) in solution

12 mg of (PONOP)RuH(Cl)(CO) (0.02 mmol) was placed in a small round-bottom flask. 20 mmol of alcohol was added. The mixture was degassed by an applied vacuum. The mixture was then heated with slow stirring under at an inert atmosphere of argon. The reaction mixture was cooled to room temperature. The liquid product mixture was analyzed by GC-MS, using an HP 5 column on an Agilent 6890N GC-MS system. Total alcohol conversion and reaction conditions for each alcohol catalysis are summarized in Table 5.1.

Table 5.1: Conversion of alcohol to corresponding esters and hydrogen with (PONOP)RuH(Cl)(CO) in solution in the absence of a base and with KOH.

Alcohol	Base (mmol)	Catalyst / Alcohol ratio (mmol)	Reaction Temp (°C)	Reaction Time (Hours)	Total alcohol conversion (%)	Turnover frequency (Hour $^{-1}$)
1-Hexanol	-	0.01/10	157	36	0	-
	0.01	0.01/10	157	36	61 (60% Hexyl hexanoate and 0.5% 1-Hexanal) Range: 60-62	17
1-Heptanol	-	0.01/10	176	24	0	-
	0.01	0.01/10	176	24	69 (67% Heptyl heptanoate and 2% 1-Heptanal) Range: 68-69	28
Benzyl alcohol	-	0.01/10	178	24	0	-
	0.01	0.01/10	178	24	66 (62% Benzyl benzoate and 4% Benzaldehyde) Range: 65-67	27
2-octanol	-	0.01/10	178	24	0	-
	0.01	0.01/10	178	24	65% 2-octanone Range: 64-65	28

5.2.2 Reaction protocols for conversion of 1-heptanol to heptyl heptanoate, 1-heptanal, and hydrogen with (PONOP)RuH(Cl)(CO)-n-butyl amine (6) in the presence of KOH

13 mg of (PONOP)RuH(Cl)(CO)-n-butyl amine (**6**) (0.02 mmol) and 0.02 mmol of KOH were mixed in a small round-bottom flask. 20 mmol of 1-heptanol was added. The mixture was degassed by an applied vacuum. The mixture was then heated at 176°C with slow stirring under an inert atmosphere of argon for 48 hours. The reaction mixture was cooled to room temperature. The liquid product mixture and catalyst were separated by filtration. The liquid product mixture was analyzed by GC-MS using an HP 5 column on an Agilent 6890N GC-MS system. Total 1-heptanol conversion (after 24 hours): 42%, after 48 hours: 54%. Heptyl heptanoate: 52%. 1-Heptanal: 2%. 1-Heptanol conversion after 48 hours, from the similar reaction between (PONOP)RuH(Cl)(CO)-n-butyl amine (6) and 1-heptanol in the absence of KOH : 0%

5.2.3 Experimental procedures for alcohol dehydrogenation reactions catalyzed by immobilized (PONOP)RuH(Cl)(CO) on BP-1 in the absence of a base and with KOH

200 mg of BP-1-Ru-PONOP (**1**) (0.007 mmol catalyst on BP-1) was placed in a small round-bottom flask. 21 mmol of alcohol was added. In the case of 1-hexanol, 400 mg of BP-1-Ru-PONOP was added into 35 mmol of alcohol. The mixture was degassed by an applied vacuum. The mixture was then heated with slow stirring under an inert atmosphere of argon. The reaction mixture was cooled to room temperature and the composite catalyst was separated by filtration. The resulting liquid product mixture was analyzed by GC-MS using an HP 5 column on an Agilent 6890N GC-MS system. Total alcohol conversion and reaction conditions for each of alcohol catalysis are summarized in Table 5.2

Table 5.2: Conversion of alcohol to corresponding esters and hydrogen with immobilized (PONOP)RuH(Cl)(CO) on BP-1 (1) in the absence of a base and with KOH

Alcohol	Base (mmol)	Catalyst / Alcohol ratio (mmol)	Reaction Temp (°C)	Reaction Time (Hours)	Total alcohol conversion (%)	Turnover frequency (Hour $^{-1}$)
1-Hexanol	-	0.02/50	157	56	43 (42% Hexyl hexanoate and 0.6% 1-Hexanal) Range: 42-43	19
	0.01	0.02/50	157	56	47 (46% Hexyl hexanoate and 0.7% 1-Hexanal) Range: 46-48	21
1-Heptanol	-	0.01/30	176	48	55 (52% Heptyl heptanoate and 3% 1-Heptanal) Range: 54-55	34
	0.01	0.01/30	176	48	60 (56% Heptyl heptanoate and 4% 1-Heptanal) Range: 59-61	38
Benzyl alcohol	-	0.01/30	178	60	49 (38% Benzyl benzoate and 11% Benzaldehyde) Range: 47-50	25
	0.01	0.01/30	178	60	56 (42% Benzyl benzoate and 14% Benzaldehyde) Range: 55-59	28
2-octanol	-	0.01/30	178	48	48% 2-octanone Range: 47-48	30
	0.01	0.01/30	178	48	54% 2-octanone Range: 53-56	34

5.2.4 Experimental procedures for alcohol dehydrogenation reactions catalyzed by immobilized (PONOP)RuH(Cl)(CO) on BP-1 in the presence of solvent

5.2.4.1 Reaction protocols for 1-hexanol catalysis with immobilized (PONOP)RuH(Cl)(CO) on BP-1 in the presence of toluene

400 mg of BP-1-Ru-PONOP (**1**) (0.014 mmol Ru-PONOP on BP-1) and 35 mmol of 1-hexanol were mixed in a small round-bottom flask. 2mL of toluene was added. The mixture was degassed by an applied vacuum. The mixture was then refluxed with slow stirring under an inert atmosphere of argon for 56 hours. Reaction mixture was cooled to room temperature. The liquid

product mixture and catalyst were separated by filtration. The formation of hexyl hexanoate was determined by GC using an HP 5 column on an Agilent 6890N GC-MS system. Total 1-hexanol conversion: 0 %

5.2.4.2 Reaction protocols for 1-hexanol catalysis with immobilized (PONOP)RuH(Cl)(CO) on BP-1 in the presence of toluene and KOH

400 mg of BP-1-Ru-PONOP (**1**) (0.014 mmol Ru-PONOP on BP-1) and 0.014 mmol KOH were suspended into 35 mmol of 1-hexanol in a small round-bottom flask. 2mL toluene was added. The mixture was degassed by an applied vacuum. The mixture was then refluxed with slow stirring under at an inert atmosphere of argon for 56 hours. The reaction mixture was cooled to room temperature. The liquid product mixture and catalyst were separated by filtration. The formation of hexyl hexanoate was determined by GC using an HP 5 column on an Agilent 6890N GC-MS system. Total 1-hexanol conversion: 0 %

5.2.4.3 Reaction protocols for 1-heptanol catalysis with immobilized (PONOP)RuH(Cl)(CO) on BP-1 in the presence of dichlorobenzene

200 mg of BP-1-Ru-PONOP (**1**) (0.007 mmol Ru-PONOP on BP-1) and 21 mmol of 1-heptanol were mixed in a small round-bottom flask. 2mL of 1,2-dichlorobenzene was added. The mixture was degassed by an applied vacuum. The mixture was then refluxed with slow stirring under an inert atmosphere of argon for 48 hours. The reaction mixture was cooled to room temperature. The liquid product mixture and catalyst were separated by filtration. The formation of heptyl heptanoate and 1-heptanal was determined GC using an HP 5 column on a Agilent 6890N GC-MS system. Total 1-heptanol conversion: 30% (Heptyl heptanoate 29 % and 1-Heptanal 1%)

5.2.4.4 Reaction protocols for 1-heptanol catalysis with immobilized (PONOP)RuH(Cl)(CO) on BP-1 in the presence of dichlorobenzene and KOH

200 mg of BP-1-Ru-PONOP (**1**)(0.007 mmol Ru-PONOP on BP-1) and 0.007 mmol KOH were suspended into 21 mmol of 1-heptanol in a small round-bottom flask. 2mL of 1,2-dichlorobenzene was added. The mixture was degassed by an applied vacuum. The mixture was then refluxed with slow stirring under at an inert atmosphere of argon for 48 hours. Reaction mixture was cooled to room temperature. The liquid product mixture and catalyst were separated by filtration. The formation of heptyl heptanoate and 1-heptanal was determined by GC using an HP 5 column on a Agilent 6890N GC-MS system. Total conversion: 36% (Heptyl heptanoate 33 % and 1-Heptanal 3%)

5.2.5 Experimental procedures for cycle study in alcohol dehydrogenation reactions by immobilized (PONOP)RuH(Cl)(CO) on BP-1 (1)

5.2.5.1 Reaction protocols for conversion of alcohols to corresponding esters and hydrogen by BP-1-Ru-PONOP (**1**) with the solid-liquid method

200 mg of BP-1-Ru-PONOP (**1**) (0.007 mmol complex on BP-1) and 21 mmol of alcohols (except 1-hexanol where 400 mg Ru-PONOP-BP-1 and 35 mmol alcohol were used) were mixed in a small round-bottom flask. The flask was equipped with a condenser. The mixtures were stirred slowly by heating an inert atmosphere of argon. Temperature and other reaction conditions were described in experimental section 5.2.3 and Table 5.2. When the reaction was complete, the reaction mixture was cooled to room temperature. The composite catalyst and liquid product mixture were separated by filtration and then the catalyst BP-1-Ru-PONOP (**1)** was washed with acetone, toluene, and CH_2Cl_2 and then dried under high vacuum. The liquid product mixtures were analyzed by GC using an HP 5 column on an Agilent 6890N GC-MS system. The dried BP-1-Ru-

PONOP (**1)** was used for the next cycle and the overall procedure was repeated. Yields and conversion of alcohols to corresponding esters in each of the successive cycles are given in Table 5.5-5.10.

5.2.5.2 Reaction protocols for conversion of alcohols to corresponding esters and hydrogen by BP-1-Ru-PONOP (**1**) with the solid-vapor method

The ratio of catalyst, BP-1-Ru-PONOP **(1)** to alcohol used in the solid-vapor method was similar to those applied in the solid-liquid method. In the solid-vapor method, the required amount of composite catalyst (as described in section 5.2.3 and Table 5.2) was placed in a glass frit. The frit was then equipped with a small round bottom flask containing the appropriate amount of alcohols (section 5.2.3 and Table 5.2). A water condenser was placed on the top of the frit. The whole system was then degassed by an applied vacuum. Alcohol vapor was created by heating the round bottom flask which then passed through the composite catalyst bed. Alcohol vapor passed through the catalyst bed as it moved up and then condensed back into the round bottom flask, and the process was repeated as the reaction proceeded. After the reaction was over, the system was cooled to room temperature and the set up was disassembled. The liquid product mixture was analyzed by GC using an HP 5 column on an Agilent 6890N GC-MS system. The composite catalyst was washed with acetone, toluene, and CH_2Cl_2, and dried under high vacuum. The dried composite catalyst was used for the next cycles and the overall procedure was repeated. Yields and conversion of alcohols to corresponding esters are given in Table 5.5-5.10. Solid state CPMAS NMR data and FT-IR data on BP-1-Ru-PONOP (**1**) after catalysis are given in Table 5.3. The results of elemental analysis and metal digestion study on BP-1-Ru-PONOP (**1**) after catalysis are shown in Table 5.4.

Table 5.3: Characterization of BP-1-Ru-PONOP (**1**) after 1-hexanol catalysis

Alcohol catalysis	Solid-state CPMAS ^{13}C NMR, δ (ppm)	Solid-state CPMAS ^{31}P NMR, δ (ppm)	IR spectra (KBr pellet) (ν CO)
Cycle 1	163.3 (pyridine), 29.4 (CH_2 polyamine), 25.3 (*tert*-butyl), 13.7 (*tert*-butyl), - 3.9(Si-CH_3)	50.3, 72.0	1956 cm^{-1}
Cycle 2	162.4 (pyridine), 28.3 (CH_2 polyamine), 25.2 (*tert*-butyl), 13.8 (*tert*-butyl), - 4.4 (Si-CH_3)	No resonance	1956 cm^{-1}
Cycle 3	160.0 (pyridine), 31.5(CH_2 polyamine), 25.2 (*tert*-butyl), 13.6 (*tert*-butyl), - 4.1 (Si-CH_3)	No resonance	-

Table 5.4: Elemental analysis data of BP-1-Ru-PONOP (**1**) after catalysis using sold-vapor method

Alcohol catalysis	Cycle 1			Cycle 3		
	Elemental analysis	Amount of complex remaining (mmol/gm BP-1) from elemental	Amount of complex remaining (mmol/gm BP-1) from metal digestion	Elemental analysis	Amount of complex remaining (mmol/gm BP-1) from elemental	Amount of complex remaining (mmol/gm BP-1) from metal digestion
1-Hexanol	C 13.47%, H 3.13%, N 2.10%, P 0.148%, Cl 0.24%	0.024	0.030	C 15.39%, H 3.65%, N 1.87%, P 716ppm, Cl 0.19%	0.012	0.019
1-Heptanol	C 13.80%, H 3.18%, N 1.98%, P 0.135%, Cl 0.22%	0.021	0.029	C 15.19%, H 3.74%, N 1.64%, P 601 ppm, Cl 0.15%	0.009	0.015
Benzyl alcohol	C 13.93%, H 3.24%, N 1.76%, P 0.118%, Cl 0.19%	0.019	0.028	C 15.57%, H 3.81%, N 1.57%, P 295 ppm, Cl 0.14%	0.005	0.008

Table 5.5: Cycle study on 1-hexanol catalysis with BP-1-Ru-PONOP (1) using the **solid-liquid (SL)** and **solid-vapor (SV)** methods

Alcohol	Reaction configuration	Catalyst/ Alcohol ratio (mmol)	Reaction Temp (°C)	Reaction Time (Hours)	Total 1-hexanol conversion (%)	Decrease in 1-hexanol conversion between two cycles (%)	Turnover frequency (Hour $^{-1}$)
1-Hexanol 1st Cycle	SL	0.02/50	157	56	43	-	19
	SV	0.02/50	Passing alcohol vapor over catalyst bed	56	41	-	18
1-Hexanol 2nd Cycle	SL	0.02/50	157	56	32	26	14
	SV	0.02/50	Passing alcohol vapor over catalyst bed	56	35	15	16
1-Hexanol 3rd Cycle	SL	0.02/50	157	56	20	37	9
	SV	0.02/50	Passing alcohol vapor over catalyst bed	56	26	26	12
1-Hexanol 4th Cycle	SL	0.02/50	157	56	10	50	4
	SV	0.02/50	Passing alcohol vapor over catalyst bed	56	16	38	7

Table 5.6: Comparison between the decrease in 1-hexanol conversions and the loading of the complex remaining on BP-1 after catalysis with BP-1-Ru-PONOP (1) using the **solid-vapor (SV)** and **solid-liquid (SL)** methods

Cycle	Method	Total conversion of 1-hexanol (%)	Decrease in conversion (%) between the cycles	Amount of complex remaining (mmol/gm BP-1) after cycle based on Ru analysis	Decrease in loading of Ru-PNN (%)between the cycles
1	SV	41 (Hexyl hexanoate 40% and 1-Hexanal 0.6%)	-	0.030	14
	SL	43 (Hexyl hexanoate 42% and 1-Hexanal 0.7%)	-	0.025	28
3	SV	26 (Hexyl hexanoate 25% and 1-Hexanal 0.5%)	36	0.019	37
	SL	20 (Hexyl hexanoate 19% and 1-Hexanal 0.6%)	53	0.011	56
4	SV	16 (Hexyl hexanoate 15% and 1-Hexanal 0.4%)	38	0.012	37
	SL	10 (Hexyl hexanoate 9% and 1-Hexanal 0.5%)	50	0.006	45

Table 5.7: Cycle study on 1-heptanol catalysis with BP-1-Ru-PONOP (**1**) using the **solid-liquid (SL)** and **solid-vapor (SV)** methods

Alcohol	Reaction configuration	Catalyst/ Alcohol ratio (mmol)	Reaction Temp (°C)	Reaction Time (Hours)	Total 1-heptanol conversion (%)	Decrease in 1-heptanol conversion between two cycles (%)	Turnover frequency (Hour $^{-1}$)
1-Heptanol	SL	0.01/30	176	48	55	-	34
1st Cycle	SV	0.01/30	Passing alcohol vapor over catalyst bed	48	51	-	32
1-Heptanol	SL	0.01/30	176	48	37	32	23
2nd Cycle	SV	0.01/30	Passing alcohol vapor over catalyst bed	48	42	18	26
1-Heptanol	SL	0.01/30	176	48	20	46	13
3rd Cycle	SV	0.01/30	Passing alcohol vapor over catalyst bed	48	27	36	17
1-Heptanol	SL	0.01/30	176	48	7	65	4
4th Cycle	SV	0.01/30	Passing alcohol vapor over catalyst bed	48	14	48	9

Table 5.8: Comparison between the decrease in 1-heptanol conversions and the loading of the complex remaining on BP-1 after catalysis with BP-1-Ru-PONOP (**1**) using the **solid-vapor (SV)** and **solid-liquid (SL)** methods

Cycle	Method	Total conversion of 1-heptanol (%)	Decrease in conversions between the cycles (%)	Amount of complex remaining (mmol/gm BP-1) after each cycle based on Ru analysis	Decrease in loading of Ru-PNN between the cycles (%)
1	SV	51 (Heptyl heptanoate 48% and Heptanal3%)	-	0.029	17
	SL	55 (Heptylheptanoate52% and 1-Heptanal3%)	-	0.024	31
3	SV	27 (Heptyl heptanoate 25% and Heptanal2%)	47	0.015	48
	SL	20 (Heptylheptanoate18% and 1-Heptanal2%)	64	0.009	63
4	SV	14 (Heptyl heptanoate 13% and 1-Heptanal 1%)	48	0.007	53
	SL	7 (Heptylheptanoate6% and1-Heptanal0.5%)	65	-	-

Table 5.9: Cycle study on benzyl alcohol catalysis with BP-1-Ru-PONOP (**1**) using the **solid-liquid (SL)** and **solid-vapor (SV)** methods

Alcohol	Reaction configuration	Catalyst/ Alcohol ratio (mmol)	Reaction Temp (°C)	Reaction Time (Hours)	Total benzyl alcohol conversion (%)	Decrease in benzyl alcohol conversion between two cycles (%)	Turnover frequency (Hour $^{-1}$)
Benzyl alcohol 1st Cycle	SL	0.01/30	178	60	49	-	25
	SV	0.01/30	Passing alcohol vapor over catalyst bed	60	47	-	24
Benzyl alcohol 2nd Cycle	SL	0.01/30	178	60	28	43	14
	SV	0.01/30	Passing alcohol vapor over catalyst bed	60	35	26	18
Benzyl alcohol 3rd Cycle	SL	0.01/30	178	60	16	43	8
	SV	0.01/30	Passing alcohol vapor over catalyst bed	60	24	30	12
Benzyl alcohol 4th Cycle	SL	0.01/30	178	60	4	75	3
	SV	0.01/30	Passing alcohol vapor over catalyst bed	60	12	50	6

Table 5.10: Comparison between the decrease in benzyl alcohol conversions and the loading of the complex remaining on BP-1 after catalysis with BP-1-Ru-PONOP (**1**) using the **solid-vapor (SV)** and **solid-liquid (SL)** methods

Cycle	Method	Total conversion of benzyl alcohol (%)	Decrease in conversions between the cycles (%)	Amount of complex remaining (mmol/gm BP-1) after each cycle based on Ru analysis	Decrease in loading of Ru-PNN between the cycles (%)
1	SV	47 (Benzyl benzoate 37% and Benzaldehyde10%)	-	0.028	20
	SL	49 (Benzyl benzoate 38% and Benzaldehyde11%)	-	0.023	34
3	SV	24 (Benzylbenzoate18 % and Benzaldehyde 6%)	49	0.013	52
	SL	16 (Benzylbenzoate13% and Benzaldehyde 3%)	67	0.008	65
4	SV	12 (Benzyl benzoate 10% and Benzaldehyde2%)	50	0.007	46
	SL	4 (Benzyl benzoate 4% and Benzaldehyde1%)	75	-	-

5.2.6 Experimental procedures for control experiments with immobilized (PONOP)RuH(Cl)(CO) on BP-1 (1)

5.2.6.1 Experimental procedure for the control experiment between 1-hexanol and BP-1-Ru-PONOP (**1**) in the absence of a base

400 mg of BP-1-Ru-PONOP (**1**) (0.014 mmol Ru-PONOP on BP-1) and 35 mmol of 1-hexanol were mixed in a small round-bottom flask. The mixture was degassed by an applied vacuum. Then the reactions were conducted following steps 1 to 4 described in section 4.2.9. Conversion of 1-hexanol to hexyl hexanoate in each of the steps was determined by using GC-MS. Yields: Step1: No conversion; Step 2: 25% ; Step 3: 4% and Step 4: 2%

5.2.6.2 Experimental procedure for the control experiment with 1-hexanol and BP-1-Ru-PONOP (**1**) in the presence of KOH

400 mg of Ru-PONOP-BP-1 (**1**) (0.014 mmol Ru-PONOP on BP-1) and 0.014 mmol of KOH were mixed in a small round-bottom flask. 35 mmol of 1-Hexanol was added. The mixture was degassed by an applied vacuum. Then the reactions were carried out following steps 1 to 4 described in section 4.2.9. Conversion of 1-hexanol to hexyl hexanoate in each of the steps was determined by using GC-MS. Yields: Step1: No conversion; Step 2: 29% ; Step 3: 6% and Step 4: 3%

5.3 Results and discussion

5.3.1 Dehydrogenative coupling of alcohols to esters and hydrogen catalyzed by (PONOP)RuH(Cl)(CO) in solution

(PONOP)RuH(Cl)(CO) successfully catalyzed the dehydrogenative coupling reactions of alcohols in solution and produced corresponding esters and hydrogen. The catalytic reactions were carried out in 1-hexanol, 1-heptanol, benzyl alcohol, and 2-octanol systems in the absence of a base as well as with KOH. The results of alcohol catalysis are presented in Table 5.1. No alcohol conversion was realized without a base in the catalytic reactions irrespective of the alcohols used. However, when the reactions were conducted in the presence of KOH equivalent to Ru-PONOP, all alcohols produced corresponding esters and hydrogen, which suggested that a base is required to generate active catalyst from (PONOP)RuH(Cl)(CO) in alcohol dehydrogenation reactions. The chemical reaction of 1-hexanol with 0.1 mol% Ru-PONOP for 36 hours at 157°C under the flow of argon yielded 61% hexyl hexanoate (Scheme 5.2). Similarly 1-heptanol was catalyzed by 0.1 mol% Ru-PONOP for 24 hours at 176°C under argon and produced 67% heptyl heptanoate, 2% 1-heptanal, and hydrogen with a turnover frequency of 58 h^{-1}. Chemical treatment of benzyl

alcohol with Ru-PONOP at 178°C under argon following similar alcohol-to-catalyst ratio resulted in the formation of benzyl benzoate, benzaldehyde, and hydrogen with an overall conversion of 66%. The secondary alcohol, 2-octanol generated a ketone, 2-octanone with a 65% yield and hydrogen by treatment with 0.1 mol% Ru-PONOP at 178°C for 24 hours under the flow of argon (Scheme 5.5)

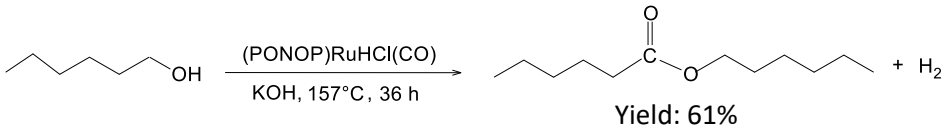

Scheme 5.2: Reaction of 1-hexanol with Ru-PONOP in the presence of KOH

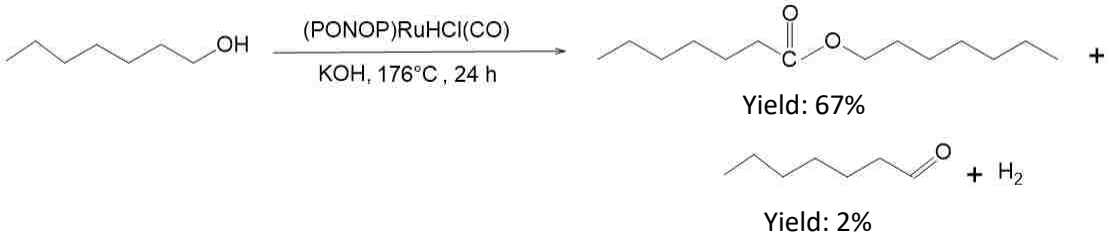

Scheme 5.3: Reaction of 1-heptanol with Ru-PONOP in the presence of KOH

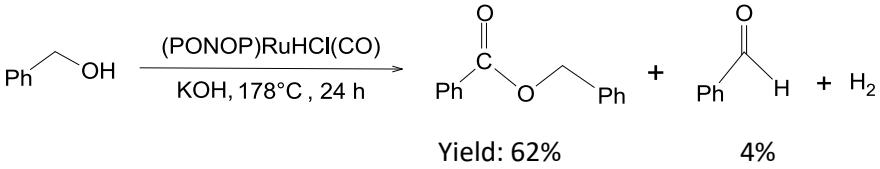

Scheme 5.4: Reaction of benzyl alcohol with Ru-PONOP in the presence of KOH

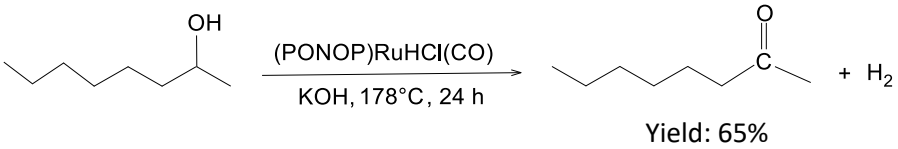

Scheme 5.5: Reaction of 2-octanol with Ru-PONOP in the presence of KOH

5.3.2 Dehydrogenative coupling of alcohols to esters and hydrogen catalyzed by (PONOP)RuH(Cl)(CO)-n-butyl amine (6) in solution

Our interesting catalytic results with Ru-PONOP in alcohol dehydrogenation reactions encouraged us to further investigate the structure and reactivity of the complex, since there was no prior record of catalytic reactivity of (PONOP)RuH(Cl)(CO) complex. The goal of this catalytic experiment was to see whether the presence of a substituent in the structure of Ru-PONOP affected its catalytic reactivity in alcohol dehydrogenation reactions. It would also verify the reactivity of (PONOP)RuH(Cl)(CO) as a suitable catalyst in solution. Chemical reaction of 1-heptanol with 0.01 mol% Ru-PONOP-n-butylamine in the presence of KOH (equivalent to Ru) at 176°C under argon yielded 42% conversion of 1-heptanol after 24 hours and continuation of the reaction up to 48 hours resulted in 54% 1-heptanol conversion (Scheme 5.6). This result further confirmed the catalytic reactivity of Ru-PONOP in homogeneous systems. However, the introduction of alkyl substituent in the structure of Ru-PONOP decreased its catalytic activity, which could be due to the steric hindrance and orientation effect of the long alkyl chain. A similar reaction between Ru-PONOP-n-butylamine (6) and 1-heptanol in the absence of KOH did not result in the formation of any ester. This suggested that amine functionality in the n-butyl substituent was not involved in the catalytic reaction.

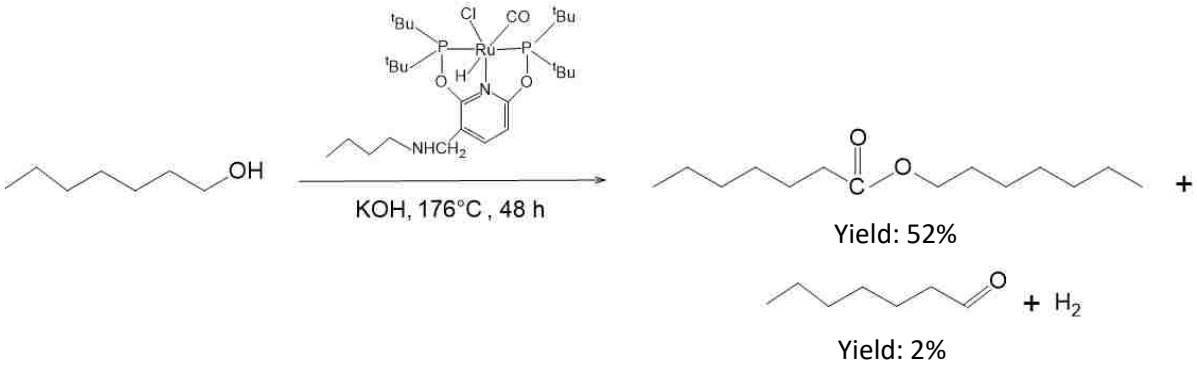

Scheme 5.6: Reaction of 1-heptanol with Ru-PONOP-n-butylamine in the presence of KOH

5.3.3 Dehydrogenative coupling of alcohols to esters and hydrogen catalyzed by immobilized (PONOP)RuH(Cl)(CO) on BP-1 (1)

The catalytic reactivity of immobilized (PONOP)RuH(Cl)(CO) on BP-1 surface was investigated in four alcohol systems: 1-hexanol, 1-heptanol, benzyl alcohol, and 2-octanol. The reactions conditions and catalyst-to-alcohol ratios used were similar to that of the Ru-PNN-BP-1 (**7**) system. The catalytic reaction of 1-hexanol on BP-1 surfaces with immobilized 0.02 mol% Ru-PONOP (**1**) at 157°C for 56 hours under an inert atmosphere of argon yielded only 26% of hexyl hexanoate. When KOH (equivalent to Ru-PONOP) was used, 1-hexanol conversion increased to 36%. Repetition of the reaction with more catalyst (0.04 mol%) with same amount of 1-hexanol following similar reaction conditions increased the alcohol conversion to 43% without a base and 47% when KOH was applied (Scheme 5.7). Other alcohols reacted similarly with BP-1-Ru-PONOP (**1**). Upon heating of 1-heptanol on the BP-1 with 0.03 mol% of loaded catalyst at 176°C for 48 hours under argon, heptyl heptanoate, 1-heptanal, and H_2 were formed with overall conversion of 55% with turnover frequency of 46 h^{-1} (Scheme 5.8). With KOH (1 equivalent to Ru), 60% of total 1-heptanol conversion was observed.

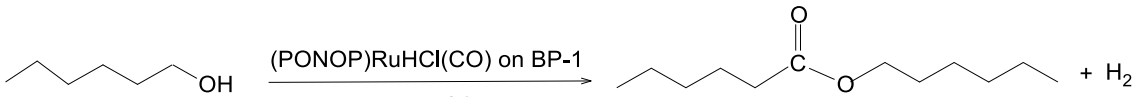

Yield: 43%

a

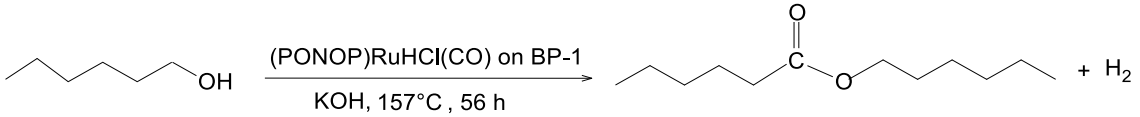

Yield: 47%

b

Scheme 5.7: Reaction of 1-hexanol with BP-1-Ru-PONOP (**1**): (a) in the absence of base and (b) with KOH

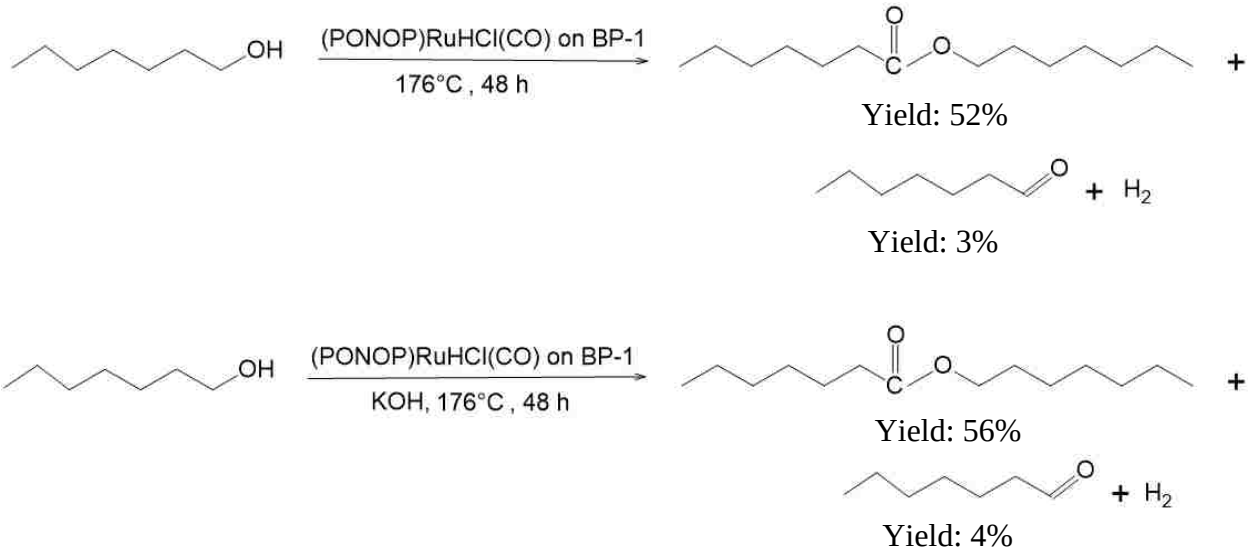

Scheme 5.8: Reaction of 1-heptanol with BP-1-Ru-PONOP (**1**): (a) in the absence of base and (b) with KOH

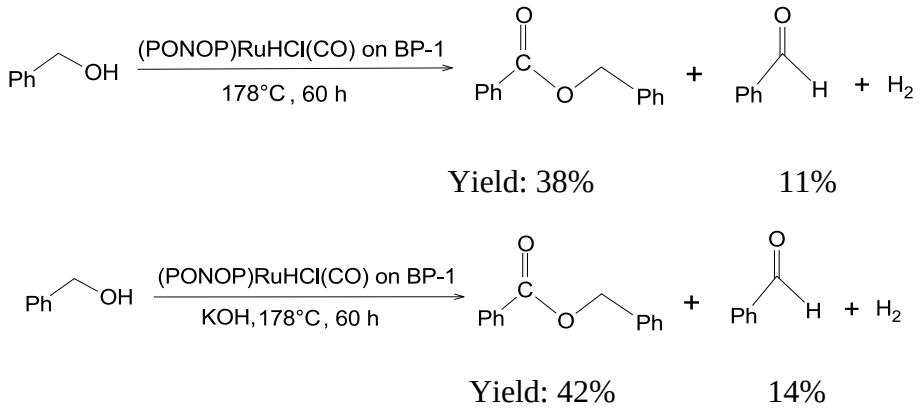

Scheme 5.9: Reaction of benzyl alcohol with BP-1-Ru-PONOP (**1**): in the absence of base and (b) with KOH

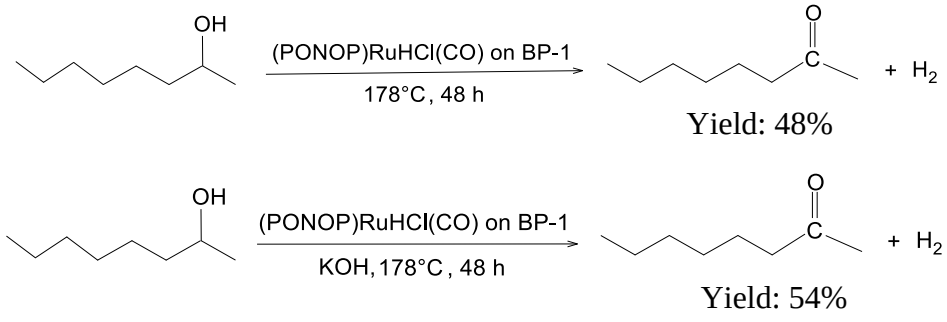

Scheme 5.10: Reaction of 2-octanol with BP-1-Ru-PONOP (**1**): (a) in the absence of base and (b) with KOH

Benzyl alcohol reacted in a similar way, with BP-1-Ru-PONOP (**1)** following a 1: 30 mmol ratio of catalyst with alcohol at 178°C under argon for 60 hours resulted in 49% conversion with 38% benzyl benzoate, 11% benzaldehyde as well as H_2 (Scheme 5.9). As in the 1-heptanol catalysis, an increase in reaction yield was realized upon the application of an equivalent amount of KOH in the benzyl alcohol reaction system (Scheme 5.9). Secondary alcohol, 2-octanol, showed the formation of a ketone, 2-Octanone and H_2 with total conversion 48% upon reaction on BP-1 by 0.03 mol% of Ru-PONOP at 175°C for 48 hours with a turnover frequency 33 h^{-1}. Addition of KOH (equivalent to Ru) increased the ketone yield to 54% (Scheme 5.10).

It has been a long time since (PONOP)RuH(Cl)(CO) and *trans*-hydride ruthenium PONOP pincer complexes were first reported in the literature.[87] However, no record of catalysis with (PONOP)RuH(Cl)(CO) in homogeneous reaction systems was found in recent literature, which predicted that the complex might not be stable enough in catalytic reaction processes. In our study, both in homogeneous and upon immobilization on BP-1 surfaces, the (PONOP)RuH(Cl)(CO) complex displayed interesting catalytic reactivity in the alcohol dehydrogenation reaction systems with moderate to good reaction yields.[92]

We propose here a mechanism of alcohol dehydrogenation reactions by homogeneous and immobilized (PONOP)RuH(Cl)(CO) on BP-1, which is depicted in scheme 5.11. Alcohol dehydrogenation to esters by Ru-PONOP might proceed by a mechanism similar to the Ru-PNN system involving an aldehyde intermediate.[41] In the first step, dehydrohalogenation of (PONOP)RuH(Cl)(CO) occurs with a base and generates a Ru(0)PONOP complex which functions as an active catalyst in the catalytic reaction. Alcohol molecules then combine with Ru(0)PONOP in the second step and form Ru(II)-hydride complex. The next step is the formation of an aldehyde accompanied by ruthenium dihydride complex, which subsequently

dehydrogenated to generate Ru(0) PONOP species again. On the other hand, the aldehyde compound reacts with another alcohol molecule to yield hemiacetal intermediate, which, followed by a second cycle, produces esters with the liberation of hydrogen. Both four-coordinate Ru(0) PONOP and dihydride-Ru(II)PONOP complexes were isolated and reported in the literature, but with P(^{i}Pr)$_3$ instead of P(^{t}Bu)$_3$.[87] As with BP-1-Ru-PNN (**7**) system, we hypothesize that amine functionality on the BP-1 surface is the base causing the dehydrohalogenation of (PONOP)RuH(Cl)(CO) to generate the active catalytic complex Ru(0)PONOP on BP-1 (Scheme 5.11).[91,92]

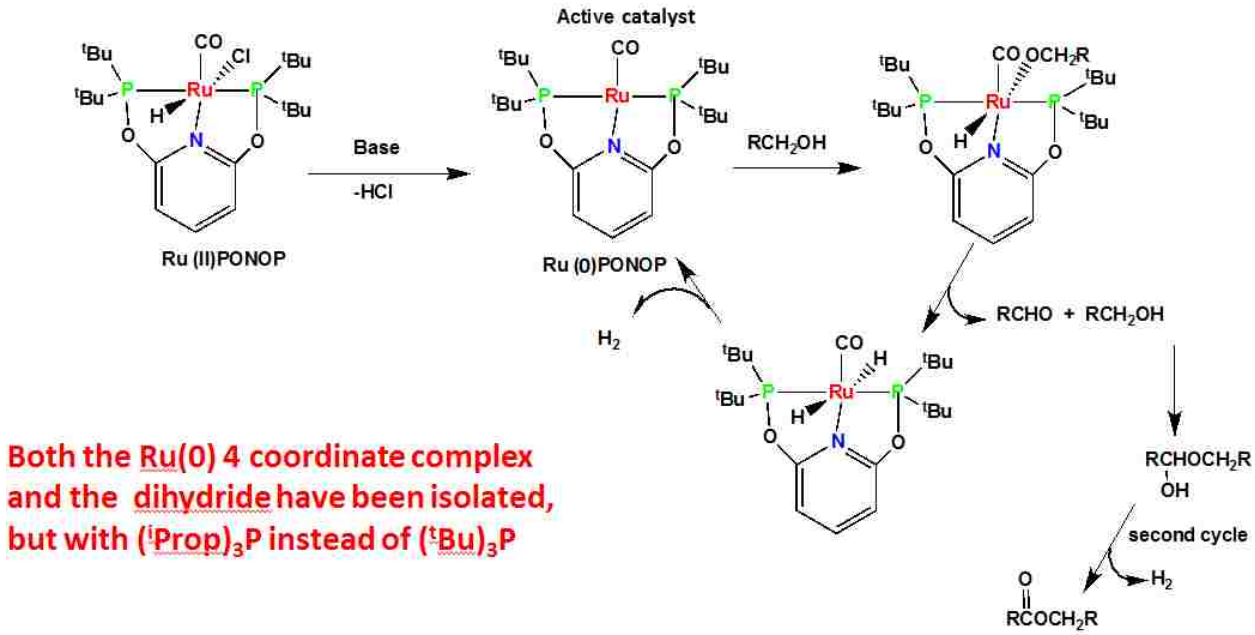

Scheme 5.11: A plausible mechanism of alcohols dehydrogenation to esters on BP-1catalyzed by immobilized(PONOP)RuH(Cl)(CO)

It was not quite clear whether all immobilized (PONOP)RuH(Cl)(CO) was converted to active catalytic species, Ru(0)complex by the amines on the BP-1 surfaces during the loading of the complex on BP-1. FT-IR data was not very informative in finding out the relative proportion

of both original complex and Ru(0)species on BP-1, since only one νCO stretch was observed in the spectra for the metal carbonyl group. The results of the model solution experiments indicated that the carbonyl stretching frequencies for Ru-PONOP compound can be shifted significantly by the attachment of a group to the pyridine ring moiety of the complex (Figure B2 in Appendix B). In fact, upon immobilization of Ru-PONOP on BP-1, metal carbonyl stretching frequency was found to be shifted by about 20 cm^{-1} (Figures B1 & B3 in Appendix B). However, there might not be considerable differences between the CO stretching frequencies of the original (PONOP)RuH(Cl)(CO) and dehydrohalogenated active catalyst-(PONOP)Ru(CO) on BP-1 surfaces based on our previous results with the BP-1-Ru-PNN (**7**) system. Solid state CPMAS ^{13}C and ^{31}P NMR data were not very helpful in figuring out the relative ratio of both species on BP-1because of the low resolution. The chemical shifts for the expected resonances of the two form of Ru-PONOP complex in the NMR spectra might be very close. Since the resonances in the solid-state NMR spectra usually appeared as a broad band, two different resonances with a small difference in chemical shifts could not be observed clearly in the corresponding spectra and they could easily overlap with each other and could appear as a single resonance.

5.3.4 The effects of solvents in the catalysis of alcohols by immobilized (PONOP)RuH(Cl)(CO) on BP-1 (1)

The chemical treatment of 1-hexanol with BP-1-Ru-PONOP (**1**) in toluene with refluxing for 56 hours under argon did not produce any ester (Scheme 5.12). Repetition of the reaction with 0.014 mmol of KOH also showed no formation of product, which indicates that alcohol catalysis on BP-1-Ru-PONOP system did not occur at a lower temperature as was noticed in the BP-1-Ru-PNN catalyst. Conducting the catalysis reaction in dichlorobenzene with 1-heptanol and 0.03 mol% Ru-PONOP on BP-1 (**1)** at refluxing for 48 hours produced 29 % heptyl heptanoate with a

trace amount of 1-heptanal (Scheme 5.13). Application of KOH (1 equivalent to Ru) in 1-heptanol catalysis with dichlorobenzene system increased the reaction yield to 36%. Similar reactions without using any solvent system at 176°C showed 1-heptanol conversion 55% without a base and 60% in KOH after 48 hours (Scheme 5.8). The presence of solvent decreased the alcohol catalysis in the heterogeneous environment. This might probably be due to the decrease in selectivity in the heterogeneous reaction system as well as for the effect of mass transfer kinetics.

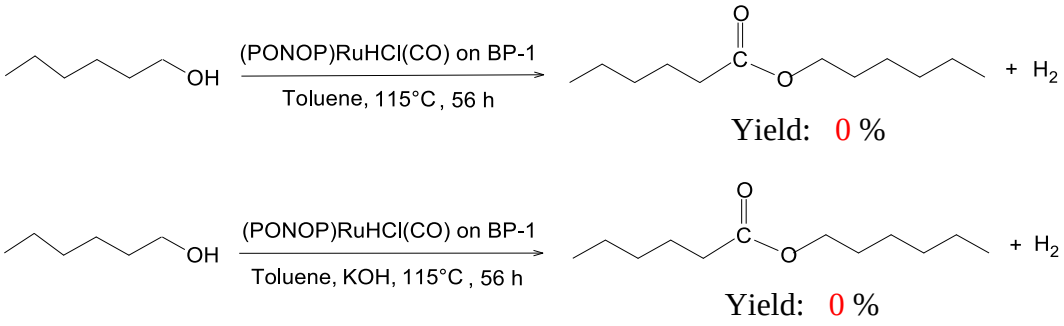

a

b

Scheme 5.12: Reaction of 1-hexanol with BP-1-Ru-PONOP (**1**) in toluene: (a) in the absence of base and (b) with KOH

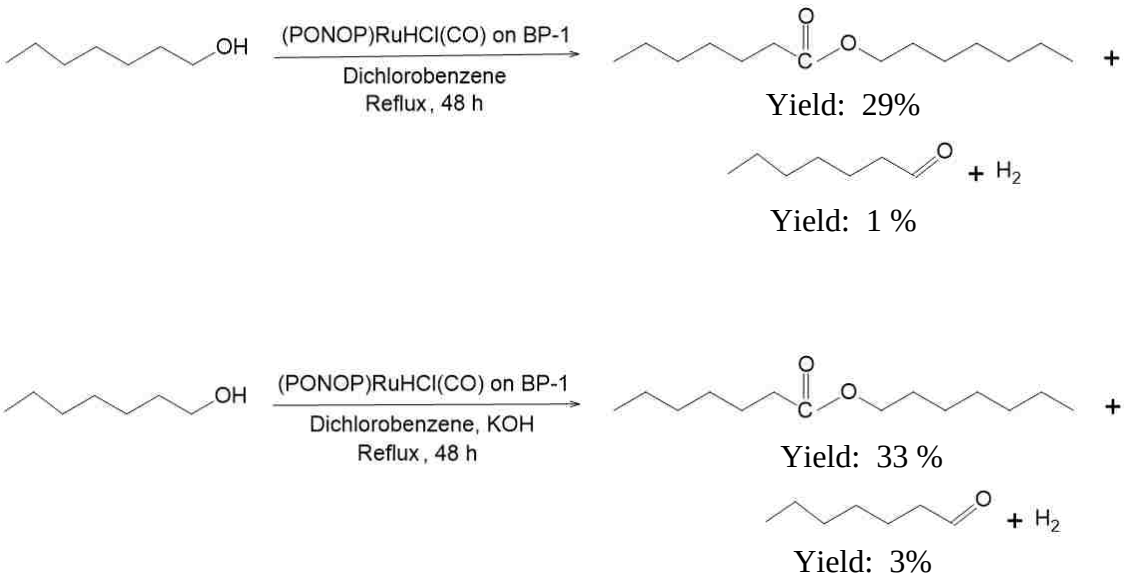

a

b

Scheme 5.13: Reaction of 1-heptanol with BP-1-Ru-PONOP (**1**) in dichlorobenzene: (a) in the absence of base and (b) with KOH

5.3.5 Cycle study on dehydrogenative coupling of alcohols to esters and hydrogen by immobilized (PONOP)RuH(Cl)(CO) on BP-1 (1) by solid-liquid and solid-vapor methods

The first attempt of homogeneous and heterogeneous catalysis with (PONOP)RuH(Cl)(CO) in alcohol dehydrogenation reactions showed us the interesting results.[92] The appearance of moderate to good conversion of starting alcohols to corresponding esters and H_2 inspired us to find out the catalytic reactivity of BP-1-Ru-PONOP (**1**) in multiple cycles of catalytic reactions. However, surface confinement and amine functionality on the BP-1 surface might allow the complex to function suitably as a catalyst in multiple catalytic cycles. In addition, attaching of an alkyl chain or other functional group with the pyridine moiety in the structure of the (PONOP)RuH(Cl)(CO) complex could influence the electron density in the metal center and might provide extra stability in the complex for functioning as a suitable catalyst in alcohol dehydrogenation reactions.[92] Very few examples have been reported in the literatures about how the substituents in the pincer complex structures affect their catalytic reactivity.[97] The main objective of this project was to investigate the recyclability of BP-1-Ru-PONOP (**1**) in alcohol dehydrogenation reactions. Another goal was to understand the stability of Ru-PONOP on the BP-1 surface in multiple cycles of catalysis. As in the BP-1-Ru-PNN (**7**) systems, in this case all the cycles reactions were also carried out by using both the old and the new methods. Catalyst-to-alcohol ratios and reaction conditions were similar to those of BP-1-Ru-PNN (**7**). In this study the recyclability of BP-1-Ru-PONOP (**1)** was evaluated up to the 4th cycle of alcohol catalysis. Cycle study was carried out in the 1-hexanol, 1-heptanol, and benzyl alcohol reaction systems. No base was used in the cycle study. After catalysis, the resulting composites were characterized by solid state NMR, FT-IR, elemental analysis, and metal digestion study.

5.3.5.1 Cycle study on 1-hexanol catalysis by immobilized (PONOP)RuH(Cl)(CO) on BP-1

1-hexanol when heated with 0.04 mol% of immobilized Ru-PONOP on BP-1 at 157°C for 56 hours under argon yielded 43% hexyl hexanoate accompanied by the liberation of H_2 in the first cycle using the solid-liquid method. With the solid-vapor method similar conversion of 1-hexanol was observed with a turnover frequency of 18 h^{-1}. The catalyst-to- alcohol ratio used in both methods was 0.014:35 in mmol. Table 5.5 shows the results of 1-hexanol catalysis with BP-1-Ru-PONOP (**1**) in multiple cycles. The comparison of the alcohol conversions with the corresponding decrease of the loading of the complex on BP-1 for cycles 1, 3 and 4 is also presented in Table 5.6. In the second cycle, the solid-vapor method showed an ester yield of 35% which was 15 % decrease from cycle 1, and the solid-liquid method provided similar conversion of 32%, which was 26% less than in cycle 1 (Table 5.5). As the catalytic reaction was repeated for cycle 3, 1-hexanol conversion decreased to 20% with solid-liquid method and 26% with the solid-vapor method, which was 26% less than cycle 2 in the solid-vapor method but 37% lower than the same cycle with the solid-liquid method. Further reduction of hexyl hexanoate yield was observed with both the solid-liquid and solid-vapor methods when the reaction was repeated in a 4^{th} cycle. From cycles 1 to 3, the overall decrease of 1-hexanol conversion was 53% with the solid-liquid method whereas in the solid-vapor method it was 36% which showed a good agreement with corresponding reduction of the loadings of the complex observed on the resulting composite, 37% and 56% respectively (Table 5.6). The reduction of hexyl hexanoate yields in cycles 1 to 4 was due to the leaching off the catalyst Ru-PONOP from the BP-1 surfaces which was evidenced from the decrease of loading of Ru-PONOP- on BP-1observed in the resulting composite BP-1-Ru-PONOP (**1**) after catalysis (Table 5.6). In both methods, the decrease of 1-hexanol conversions was highly consistent with the relative loss of the catalyst in between two successive cycles. Turnover

frequencies for all four reaction cycles were relatively lower and varied from 4 h^{-1} to 19 h^{-1}, as one could expect because of low yields of products in the catalytic reactions.

5.3.5.2 Cycle study on 1-heptanol catalysis by immobilized (PONOP)RuH(Cl)(CO) on BP-1

1-heptanol catalysis with 0.03 mol% immobilized Ru-PONOP on BP-1 (**1**) at 176°C under argon resulted in 55% conversion of alcohol to 52% heptyl heptanoate, and 3% 1-heptanal in the first cycle with the solid-liquid method, whereas 51% conversion was realized in the solid-vapor method with a similar ratio of ester to aldehyde. Ester yields dropped to 42% with solid-vapor method and 37% using solid-liquid method when the reaction was conducted for the second run with recycled BP-1-Ru-PONOP (**1)** (Table 5.7). Ru analysis data on the resulting composite showed that 17% of the catalyst leached off in cycle 1 which explains the reduction of 1-heptanol conversion from cycles 1 to 2 by 18% using the solid-vapor method (Table 5.7 & 5.8). Similarly, further decrease in heptyl heptanoate yields was observed from cycle 2 to 3 with both methods (Table 5.7). However, the decrease was higher than in the previous cycles. Cycle 4 provided 14 % yield with the solid-vapor method and only 7% using the solid-liquid method. The overall decrease of 1-heptanol conversion from cycles 1 to 4 was 72% with solid-vapor method and 88 % decrease was noticed in the solid-liquid method, which indicated that most of the catalyst was leached off at the end of the 4^{th} cycle of catalysis. This was supported by the corresponding loss of the complex from the resulting composite BP-1 (Table 5.8), which was about 76 % from cycle 1 to 4 with the solid-vapor method. There was no Ru-PONOP remaining on the BP-1 surface after the 4^{th} catalytic cycle as evidenced from Ru analysis (Table 5.7). Turnover frequencies were more or less similar to the 1-hexanol system, with a maximum of 34 h^{-1} observed in the first cycle and lower TOF as the reaction cycles increased because of lower reaction yields.

5.3.5.3 Cycle study on benzyl alcohol catalysis by immobilized (PONOP)RuH(Cl)(CO) on BP-1 (1)

The first cycle of benzyl alcohol catalysis with BP-1-Ru-PONOP (**1**) (0.03 mol% Ru-PONOP on BP-1) at 178°C produced 39% of benzyl benzoate and 10% of benzaldehyde by the solid-liquid method. Almost similar conversion of benzyl alcohol (total 47%) was observed in that cycle with the solid-vapor method as well (Table 5.9). The repetition of the reaction with recycled BP-1-Ru-PONOP (**1**) reduced benzyl alcohol conversion to 28% by the solid-liquid method and by 35 % using the solid-vapor method in the second cycle (Table 5.9). From cycles 2 to 3, the reaction yields decreased by 30% with the solid-vapor method. However, the decrease was 43% when the solid-liquid method was applied (Table 5.9). The loading of the complex in cycle 3 was found to be 0.013 mmol complex/gm BP-1 after cycle 3 which was a decrease of 52% from cycle 1 and was consistent with the decrease of alcohol conversion in the corresponding reaction cycles 1 to 3 by the solid-vapor method (Table 5.10). A similar correlation was also observed in cycles 1 to 3 with the solid-liquid method. However, the decrease of benzyl alcohol conversions and the corresponding loss of catalyst from the BP-1 surface were much higher in this case (Table 5.10). 12% Benzyl alcohol conversion was observed in cycle 4 with the solid-vapor method, while the solid-liquid method provided only 4%, indicating that almost all the catalyst had leached off. Turnover frequencies were in the range of 3 h^{-1} to 25 h^{-1}.

5.3.5.4 Comparison of cycle study on the catalysis of three alcohol systems by BP-1-Ru-PONOP (1) using the solid-liquid and solid-vapor methods

Out of three alcohols used in the catalytic cycle study with the BP-1-Ru-PONOP (**1**) system, 1-hexanol displayed better conversion in the repeated reaction cycles with both methods. On the other hand, in the first cycle of catalysis, 1-heptanol showed the highest conversion in

comparison to the other two alcohols. The percent of decrease of reaction yields in between the two successive cycles was also comparatively lower in the case of 1-hexanol catalysis, but it was found to be relatively higher in the 1-heptanol and benzyl alcohol reaction systems. There was no particular trend observed in the reduction of alcohol conversions in between the two consecutive cycles. In all cases, the highest decrease of ester yield was realized in cycle 4 and the lowest was in cycle 1, as one would predict. The decrease of alcohol conversions from cycle to cycle using both methods was due to the leaching of the catalyst Ru-PONOP from BP-1 surface during the reactions, which was evidenced by the reduction of the loading of the complex observed on the resulting composite after catalysis by both metal digestion and elemental analysis study (Table 5.4, 5.6, 5.8 & 5.10). There was very good agreement between the percent of decrease of alcohol conversions and the percentage of loss of loading of Ru-PONOP on BP-1 surface in the successive cycles of reactions in 1-hexanol, 1-heptanol, and benzyl alcohol reaction systems. This provides further evidence the loss of the Ru-PONOP from the BP-1 surface, which caused the respective decrease of alcohol conversions from cycles 1 to 4.

In all cases, application of the solid-vapor method in the alcohol catalytic systems favored the formation of more esters irrespective of the alcohols and the reaction cycle. Leaching of the catalyst from BP-1 surface was relatively higher with the solid-liquid method in comparison to that observed with the solid-vapor method. The mechanical stirring of the BP-1-Ru-PONOP (**1**) composite with alcohols for a longer reaction period might cause the degradation of some BP-1 particles and thus enhance the leaching of the catalyst and cause the decrease of the reaction yields more in the solid-liquid method. Higher reaction temperatures could also influence the decomposition of the loaded Ru-PONOP from BP-1 surfaces, evidenced by the relatively higher loss of the ester yields in the benzyl alcohol as well as in the 1-heptanol reaction systems in

comparison to the 1-hexanol reaction system. In comparison to the BP-1-Ru-PNN-BP-1 system, the differences in alcohol conversions between solid-liquid and solid-vapor methods from cycle 1 to 4 were relatively lower with BP-1-Ru-PONOP catalyst. This indicates that (PONOP)RuH(Cl)(CO) complex is comparatively less stable than (PNN)RuH(Cl)(CO) in the catalytic reactions and might have decomposed faster than Ru-PNN after catalysis. The results of the cycle study on both immobilized systems also supported this. Immobilized Ru-PNN on BP-1 showed catalytic activity up to fifth cycles in alcohol dehydrogenation reactions whereas the immobilized Ru-PONOP survived up to fourth catalytic cycles.

FT-IR spectra of Ru-PONOP on BP-1 (**1**) after catalysis showed an expected metal carbonyl stretching frequency at 1956 cm^{-1} (Figure B4 in Appendix B), which was similar to that observed before catalysis, confirming the presence of the complex on BP-1 after catalysis.[85] However, after cycles 3 and 4, FT-IR spectra were not very informative since the νCO stretch was too weak because of the low abundances of the complex on the resulting composites. There was no Ru content found on the resulting composite with the solid-liquid method after the 4^{th} catalytic cycle which showed that the loaded Ru-PONOP completely decomposed/ leached off with the repeated catalytic cycles. The elemental analysis data of BP-1-Ru-PONOP (**1**) after cycle 3 showed slightly higher percentage of carbon and hydrogen than those of cycle 1 which could be due to the remaining alcohol or product in the composite after repeated washing. Solid-state CPMAS ^{13}C NMR spectra of BP-1-Ru-PONOP (**1)** after catalysis showed the expected resonances for pyridine carbons at δ 163.3 and the resonance for *tert*-butyl carbons appeared at δ 25.3, which were very similar to those observed for the immobilized Ru-PONOP before catalysis (Figures A3 & A12 in Appendix A).[90] This suggests that the complex retained its structure on BP-1 even after catalysis. In addition, solid state CPMAS ^{31}P NMR spectra displayed resonance at δ 50.3 ppm which was

similar to that observed for BP-1-Ru-PONOP (**1)** (δ 58 ppm) before catalysis (Figures A4 & A11). This further confirmed the presence of Ru-PONOP on BP-1 after catalysis. In addition, a second ^{31}P resonance was observed at δ 72 ppm and suggested the presence of Ru(0)PONOP complex on BP-1. However, the intensity of the resonances in the solid-state CPMAS ^{13}C NMR was found to have decreased from cycles 1 to cycle 3, which can be attributed to the leaching of the Ru-PONOP from the BP-1 surfaces as the composite catalyst was recycled for multiple runs of the reactions (Figures A12-A14 in Appendix A).

5.3.6 Control experiments with 1-hexanol and BP-1-Ru-PONOP (1)

The procedures of the control experiments with BP-1-Ru-PONOP (**1**) system were similar to those conducted on BP-1-Ru-PNN (**7)**. The experiments were carried out with 1-hexanol and BP-1-Ru-PONOP (**1**) in the absence of base and in the presence of KOH involving four steps reactions. Slow stirring of the mixture of 1-hexanol with 0.04 mol% of Ru-PONOP on BP-1 at room temperature under argon for 4-5 hours did not produce any ester in step 1, indicating that no alcohol catalysis occurred on BP-1-Ru-PONOP (**1**) at room temperature. Heating of the mixture of alcohol and the catalyst BP-1-Ru-PONOP (**1**) at 157°C for about15 hours under argon in step 2 resulted in 25% yield of hexyl hexanoate. These results suggested that alcohol catalysis on BP-1 by immobilized Ru-PONOP occurred at higher reaction temperature. Step 3 showed 4% conversion of 1-hexanol when the resultant mixture of BP-1-Ru-PONOP (**1**) and 1-hexanol from step 2 was further heated at 157°C under argon for another 3-4 hours which demonstrated that the reaction was not completed at 15 hours, and the catalyst remained on the BP-1 surface and did not fall off during the catalysis. Also, a longer reaction period was required to complete the catalysis. In step 4 the resulting liquid mixture was separated from BP-1-Ru-PONOP (**1**), and was heated without any catalyst at 157°C for 15 hours under argon which yielded very little ester (2%). The

results of step 4 indicate that the immobilized Ru-PONOP remained on the BP-1 surface during alcohol catalysis and didn't leach off at the beginning of the reaction. It confirmed that alcohol catalysis occurred by immobilized Ru-PONOP on BP-1 and the catalytic process was truly heterogeneous in nature. As in the Ru-PNN-BP-1 system, we believe that alcohol catalysis on BP-1 also proceeds by the immobilized Ru-PONOP complex. The complex performs the alcohol catalysis on BP-1 surfaces and then might decompose. The very little alcohol conversion observed in step 4 also suggested that there was no significant loss of the catalyst at the beginning of the catalytic reactions. The control experiment of 1-hexanol with BP-1-Ru-PONOP (**1**) in the presence of KOH (1 equivalent to Ru) showed similar results in all four steps which further strengthened the evidence for the heterogeneity of alcohol catalysis on BP-1-Ru-PONOP- system.

Chapter 6

Formation of imines from primary amines on the silica polyamine composite, BP-1, by immobilized (PNN)RuH(Cl)(CO) and (PONOP)RuH(Cl)(CO)

6.1 Introduction

The interesting catalytic results with BP-1-Ru-PNN (**7**) and BP-1-Ru-PONOP (**1**) systems in the dehydrogenation of alcohol reactions motivated us to extend the applications of these catalytic systems to other chemical transformations. The objective of this project was to investigate the amide formation reactions from amines and alcohols. In 2007, David Milstein reported the synthesis of amides from amines and alcohols catalyzed by (PNN)RuH(Cl)(CO) (Scheme 6.1).[45]

Scheme 6.1: General reaction- amide formation from alcohols and amines catalyzed by dearomatized (PNN-)RuH(CO).[45]

We thought that it would be interesting to study the amide formation reactions on our immobilized systems. We conducted the reactions by using different amines: hexyl amines, benzyl amines and alcohols: 1-hexanol, 1-heptanol and benzyl alcohol. No amide formations was found, irrespective of the types of alcohols and amines used in the reaction systems. Surprisingly, instead of amide, we found the formation of imines by the coupling of the respective amine compounds in each case. These interesting observations led us to investigate the imine formation reactions on BP-1 by the immobilized Ru-PNN and Ru-PONOP complexes using primary amines.

Imines are important compounds in organic chemistry because they contain C=N bonds which show diverse reactivity to various types of chemical transformations.[112,113] They function as electrophilic reagents in many organic syntheses such as additions, condensations, asymmetric organo-catalysis, cross-dehydrogenative coupling and cycloadditions.[114,115] Imines are highly reactive and can be widely used as nitrogen sources in the laboratory, biological, pharmaceutical, and industrial synthetic processes.[116,117] The conventional method for the synthesis of imines involves the reaction of ketones or aldehydes with amines in the presence of an acid catalyst.[115] Many other methods have also been reported in the literature for synthesis of imines which include oxidation of secondary amines,[118] direct reaction of nitroarenes and primary alcohols,[119] the aza-Wittig reaction,[120] and coupling of nitriles with amines.[121] Metal pincer complexes have also been applied in imines synthesis reactions.[115-116,122] David Milstein reported the direct synthesis of imines from alcohols and amines with the liberation of H_2 using a dearomatized (PNP-)RuH(CO) pincer complex.[116] A ruthenium(II)NNN-pincer complex catalyzed alcohol and amine conversion to imines.[115] Ruthenium N-Heterocyclic carbene complex has also been used to synthesize imines from alcohols and amines.[123] Nano-ordered mesoporous silicas (MCM-41) with an anchored sulfonic acid was used as heterogeneous catalyst for the synthesis of imines from aldehydes and amines.[124] Imines can also be synthesized from primary amines by oxidative condensation reactions.[125] Zhang *et al.* reported the direct iron catalyzed synthesis of imines from amines via aerobic oxidation reactions under air.[126] Vapor-phase selective aerobic oxidation of benzyl amine led to the formation of dibenzylimine over a silica supported vanadium-substituted tungstophosphoric acid catalyst.[127] The objective of this project was to investigate the primary amines catalysis on BP-1 using immobilized Ru-PNN and Ru-PONOP.

6.2 Experimental

6.2.1 Experimental procedure for the reaction between primary alcohols and primary amines with BP-1-Ru-PNN (**7**)

100 mg of BP-1-Ru-PNN (**7**) (0.0036 mmol Ru-PNN on BP-1) was added into a mixture of 11 mmol of primary amine and 11 mmol of alcohol in a small round-bottom flask equipped with a water condenser. The mixture was degassed by an applied vacuum. The mixture was then heated with slow stirring under an inert atmosphere of argon. The reaction mixture was then cooled to room temperature. The liquid product mixture and catalyst were separated by filtration and then settle at 12 hours. No amide precipitation was observed. The formation of imine in the product mixture was determined by GC with using an HP 5 column on an Agilent 6890N GC-MS system. The reaction conditions and corresponding yields are summarized in Table 6.1

6.2.2 Experimental procedure for the primary amine catalysis by BP-1-Ru-PNN (**7**)

100 mg of BP-1-Ru-PNN (**7**) (0.0036 mmol Ru-PNN on BP-1) was added into 11 mmol of primary amines in a small round-bottom flask equipped with a water condenser. The mixture was degassed by an applied vacuum. The mixture was then heated with slow stirring under an inert atmosphere of argon. The reaction mixture was then cooled to room temperature. The liquid product mixture and catalyst were separated by filtration. The formation of imine in the product mixture was determined by GC using an HP 5 column on an Agilent 6890N GC-MS system. The reaction conditions and corresponding yields are summarized in Table 6.1

Table 6.1: Primary amine catalysis on BP-1 by immobilized Ru-PNN and Ru-PONOP

Catalyst	Reactant	Catalyst / Amine ratio (mmol)	Reaction Temp (°C)	Reaction Time (Hours)	Imine (%)	Amide (%)
BP-1-Ru-PNN (7)	1-Hexanol and benzyl amine	0.01/30	150	96	31 (dibenzylimine) Range: 30-32	0
	1-Heptanol and benzyl amine	0.01/30	175	84	28 (dibenzylimine) Range: 27-30	0
	Heptyl amine and benzyl alcohol	0.01/30	156	84	24 (diheptylimine) Range: 23-25	0
	Benzyl alcohol and benzyl amine	0.01/30	178	90	36 (dibenzylimine) Range: 35-36	0
	Hexylamine	0.01/30	132	96	38 (dihexylimine) Range: 36-38	-
	Heptyl amine	0.01/30	156	84	46 (diheptylimine) Range: 45-46	-
	Benzyl amine	0.01/30	180	90	42 (dibenzylimine) Range: 41-42	-
BP-1-Ru-PONOP (1)	1-Hexanol and benzyl amine	0.01/30	150	96	23 Range: 22-24	0
	Hexylamine	0.01/30	132	96	33 (dihexylimine) Range: 32-33	-
	Heptyl amine	0.01/30	156	84	47 (diheptylimine) Range: 46-48	-
	Benzyl amine	0.01/30	180	90	41 (dibenzylimine) Range: 40-42	-

6.2.3 Experimental procedure for the reaction of 1-hexylamine with BP-1

100 mg of BP-1 (containing 1.6 mmol of N/g) was placed in a small round-bottom flask equipped with a water condenser. 10 mmol of hexylamine was added. The mixture was degassed by an applied vacuum. The mixture was then heated at 132°C with slow stirring under an inert atmosphere of argon for 96 hours. The reaction mixture was then cooled to room temperature. The

liquid product mixture and BP-1 were separated by filtration. The formation of imine was determined by GC using an HP 5column on an Agilent 6890N GC-MS system. Yield (dihexylimine): 14 %.

6.2.4 Experimental procedure for the control experiment between heptylamine and BP-1

100 mg of BP-1 (containing 1.6 mmol of N/g) was placed in a small round-bottom flask. 10 mmol of heptylamine was added. The mixture was degassed by an applied vacuum. The mixture was heated at 156°C with slow stirring under an inert atmosphere of argon for 84 hours. The reaction mixture was then cooled to room temperature. The liquid product mixture and BP-1 were separated by filtration. The formation of imine product mixture was analyzed by GC using an HP 5 column on an Agilent 6890N GC-MS system. Yield (diheptylimine): 32%.

6.2.5 Experimental procedure for the control experiment of heptylamine with BP-1in air

100 mg of BP-1 (containing 1.6 mmol of N/g) was placed in a small round-bottom flask. 10 mmol of heptylamine was added. The flask was equipped with a water condenser and sealed under air. The mixture was heated at 156°C with slow stirring under air for 84 hours. The reaction mixture was then cooled to room temperature. The liquid product mixture and BP-1 were separated by filtration. The formation of imine in the liquid product mixture was determined by GC using an HP 5 column on an Agilent 6890N GC-MS system. Yield (diheptylimine): 46%.

6.2.6 Experimental procedure for the control experiment between benzyl amine and BP-1

100 mg of BP-1 (containing 1.6 mmol of N/g) was placed in a small round-bottom flask. 10 mmol of benzyl amine was added. The mixture was degassed by an applied vacuum. The mixture was then heated at 180°C with slow stirring under an inert atmosphere of argon for 90 hours. The reaction mixture was then cooled to room temperature. The liquid product mixture and

BP-1 were separated by filtration. The formation of imine in the product mixture was determined by GC using an HP 5 on an Agilent 6890N GC-MS system. Yield (dibenzylimine): 27%.

6.2.7 Experimental procedure for the control experiment of with hexylamine and silica gel

200 mg of silica gel (10 nm average pore diameter, 250−600 μm particle size, 450 m^2/g surface area was obtained from Qing Dao Mei Gow, Qing Dao, China) was placed in a small round-bottom flask. 10 mmol of Hexylamine was added to it. The mixture was degassed by an applied vacuum. The mixture was then heated at 132°C with slow stirring under argon for 96 hours. The reaction mixture was then cooled to room temperature. The liquid product mixture and silica gel were separated by filtration. The formation of imine in the product mixture was determined by GC using an HP 5 column on an Agilent 6890N GC-MS system. Yield: 0 %.

6.2.8 Experimental procedure for the control experiment between heptylamine and silica gel

200 mg of silica gel (10 nm average pore diameter, 250−600 μm particle size, 450 m^2/g surface area was obtained from Qing Dao Mei Gow, Qing Dao, China) was placed in a small round-bottom flask. 10 mmol of heptylamine was added. The mixture was degassed by an applied vacuum. The mixture was then heated at 156°C with slow stirring under argon for 84 hours. The reaction mixture was then cooled to room temperature. The liquid product mixture and silica gel were separated by filtration. The formation of imine in the product mixture was determined by GC using an HP 5 column on an Agilent 6890N GC-MS system. Yield: 0 %.

6.2.9 Experimental procedure for the control experiment of heptyl amine with humidified BP-1

100 mg of BP-1 (containing 1.6 mmol of N/g) was placed in a small round-bottom flask. Humidification of the BP-1 was done by bubbling N_2 gas through H_2O in a 25 mL Erlenmeyer

flask with a rubber septum. Using plastic tubing, N_2 with H_2O vapor was allowed to pass through the BP-1. 10 mmol of heptylamine was added to humidified BP-1 in the round-bottom flask. The flask was equipped with a condenser. The mixture was heated at 156°C with slow stirring under the flow of argon for 84 hours. The reaction mixture was then cooled to room temperature. The liquid product mixture and silica gel were separated by filtration. The formation of imine in the liquid product mixture was determined by GC using an HP 5 column on an Agilent 6890N GC-MS system. Yield(diheptylimine): 35%.

6.2.10 Experimental procedure for the controlled experiment between benzyl alcohol and silica gel

100 mg of silica gel (10 nm average pore diameter, 250−600 μm particle size, 450 m^2/g surface area was obtained from Qing Dao Mei Gow, Qing Dao, China) was placed in a small round-bottom flask. 10 mmol of benzylamine was added. The mixture was degassed by an applied vacuum. The mixture was then heated at 180°C with slow stirring under argon for 96 hours. The reaction mixture was then cooled to room temperature. The liquid product mixture and silica gel were separated by filtration. The product mixture was analyzed by GC using an HP 5 column on an Agilent 6890N GC-MS system. Yield: 0 %.

6.3 Results and discussion

6.3.1 Investigation of amide formation on BP-1 by immobilized Ru-PNN (7) and Ru-PONOP (1)

The reaction of 1-hexanol with benzyl amine using 0.03 mol% of BP-1-Ru-PNN (**7**) at 150°C for 96 hours under argon did not result in any amide formation. When the mixture of benzyl amine and 1-heptanol was heated with BP-1-Ru-PNN (**7**) at 175°C under argon for 84 hours, no amide formation was realized. A similar reaction between heptylamine and benzyl alcohol with

0.03 mol% Ru-PNN on BP-1 at 156°C for 84 hours under argon yielded no amide. Further reaction between benzylamine and benzyl alcohol with BP-1-Ru-PNN (**7**) resulted in no amide formation. Again, when the reaction was carried out between 1-hexanol and benzyl amine with 0.03 mol% immobilized Ru-PONOP (**1**) similar results were observed. However, in all cases, imine formation was to be found instead of amide production (Table 6.1). The analysis of the liquid product mixtures by GC-MS revealed the generation of imines from the coupling of the respective amine molecules. The homogeneous reaction between 1-hexanol and benzyl amine with 0.1 mol% dearomatized pincer complex, (PNN-)RuH(CO) provided 96% amide as reported by David Milstein *et al*.[45] Similar reactions between other alcohols and amines with (PNN-)RuH(CO) also produced corresponding amides with very good yields in the homogeneous systems.[45] In our heterogeneous reaction systems with BP-1-Ru-PONOP (**1**) & BP-1-Ru-PNN (**7**)**,** the amines were observed to react between themselves which led to the formation of corresponding imines. These interesting catalytic results inspired us to investigate the primary amine catalysis on BP-1-Ru-PNN (**7**) and BP-1-Ru-PONOP (**1**).

6.3.2 Study of the primary amine catalysis on BP-1 by immobilized Ru-PNN (7) and Ru-PONOP (1)

The catalysis of 1-hexyl amine with 0.03 mol% of Ru-PNN on BP-1 (**7**) at 132°C for 96 hours under argon resulted in the formation of 38% dihexylimine (Scheme 6.2). Heptylamine catalysis with BP-1-Ru-PNN (**7)** in a similar catalyst-to-amine ratio at 156°C for 84 hours yielded 46% diheptylimine. Benzyl amine reacted in a similar way. Chemical treatment of benzyl amine with 0.03 mol% Ru-PNN on BP-1 at 180°C for 90 hours showed the formation of 42% dibenzylimine (Scheme 6.4). In all three cases, imines formation was accompanied by the liberation of ammonia.

Catalytic reactions of primary amines with BP-1-Ru-PONOP (**1**) produced results similar to those with the BP-1-Ru-PNN (**7**) system. The chemical reaction of hexylamine with 0.03 mol% of Ru-PONOP on BP-1 at 132°C for 96 hours under argon produced 33% dihexylimine (Scheme 6.5). Other primary amines react similarly with BP-1-Ru-PONOP (**1**) following similar catalyst-to-amine ratio. Heptylamine catalyzed by BP-1-Ru-PONOP (**1**) at 156°C under argon for 84 hours generated 47% diheptylimine. The reaction of benzylamine on BP-1 by 0.03% of Ru-PONOP at 180°C for 90 hours yielded 41% dibenzylimine. As in the BP-1-Ru-PNN system (**7**), in all three cases ammonia was produced as a byproduct. The formation of imines was confirmed by GC-MS analysis of the product mixture. The results were checked and verified by running the standard solutions of the respective imines in the GC-MS. Among three primary amines, heptylamine catalysis showed the highest (46-47%) imine formation with both BP-1-Ru-PNN (7) and BP-1-Ru-PONOP (1) systems. The homogeneous reaction system with 0.2 mol% of dearomatized (PNP-)RuH(CO) complex reported 67% imine formation from the reaction between hexyl amine and 1-hexanol.[116]

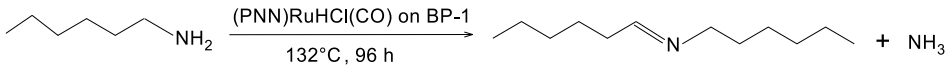

Yield: 38%

Scheme 6.2: Reaction of hexylamine with BP-1-Ru-PNN (**7**)

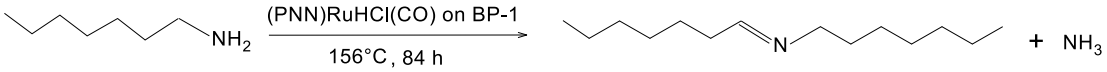

Yield: 46%

Scheme 6.3: Reaction of heptylamine with BP-1-Ru-PNN (**7**)

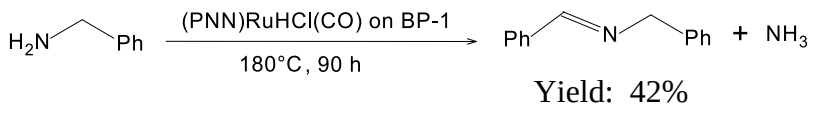

Scheme 6.4: Reaction of benzyl amine with BP-1-Ru-PNN (**7**)

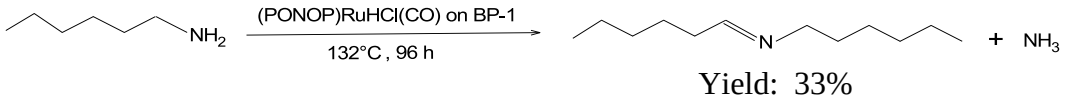

Scheme 6.5: Reaction of hexyl amine with BP-1-Ru-PONOP (**1**)

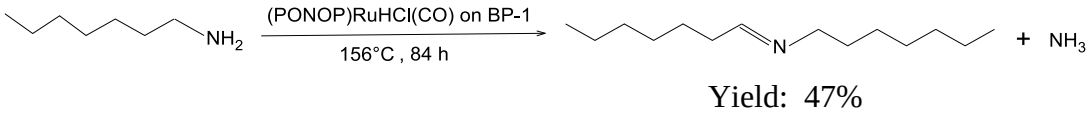

Scheme 6.6: Reaction of heptyl amine with BP-1-Ru-PONOP (**1**)

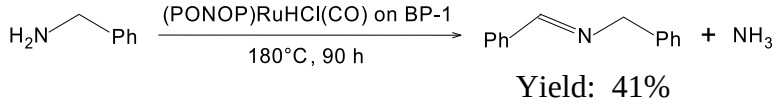

Scheme 6.7: Reaction of benzyl amine with BP-1-Ru-PONOP (**1**)

The imine yields observed from our study were considerably lower than those reported in the homogeneous systems.[116] This could be due to the use of a smaller amount of catalyst, 0.03 mol% in comparison to 0.2 mol% used in the homogeneous systems[116] as well as the heterogeneity of the reactions. As an initial investigation we decided to start amine reactions using a lower amount of catalyst to see whether catalysis would occur on the BP-1 surface with the immobilized complexes. The imine formation reactions catalyzed by pincer metal complexes needed an amine and an alcohol, as reported in the recent literature.[115-116,122] Imine synthesis on nano-ordered MCM-41-SO_3H heterogeneous catalyst also required use of an aldehyde and an amine and found

imine yields 66% to 87%.[124] However, Fe-catalyzed homogeneous synthesis of imines directly from amines was also noted in the literature, which showed 45 to 91% yields of imine irrespective of the primary amine used.[126] Vapor-phase selective aerobic oxidation of benzylamine on silica supported vanadium-substituted tungstophosphoric acid catalyst produced 50 to 90% dibenzylimines reported by Rao *et. al.*[127] They reported a plausible mechanism for imine formation from primary amines where the first step was the oxidative dehydrogenation of benzyl amine by a vanadium-substituted tungstophosphoric acid catalyst which formed benzonitrile (imine). Then the nucleophilic attack of the amine at C=N bond of benzonitrile (imine) generated an aminal intermediate which lost ammonia to form dibenzylimine (Scheme 6.8). [127]

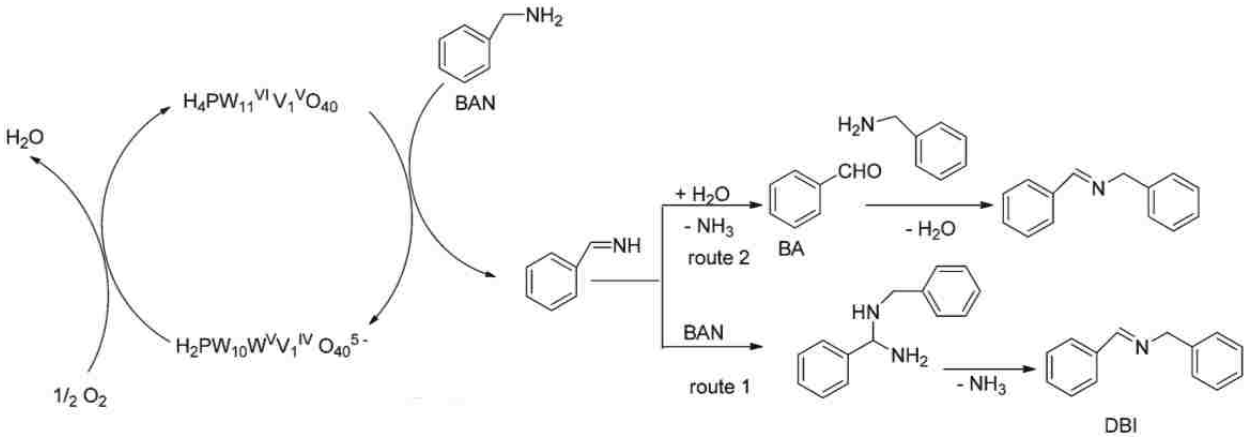

Scheme 6.8: Plausible mechanism for the formation of dibenzylimine from benzyl amine catalyzed by silica-supported vanadium-substituted tungstophosphoric acid.[121]

6.3.3 Control experiments of primary amines with BP-1 and silica gel

Control experiments were carried out between amines and BP-1as well as amines and silica gels to see the effects of support surfaces on amine catalytic reactions. The reaction of BP-1 with hexylamine at 132°C for 96 hours surprisingly resulted in the formation of 14% dihexylimine, indicating that the functionality on the composite surface actively participated in the catalytic

reactions. To verify this, a similar reaction was carried out with heptyl amine. Heating of the mixture of heptylamine and BP-1 at 156°C for 84 hours resulted in 32 % diheptylimine formation (Scheme 6.10). Similarly, benzylamine catalysis with BP-1also yielded 27% dibenzylimine after conducting the reaction at 180°C for 96 hours under argon. These results suggest that the BP-1 surface could also act as a catalyst in imine formation reactions. However, similar control experiments with silica gels and the corresponding primary amines did not produce any imines, indicating that the basic silica structure in the BP-1 composite did not have any influence on the amine catalytic reaction. This is evidence that amine functionality on the BP-1 surface caused the imine formation on BP-1 and acted as a catalyst in amine catalysis reactions. Previous research from our lab has also shown the catalytic reactivity of amine functionality on BP-1 in Knoevenagel reactions.[77]

We conducted primary amine catalysis on BP-1 in an air atmosphere as well, to see the effect of oxygen in the imine formation reactions. Catalysis of heptylamine with BP-1 in air resulted in the formation of 46% imines whereas a similar reaction under an inert atmosphere of argon showed an imine yield only 32%, which revealed that oxygen also plays a significant role in primary amines reaction systems (Scheme 6.10). The presence of moisture or H_2O does not have a significant impact in primary amine catalysis. This was confirmed from the reaction between heptylamine and humidified BP-1 which yielded almost the same amount of imines (35%) in comparison to that (32%) obtained with dried BP-1 following similar reaction conditions.

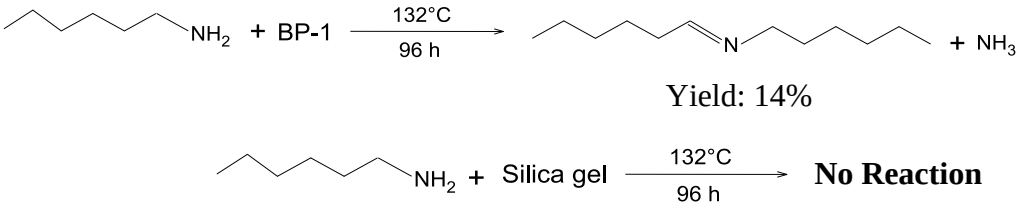

a

b

Scheme 6.9: Reaction of hexyl amine with: (a) BP-1 and (b) silica gel

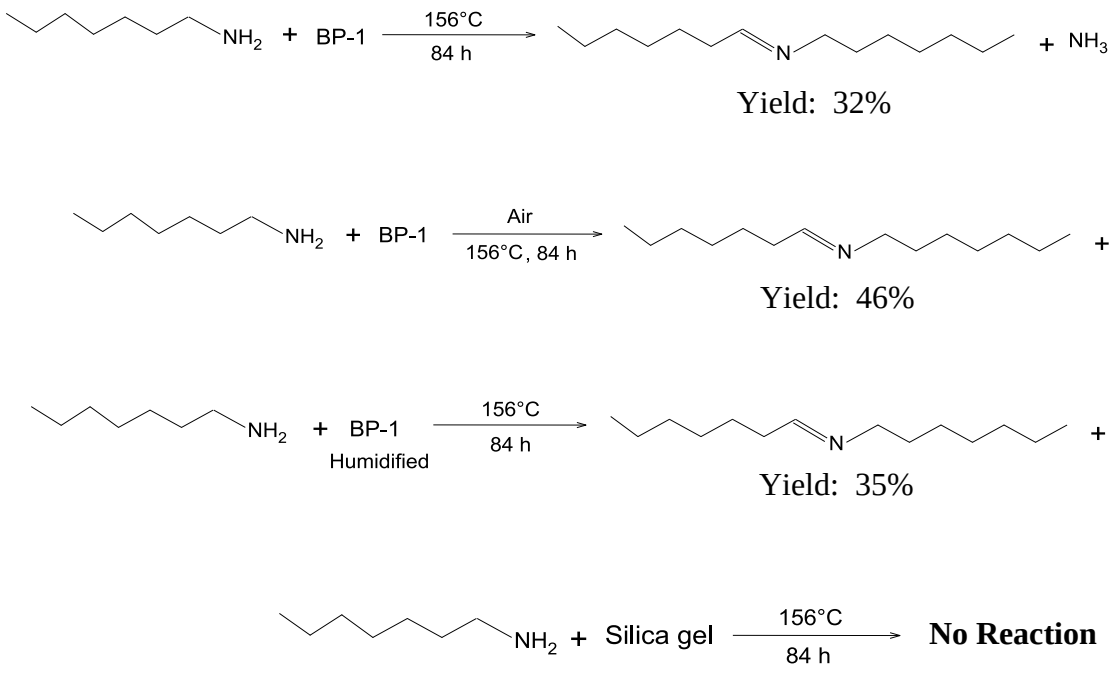

Scheme 6.10: Reaction of heptyl amine with: (a) BP-1, (b) BP-1 in air, (c) humidified BP-1, and (d) silica gel

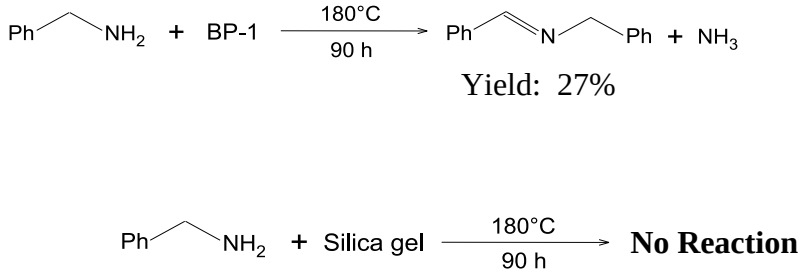

Scheme 6.11: Reaction of benzyl amine with: (a) BP-1 and (b) silica gel

We anticipated a mechanism for imine formation reactions with immobilized BP-1-Ru-PNN (**7**) and BP-1-Ru-PONOP (**1**) systems similar to those reported by Rao *et al.*[127] We believe that amines on BP-1 surfaces or the immobilized Ru-PNN and Ru-PONOP caused the initial oxidative dehydrogenation of primary amines and formed an alkyl/arylimine compounds. In the

next step, the nucleophilic attack by the amine from another molecule of primary amines at the C=N bond produced an aminal intermediate compound which then loses ammonia to form dialkyl/diarylamine compounds. The proposed mechanism for the imine formation reaction from primary amines is shown in the scheme 6.12.

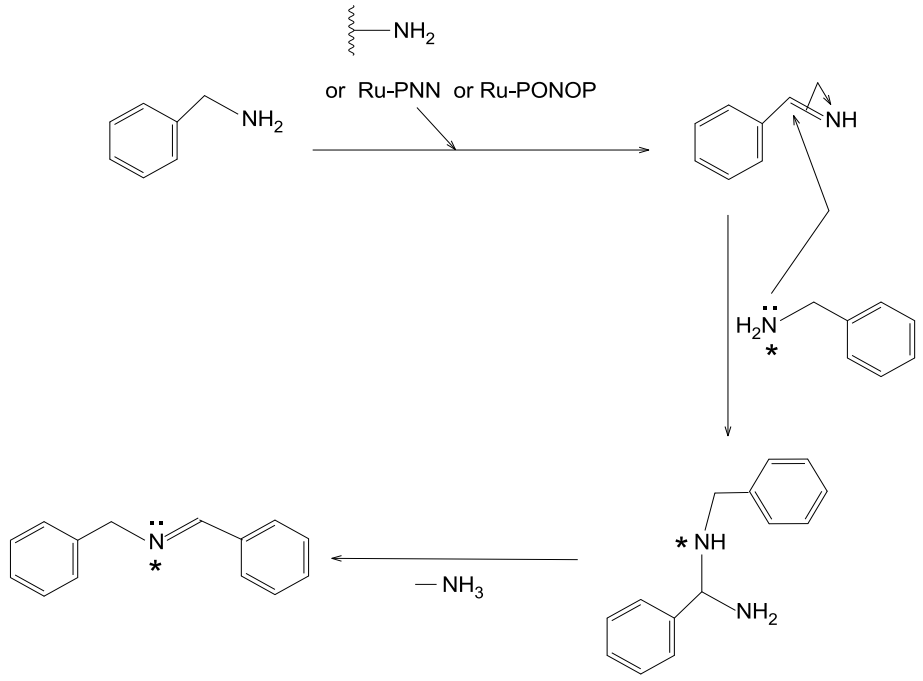

Scheme 6.12: Proposed reaction mechanism for the formation of imines from primary amines by BP-1, immobilized Ru-PNN (**7**), and Ru-PONOP on BP-1 (**1**)

Chapter 7

Conclusions and Future Work

7.1 Conclusions

7.1.1 Investigation of the methods for loading and synthesizing pincer ligands and metal pincer complexes on silica polyamine composite, BP-1

The initial focus of this project was to investigate and determine an efficient method for synthesizing and loading catalytically important pincer metal complexes on silica polyamine composites. Immobilization of catalytically active transition metal complexes on silica polyamine composite (SPC) surfaces offers many advantages for applications in catalysis, particularly for catalyst recovery and reuse. Three different methods have been investigated for synthesizing and loading metal pincer complexes on the silica polyamine composite, BP-1. The PONOP pincer ligand and its metal complexes have been chosen for the immobilization study. PONOP pincer complexes of Ru, Rh, Ni and Pd were synthesized and immobilized on the poly(allylamine)SPC, BP-1 using the Mannich reaction. Three methods were introduced and developed for synthesizing the PONOP pincer transition metal complexes on BP-1: 1) direct reaction of the preformed pincer complexes using a two-step Mannich reaction; 2) immobilization of the PONOP ligand using the Mannich reaction followed by the addition of a transition metal compound of a given metal; and 3) the stepwise construction of PONOP on BP-1 followed by the addition of a transition metal compound. The immobilized complexes on BP-1 were characterized by FT-IR, solid-state CPMAS ^{13}C and ^{31}P NMR, as well as elemental analysis. Anchoring of the complexes on BP-1 was also evaluated by the metal loading data obtained from the digestion of the loaded composites followed by Atomic Absorption Spectroscopy (AAS) or Inductively Coupled Plasma Atomic Emission Spectroscopy (ICPAES). The results showed that method 1 worked better for the loading of pincer

complexes on the SPC than methods 2 and 3. In the case of the Ru and Ni pincer complexes, reasonable agreement between metal and phosphorous analysis was realized, while for the Pd complex, the values were high relative to the loading predicted from the phosphorus analysis, indicating the formation of the Pd nanoparticles on the surface during immobilization. For the Rh and Ru immobilized complexes with methods 2 & 3, metal loading was lower than the phosphorous analysis, and this is attributed to entrained triphenyl phosphine from the starting rhodium and ruthenium complexes based on the ^{13}C and ^{31}P CPMAS NMR data. Solution experiments using the PONOP pincer ligand and the Ru(PONOP) complex with n-butyl amine were conducted to model the site of electrophilic aromatic substitution on the pyridine ring. It was found that substitution of both *meta*- and *para*-positions relative to the nitrogen takes place, and this helped in the interpretation of the solid-state data.

7.1.2 Immobilization of (PNN)RuH(Cl)(CO) on BP-1

(PNN)RuH(Cl)(CO) was covalently immobilized on BP-1 by method 1. The presence of the complex on BP-1 was confirmed by characterization with the standard spectroscopic techniques, FT-IR, solid-state NMR, elemental analysis, and metal digestion study. The model solution experiment between (PNN)RuH(Cl)(CO) and n-butyl amine showed the formation of both *meta*- and *para*- isomers, indicating the position of the electrophilic substitution at the pyridine ring of the (PNN)RuH(Cl)(CO) complex during loading on BP-1. It also helped to explain the large shift in the carbonyl frequency of the complex observed upon immobilization on BP-1. The product of the solution experiment was deprotonated by KO^{t}Bu to generate dearomatized-Ru-PNN-n-butylamine active catalyst complex. Alcohol catalysis with this complex showed less alcohol conversion in comparison to the original deprotonated catalyst (PNN-)RuH(CO)

demonstrating the effects of the substituent in the catalytic performance of the Ru-PNN pincer complex.

7.1.3 Heterogeneous catalysis on BP-1 by immobilized (PNN)RuH(Cl)(CO) (7)

The main focus of the project was to perform heterogeneous catalysis on BP-1 with immobilized pincer complexes and to apply this platform to a range of catalytic reaction systems which require using a base to generate active catalytic species or complexes. Dehydrogenative coupling of alcohols to esters and hydrogen reactions were carried out on BP-1 by the immobilized (PNN)RuH(Cl)(CO). Four alcohols were used in the heterogeneous catalytic reactions: 1-hexanol, 1-heptanol, benzyl alcohol, and 2-octanol. Primary alcohols produced corresponding esters and H_2 with aldehydes in some cases, whereas the secondary alcohol produced ketone (2-octanone) and H_2. The catalyst to alcohol ratio was 0.007: 21 (0.01:30) in mmol except in 1-hexanol where a higher amount of catalyst (0.02 mmol) was used. Moderate to good yields of esters were observed without the application of an external base in the BP-1-Ru-PNN system. Homogeneous reactions require using a base for catalysis of alcohols. Amine functionality on BP-1 functions as a base to generate active pincer catalytic complex on the BP-1 surface. However, the addition of KOH in the heterogeneous reaction systems has been shown to increase alcohol conversions in all four alcohol systems. A longer reaction period was required and overall alcohol conversion was relatively lower with the BP-1-Ru-PNN (**1**) system in comparison to the homogeneous analogs. This could be due to the use of lower amounts of catalyst (0.03%) and excess alcohols. In the homogeneous systems, 0.1 mol% catalyst was used. Application of a solvent in the catalytic reactions has been shown to decrease the alcohol conversion, whereas the solvent in the homogeneous reactions was found to increase the reaction yields. Alcohol catalysis did not occur on BP-1 at lower temperatures which was evidenced by the reactions in refluxing toluene. The catalysis of alcohol with dearomatized Ru-PNN-n-butyl amine (**9**) showed less conversion of

alcohol in comparison to that observed with the dearomatized active pincer complex (PNN-)RuH(CO) indicating the effect of the substituent in the catalytic performance of the pincer catalyst complex. It was difficult to figure out the exact percentage of the dearomatized and original form of the immobilized Ru-PNN on BP-1 from the spectroscopic data, which might be due to poor resolution as well as small differences in the resonances of the two complexes.

7.1.4 Catalytic reactivity of (PONOP)RuH(Cl)(CO) in homogeneous and heterogeneous systems

Though (PONOP)RuH(Cl)(CO) has been reported for a long time, there was no prior record of catalytic activity of this complex in the literature.[20,87,105] In our study, (PONOP)RuH(Cl)(CO) showed interesting catalytic reactivity in dehydrogenative coupling of alcohols to esters both in homogeneous and heterogeneous systems. Chemical treatment of 1-hexanol with 0.1 mol% Ru-PONOP at 157°C yielded 61% hexyl hexanoate and hydrogen. 1-heptanol catalyzed by 0.1 mol% Ru-PONOP resulted in 68% conversion with a turnover frequency of 28 h^{-1}. Similarly, benzyl alcohol produced benzyl benzoate, benzaldehyde, and hydrogen with an overall conversion of 66% when treated with Ru-PONOP following a similar catalyst-to-alcohol ratio. The secondary alcohol, 2-octanol was catalyzed by 0.1 mol% Ru-PONOP and generated 65% ketone and hydrogen. Catalytic studies with immobilized Ru-PONOP on BP-1 (**1**) in the dehydrogenative coupling of alcohols reactions also revealed the formation of esters with the liberation of hydrogen. The reactions were conducted with 1-heptanol, benzyl alcohol, and 2-octanol separately with 0.03 mol% of immobilized Ru-PONOP on BP-1. 1-hexanol catalysis was carried out with 0.04 mol% of Ru-PONOP on BP-1. All alcohol reacted similarly with BP-1-Ru-PONOP (**1**) and produced corresponding esters, H_2 and in some cases aldehyde formation was observed, except in the case of 2-octanol, which yielded only 2-octanone and H_2. The addition of

KOH (equivalent to Ru) resulted in the increase of alcohol conversion in all four alcohol systems with BP-1-Ru-PONOP. No ester formation was observed when the reaction was conducted in toluene, indicating the higher temperature requirement for catalysis by BP-1-Ru-PONOP as well as for immobilized Ru-PNN on BP-1. Application of a solvent (1,2-dichlorobenzene) in alcohol catalysis with the immobilized Ru-PONOP system also decreased the ester yield in comparison to the net alcohol systems. A mechanism was proposed for alcohol dehydrogenation reactions by Ru-PONOP-BP-1 which involved the generation of Ru(0) complex which reacted with alcohol and then catalysis proceeded with the formation of a ruthenium dihydride complex. Overall, the (PONOP)RuH(Cl)(CO) complex did not perform as well as the (PNN)RuH(Cl)(CO) complex in alcohol dehydrogenation reactions.

7.1.5 Cycle study on alcohol dehydrogenation reactions by BP-1-Ru-PNN (7) and BP-1-Ru-PONOP (1) with the solid-liquid and solid-vapor methods

Both immobilized Ru-PNN (**7**) and Ru-PONOP on BP-1 (**1**) catalysts were studied for multiple catalytic cycles. BP-1-Ru-PNN (**7**) showed catalytic reactivity for up to five catalytic cycles, whereas BP-1-Ru-PONOP (**1**) survived up to the fourth cycle of catalysis. The cycle studies were carried out using two reaction configurations: heating the mixture of alcohol and catalyst with slow stirring (solid-liquid) and passing the alcohol vapor over the catalyst bed (solid-vapor method). The catalyst-to-alcohol ratio (0.01:30) was the same in both methods. No apparent differences in alcohol conversion were found between the two methods in cycle 1 irrespective of the alcohols and the catalysts used. The conversion of alcohol was considerably decreased after cycle 1 using both methods and catalysts. Characterization of the resulting BP-1-Ru-PNN (**7**) and BP-1-Ru-PONOP (**1**) by solid-state NMR, FT-IR, elemental analysis, and metal digestion study revealed that both immobilized complexes remained intact on BP-1 after alcohol catalysis.

However, the decrease of intensity in the resonances of solid state CPMAS ^{13}C spectra as well as the loading of the complexes on the resulting composite BP-1-Ru-PONOP (**1**) & BP-1-Ru-PNN (**7**) demonstrated that catalysts were leached off and decomposed during catalysis, which caused the reductions of alcohol conversions in both methods. Elevated reaction temperatures and longer reaction periods resulted in the leaching and decomposition of Ru-PNN and Ru-PONOP from the BP-1 surface. In both BP-1-Ru-PNN (**7**) and BP-1-Ru-PONOP (**1**) systems, the solid-vapor method showed better conversions of alcohols in the successive cycles because it saved the catalyst from mechanical degradation by slow stirring. The reduction of the alcohol conversions in between two successive cycles was relatively more in the catalysis with BP-1-Ru-PONOP (**1**) in comparison to those with the BP-1-Ru-PNN (**7**) system, which implies that Ru-PONOP leached off or decomposed faster than Ru-PNN in the catalytic processes. There was good agreement between the reduction of reaction yields and the corresponding loss of the catalysts from BP-1 surfaces from cycle to cycle in both immobilized systems.

7.1.6 Heterogeneity of alcohol catalysis on BP-1-Ru-PNN (7) and BP-1-Ru-PONOP (1)

Four-step control experiments were carried out with BP-1-Ru-PNN and BP-1-Ru-PONOP systems separately using 1-hexanol to determine if catalysis with BP-1-Ru-PONOP (**1)** and BP-1-Ru-PNN (**7)** was truly heterogeneous and took place on the composite. The results revealed that catalysis which occurred on BP-1 by means of the immobilized Ru-PNN as well as Ru-PONOP proceeded in a heterogeneous manner. The immobilized catalysts might have survived on BP-1 during catalysis and then leached off or decomposed at the terminal point of the reaction. We assumed two pathways existed for alcohol catalysis on BP-1 by immobilized Ru-PNN and Ru-PONOP.

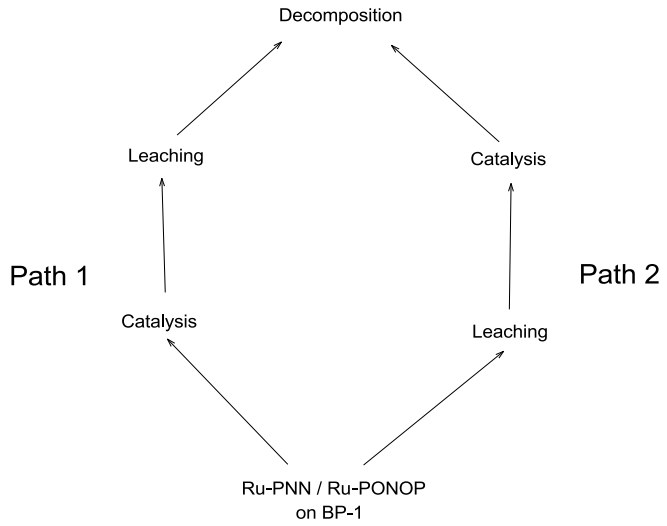

Path 2 was less likely to occur based on the results of the control experiments. We are convinced that immobilized Ru-PNN and Ru-PONOP stayed on the BP-1 surfaces during catalysis and eventually leached off the composite surface during longer reaction periods with elevated reaction temperatures, then finally decomposed.

The results of all alcohol conversions were checked and verified by running the appropriate standard solutions of corresponding alcohols in GC-MS. The results were also cross checked by running the standard solutions of the corresponding esters as well.

7.1.7 Primary amines catalysis on BP-1 by immobilized (PNN)RuH(Cl)(CO) (7) and (PONOP)RuH(Cl)(CO) (1)

The catalytic reactivity of BP-1-Ru-PNN (**7**) and BP-1-Ru-PONOP (**1**) was also investigated in amide formation reactions from amines and alcohols. No amide formation was realized. Instead, imines were formed by coupling of primary amines which revealed that primary amines could be catalyzed by BP-1-Ru-PNN (**7**) and BP-1-Ru-PONOP (**1**) to form imines. The catalysis of hexylamine and heptylamine on the immobilized catalysts BP-1-Ru-PONOP (**1)** & BP-1-Ru-PNN (**7)** yielded corresponding dialkylimines with the liberation of ammonia, whereas

in the case of benzyl amine, dibenzylimine and ammonia were formed. The control experiments with BP-1 showed that amine functionality also catalyzed imine formation but with lower conversions. A mechanism was proposed for imine formation reactions which involved the formation of a Schiff base with the oxidation of primary amines by BP-1 and/or supported pincer complexes, and the corresponding nucleophilic attack on imine carbon led to the formation of coupled imines.

7.2 Future Work

7.2.1 Optimization of loading

Though the low loading of the catalyst on BP-1 from our study provided interesting catalytic results, better reaction yields could be achieved with higher loading of the pincer complexes on BP-1. We chose the current method, the Mannich reaction, because of our prior successes with this method for loading aromatic molecules on SPC to prove the concept with a previously proven catalyst.[71,78] A pathway that may be much more efficient is the immobilization of pincer complexes by simple halide displacement. Our previous studies with a chloroacetic acid ligand provided much better loading on SPC, which was about 1.0 mmol per gm of SPC. Of course, the pincer ligands and their complexes are much larger than the chloroacetic acid ligand, but higher loading of the pincers can also be anticipated with halide displacement. This study can be done by introducing alkyl halide functionality in the pyridine moiety of the pincer complexes. Synthesis of substituted pincer complexes might not be easy and will involve multi-step synthetic and separation procedures. However, it can be accomplished by careful selection of suitable starting materials. One approach could be to synthesize *p*-bromomethyl-(PNN)RuH(Cl)(CO) pincer complex starting from 2,4,6-trimethyl pyridine, which is commercially available. NBS bromination would give two

possible bromination products that would require chromatographic separation. The desired alkyl halide substituted pincer complexes could then be synthesized following the steps used for unsubstituted pincer complexes.[41] However, in each of the steps, the formation of isomeric product mixtures may be expected, which may require extensive chromatographic separation. Binding of the *p*-bromomethyl Ru-PNN to BP-1 should take place under relatively mild conditions in the presence of a scavenging base such as ethyl-di-isopropyl amine.

7.2.2 Heterogeneous catalysis on BP-1 with higher loading of pincer complexes

Catalytic study on BP-1 with more highly loaded pincer complexes might give better reaction yields in alcohol dehydrogenation and other chemical transformations. Increasing the density of the pincer catalyst on the BP-1 surface might have significant influence on the corresponding catalytic reaction processes. However, the effects of the substituent might be an issue in the catalytic performances of the resulting pincer complexes. We observed relatively lower alcohol conversions in our catalytic study with deprotonated Ru-PNN-n-butyl amine (**9**) in comparison to those observed with unsubstituted Ru-PNN. The presence of a substituent in the basic ligand moiety of the pincer structures could influence the electron density in metal centers and thus might affect the catalytic reactivity of the resulting pincer complexes. It could also inhibit the catalytic reactivity due to the orientation effects of substituents during catalytic reactions.

7.2.3 Immobilization of other metal pincer complexes on BP-1 and extending heterogeneous catalytic study to other chemical transformations

A large number of pincer complexes which have shown interesting catalytic reactivity in various chemical reactions do require a base to function as efficient catalysts in their respective reactions. It would be interesting to apply the SPC-BP-1 surface as a platform for heterogeneous catalysis in other chemical transformations as well. Amine functionality on SPC-BP-1 surfaces

has already been proven as an efficient base and acted as a co-catalyst in alcohol dehydrogenation reactions. The immobilization and subsequent catalytic study of other important pincer complexes on SPC-BP-1 could be an interesting area of research which might eliminate the application of bases in those catalytic reactions. It could also save some relatively expensive pincer catalyst and might reduce the cost in the case of large scale commercial applications in the future.

Another important aspect could be to extend the heterogeneous catalysis on BP-1 to other reaction systems which do not have a high temperature requirement for catalysis, which might decrease the catalyst leaching from the composite surface in multiple cycles. Our catalytic studies on BP-1 with immobilized Ru-PNN and Ru-PONOP systems were carried out at relatively high temperatures. We tried to perform catalysis on BP-1 at a lower temperature (115°C). However, it did not work. This could be due to the nature and type of reactions (dehydrogenative coupling of alcohol to esters and hydrogen) we conducted on BP-1. The higher temperature requirement in alcohol dehydrogenation reactions might have resulted in significant leaching of the catalyst in multiple cycles of reactions. However, it provided a favorable environment for the deprotonation of pincer complexes on BP-1 by amine functionality on the surface, though the amine is a weak base. It would be worthwhile to try the catalytic reactions on BP-1 by immobilized Ru-PNN and Ru-PONOP, which do not need higher temperature requirements and that might reduce the loss of catalyst in the cycle study.

7.2.4 Optimization of reaction yields in primary amine catalysis and extending catalysis to other amines

Our initial catalytic investigation in primary amine catalysis by immobilized Ru-PNN and Ru-PONOP on BP-1 systems showed interesting results in imine formations. Further study is required to optimize the imine yields and to get a better understanding of the mechanism of amine

catalysis on BP-1 with immobilized pincer complexes. We must address two key issues here which are the relatively lower yields, as well as the participation of the BP-1 surface in the catalytic reactions.

Imine yields could be improved by using a higher catalyst-to-amine ratio. In addition, the role of air or oxygen in the amine catalytic process needs to be determined, since the conduction of amine reactions in air have been shown to increase imine yields. The involvement of amine functionality on BP-1 in the catalytic processes may complicate the optimization of reaction yields. Another important aspect could be to apply this heterogeneous catalytic study in other primary amines and secondary amines. Once the optimization is performed, the next step would be to study the recyclability of BP-1-Ru-PNN and BP-1-Ru-PONOP in corresponding amine catalytic reactions. Hexyl amine and heptyl amine catalysis on BP-1 by both immobilized Ru-PNN and Ru-PONOP occurred at relatively lower temperatures in comparison to the 1-heptanol and benzyl alcohol reaction systems. The catalysts' stability on BP-1 might be better in the amine catalysis reactions, particularly with amines with lower boiling points, and cycle study might provide better amine conversions to imines. The catalyst may display reactivity in a greater number of cycles in this case, in comparison to those observed in alcohol dehydrogenation reactions.

Bibliography

1. Mohr, J.T.; Michael R. Krout, M.R.; Brian M. Stoltz, B.M. *Nature* **2008**, *455*, 323-332.
2. Taylor, A. I.; Pinheiro, V.B.; Smola, M.J.; Morgunov, A.S.; Peak-Chew, S.; Cozens, C.; Herdewijn, P.; Hollinger, P. *Nature* **2015**, *518*, 427–430.
3. Kung, H.H. & Kung, M.C. *Catal. Lett.* 2014,144, 1643–1652.
4. http://2012books.lardbucket.org/books/principles-of-general-chemistry-v1.0/s18-08-catalysis.html
5. http://web.uvic.ca/~mcindoe/423/homovshet.pdf
6. Mehendale, N.C.; Bezemer, C.; van Walree, C.A.; Gebbink, R.J.M.K.; van Koten, G.; *J. Mol. Catal. A: Chem.* **2006**, *257*, 167–175.
7. Cornils, B.; Herrmann, W. A. *J. Catal.* **2003**, *216*, 23-31.
8. Blaser, H.U.; Pugin, B.; Studer, M. in :Chiral Catalyst Immobilization and Recycle, eds. De Vos, D.E.; Vankelecom, I.F.J.; Jacobs, P.A. (VCH, Weinheim, 2000) p. 9.
9. Design of silica-tethered metal complexes for polymerization catalysis. *Topic in Catal.* **2005**, *34*, 67-76.
10. Duca, G. Homogeneous catalysis with metal complexes, Springer series in Chemical Physics 102, DOI 10.1007/978-3-642-24629-6_1. Springer-Verlag Berlin Heidelberg 2012.
11. Gemeay, A.H.; Zaki, A.B.; El-Sheikh, M.Y.; El-Saied, H.F. *Transition Met. Chem.* **2003**, *28*, 625-631.
12. Choplin, A.; Quignard, F. *Coord. Chem. Rev.* **1998**, *178-180*, 1679-1702.
13. Pozo, C.D. ;Corma, A.; Iglesias, M.; Sanchez, F. *Organometallics* **2010**, 29, 4491.
14. Chase, P.A.; Klein Gebbink,R.J.M.; van Koten,G. *J. Organomet. Chem.* **2004**, 689, 4016-4054.
15. Bergbreiter, D.E.; Osborn, P.L.; Frels, J.D. *J. Am. Chem. Soc.* **2001**, *123*, 11105-11106.
16. Mehendale, N.C.; Sietsma, J.R.A.; de Jong, K.P.; van Walree, C.A.; Gebbink, R.J.M.K.; Van Koten, G. *Adv. Synth. Catal.* **2007**, *349*, 2619-2630.

17. Bhattacharya, P.; Krause, J.A.; Guan, H. *Organometallics*, **2011**, *30*, 4720–4729.
18. Arashiba, K.; Miyake, Y.; Nishibayashi, Y. *Nat. Chem.* **2011**, *3*, 120.
19. Tanaka, R.; Yamashita, M.; Nozaki, Y. *J. Am. Chem. Soc.* **2009**, *131*, 14168.
20. Kundu, S.; Willium, W. B.; Jones, W. D. *Inorg. Chem*. **2011**, *50*, 9443.
21. De Rieux, W.; Wong, A.; Schrod, Y. *J. Organomet. Chem.* **2014**, *772-773*,60-67.
22. Morales-Morales, D.; Jensen, C., Eds. *The Chemistry of Pincer Compounds*; Elsevier Science: Amsterdam, **2007**.
23. Boro, B. J.; Duesler, E. N.; Goldberg, K. I.; Kemp, R. A. *Inorg. Chem*. **2009**, *48*, 5081-5087.
24. Moulton, C.J.; Shaw, B.L. *J. Chem. Soc.*, *Dalton Trans*. **1976**, *11*, 1020-1024.
25. Rybtchinski, B.; Milstein, D. Metal Insertion into C-C Bonds in Solution. *Angew. Chem. Int. Ed.* **1999**, *38*, 871-883.
26. van der Boom, M. E.; Milstein, D. *Chem. Rev.* **2003,** *103*, 1759-1792.
27. Leonard, N.G.; Williard, P.G.; Bernskoetter, W. H. *Dalton Trans.***2011**, *40*, 4300-4306.
28. Fryzuk, M.D.; Berg, D.J.; Haddad, T.S. *Coord. Chem. Rev.* **1990**, *99*,137-212.
29. Liang, L.-C.; Lin, J.-M.; Hung, C.-H. *Organometallics* **2003**, *22*, 3007-3009.
30. Benito-Garagorri, D.; Kirchner, K. *Acc. of Chem. Res.* **2008**, *41*, 201-213.
31. Tamami, B.; Nezhad, M.M.; Ghasemi, S.; Farjadian, F. *J. of Organomet. Chem.* **2013**,*743*, 10-16.
32. Castonguay, A.; Beauchamp, A.L.; Zargarian, D. *Organometallics* **2008**, *27*, 5723-5732.
33. Tanaka, R.;Yamashita, M.; Nozaki, K. *J. Am. Chem. Soc.***2009**, *131*, 14168-14169.
34. Albrecht, M.; van Koten, G. *Angew. Chem. Int. Ed.* **2001**, 40, 3750-3781.
35. Mizoroki, T.; Mori, K.; Ozaki, A. *Bull. Chem. Soc. Jpn.* **1971**,*44*, 581.
36. Blaser, H.-U.; Indolese, A.; Naud, F.; Nettekoven, U.; Schnyder, A. *Adv. Synth. Catal.* **2004**, *346*, 1583.
37. Beller, M.; Fischer, H.; Herrmann, W. A.; Ofele, K.; Brossmer, C. *Angew. Chem., Int. Ed. Engl.* **1995**, *34*, 1848.

38. Beller, M.; Riermeier, T. H.; Haber, S.; Kleiner, H.-J.; Herr-mann, W. A. *Chem. Ber.* 1996.

39. Beller, M.; Riermeier, T. H. *Eur. J. Inorg. Chem.* 1998, 29.

40. Beller, M.; Riermeier, T. H.; Magerlein, W.; Muller, T. E.; Scherer, W. *Polyhedron* **1998**, 17, 1165.

41. Zhang, J.; Leitus, G.; Ben-David, Y.; Milstein, D. *J. Am. Chem. Soc.* **2005**, *127*, 10840-10841.

42. Zhang, J.; Gandelman, M.; Linda J. W. Shimon, L.J.W.; HaimRozenberg, H.; David Milstein, D. *Organometallics* **2004,** *23*, 4026-4033.

43. Prechtl, M.H.G.; Wobser, K.; Theyssen, N.; Yehoshoa Ben-David, Y.; Milstein, D.; Walter Leitner, W. *Catal. Sci. Technol.*, **2012**, *2*, 2039–2042.

44. Balaraman, E.; Gnanaprakasam, B.; Shimon, L.J.W.; Milstein, D. *J. Am. Chem. Soc*. **2010**, *132*, 16756–16758.

45. Gunanathan, C.; Ben-David, Y.; Milstein, D. *Science*, **2007**, *317*, 790-792.

46. Langer, R.; Leitus, G.; Ben-David, Y.; Milstein, D. *Angew. Chem. Int. Ed.***2011**, *50* 2120–2124.

47. Balaraman, E.; Gunanathan, C.; Zhang, J.; Shimon, L.J.W.; Milstein, D. *Nat. Chem*. **2011**, *3*, 609-614.

48. Zhang, J.; Gandelman, M.; Linda J. W. Shimon, L.J.W.; Milstein, D. *Dalton Trans.*, **2007**, 107–113.

49. Gnanaprakasam, B.; Balaraman, E.; Ben-David, Y.; David Milstein, D. *Angew. Chem. Int. Ed.* **2011**, *50*, 12240 –12244.

50. Langer, R.; Diskin-Posner, Y.; Leitus, G.; Shimon, L.J.W.; Ben-David, Y.; Milstein, D. *Angew.Chem. Int. Ed.* **2011**, *50*, 9948 –9952.

51. Gnanaprakasam, B.; Ben-David, Y.; Milstein, D. *Adv. Synth. Catal.* **2010**, *352*, 3169 – 3173.

52. Gnanaprakasam, B.; Milstein, D.*J. Am. Chem. Soc.* **2011**, *133*, 1682–1685.

53. Balaraman, E.; Ben-David, Y.; Milstein, D. *Angew. Chem. Int. Ed.* **2011**, *50*, 11702 –11705.

54. Chase, P.A.; KleinGebbink, R.J.M.; van Koten, G. *J. Organomet. Chem.* **2004**, *689*, 4016–4054.

55. Knapen, J.W.J.; van der Made,A.W.; de Wilde, J.C.; van Leeuwen, P.W.M.N.; Wijkens, P.; Grove, D.M. ;van Koten, G. *Nature* **1994**, *372*.

56. Bergbreiter, D.E.; Osborn, P.L.; Frels, J.D. *J. Am. Chem. Soc*. **2001**, *123*, 11105–11106.
57. Karakhanov, E.; Maximov, A. in: Wohrle, D.; Pomogajlo (Eds.), A., Metal Complexes and Metals in Macromolecules, John Wiley & Sons, New York, 2003, p.457.
58. McDonald, A.R.; Dijkstra, H.P.; Suijkerbuijk, B.M.J.M.; van Klink, G.P.M.; van Koten, G. *Organometallics* **2009**, 28, 4689–4699.
59. Sommer, W.J.; Yu, K.; Sears, J.S.; Ji, Y.; Zheng, X.; Davis, R.J.; Sherrill, C.D.; Jones, C.W.; Weck, M. *Organometallics* **2005**, *24*, 4351–4361.
60. Z. Huang, Z.; Brookhart, M.; Goldman, A.S.; Kundu, S.; Ray, A.; Scott, S.L.; B.C. Vicente, B.C. *Adv. Synth. Catal.* **2009**, *351*, 188–206.
61. Vicente, B.C.; Huang, Z.; Brookhart, M.; Goldman, A.S.; Scott, S.L. *Dalton Trans*. **2011**, *40* 4268–4274.
62. Rimoldi, M.; Fodor, D.; van Bokhoven, J.A.; Mezzetti, A. *Chem. Commun*. **2013**, *49* 11314–11316.
63. Yu, K.; Sommer, W.; Weck, M.; Jones, C.W. *J. Catal.* **2004,** *226*, 101–110.
64. Yu, K.; Sommer, W.; Richardson, J.M.; Weck, M.; Jones, C.W. *Adv. Synth. Catal.* **2005**, 347, 161–171.
65. Milstein, D. *Top. Catal.* **2010**, *53*, 915–923.
66. Kang, P.; Cheng, C.; Chen, Z.; Schauer, C.K.; Meyer, T.J.; Brookhart, M. *J. Am. Chem. Soc.* **2012**,134, 5500–5503.
67. Chakraborty, S.; Krause, J.A.; Guan, H. *Organometallics* **2009**, *28*, 582–586.
68. Selander, N.; Szabo, K.J. *Chem. Rev.* **2011**, *111*, 2048–2076.
69. Hughes, M.; Nielsen, D.; Rosenberg, E.; Gobetto, R.; Viale, A.; Burton, S.D. *Ind. Eng. Chem. Res.* **2006**, *45*, 6538.
70. Beatty, S.T.; Fischer, R.J.; Hagers, D.L.; Rosenberg, E. *Ind. Eng. Chem. Res.***1999**, *38* 4402–4408.
71. Wong, Y.O.; Miranda, P.; Rosenberg, E. *J. Appl. Poly. Sci.***2010**, *115*, 2855–2864.

72. Hughes, M.; Miranda, P.; Nielsen, D.; Rosenberg, E.; Gobetto, R.; Viale, A.; Burton, S. Silica polyamine composites: new supramolecular materials for cation and anion recovery and remediation, in: R. Barbucci, F. Ciardelli, G. Ruggeri (Eds.), Recent Advances and Novel Approaches in Macromolecule metal Complexes, Wiley- VCH, Weinheim, 2006, p. 161 (Macromolecular Symposia 235).
73. Nishimura, S. Handbook of heterogeneous catalytic hydrogenation for organic synthesis, John Wiley & Sons, New York, 2001.
74. Thomas, J.M. *J. Mol. Catal. A: Chem.* **1999**, *146*, 77–85.
75. Allen, J.; Rosenberg, E.; Karakhanov, E.; Kardashev, S.V.; A. Maximov, A.; Zolotukhina, A. *Appl. Organometal. Chem.* **2011**, *25*, 245–254.
76. Bandosz, T.J.; Seredych, M.; Allen, J.; Wood, J.; Rosenberg, E. *Chem. Mater.***2007**, *19*, 2500–2511.
77. Abbott, G.; Brooks, R.; Rosenberg, E.; Terwilliger, M.; Alexander Ross, J.B.; Ichire, O.L. *Organometallics* **2014**, *33*, 2467–2478.
78. Rosenberg, E.; Miranda, P.; Wong, Y.O. U.S. Patent 8,343,446, 2012.
79. Mannich, C.; Krösche, W. *Arch. Pharm. Pharm. Med. Chem.* **1912**, *250*, 647–667.
80. (a) Majid, M.H.; Vahideh, Z.; ; Bozorgpour Savadjani, Zahra, B.S. *Curr. Org. Chem.* **2014**, *18 (22)*, 2857-2891. (b) http://en.wikipedia.org/wiki/Mannich_reaction
81. Quevedo, R.; Moreno-Murillo, B. *Tetrahedron Lett.* **2008**, *50(8)*, 936–938.
82. Rivera, A.; Quevedo, R. *Tetrahedron Lett.* **2004**, *45*, 8335–8338.
83. Szlosek, D.; Currie, D. *Green and Sustainable Chem.* **2016**, *6*, 110-115.
84. Yang, J.W.; Chandler, C.; Stadler, M.; Kampen, D.; List, B. *Nature* **2008**, *452*, 453-455.
85. Inorganic Syntheses, Vol. VI, p. 218, McGraw-Hill Book Company, NY.
86. Andrews, M.A.; Chang, T.C.-T.; Chi-Wen, Cheng, F.; Emge, T.J.; Kelly, K.P.; Koetzle, T.F. *J. Am. Chem. Soc.* **1984**, *106*, 5913–5920.
87. Salem, H.; Shimon, L.J.W.; Diskin-Posner, Y.; Leitus, G.; Ben-David, Y.; Milstein, D. *Organometallics* **2009**, *28*, 4791–4806.
88. Bernskoetter, W.H.; Schauer, C.K.; Goldberg, K.I.; Brookhart, M. *Science* **2009**, *326* 553–556.
89. Panigati, M.; Mercandelli, P.; Alfonso, G.D.O.; Berrenghelli, T.; Sironi, A. *J. Organometal. Chem.* **2005**, *690*, 2044–2051.

90. Goni, M.A.; Rosenberg, E.; Meregude, S.; Abbott, G. *J. of Organomet. Chem.* **2016**, *807*, 1-10.

91. Goni, A.; Rosenberg, E. in: Abstracts 2015 ACS Northwest Regional Meeting held in Pocatello, ID, June 21-24, 2015. Abstract # 33.

92. Goni, A.; Rosenberg, E. in: Abstracts 2016 ACS National Meeting held in Philadelphia PA, August 20-25, 2016. Abstract # 2517419.

93. Zhang, J.; Leitus, G.; Ben-David, Y.; Milstein, D. *Angew. Chem. Int. Ed.***2006**, *45*, 1113-1115.

94. https://application.wiley-vch.de/books/sample/3527334424_c01.pdf

95. Gunanathan, C. and Milstein, D. *Top. Organomet. Chem.* **2011**, *37*, 55–84.

96. Gunanathan, C. and Milstein, D. *Acc. Chem. Res*. **2011**,*44*, 588 – 602.

97. Chen, T.; Yang, L.; Li, L.; Huang, K-W. *Tetrahedron* **2012**, *68*, 6152-6157.

98. Gilbert, L.; Mercier, C. *Studies in Surfaces Science and Catalysis* **1993**, *78*, 51-66

99. Akpa, B.S.; Agostino, C.D.; Gladden, L.F.; Hindle, K.; Manyar, H.; McGregor, J.; Li, R.; Neurock, M.; Sinha, N.; Stitt, E.H.; Weber, D.; Zeitler, J.A.; Rooney, D.W. *J. of Catal.* **2012**, *289*, 30-41.

100. George, S.M. *Chem. Rev.*, **1995**, 95 (3), 475–476.

101. http://www.nature.com/subjects/heterogeneous-catalysis

102. Rosentha, D. *Phys. Status Solidi A* **2011**, *208 (6)*, 1217–1222.

103. Rosenberg, E.; Abbott, G.; Goni, A., McVay, R.; Ross, J.B.A. in: Abstracts 2016 ACS National Meeting held on San Diego, March 17, 2016. Abstract #

104. Richardson, J.M.; Jones, C.W. *J. Mol. Catal. A: Chem.* **2009**, *297*, 125–134.

105. De Rieux, W.W.; Wong, A.; Schrodi, Y. *J. Org. Metallic. Chem.* **2014**, *772-773*, 60-67.

106. Salem, H.; Shimon, L.J.W.; Leitus, G.; Weiner, L.; Milstein, D. *Organometallics* **2008,** *27*, 2293–2299.

107. Salem, H.; Ben-David, Y.; Shimon, L.J.W.; Milstein, D. *Organometallics* **2006,** *25*, 2293–2299.

108. Polukeev, A.L.; Petrovsk, P.V.; Peregudov, A.S.; Ezernitskaya, M.G.; Avthandil A. Koridze A. A. *Organometallics* **2013**, *32*, 1000−1015.

109. Go¨ttker-Schnetmann, I.; White, P.; Brookhart, M. *J. Am. Chem. Soc.* **2004**, *126*, 1804-1811.

110. Morales-Morales, M.; Cathleen Yung, C.; Jensen, C.M. *Inorg. Chimic. Acta* **2004**, *357*, 2953–2956.

111. Ankan Paul, A.; Musgrave, C.B. *Angew. Chem. Int. Ed.* **2007**, *119*, 8301 –8304

112. Martin, S.F. *Pure. Appl. Chem.* **2009**, *81*, 195-204.

113. Gawronski, J.; Wascinska, N.; Gajewy, I. *Chem. Rev.* **2008**, *108*, 5227-5252.

114. Adams, J.P. *J. Chem. Soc. Perkins Trans.* **2000**, 125-139.

115. Sindhuja, E.; Ramesh, R. *Tetrahedron Letters* **2014**, *55*, 5504-5507.

116. Gnanaprakasam, B.; Zhang, J.; Milstein, D. *Angew. Chem. Int. Ed.* **2010**, *49*, 1468 –1471.

117. Tang, W.; Zhang, X. *Chem. Rev.* **2003**, *103*, 3029-3069.

118. (a) Jiang, G.; Chen, J.; Huang, J.S.; Che, C.M. *Org. Lett.* **2009**, *11*, 4568-4571.

(b) Yuan, H.; Yoo, W. J.; Miyamura, H.; Kobayashi, S. *J. Am. Chem. Soc.* **2012**, *134*, 13970-13973.

119. Zanardi, A.; Mata, J.A.; Perris, E. *Chem. Eur. J.* **2010**, *16*, 10502-10506.

120. Palacios, F.; Alonso, C.; Aparicio, D.; Rubiales, G.; Delos-Santos, J.M. *Tetrahedron* **2007**, *63*, 523-575.

121. Srimani, D.; Feller, M.; David, Y.B. Milstein, D. *Chem Commun*. **2012**, 11853-11855.

122. Balaraman, E.; Srimani, D.; Diskin-Posner, Y.; Milstein, D. *Catal. Lett.* **2015**, *145*, 139-144.

123. Maggi, A,; Madsen, R. *Organometallics* **2012**, *31*, 451-455.

124. Ali, E.; Naimi-Jamal, M.R.; Dekamin, M.G. *Scientia Iranica* **2013**, *20(3)*, 592-597.

125. (a) Orito,K.; Hatakeyama, T.; Takeo, M.; Uchiito, S.; Tokuda, M.; Suginome, H. *Tetrahedron* **1998**, *54*, 8403-8410.

(b) Prades, A.; Perris, E.; Albrecht, M. *Organometallics* **2011**, *30*, 1162-1167.

(c) Huang, H.; Huang, J.; Liu, Y.M.; He, H.Y.; Cao, Y.; Fan, K.N. *Green Chem.* **2012**, *14*, 930-934.

126. Zhang, E.; Tian, H.; Xu, S.; Yu, X.; Xu, Q. *Org. Lett* **2013**, *11*, 2704-2707.

127. Rao, K.T.V.; Haribabu, B.; Prasad, P.S.S.; Ligaiah, N. *Green Chem.* **2013**, *15*, 837-846.

Appendix A

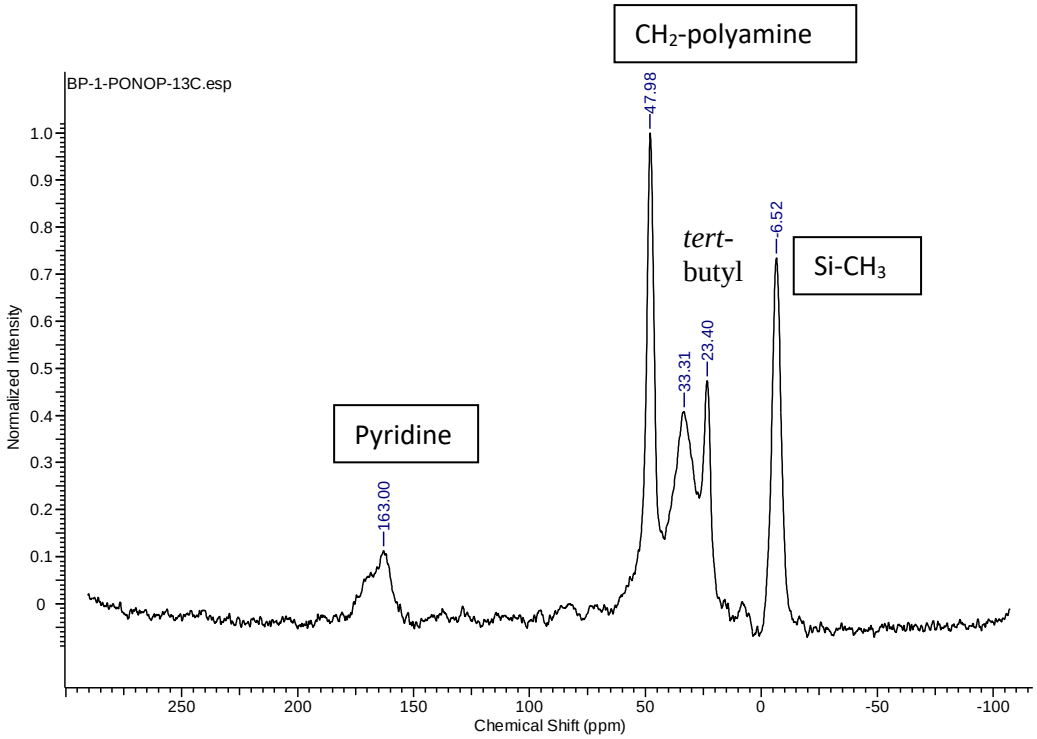

Figure A1: Solid-state CPMAS ^{13}C NMR spectrum of BP-1-PONOP

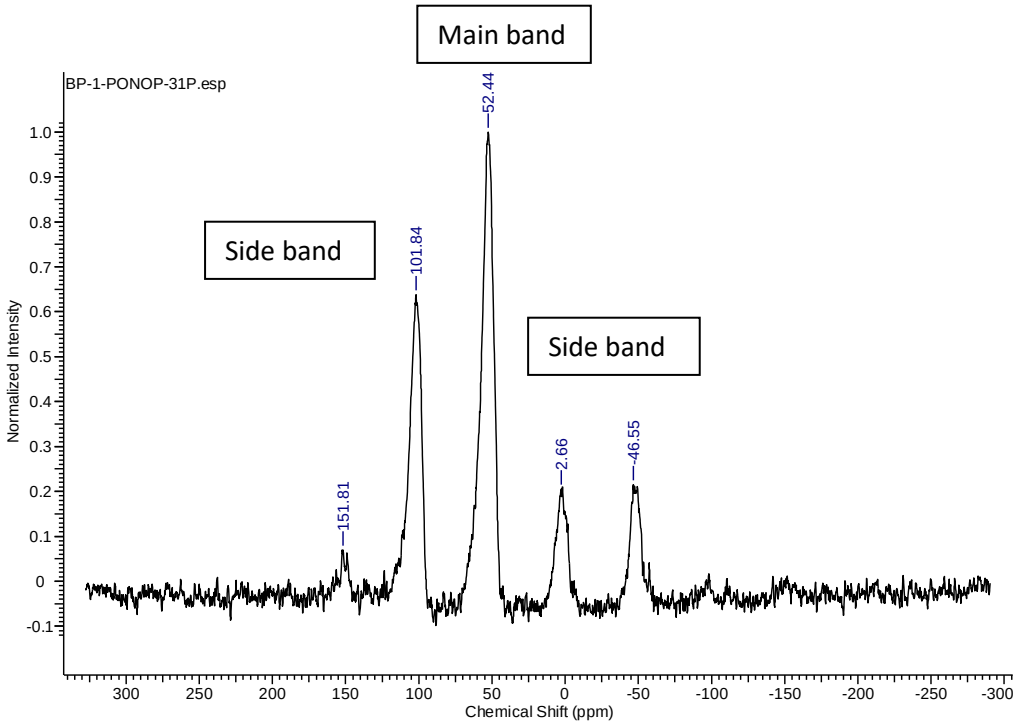

Figure A2: Solid-state CPMAS ^{31}P NMR spectrum of BP-1-PONOP

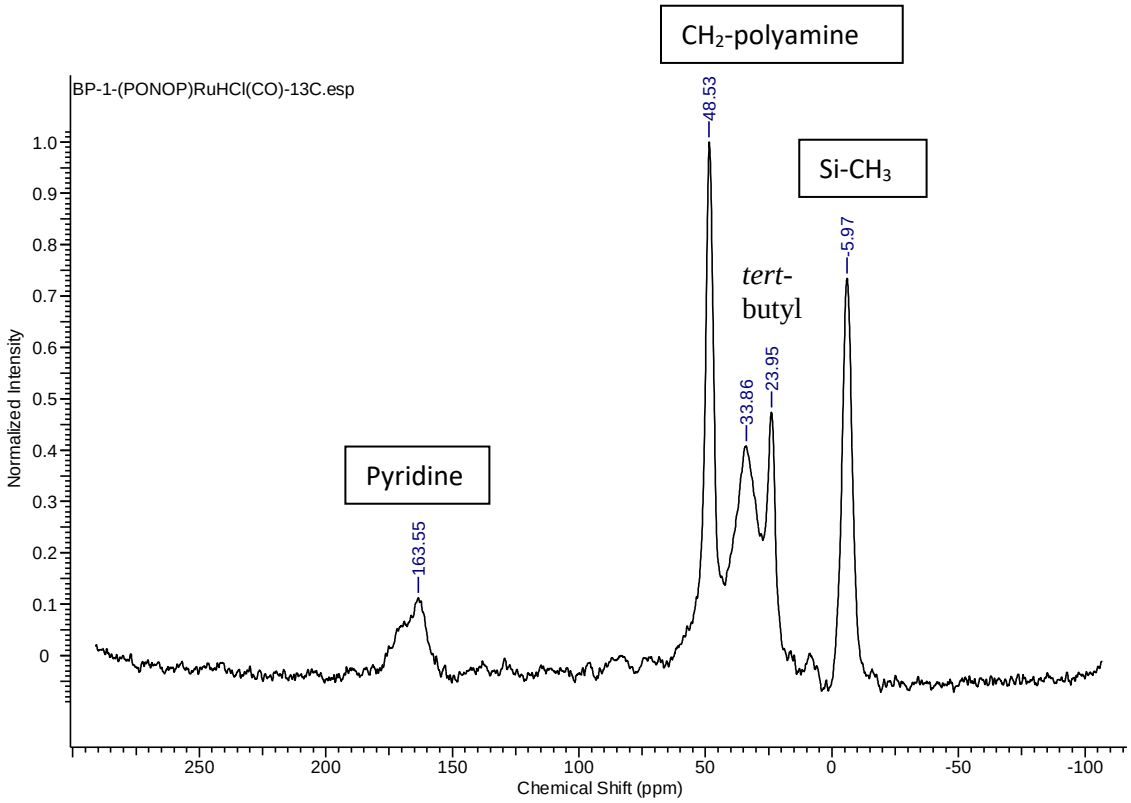

Figure A3: Solid-state CPMAS ^{13}C NMR spectrum of BP-1-(PONOP)RuH(Cl)(CO) (**1**)

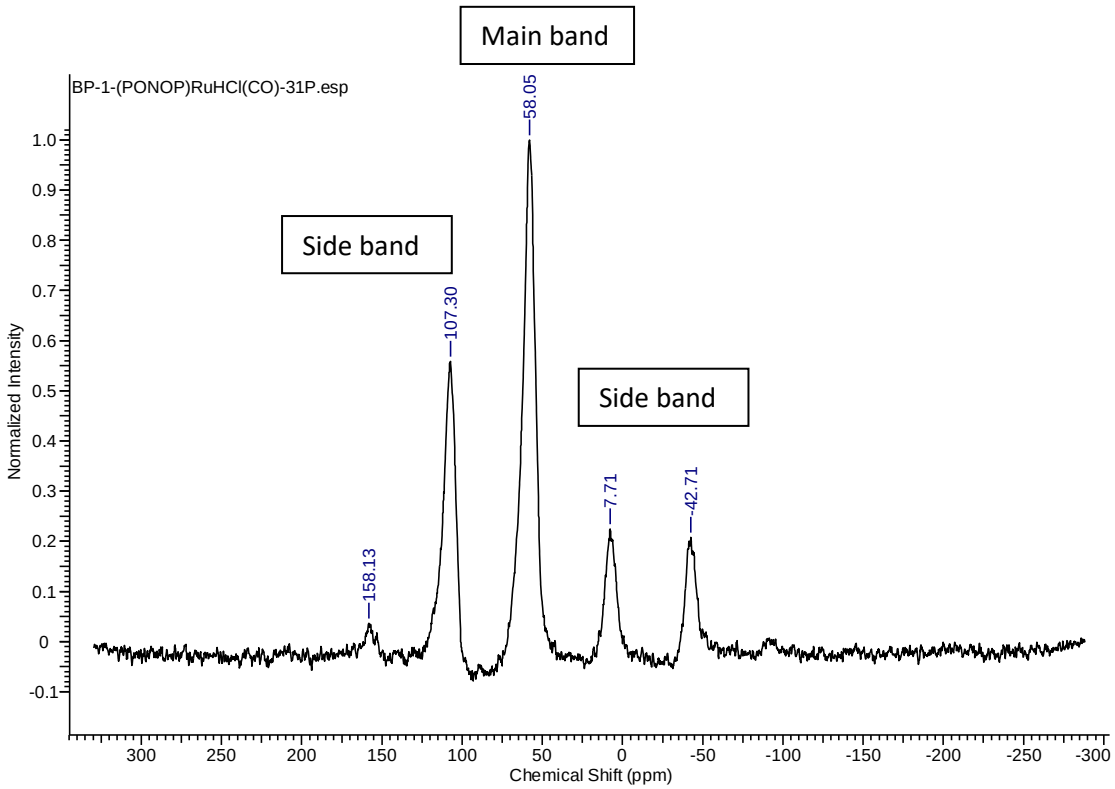

Figure A4: Solid-state CPMAS ^{31}P NMR spectrum of BP-1-(PONOP)RuH(Cl)(CO) (**1**)

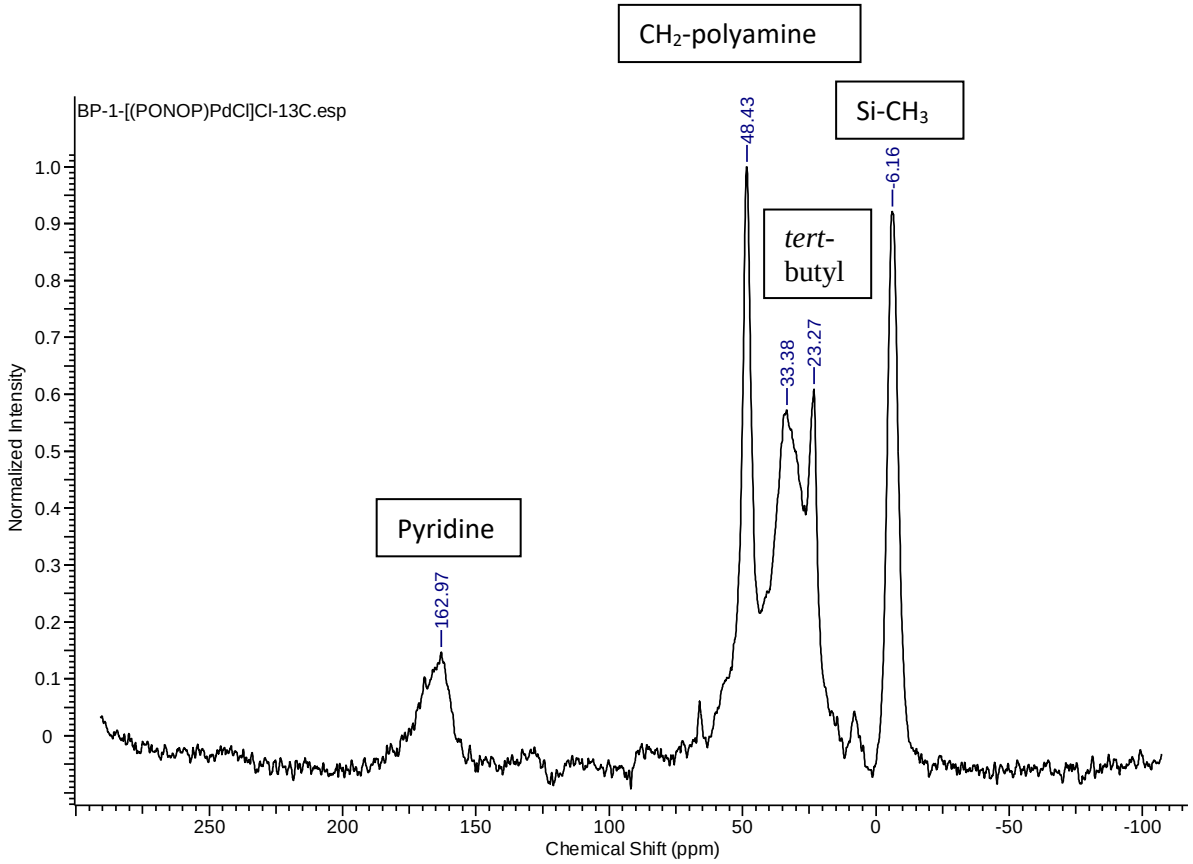

Figure A5: Solid-state CPMAS ^{13}C NMR spectrum of BP-1-[(PONOP)PdCl]Cl (**2**)

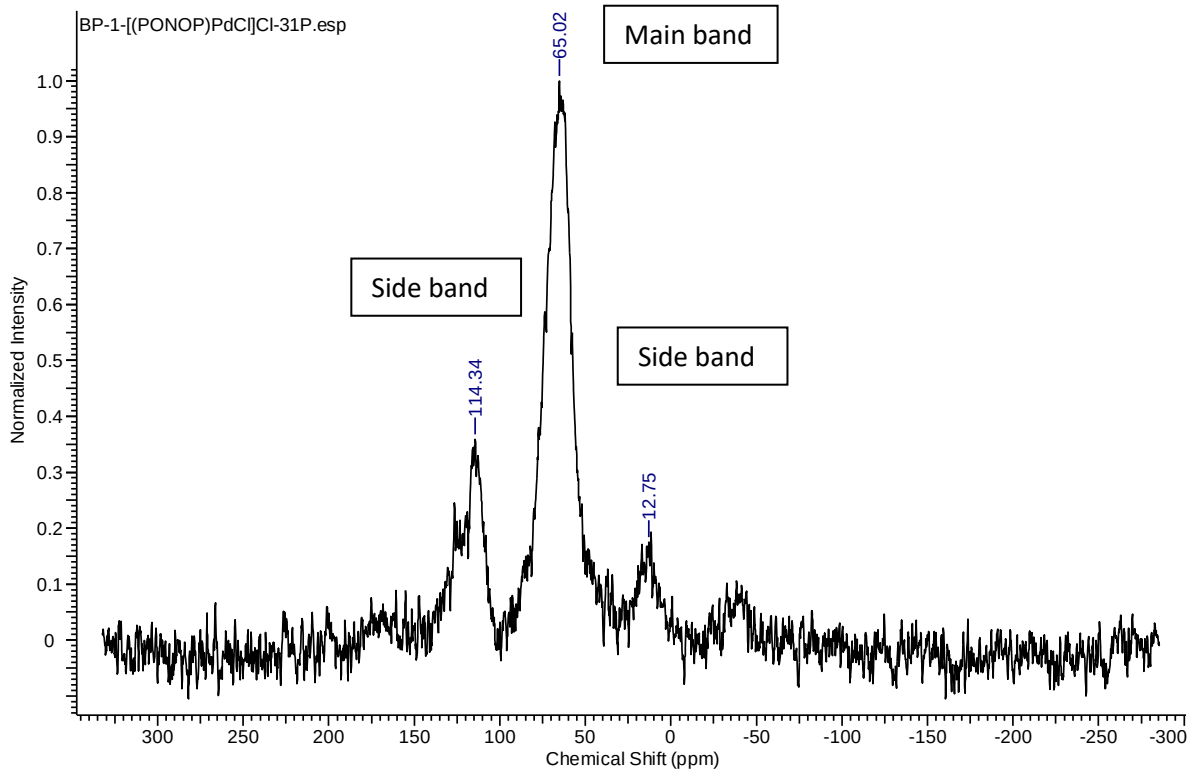

Figure A6: Solid-state CPMAS ^{31}P NMR spectrum of BP-1-[(PONOP)PdCl]Cl (**2**)

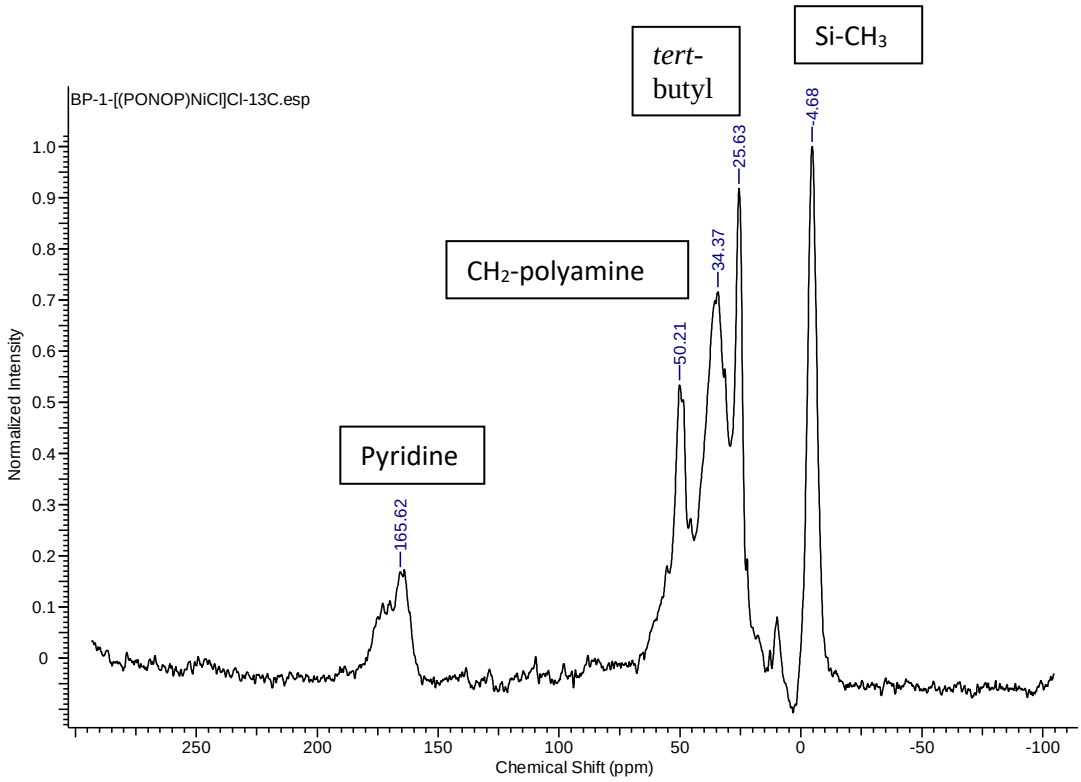

Figure A7: Solid-state CPMAS ^{13}C NMR spectrum of BP-1-[(PONOP)NiCl]Cl (**3**)

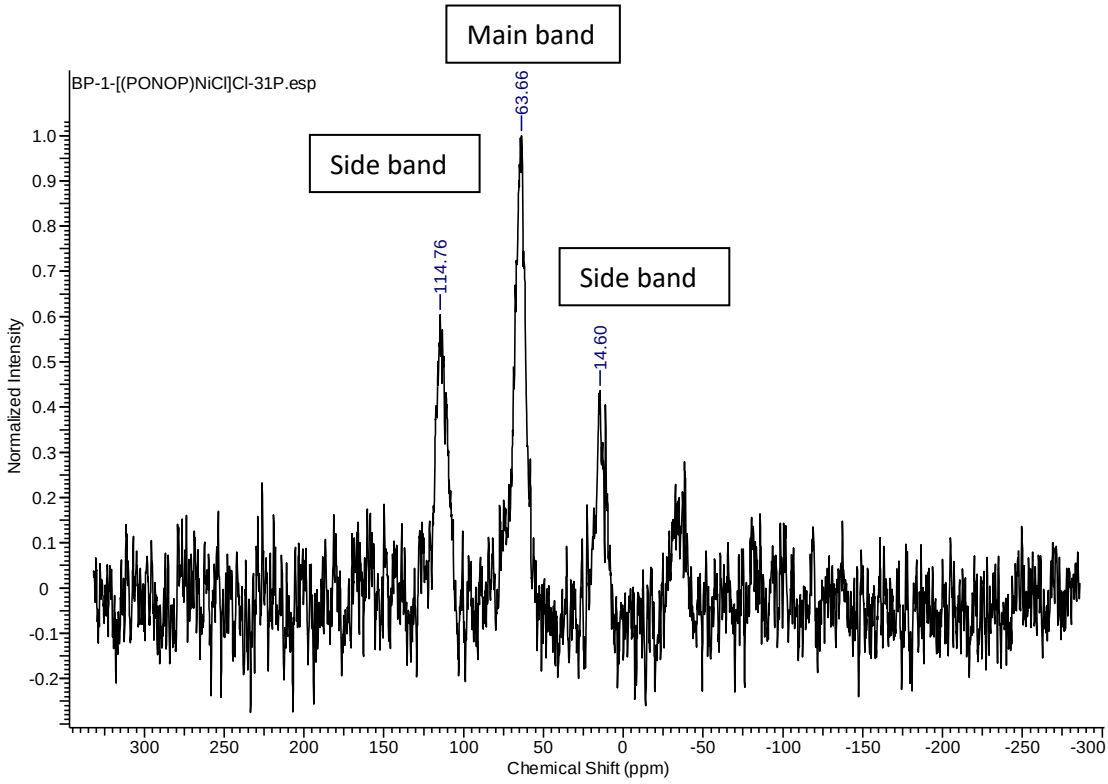

Figure A8: Solid-state CPMAS ^{31}CP NMR spectrum of BP-1-[(PONOP)NiCl]Cl (**3**)

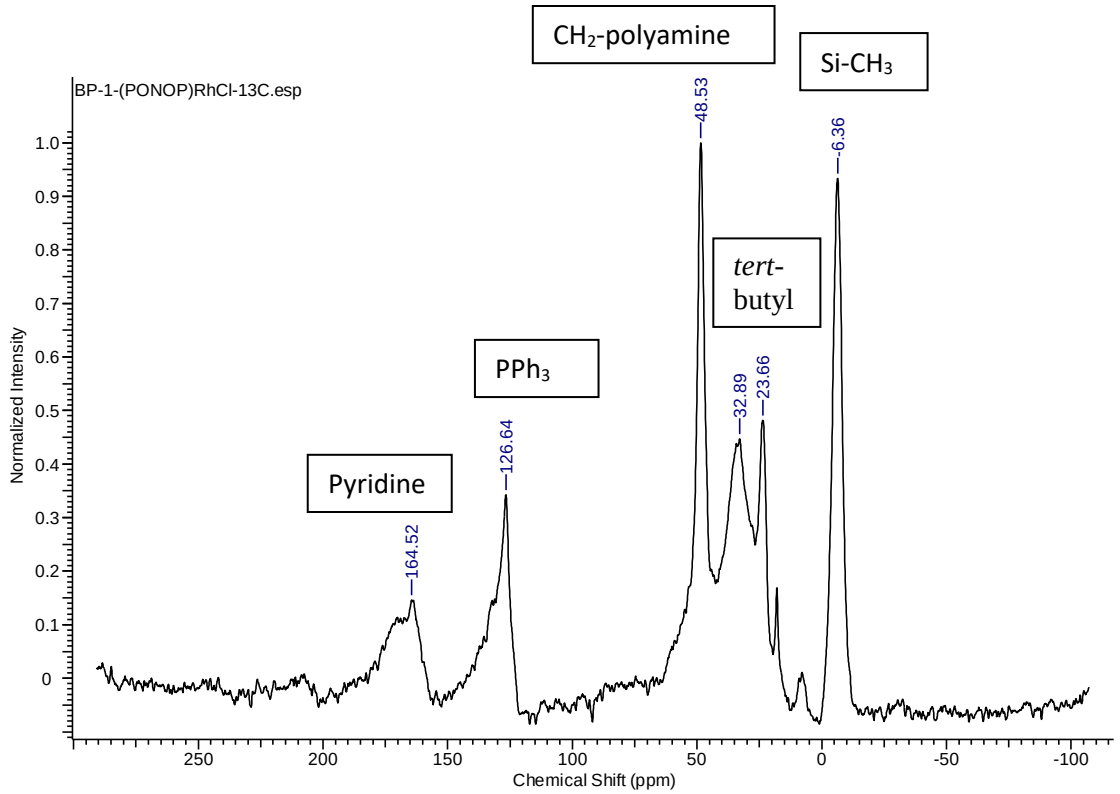

Figure A9: Solid-state CPMAS ^{13}C NMR spectrum of BP-1-(PONOP)RhCl (**4**)

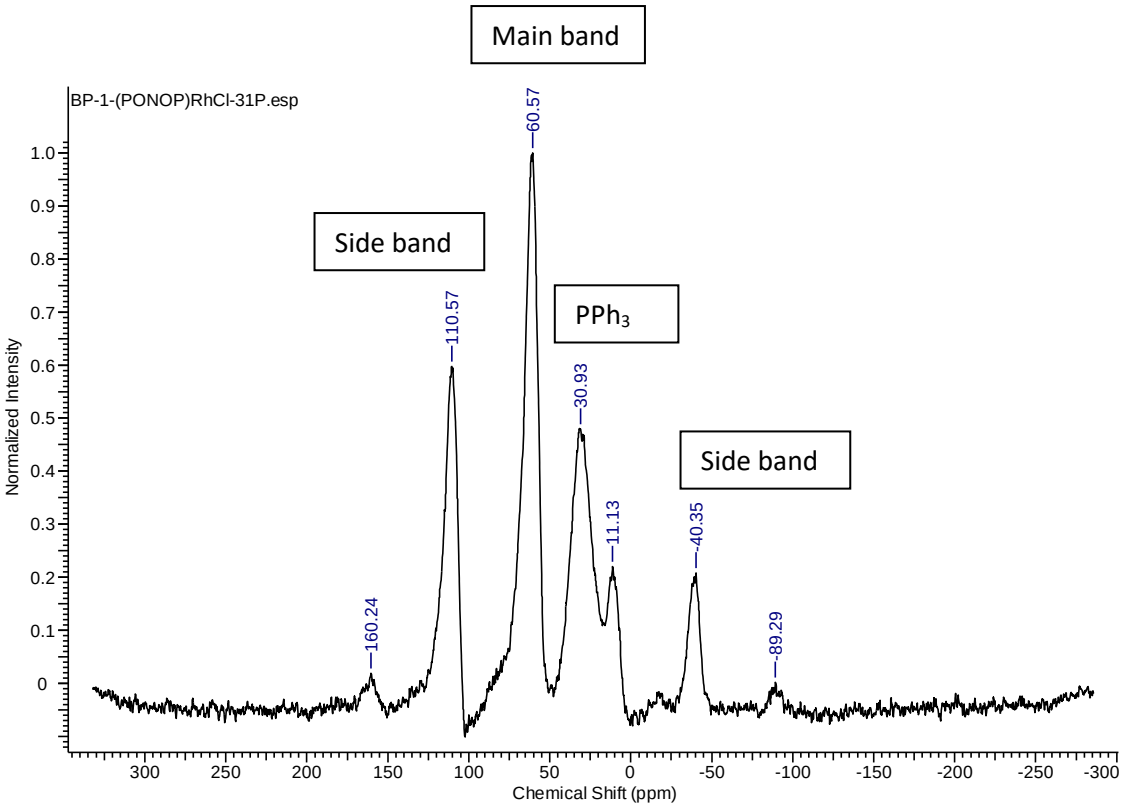

Figure A10: Solid-state CPMAS ^{31}P NMR spectrum of BP-1-(PONOP)RhCl (**4**)

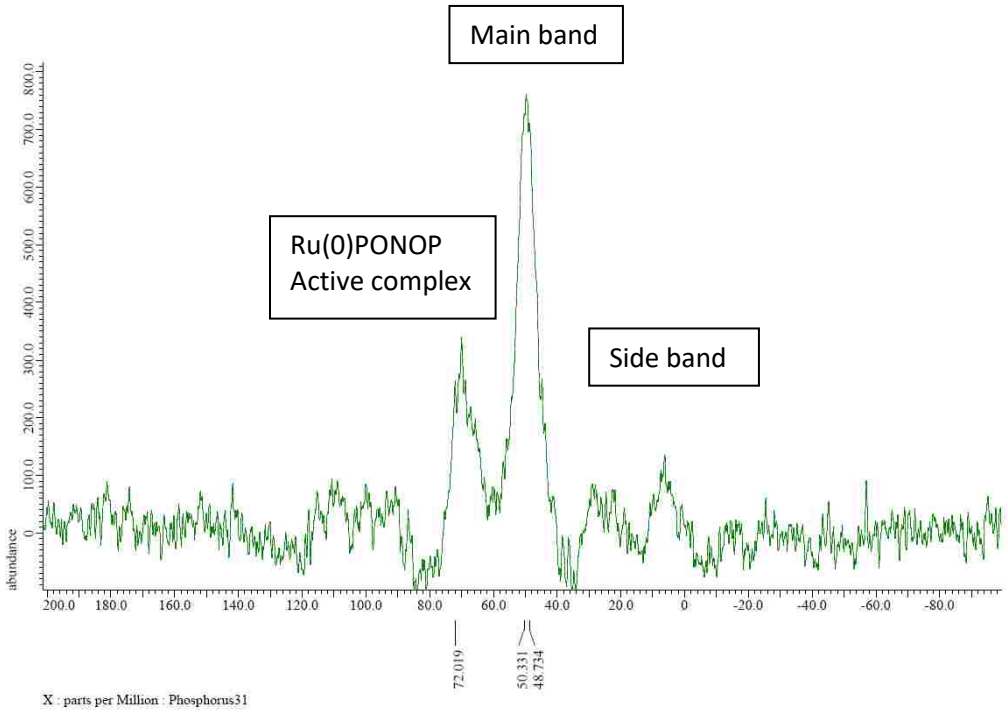

Figure A11: Solid-state CPMAS ^{31}P NMR spectrum of BP-1-(PONOP)RuH(Cl)(CO) (**1**) after 1st cycle of catalysis

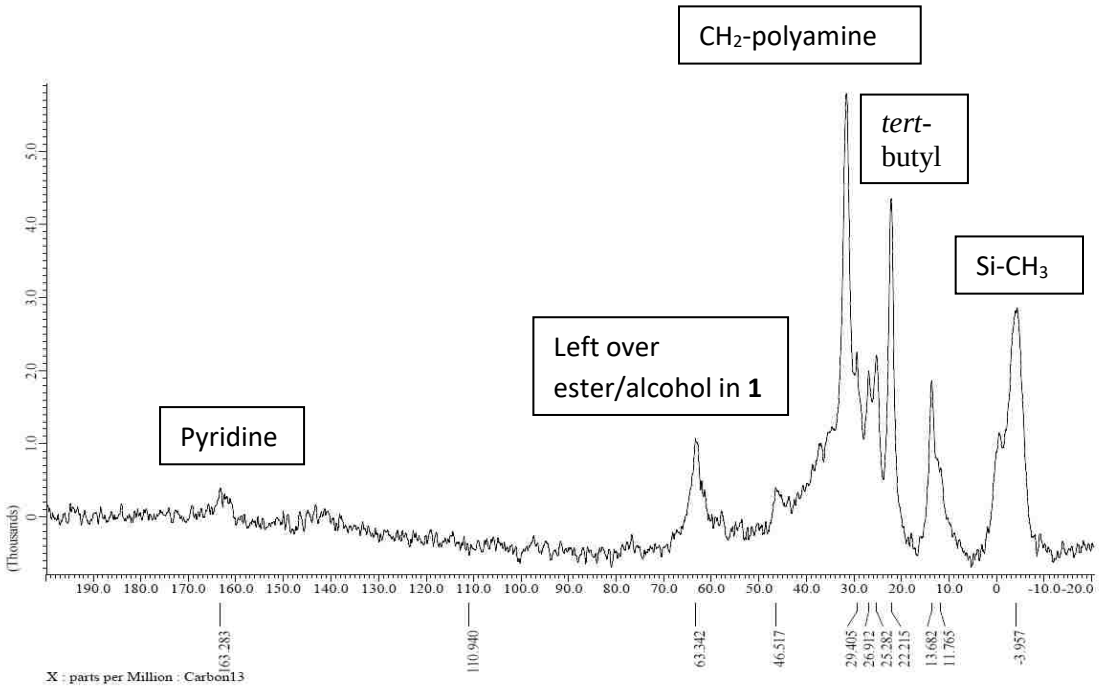

Figure A12: Solid-state CPMAS ^{13}C NMR spectrum of BP-1-(PONOP)RuH(Cl)(CO) (**1**) after 1st cycle of catalysis

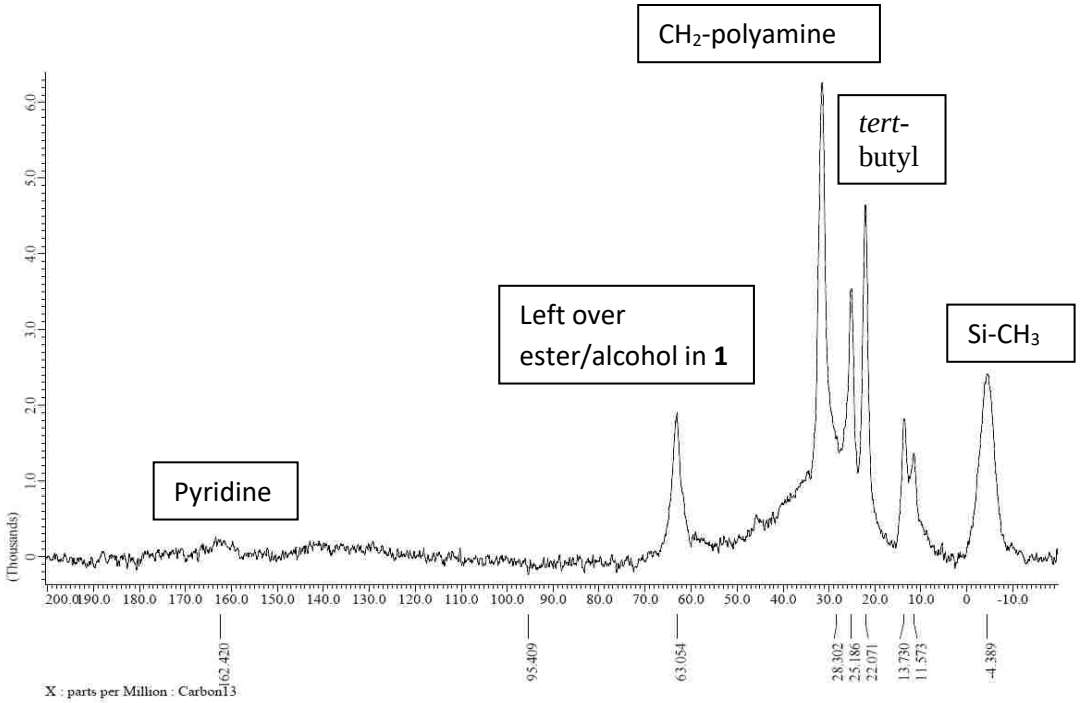

Figure A13: Solid-state CPMAS ^{13}C NMR spectrum of BP-1-(PONOP)RuH(Cl)(CO) (**1**) after 2nd cycle of catalysis

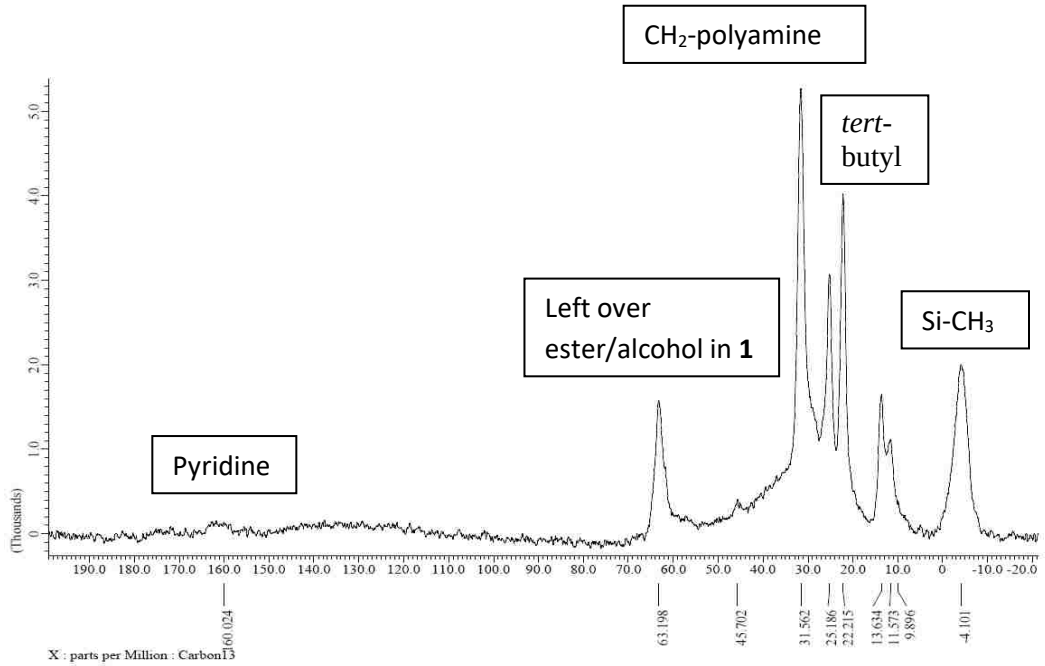

Figure A14: Solid-state CPMAS ^{13}C NMR spectrum of BP-1-(PONOP)RuH(Cl)(CO) (**1**) after 3rd cycle of catalysis

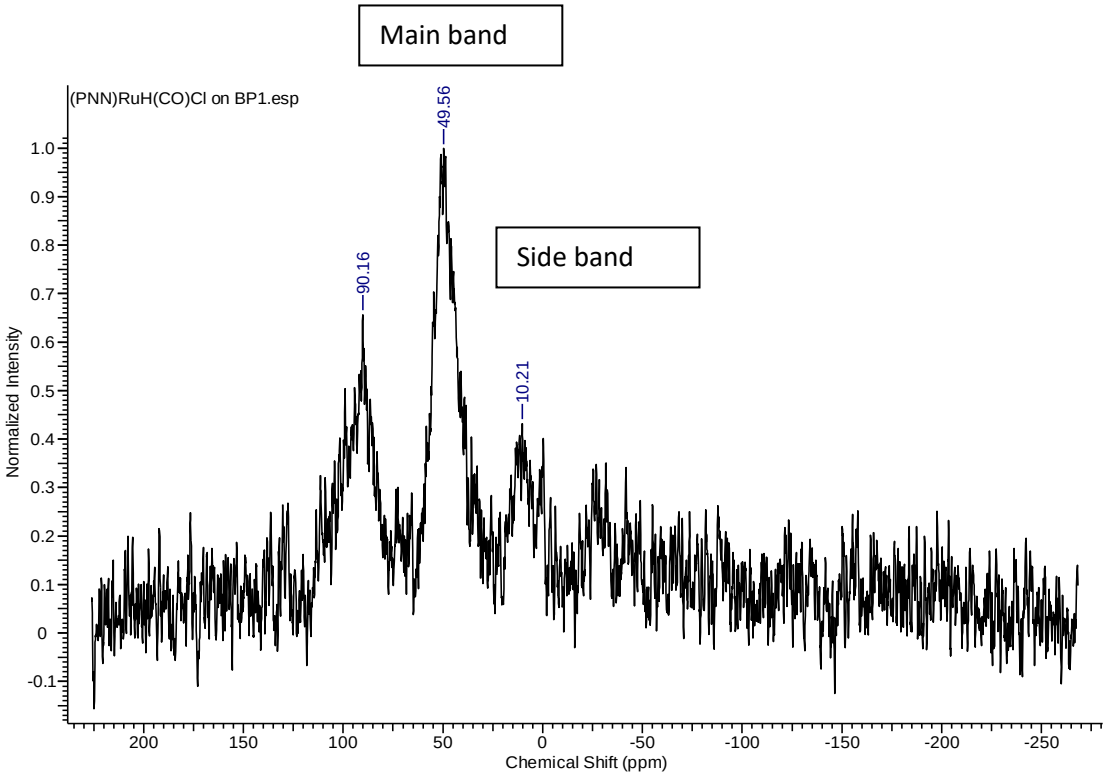

Figure A15: Solid-state CPMAS ^{31}P NMR spectrum of BP-1-(PNN)RuH(Cl)(CO)Cl (7)

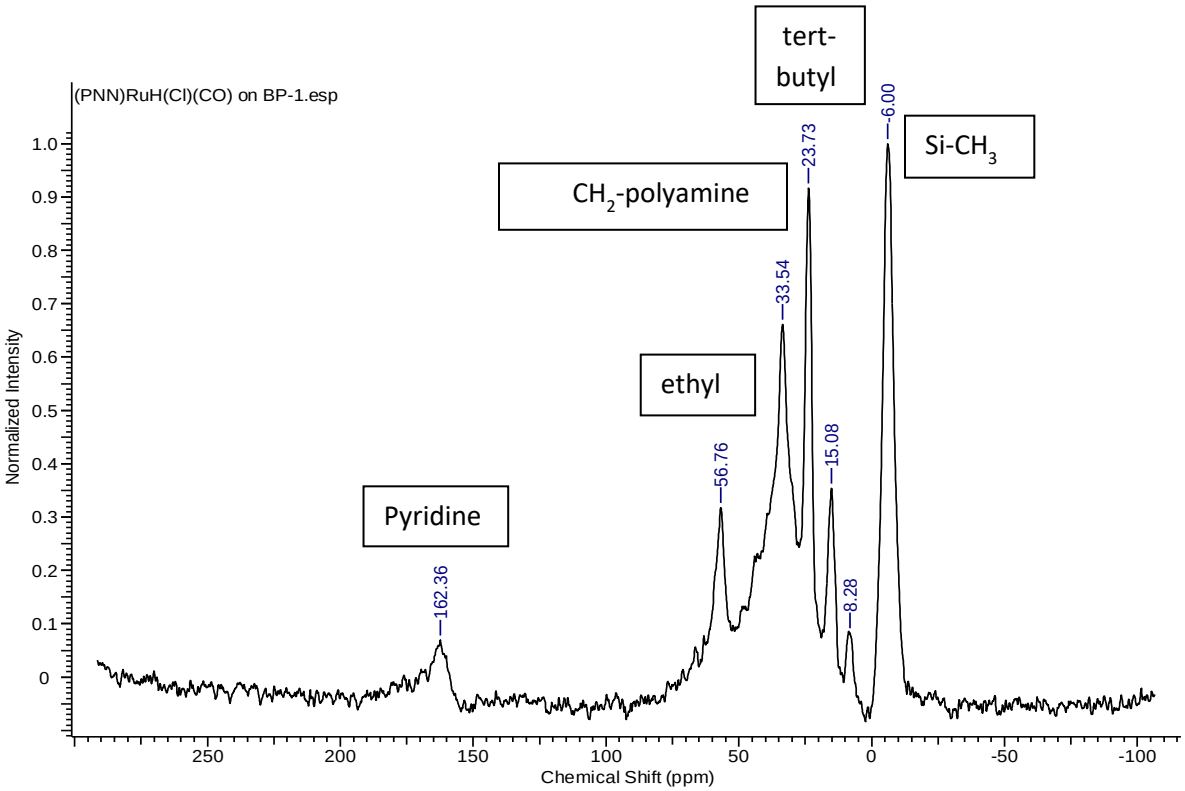

Figure A16: Solid-state CPMAS ^{13}C NMR spectrum of BP-1-(PNN)RuH(Cl)(CO)Cl (**7**)

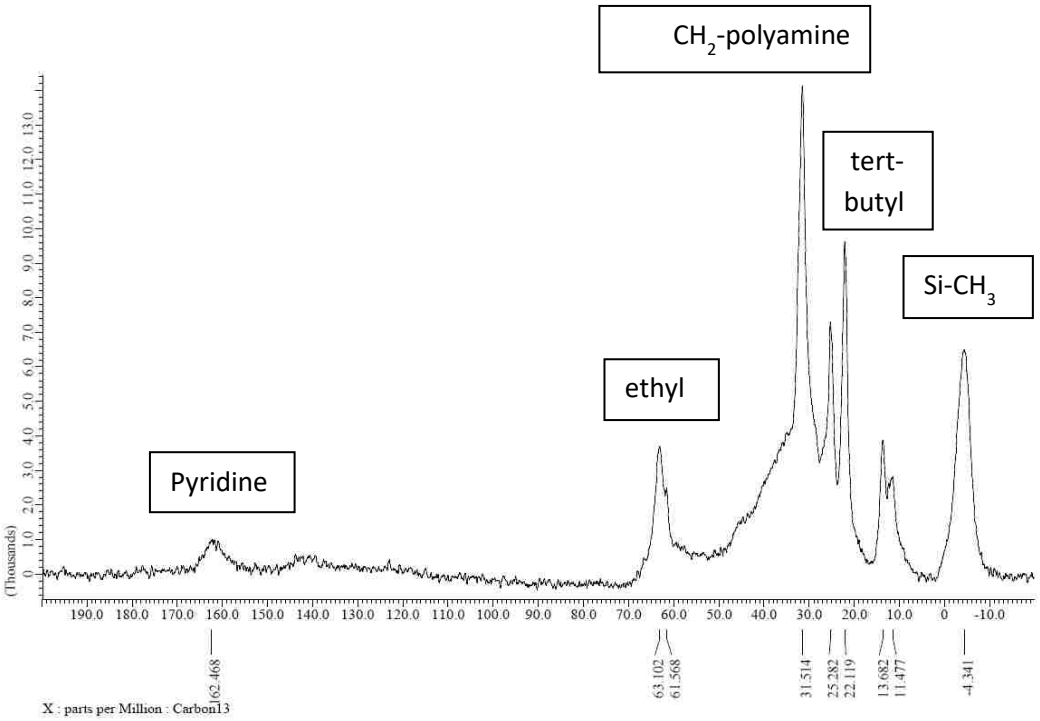

Figure A17: Solid-state CPMAS ^{13}C NMR spectrum of BP-1-(PNN)RuH(Cl)(CO)Cl (**7**) after 1st cycle of catalysis

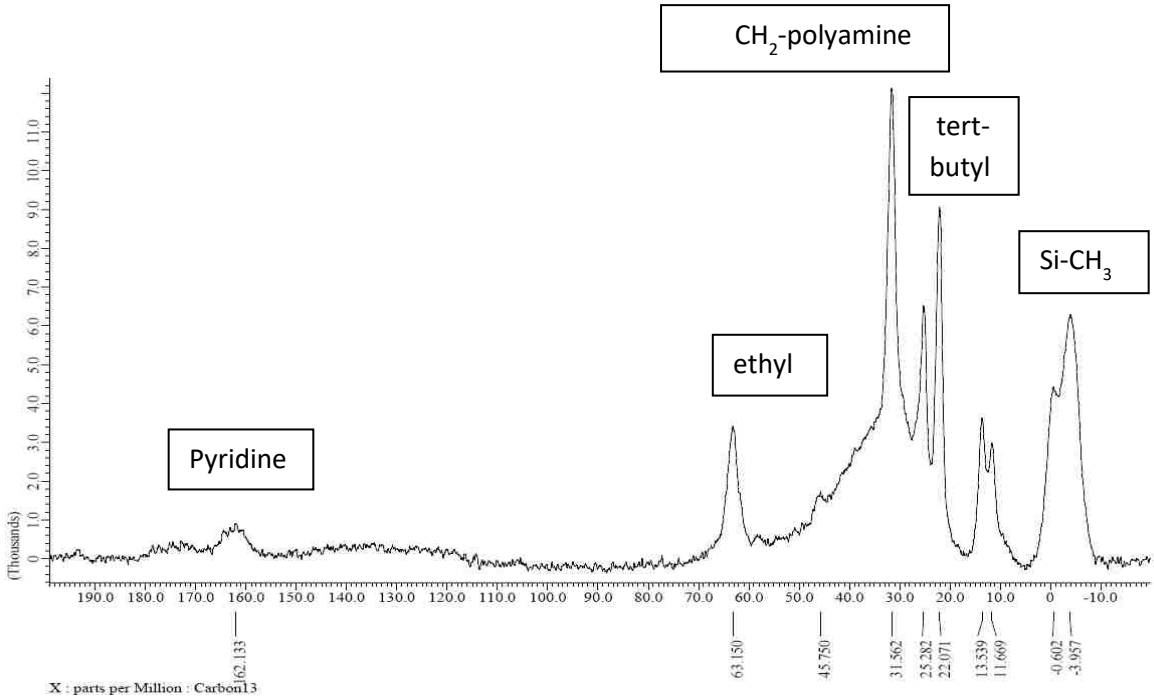

Figure A18: Solid-state CPMAS ^{13}C NMR spectrum of BP-1-(PNN)RuH(Cl)(CO)Cl (**7**) after 2nd cycle of catalysis

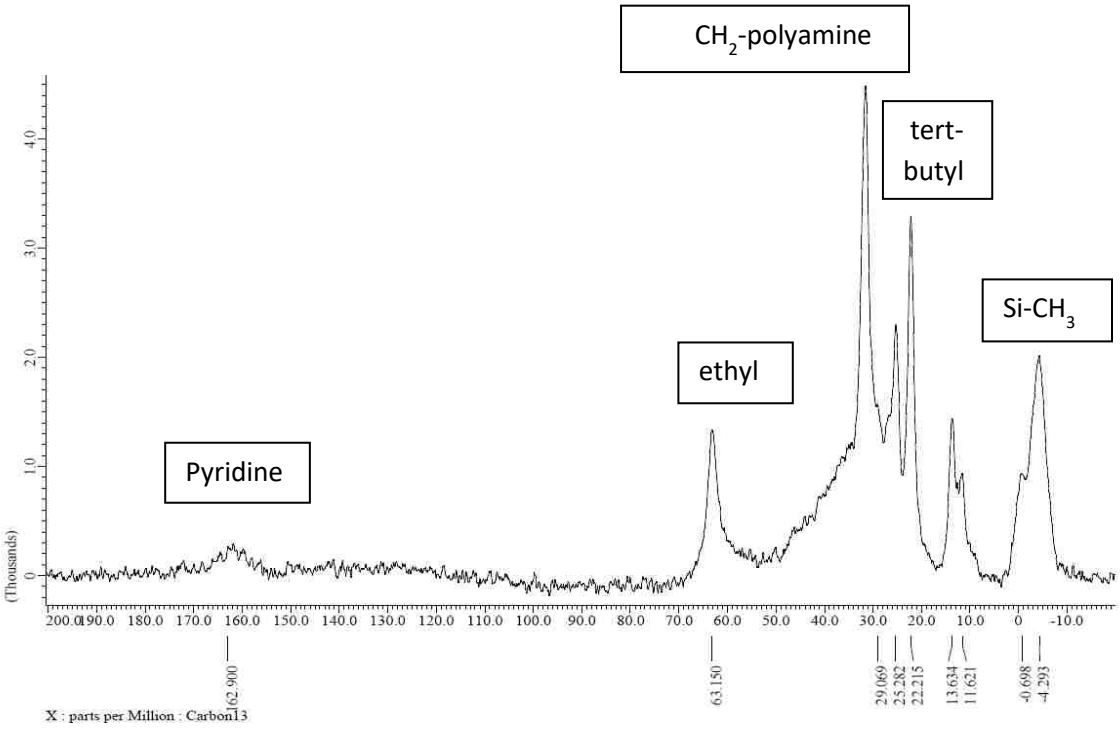

Figure A19: Solid-state CPMAS ^{13}C NMR spectrum of BP-1-(PNN)RuH(Cl)(CO)Cl (**7**) after 3rd cycle of catalysis

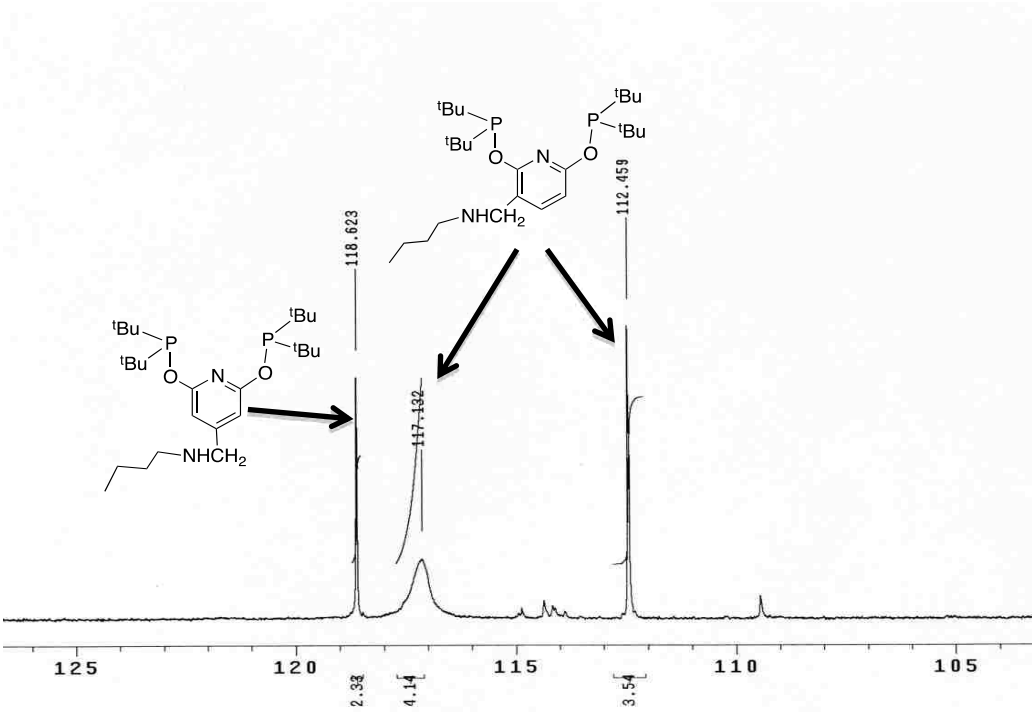

Figure A20: ^{31}P NMR spectrum of the isomers (**5**) formed from n-butyl amine reaction with PONOP

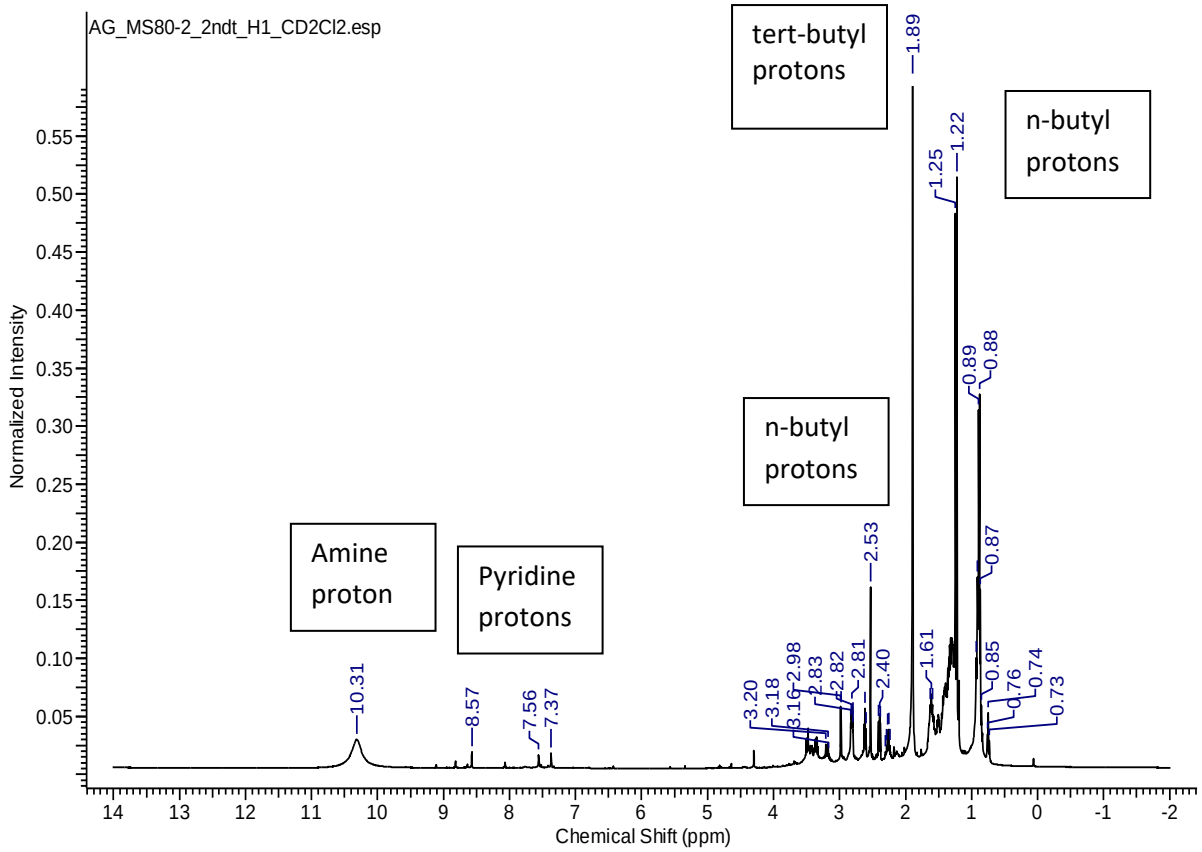

Figure A21: ^{1}H NMR spectrum of the isomers (**5**) formed from n-butyl amine reaction with PONOP

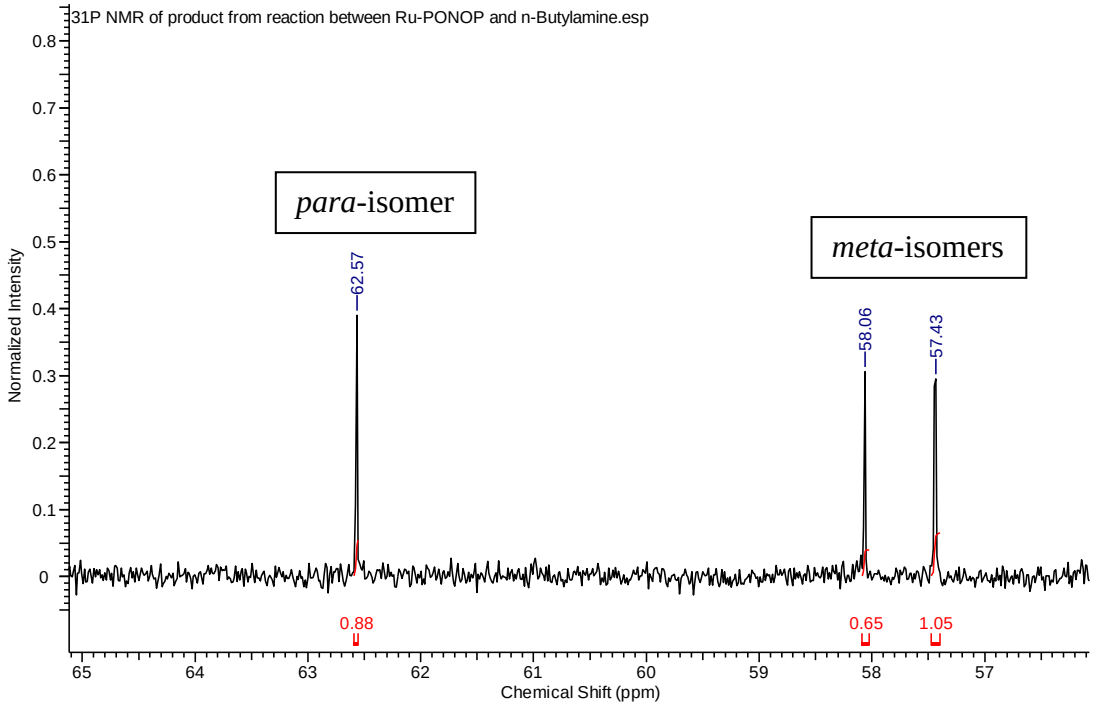

Figure A22: ^{31}P NMR spectrum of the isomers (**6**) formed from n-butylamine reaction with (PONOP)RuH(Cl)(CO)

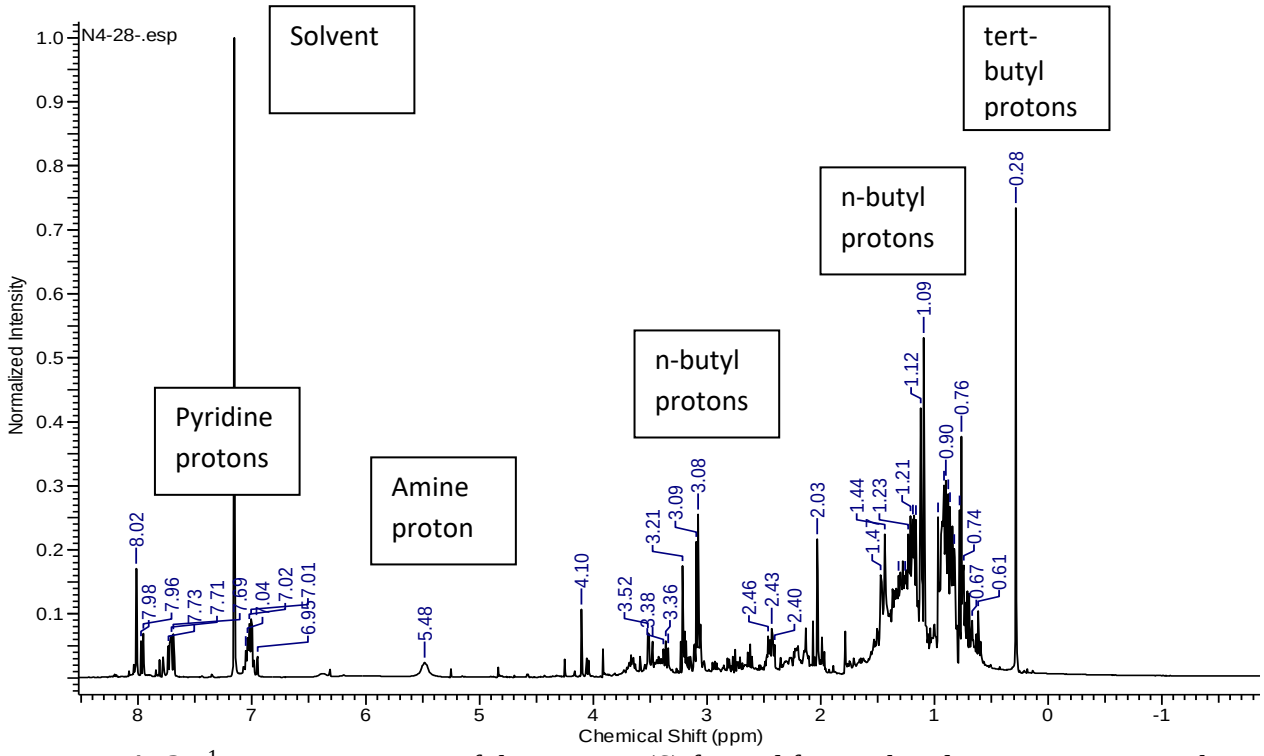

Figure A23: ^{1}H NMR spectrum of the isomers (**6**) formed from n-butylamine reaction with (PONOP)RuH(Cl)(CO). [The additional resonances might be due to the presence of a trace amount of impurities such as unreacted amine, formaldehyde, imine, and remaining starting complex after separation and purification of the product]

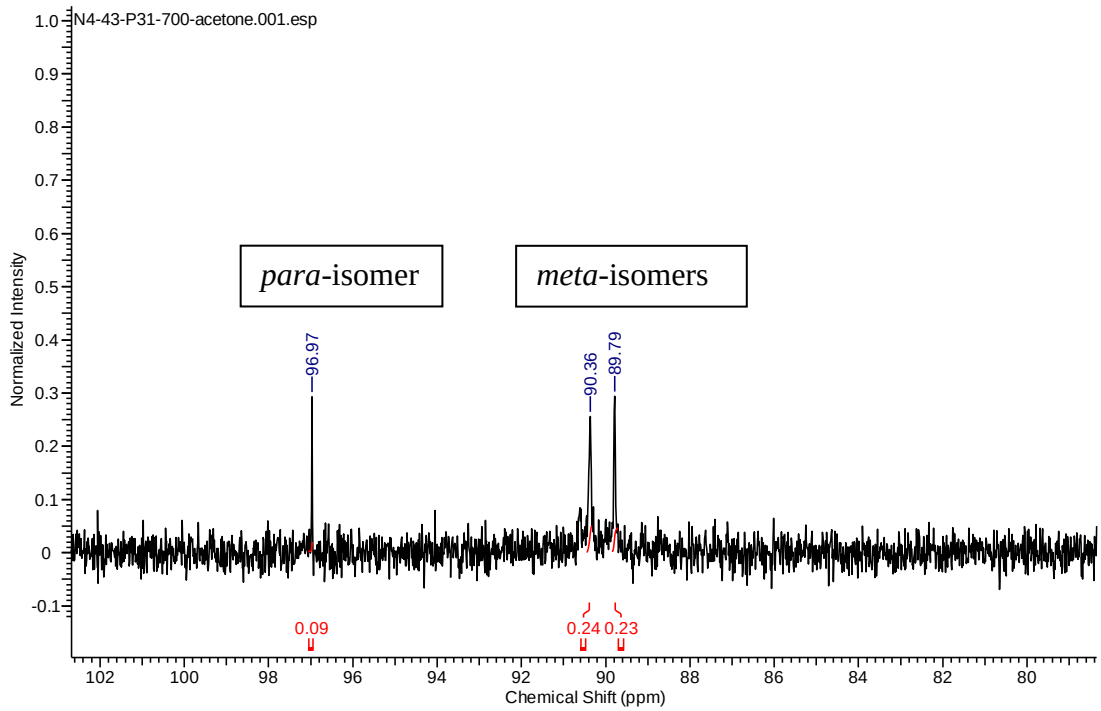

Figure A24: ^{31}P NMR spectrum of the isomers (**8**) formed from n-butylamine reaction with (PNN)RuH(Cl)(CO)

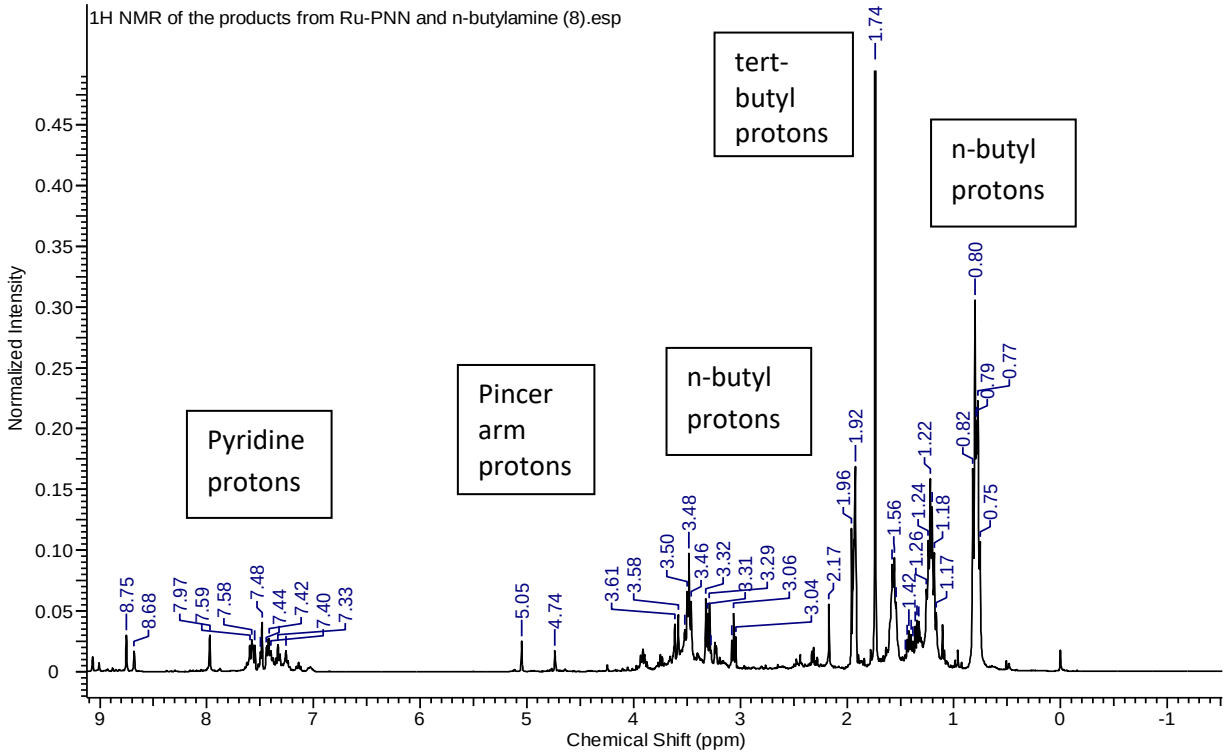

Figure A25: ^{1}H NMR spectrum of the isomers (**8**) formed from n-butylamine reaction with (PNN)RuH(Cl)(CO). [The additional resonances might be due to the presence of a trace amount of impurities such as unreacted amine, formaldehyde, imine, and remaining starting complex after separation and purification of the product]

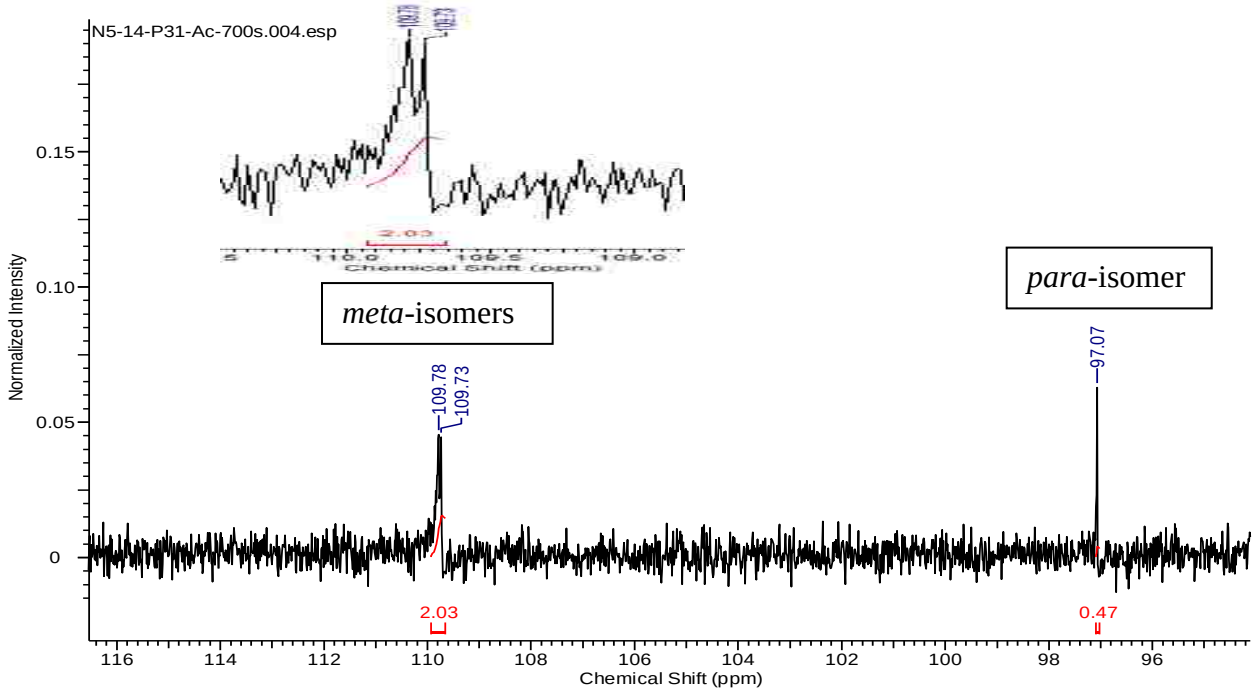

Figure A26: ^{31}P NMR spectrum of t he isomers (**9**) formed from n-butylamine reaction with (PNN)RuH(Cl)(CO)

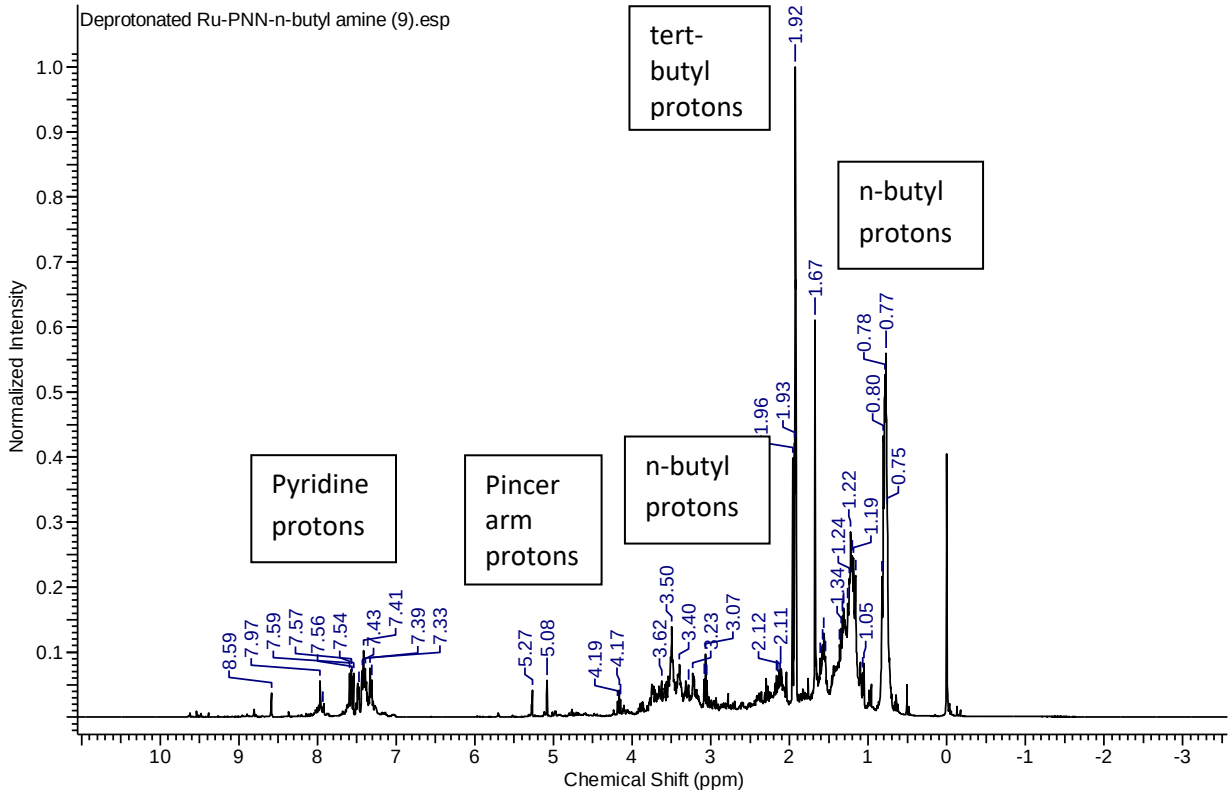

Figure A27: ^{1}H NMR spectrum of the isomers (**9**) formed from n-butylamine reaction with (PNN)RuH(Cl)(CO)

Appendix B

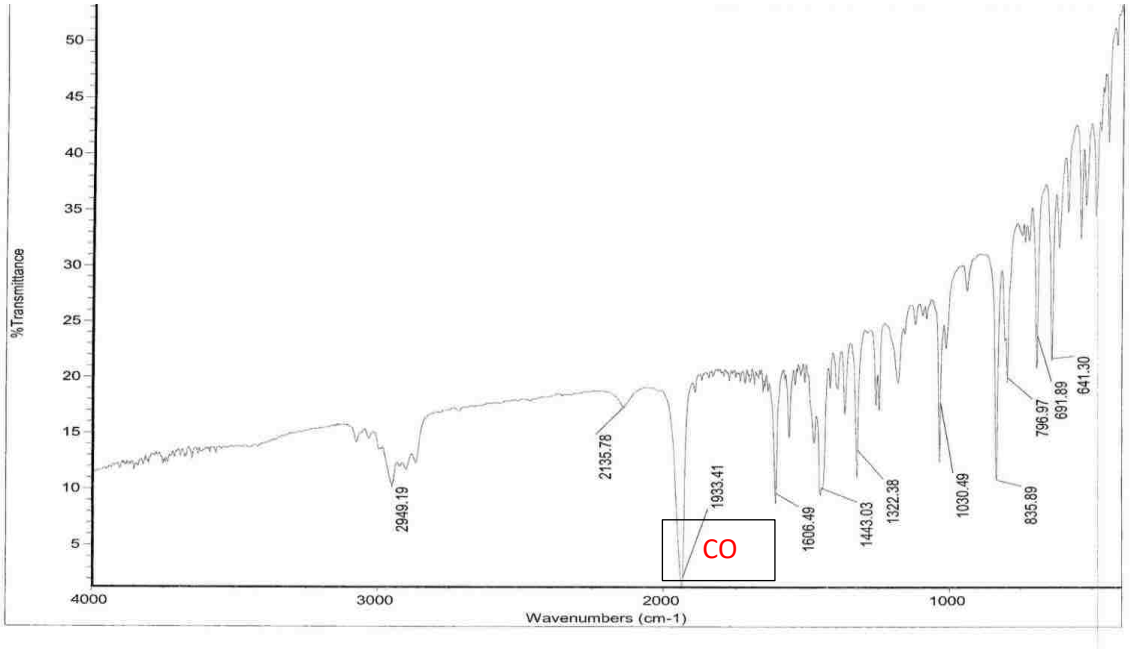

Figure B1: FT-IR spectrum of (PONOP)RuH(Cl)(CO)

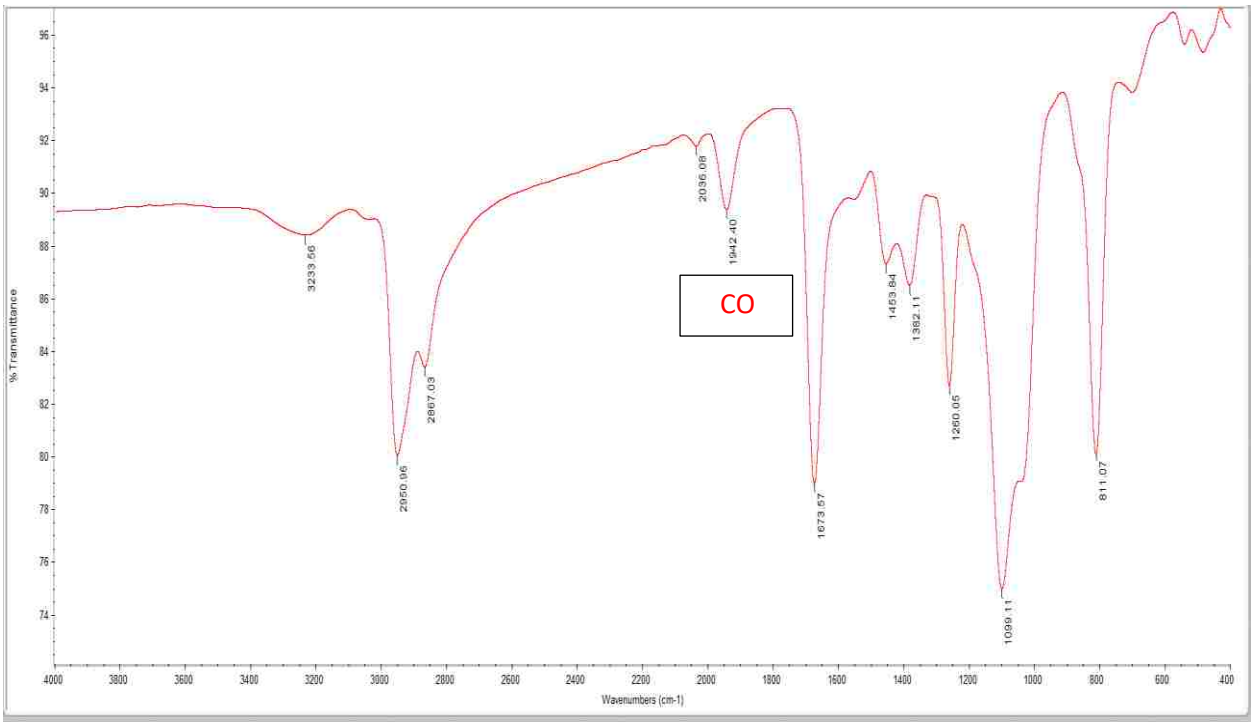

Figure B2: FT-IR spectrum of (PONOP)RuH(Cl)(CO)-n-butyl amine (**6**)

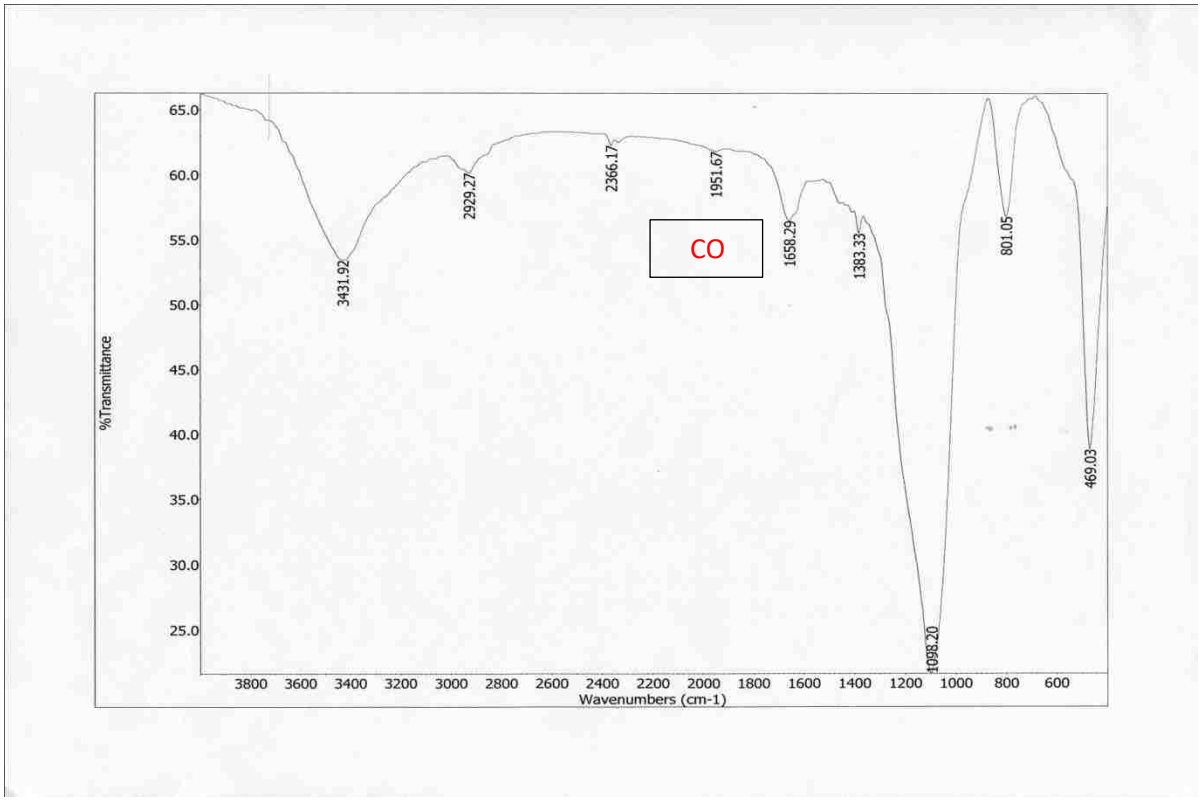

Figure B3: FT-IR spectrum of BP-1-Ru-PONOP (**1**)

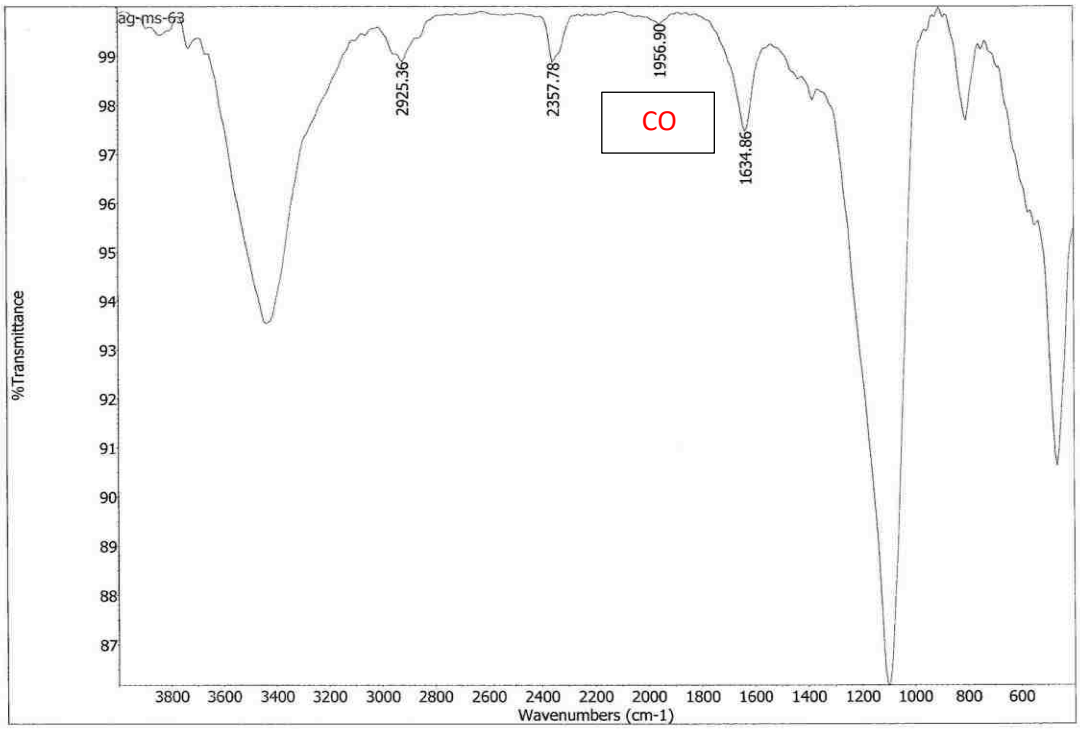

Figure B4: FT-IR spectrum of BP-1-Ru-PONOP (**1**) after catalysis

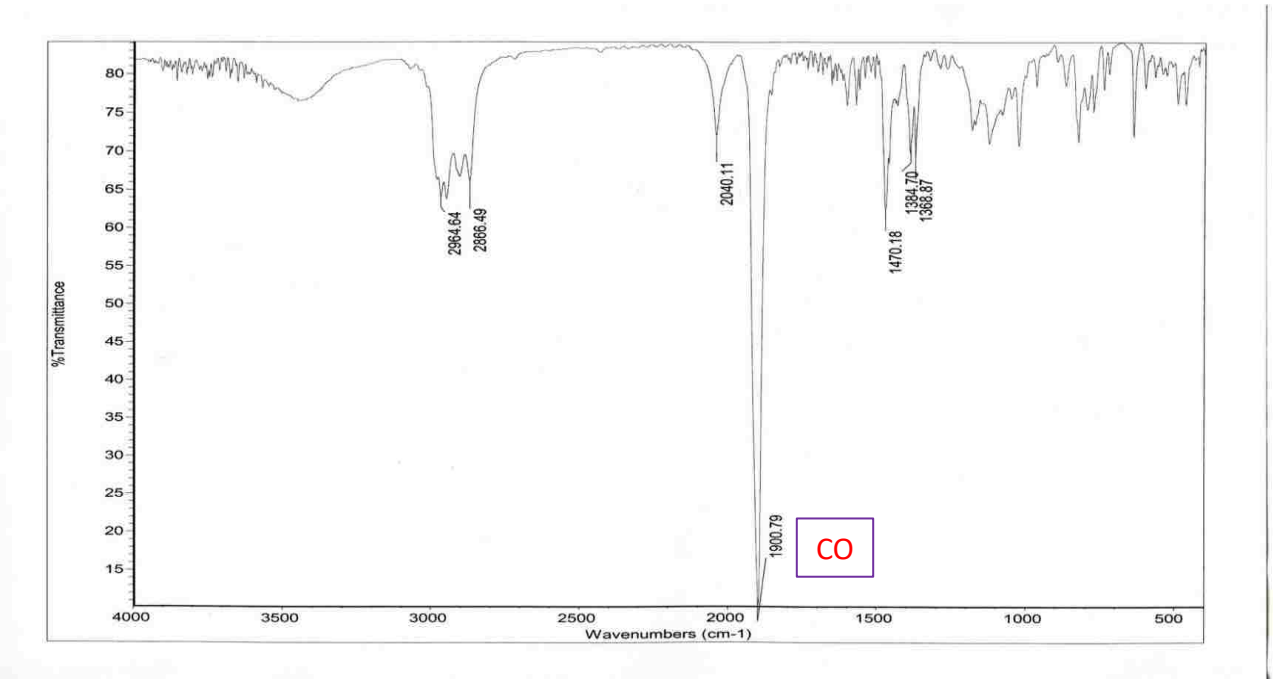

Figure B5: FT-IR spectra of the complex, (PNN)RuH(Cl)(CO)

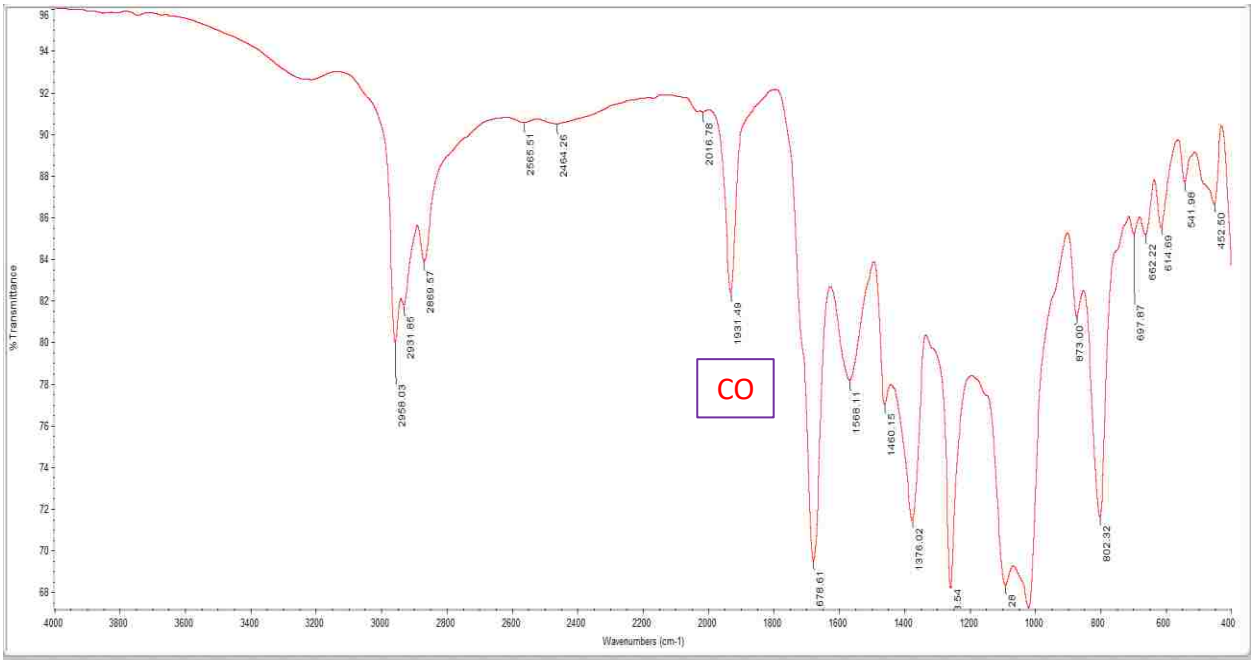

Figure B6: FT-IR spectra of RuH(Cl)(CO)(PNN)-n-butyl amine (**8**)

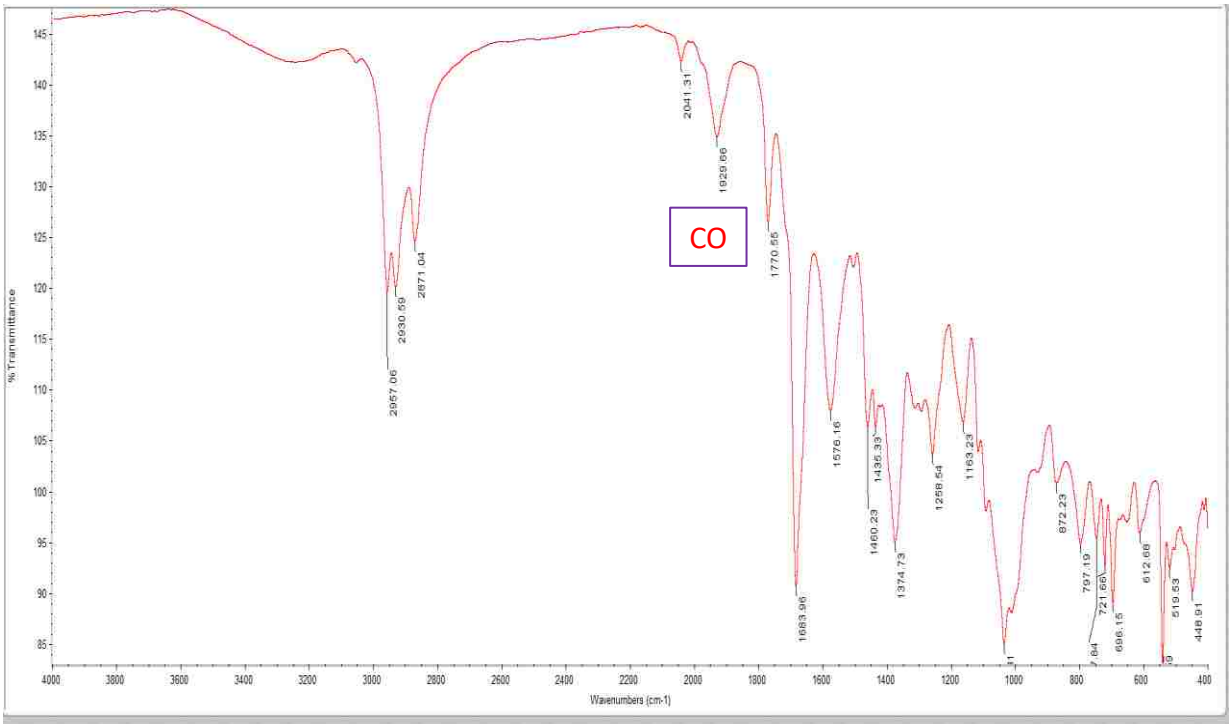

Figure B7: FT-IR spectra of dearomatized Ru-PNN-n-butyl amine (**9**)

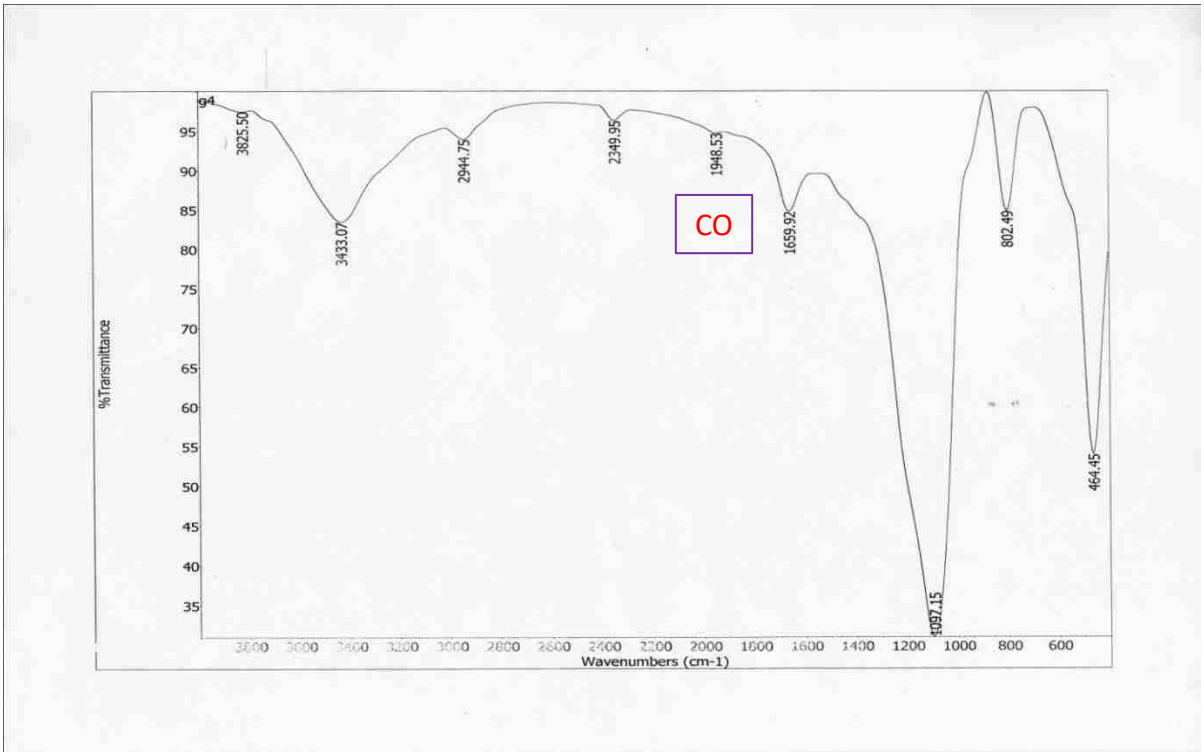

Figure B8: FT-IR spectra of BP-1-Ru-PNN (**7**)

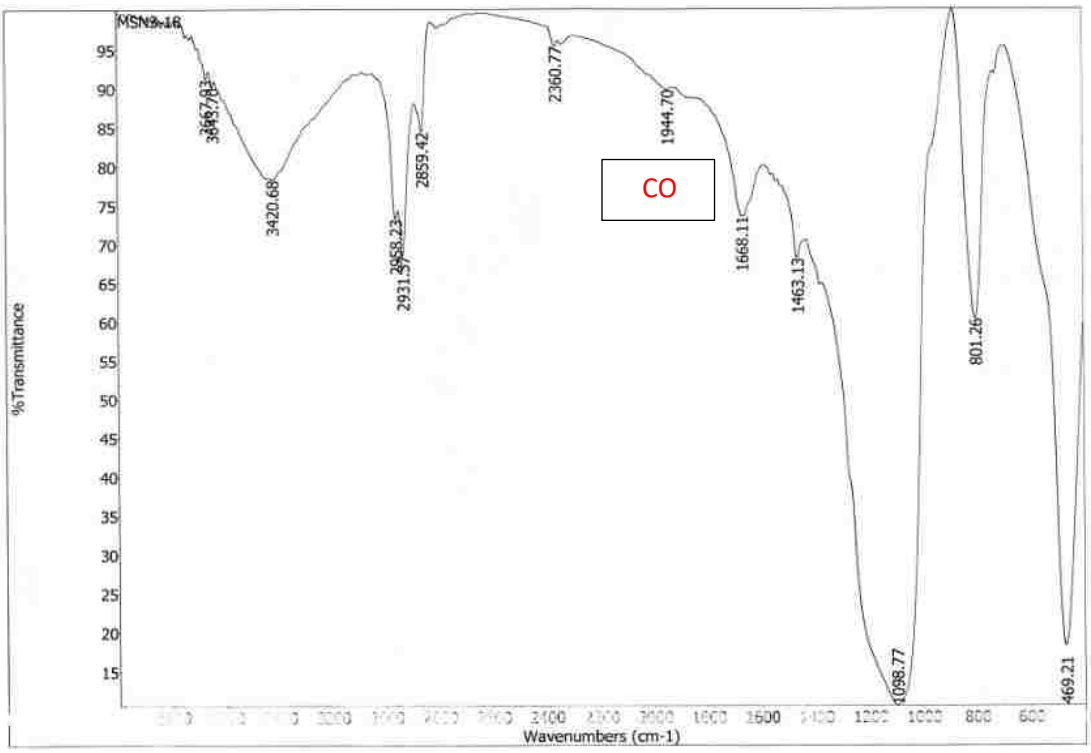

Figure B9: FT-IR spectra of BP-1-Ru-PNN (**7**) after catalysis

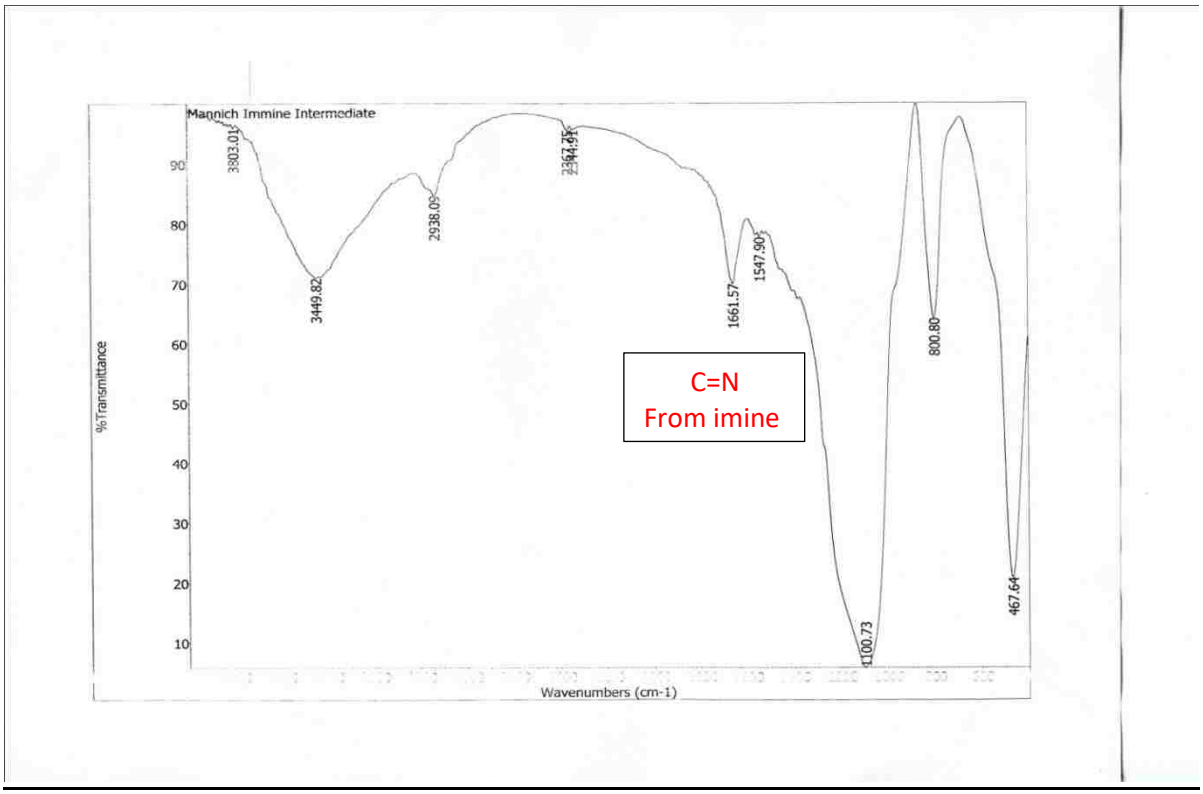

Figure B10: FT-IR spectra of the imine intermediate